

TESIS DOCTORAL

Molecular and metabolomics techniques for the nutritive and organoleptic quality improvement of strawberry (*Fragaria x ananassa*)

Delphine M. Pott

Directores: Prof. Dr. Sonia Osorio Algar / Dr. José G. Vallarino

Universidad de Málaga, Facultad de Ciencias. 2019

Programa de doctorado en Biotecnología avanzada





UNIVERSIDAD
DE MÁLAGA

AUTOR: Delphine M. Pott

 <http://orcid.org/0000-0002-2545-8777>

EDITA: Publicaciones y Divulgación Científica. Universidad de Málaga



Esta obra está bajo una licencia de Creative Commons Reconocimiento-NoComercial-SinObraDerivada 4.0 Internacional:

<http://creativecommons.org/licenses/by-nc-nd/4.0/legalcode>

Cualquier parte de esta obra se puede reproducir sin autorización pero con el reconocimiento y atribución de los autores.

No se puede hacer uso comercial de la obra y no se puede alterar, transformar o hacer obras derivadas.

Esta Tesis Doctoral está depositada en el Repositorio Institucional de la Universidad de Málaga (RIUMA): riuma.uma.es





Departamento de Biología Molecular y Bioquímica

Facultad de Ciencias

Prof. Dr. SONIA OSORIO ALGAR,

Departamento de Biología Molecular y Bioquímica de la Universidad de
Málaga.

Dr. JOSÉ GABRIEL VALLARINO,

Max Planck Institute of Molecular Plant Physiology, Potsdam-Golm (Germany)

INFORMAN:

Bajo nuestra dirección, Dña. **Delphine M. Pott** ha realizado trabajos teórico-experimentales conducentes para la obtención del grado de Doctor y, tanto sus resultados como su interpretación en contexto, son reflejados en la presente Memoria de Tesis Doctoral.

Y para que así conste, y tenga los efectos que correspondan, en cumplimiento de la legislación vigente, se extiende el presente informe en Málaga, a 11 de diciembre de 2018.

Fdo: Prof. Dr. Sonia Osorio Algar

Fdo: Dr. José Gabriel Vallarino

Look deep into nature, and then you will understand everything better

Albert Einstein

Agradecimientos / Remerciements

Aunque no se me da bien tanto sentimentalismo, quiero agradecer a las personas que me han acompañado durante esta etapa, y que han hecho que sea una de las mejores experiencias que he vivido hasta ahora.

En primer lugar, a Sonia, por confiar en mí sin apenas conocerme, por transmitirme su energía y motivación, por obligarme a conseguir siempre más. Creo que hemos sido un buen equipo, y espero que lo podamos seguir siendo.

A José por cuidar de mí en los inicios de esta etapa, por ser el responsable de que ya no me disgusta tanto la bioinformática, por las largas conversaciones y por abrirme los ojos sobre lo que es la ciencia.

A Victoriano, Josan y Ana...porque empecé la bioquímica vegetal con ellos, por la bonita experiencia de Grenoble, y por todo lo que he aprendido con ellos.

A Karen...por su amistad, por lo que hemos compartido dentro y fuera del laboratorio, y por los viajes que nos quedan por hacer. Por ser una maravillosa compañera de trabajo, y por tener esta visión de la ciencia, que me encanta.

A David y Carmen, por ser una gran pareja de científicos, y unos súper compañeros de laboratorio. Por toda la ayuda que me han aportado a lo largo de estos años, y porque, sin Carmen, los beer meetings no serían iguales.

A Iri, por su ayuda en mi tesis, por su simpatía y sus buenos consejos.

A Miguel Ángel...por siempre tomar el tiempo de escuchar mis lab meetings y darme buenas ideas.

A Lidia, por ser la mejor compañera de tesis que se podía imaginar, por todos los buenos (y algunos menos buenos) momentos compartidos, por lo que hemos conseguido juntas. Gracias a ella, mi tesis ha ido viento en popa.

A Sara...por su eficiencia, su siempre buen humor y energía, incluso cuando no salen las cosas. Ha sido un gran aporte al grupo.

A mis compañeros de carrera, de máster y tesis, porque llevamos 10 años estudiando juntos en la UMA y por todos los momentos que hemos compartido. A Bego por estar siempre pendiente de todos, a Blanca por sus conversaciones, a Alba por su sentido del humor, a Álvaro Melillero por pasármelo siempre bien con él y a Álvaro Piedra por su compañerismo.

A todos mis compañeros de laboratorio... por lo bien que me lo pasé con ellos, por todas las quedadas, las comilonas en la Pepa, los beer meetings y los viajes...

A los que estaban al principio, por acogerme en el grupo tan fácilmente... a Vitor por su ayuda en el lab y por ser tan buen vecino, a Eli por su alegría contagiosa, a Jessi por su buen rollo y a Ali por su amistad.

...Y a los que llegaron más tarde...a Eva por ayudarme cada vez que lo necesitaba con las qPCR, a Vito por compartir conmigo su conocimiento sobre el cultivo de fresa *in vitro*, a Noemí por sus consejos y su manera tan espontánea de decir las cosas, a Mario por hacernos reír tanto, a José por nunca dejarme sentada sola con una cerveza y a Almu por ser también parte del equipo A.

A Sophia, Yulia, Amalia, Mariem, Annika, Selene, Carlos y Pepe, por haber sido parte de esta aventura.

A los genéticos, Araceli, Miguel, Pepe, Ana, Bea, Ale y Tábata por los momentos compartidos.

Quiero agradecer a Björn y a Alisandra, que han tenido la paciencia de enseñarme algo de bioinformática. Igualmente, quiero dar las gracias a Harry Klee y a Denise por darme la oportunidad de trabajar dos meses en la University of Florida y tratarme tan bien.

A Elsa y Pepe Sevilla, por su ayuda en Churriana.

A la gente que tuve la suerte de conocer durante estos años... A Daniela, por enseñarme esa parte de Alemania, a Verena, Dennis, Farhan, John y Deborah por ser grandes compañeros de piso, a Serdal por llevarme al Golfo de México.

À Pol, pour plus de 20 ans d'amitié, malgré la distance. Pour toutes nos rigolades en Irlande, au Maroc, en Belgique, en Allemagne, à la feria de Málaga et à Paris. Pour avoir toujours le détail fraise à apporter.

À mes parents...pour m'avoir toujours soutenue, même dans mes décisions les plus folles. J'espère que vous êtes fiers de moi et de mon travail. Cette thèse vous est dédiée.

A Fran... porque, después de todo, ha sido lo mejor que me ha ocurrido durante esta etapa de mi vida. Te quiero, y espero seguir creciendo a tu lado.

Esta tesis ha sido financiada por el proyecto AGL2012-40066-C02-02, concedido a Sonia Osorio, así como una ayuda predoctoral para la formación de doctores (BES-2013-062865) y dos estancias breves (EEBB-C-16-11304 y EEBB-I-17-12456).

Chapter 1: General introduction	8
The Rosaceae family	10
<i>Fragaria</i> genus	10
Fruit quality traits in strawberry	13
Postharvest	17
Analysis of the fruit metabolome	18
Breeding for quality traits	20
Quantitative Trait Loci (QTL) analysis	21
Linkage maps in strawberry	23
QTL analysis for fruit quality traits	24
Aims	28
Chapter 2: Identification of Quantitative Trait Loci (QTL) and Candidate Genes for Primary Metabolite Content in Strawberry Fruit	29
Chapter 3: Quantitative Trait Loci and Underlying Candidate Genes Controlling Secondary Metabolites in Strawberry Fruit	47
Introduction	48
Materials and Methods	54
Results	58
Discussion	104
Chapter 4: Metabolomic Profiling of Postharvest Senescence in Different Strawberry Cultivars	114
Introduction	115
Materials and Methods	120
Results	125
Discussion	193
Conclusions	201
Resumen de la tesis en castellano	203
CAPÍTULO 1: Introducción general	203
Objetivos	205
CAPÍTULO 2: Identificación de <i>loci</i> de carácter cuantitativo (QTL) y genes candidatos para el contenido en metabolitos primarios del fruto de fresa...	205
CAPÍTULO 3: Identificación de <i>loci</i> de carácter cuantitativo (QTL) y genes candidatos que regulen el contenido en metabolitos secundarios del fruto de fresa	209
CAPÍTULO 4: Perfil metabolómico durante la senescencia de postcosecha en frutos de diferentes cultivares de fresa	213

Conclusiones generales	218
References	220
Annexes	244

Chapter 1: General introduction

Strawberry (*Fragaria x ananassa*) is one of the most consumed berry crops in the world, appreciated for its delicate taste and aroma, and its high nutritional value. In 2016, more than 9 million metric tons were produced on a harvested area of 401862 Ha. Spain, with a production of 366161 metric tons, is the sixth world producer, and concentrates 95% of its total production in the province of Huelva, Southern Spain (FAOSTAT, www.fao.org/faostat). During the 2016-2017 season, ‘Fortuna’ was the main cultivar in Huelva (33.75%), followed by ‘Primoris’ (16.28%), ‘Rociera’ (10.058%) and ‘Rabida’ (9.989%) (Figure 1). It is worth noting that an important change took place, between the beginning of the 21st century, when ‘Camarosa’ was almost the unique cultivated cultivar in all the Huelva region, and the current situation, where every producer grows at least 4 or 5 different varieties. This increase in the number of cultivated varieties is a consequence of breeding programs developed in collaboration with producers, and prevents also production excess due to the monovarietal culture of strawberry (Medina-Minguez, 2017).

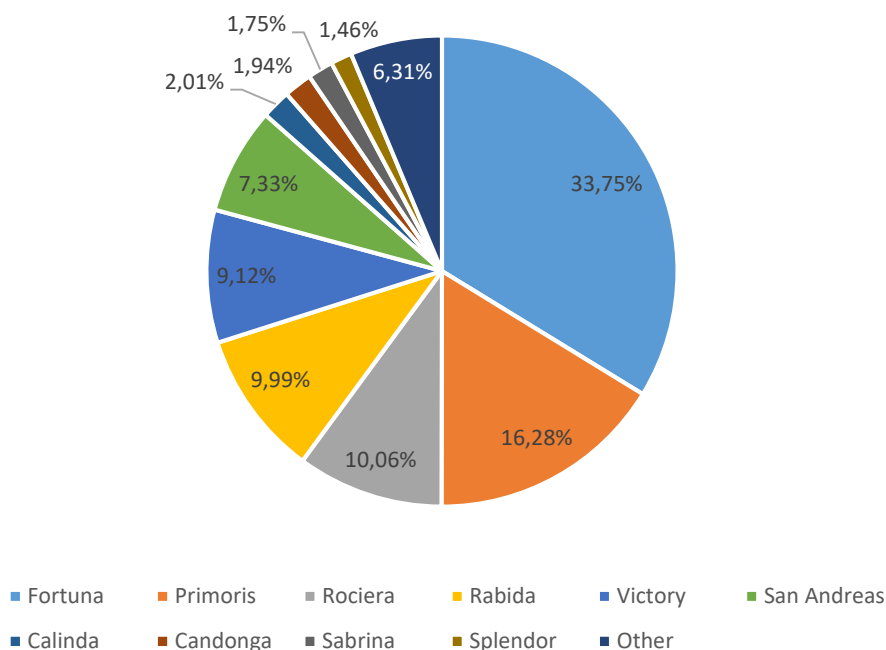


Figure 1: Cultivars grown in Huelva during 2016-17 season (adapted from Medina-Minguez, 2017).

The Rosaceae family

Strawberry belongs to the genus *Fragaria*, within the Family Rosaceae which comprises over 100 genera and 3000 species. It is the third most economically important plant family in temperate regions (Dirlewanger *et al.*, 2002) and includes important edible fruits, such as almond, apple, plum, peach, pear, raspberry, cherry or strawberry, and nonedible species with high ornamental value, such as rose. Phylogenetic analysis supported for the division of Rosaceae into three subfamilies, Dryadoideae, Rosoideae (including *Fragaria*) and Spiraeoideae. Patterns of diversification within the family Rosaceae suggested the use of different rosaceous species as reference genomic models. The best-developed model species include apple (*Malus x domestica*), peach (*Prunus persica*) and diploid strawberry (*Fragaria vesca*) (Shulaev *et al.*, 2008). The Genome Database for Rosaceae (GDR, www.rosaceae.org) was created as a repository of genetic and genomics data for the Rosaceae family (Jung *et al.*, 2008).

***Fragaria* genus**

Around 20 different species are included within *Fragaria* genus (Table 1), with a ploidy series ranging from diploid ($2n=2x=14$) to decaploid ($2n=10x=70$), converting the genus in a good model to study the evolution of polyploidy in angiosperms. In addition, the biological diversity of wild *Fragaria* has been used in breeding efforts as a source of novel genetic variation that can be introgressed into the cultivated strawberry (Chambers *et al.*, 2013). The distribution of *Fragaria* species occurs across a broad range of temperate habitats, in the northern hemisphere and disjunctly in southern South America, and molecular phylogenetic analyses consistently resolve two clades, the 'China clade' and the 'Vesca clade' (Liston *et al.*, 2014). Strawberry is normally a short-day plant, flowering in response to short-day lengths and low temperatures, even if day neutral forms have been identified in some species, including *F. vesca* and *F. x ananassa* (Battey *et al.*, 1998). Sex determination differs among species, being modern cultivars of *F. x ananassa* hermaphroditic (Hancock, 1999).

All *Fragaria* species are herbaceous perennials, capable of clonal growth via the production of runners (stolons) and have animal-dispersed fleshy ‘false’ fruits (Johnson *et al.*, 2014, Figure 2). The berry results from the development of the flower receptacle in which are embedded the real fruits, which are dry achenes. Each achene contains a single seed and a hard pericarp, which is attached to the receptacle by vascular strands (Perkins-Veazie, 1995). A coordinated development of seed maturation within the achenes and receptacle expansion and softening occurs during fruit growth and ripening.

The common cultivated species, *F. x ananassa* is one of the youngest domesticated plant. It is an octoploid ($2n=8x=56$), and originated by chance in Europe in the mid-18th century, as the result of a hybridization between two wild octoploid species, *F. virginiana* and *F. chiloensis* (Njuguna *et al.*, 2013). Recent study of Tennessen *et al.* (2014) suggested a *F. x ananassa* genomic formula of AABBB'B'B''B''', with four different subgenomes, one grouping with *F. vesca* (A) and three grouping with the Japanese diploid *F. iinumae* (B, B' and B''). A *F. vesca*-like diploid could have hybridized with a *F. iinumae*-like diploid to form an allotetraploid, which then hybridized with an unknown *F. iinumae*-like autotetraploid, forming the octoploid ancestor of *F. chiloensis* and *F. virginiana*. The octoploid subgenomes are highly diploidized and inheritance in octoploid *Fragaria* is basically disomic (Rousseau-Gueutin *et al.*, 2008), even if there is some evidence of a small amount of polysomic inheritance (Lerceteau-Köhler *et al.*, 2003).

The wild diploid strawberry *F. vesca* emerged as an attractive model for Rosaceae genomics due to several advantages it presents. It is a small plant, with a short generation time for a perennial, self-compatible and easy to propagate sexually and asexually (Slovin and Michael, 2011). *F. vesca* genetic manipulation was made possible by the development of transformation protocols (Oosumi *et al.*, 2006). In addition, strawberry fruit became a good model to study molecular mechanism of fruit development and non-climacteric ripening. Finally, *F. vesca* has a small genome (around 200 Mb), which shows a high macrosynteny and collinearity with the genome of the cultivated octoploid *F. x ananassa* (Rousseau-Gueutin *et al.*, 2008; Sargent *et al.*, 2009). Its available sequence turned the wild species into a reference for genomic and genetic

studies within the genus (Shulaev *et al.*, 2011; Tennessen *et al.*, 2014). A new assembly (Fragaria vesca Whole Genome v4.0.a1 Assembly & Annotation) is available in GDR since the beginning of the year (Edger *et al.*, 2018).

Table 1: *Fragaria* species with their ploidy levels and geographic distribution (adapted from Liston *et al.*, 2014; Tennessen *et al.*, 2014)

Species	Ploidy	Geographic distribution
<i>F. bucharica</i>	2x	Himalaya
<i>F. iinumae</i>		Japan
<i>F. mandschurica</i>		North China
<i>F. nilgerrensis</i>		Southeastern Asia
<i>F. vesca</i>		Europe, west of the Urals, North America
<i>F. nipponica</i>		Japan
<i>F. daltoniana</i>		Himalaya
<i>F. nubicola</i>		Himalaya
<i>F. pentaphylla</i>		North China
<i>F. viridis</i>		Europe and Asia
<i>F. yeozoensis</i>		Japan
<i>F. gracilis</i>	4x	Northwestern China
<i>F. corymbosa</i>		Northern China
<i>F. moupiensis</i>		Northern China
<i>F. orientalis</i>		Russia/China
<i>F. tibetica</i>		China
<i>F. x bringhyrstii</i>	5x	California
<i>F. moschata</i>	6x	Euro-Siberia
<i>F. chiloensis</i>	8x	Western North America, Hawaii and Chile
<i>F. virginiana</i>		North America
<i>F. x ananassa</i>		Cultivated worldwide
<i>F. iturupensis</i>	10x	Iturup Island, Kurile Islands



Figure 2: Morphology of *Fragaria* genus. a: crown, b and e: runners (stolons), c: axillary bud, d: daughter plant.

Fruit quality traits in strawberry

Quality traits can be defined by the organoleptic and the nutritional characteristics of the fruit. The organoleptic component is related to the overall impression perceived by the olfactory and taste systems, vision and tactile sensation. It includes aspects of the fruit such as flavor (taste and aroma), color and firmness. The nutritional component depends on the chemical composition of the fruit, which englobes compounds with healthy value and which are highly recommended for a balanced diet.

Strawberry fruit growth and maturation from anthesis to ripe stage encompasses a period of approximately 30 days, and can be divided visually into four stages: green, white, turning and red (Figure 3). The first stages correspond to the fruit growth by cell division and cell enlargement after the fertilization and

development of the ovary. They are accompanied by seed and embryo formation and maturation. Once the maturation of the embryo is almost completed, ripening of the receptacle occurs, with a series of physiological processes leading to increase the attractiveness of the fruit to animals (Gillaspy *et al.*, 1993; Aharoni and O'Connell, 2002; Fait *et al.*, 2008a). These physiological processes, together with events which occur during postharvest life of the fruit, contribute to the final quality of strawberry found in the market by the consumer.



Figure 3: Strawberry fruit growth and ripening stages (from Pott *et al.*, 2018). The developmental stages shown here are green, white, turning and red (from left to right).

Softening of the receptacle by cell wall degrading enzymes during ripening contribute to the texture of the fruit, which is one of the most important quality characteristics in breeding programs. The reduction of firmness starts at the white stage, and pectin depolymerization and solubilisation are the main mechanisms responsible for tissue softening (Nogata *et al.*, 1996; Rosli *et al.*, 2004; Osorio *et al.*, 2008; Molina-Hidalgo *et al.*, 2013; Paniagua *et al.*, 2016).

Achene and receptacle metabolism during ripening involves a series of changes leading to the conversion of high molecular weight precursors to smaller compounds which play a key role in seed development and dispersal. One of the important changes is the loss of green color and the increase of non-photosynthetic pigments, conferring the bright red color of the mature strawberry. Anthocyanins are responsible of the coloration of the ripe receptacle, being the two more abundant pigments pelargonidin-3-O-glucoside (92%) and cyanidin-3-O-glucoside (4%) (Bakker *et al.*, 1994; Griesser *et al.*, 2008). They are polyphenol compounds, synthesized via the phenylpropanoid and flavonoid pathways,

together with a multitude of metabolites involved in the nutritional characteristics of the fruit (Tulipani *et al.*, 2009).

Metabolites present in the receptacle, mainly sugars, amino and organic acids, as a consequence of the central carbohydrate metabolism of the plant (primary metabolism), play a key role in the overall taste of the fruit. Sweetness, determined by the total sugar content and by the ratios among those sugars, is the key character determining fruit flavor and quality (Vandendriessche *et al.*, 2013). The main sugars in strawberry fruit are glucose, fructose and sucrose, and their content increase significantly during ripening (Hancock, 1999; Fait *et al.*, 2008a; Crespo *et al.*, 2010). Another important parameter in flavor perception, is the acidity of the fruit, which is related to the content of organic acids, being citrate and malate the most abundant in strawberry fruits. Malate content shows an increase during ripening, while citrate content remains steady throughout development (Fait *et al.*, 2008a). It has been demonstrated that a high ratio between sugars and organic acids is a major determinant of the acceptance of the fruit by consumers (Zhang *et al.*, 2011). In addition, sugars, amino and organic acids are precursors for volatiles and other secondary metabolites involved in the aroma, color and nutritional traits ((Vandendriessche *et al.*, 2013, Figure 4).

While taste depends mainly on sugars/acids ratio (Kallio *et al.*, 2000), the delicate strawberry aroma perceived by the olfactory system is consequence of the complex pattern of volatile organic compounds (VOCs) emitted by the fruit (Klee, 2010). More than 360 VOCs have been identified in strawberry, varying among different species within *Fragaria* and displaying a strong developmental and environmental regulation. However, it is thought than less than 20 compounds contribute significantly to the aroma (Schieberle and Hofmann, 1997; Ulrich *et al.*, 2007; Olbricht *et al.*, 2011; Ulrich and Olbricht, 2013; Schwieterman *et al.*, 2014). Furanones and esters are considered the dominating aroma compounds, together with linalool, γ -decalactone, 2,3-butanedione, alcohols and aldehydes (Jetti *et al.*, 2007). Several enzymes responsible of the biosynthesis of these compounds have been previously identified, even if the genetic mechanisms underlying these pathways are still broadly unknown (Lunkenbein *et al.*, 2006;

Raab *et al.*, 2006; Chambers *et al.*, 2014; Sánchez-Sevilla *et al.*, 2014; Song *et al.*, 2016).

Strawberry is also very appreciated for its nutritional quality. Indeed, it contains carotenoids, vitamin A, vitamin E, vitamin K, thiamin, riboflavin, niacin, vitamin B6, and it is a particularly rich source of ascorbic and folic acids (Tulipani *et al.*, 2008, 2009; Giampieri *et al.*, 2015). Moreover, phenolic compounds, the main class of secondary metabolites found in strawberry fruit, convert it to an indispensable source of phytochemicals. Polyphenols, synthesized via the phenylpropanoid pathway, show antioxidant, anti-inflammatory, antihypertensive and antiproliferative abilities in human (Hannum, 2004; Giampieri *et al.*, 2012, 2015; Mazzoni *et al.*, 2016). In addition, new studies demonstrated that phenols could regulate the activity of transcription factors involved in cellular metabolism and survival, even if more *in vivo* research is needed (Forbes-Hernandez *et al.*, 2016).

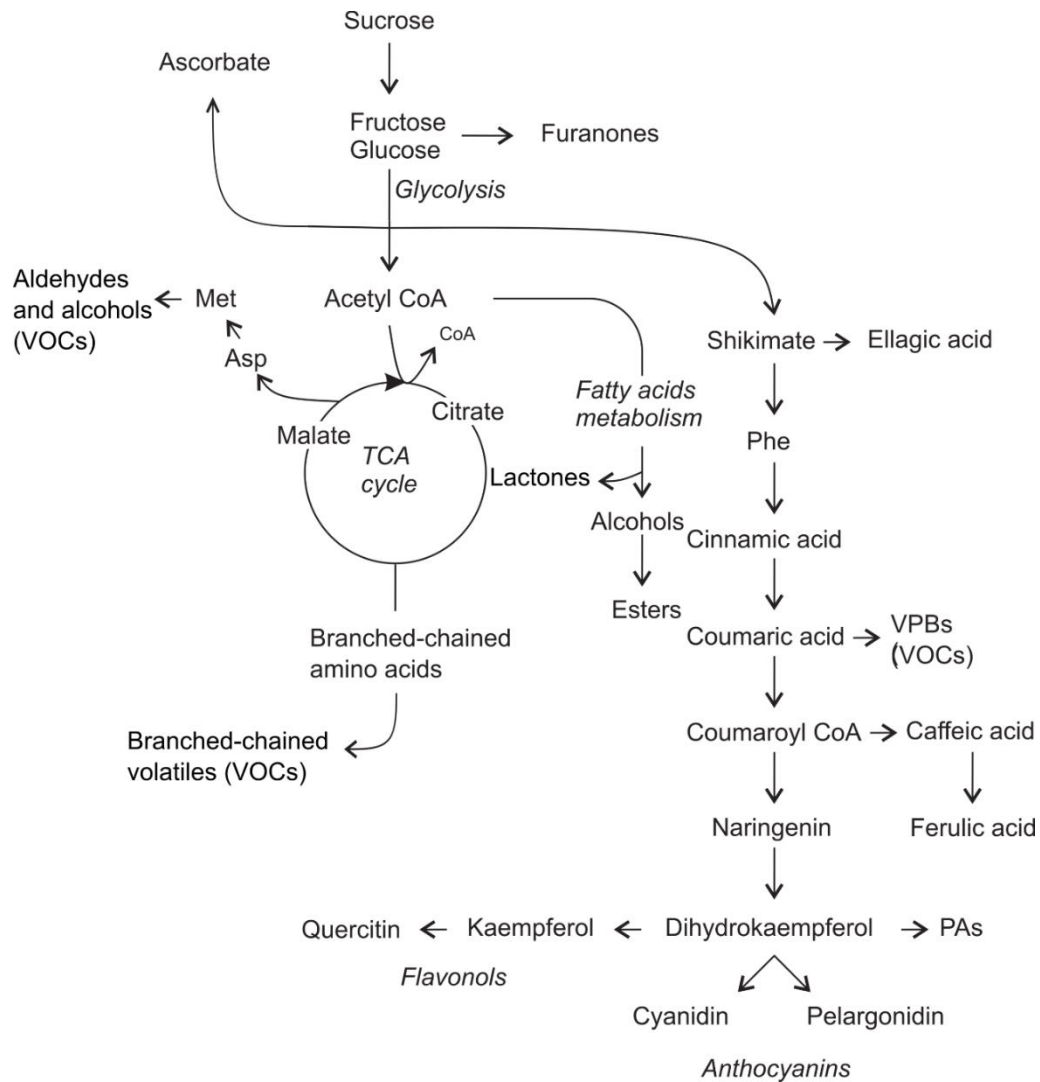


Figure 4: General overview of primary and secondary metabolism in strawberry fruit (from Pott *et al.*, 2018). VPBs: volatiles phenylpropanoids and benzenoids; PA: proanthocyanidins.

Postharvest

Postharvest life of the fruit also influences fruit quality traits and organoleptic characteristics. Strawberry fruit is especially sensitive to postharvest conditions, having a high rate of respiration and being susceptible to water loss and mechanical damage. They are also vulnerable to fungal deterioration. Unlike many other fruits, they are harvested fully ripe, resulting in a shorter shelf life (Feliziani and Romanazzi, 2016).

Commercially, different postharvest treatments are used, in order to delay ripening and senescence, to prevent pathogen growth and increase shelf life. These procedures include low temperature, controlled atmosphere or chemical treatments, being the first one the most commonly applied (Pedreschi and Lurie, 2015).

In strawberry, studies have demonstrated that cold storage during postharvest life decreases the loss of soluble solids observed (Ayala-Zavala *et al.*, 2004; Li *et al.*, 2015). Both storage time and temperature have a significant effect on organic acids, ascorbate, phenolic compounds and volatiles (Forney *et al.*, 2000; Ayala-Zavala *et al.*, 2004; Koyuncu and Dilmaçunal, 2010; Piljac-Žegarac and Šamec, 2011; Li *et al.*, 2015).

Controlled atmosphere is another strategy used to delay senescence during postharvest. It has been seen that strawberry total acidity decreases during storage period, but controlled atmosphere (2% O₂ and 12% CO₂) can delay this decrease, and consequently postpone loss of postharvest quality (Li *et al.*, 2016). In addition, it seems that controlled atmosphere leads to an overall higher concentration of volatiles than low temperature treatment (Li *et al.*, 2015).

Analysis of the fruit metabolome

As mentioned above, a wide range of metabolites is responsible of the organoleptic and nutritional characteristics of the fruit. Even if important technical advances in the metabolomics platforms have been made recently, none is able to provide complete coverage of all classes of metabolites in a single separation. There are two types of platforms used for metabolome analysis: mass spectrometry (MS) and nuclear magnetic resonance (NMR). MS instruments are very sensitive and can be used in combination with separation techniques, such as gas (GC) and liquid chromatography (LC), allowing the analysis of complex biological extracts (Dettmer *et al.*, 2007).

LC-MS is the most widely applied platform for the targeted profiling of both polar and non-polar compounds, followed by GC-MS, which is most often used for the analysis of volatile metabolites, or those that can be made volatile by chemical derivatization (Begou *et al.*, 2017).

GC-MS is a standard technology for the detection of small plant metabolites, such as sugars, amino and organic acids (primary metabolites), due to a series of advantages. It presents reproducible chromatography, high separation efficiency, good sensitivity and a standardized electron ionization method, which allows the establishment of mass spectral libraries (Fiehn *et al.*, 2008). The analysis of polar primary metabolites requires a step of derivatization to reduce polarity and increase volatility. To obtain broad coverage of the metabolome, a two-step derivatization procedure including methoximation followed by silylation is often used (Jonsson *et al.*, 2004). Mass analyzers for GC-MS commonly used are quadrupole or time-of-flight (TOF) instruments (Roessner *et al.*, 2001; Stewart *et al.*, 2015).

GC-MS is also the reference analytical method for volatiles detection. It is coupled with HS-SPME which allows to lower the detection limits. A silica fiber, coated with a polymeric phase is mounted on a syringe device, allowing the adsorption of the volatiles in the fiber until an equilibrium phase is reached. Headspace extraction protects the fiber from the nonvolatile compounds present in the matrix (Azzi-Achkouty *et al.*, 2017). SPME-GC-MS provides many advantages such as it is easily automatized, simple to manage, inexpensive to workup, and do not use organic solvents. The success of its use depends on factors such as the chemical nature of the compounds to be extracted, the temperature used during extraction, extraction time, and amount of added salts to enhance volatility (Moreira *et al.*, 2016).

Reverse phase liquid chromatography is a standard tool for the separation of semi-polar metabolites, and ultraperformance liquid chromatography increases chromatographic resolution and peak capacity. To obtain a broad coverage of the metabolome, ionization must be performed in positive and negative mode (Dettmer *et al.*, 2007). LC-MS is the method of choice for qualitative and quantitative analysis of polyphenol compounds (Motilva *et al.*, 2013). LC can also be coupled to tandem MS (MS/MS), which involves a fragmentation of the precursor ion to product ions which are detected in a second stage of mass spectrometry and which helps structural identification. Orbitrap mass analyzer is one of the choice instrument in LC-MS, as it shows high resolution, high mass accuracy and good dynamic range (Perry *et al.*, 2008; Ernst *et al.*, 2014).

Table 2: Advantages and disadvantages of hyphenated mass spectrometry methods (adapted from Ernst *et al.*, 2014).

	Advantages	Disadvantages
GC-MS	Analysis of low molecular weight Hydrophobic compounds can be directly analysed Volatile compounds can be directly analysed Electron ionization is very robust and reproducible Databases available There is no ion suppression	Derivatisation is required for non-volatile compounds Derivatisation can mask the result Not suitable for non-volatile or thermo-unstable compounds
LC-MS	Much wider range of metabolites Suitable for analysis of relatively polar compounds with low or high molecular weights Derivatisation is not required Thermo-unstable compounds can be analysed	Fragmentation patterns are poorly reproducible No databases available Possible ion suppression

Breeding for quality traits

Since the beginning of agriculture, human beings have been selecting favorable traits, such as yield, fruit size or color, in order to obtain superior plant phenotypes and to suit the needs of farmers and consumers. This process is known as plant breeding and has been globally successful, with the introduction of hybrid maize (*Zea mays*), wheat (*Triticum aestivum*) and rice (*Oryza sativa*). Molecular plant breeding integrates advances in biotechnology, molecular marker applications and genomics with traditional breeding. Molecular marker systems were developed to create high-resolution genetic maps and use genetic linkage between markers and important crop traits (Paterson *et al.*, 1988). Since the beginning of 1980s, important efforts have been made to develop molecular markers such as random-amplified polymorphic DNAs (RAPD), amplified fragment length polymorphisms (AFLP), simple sequence repeats (SSR) or single nucleotide polymorphisms (SNP).

Marker-assisted selection (MAS) has allowed breeders to drive the selection of genomic regions involved in the expression of traits of interest (Grover and Sharma, 2016). In addition, MAS can be used in association with backcrossing for the introgression of a gene of interest in elite genotypes, when targeted traits are controlled by one or a few loci (Moose and Mumm, 2008). Together with the recent advances of next generation-sequencing, SNP markers have allowed the development of genome wide association studies, enabling the identification of linkage between SNP and traits of interest (Fu *et al.*, 2017b).

Traditionally, breeders focused on yield, disease resistance and firmness, which are essential traits for transportation, long-term storage and external appearance. Breeding for fruit quality characteristics have been neglected because of its complexity. Indeed, flavor phenotyping is expensive and not adaptable to high-throughput analysis. Most quality traits are genetically complex, with polygenic inheritance. Their regulation varies greatly between different species or varieties, and they are subject to environmental variation (Carbone *et al.*, 2009; Sánchez *et al.*, 2014; Tieman *et al.*, 2017).

Quantitative Trait Loci (QTL) analysis

As most agronomic and quality traits are quantitatively inherited, and their expression is controlled by many quantitative trait loci (QTL), mapping studies have to be conducted to detect these QTL with the help of molecular markers. A QTL can be described as a genomic region hypothetically responsible for quantitative genetic variation of a trait where the allelic variation of a *locus* is associated with the variation of the trait (Collard *et al.*, 2005; Würschum, 2012).

In addition, quantitative phenotypic variation of a trait can be associated with environmental factors, and thus can be described as followed (Tanksley, 1993):

$$V_P = V_G + V_E$$

where V_P is the phenotypic variance and has been divided into components of genetic (V_G) and environmental (V_E) variances. The ratio between V_G and V_E results in the broad sense heritability (H^2) and described the degree of phenotypic variance explained by genetic factors.

Previous to QTL mapping, it is necessary to obtain a genome-wide set of polymorphic markers and a mapping population that shows heritable variation for quantitative traits. Both genotyping for molecular markers and phenotyping for the traits of interest the whole population are needed to perform QTL analysis. Traditionally, QTL detection started with linkage mapping in populations which derive from the cross between phenotypically divergent lines (Würschum, 2012; Phan and Sim, 2017).

Several statistical methods have been developed to locate QTL, based on the non-random association, also called *linkage disequilibrium*, between QTL and markers. Single-marker analysis, simple interval mapping (SIM) and multiple QTL models are the most frequently used methods (Tanksley, 1993; Liu, 1998; Doerge, 2002).

For single-marker analysis, statistical tests such as the nonparametric test of Kruskal-Wallis (Lehman, 1975) are applied, calculating whether phenotype values differ among genotypes for a given molecular marker. Significant differences suggest a linkage between phenotype and the given marker. It is the easiest method for QTL mapping, and simple statistical software can be used. However, the method presents some limitations. First, it does not provide a good estimation of the QTL position, and secondly the QTL effects can be underestimated due to recombination between marker and QTL (Collard *et al.*, 2005).

SIM requires a linkage map to be constructed, and simultaneously analyses intervals between adjacent pairs of linked markers to locate QTL. As a consequence, both the position and the size of the QTL effect are estimated more accurately. At each tested position along the chromosome, SIM method calculated a LOD score, which indicates the probability to find a QTL at that position. Only the LOD scores which exceed a threshold significance level suggest the presence of a QTL in that genomic region. The threshold significance level is calculated with a permutation test (Churchill and Doerge, 1994). Even if the most likely position of the QTL is the one at which the highest LOD score is found, confidence intervals are calculated where QTL can actually occur. The simplest way to estimate confidence intervals is to calculate 1-LOD and 2-LOD

intervals, which correspond to the regions on both sides of the QTL peak corresponding to a decrease of one and two LOD scores respectively (Lander and Botstein, 1989). In addition, the percent of phenotypic variation explained by a QTL is calculated with SIM. It informs about the importance of a single QTL on the trait of interest (Lander and Botstein, 1989; Hackett, 2002). The main limitation of SIM is that it ignores the effects of QTL at other positions.

To overcome SIM constraints, multiple QTL models have been developed, including composite interval mapping (Zeng, 1993, 1994) and multiple QTL mapping (Jansen, 1993; Jansen and Stam, 1994). These methods combine interval mapping with multiple regression. A set of cofactors, which are markers linked to other QTL, are incorporated into the model, allowing to reduce the background noise which affects QTL detection.

Linkage maps in strawberry

The first linkage map of octoploid strawberry was constructed using AFLP markers by Lerceteau-Köhler *et al.* (2003). Strategy in the construction of linkage maps in polyploid species depends on chromosome pairing behavior (disomic or polysomic) at meiosis (Osborn *et al.*, 2003). Rousseau-Gueutin *et al.* (2008) did comparative mapping in diploid and octoploid strawberry genomes, and showed that the octoploid genome was organized in seven homoeologous groups (HG) corresponding to the seven linkage groups (LG) present in the diploid genome and to the base chromosome number of $x = 7$ in *Fragaria* genus. As mentioned above, the comparative mapping revealed high levels of macrosynteny and collinearity between diploid and octoploid genomes. Several maps were developed for QTL mapping and comparative studies in *F. x ananassa* or other strawberry wild species (Weebadde *et al.*, 2008; Spigler *et al.*, 2010; Zorrilla-Fontanesi *et al.*, 2011). However, they are low-density genetic maps which contain different marker types, hindering comparisons between studies. The release of *F. vesca* genome in 2011 by Shulaev *et al.* permitted the characterization of thousands of SSR markers which have been used for the development of extensive linkage maps of the cultivated strawberry (Sargent *et al.*, 2012; Isobe *et al.*, 2013; Dijk *et al.*, 2014).

A whole genome genotyping array (Axiom® IStraw90® array) was developed for the octoploid strawberry (Bassil *et al.*, 2015), containing more than 90K well-defined SNP distributed across the 28 linkage groups of the octoploid genome. This tool enables rapid linkage map construction for QTL analysis (Sargent *et al.*, 2016; Verma *et al.*, 2017). Nevertheless, the cost per sample is relatively high and the reliance on the *F. vesca* reference genome for SNP discovery has led to a preference towards markers in the *F. vesca*-derived sub-genome compared to the other 3 sub-genomes (Sánchez-Sevilla *et al.*, 2015; Sargent *et al.*, 2016). As a cheaper alternative to Axiom® IStraw90® array, Sánchez-Sevilla *et al.* (2015) developed two platforms based on the implementation of Diversity Array Technology (DArT) markers. The second platform, taking benefit from the development of next-generation sequencing, was used to develop a high-density genetic map of the *F. x ananassa* '232' x '1392' population, which was applied for the QTL analysis of chapters 2 and 3 of this thesis. 2089 markers were positioned in the consensus '232' x '1392' linkage map, providing high coverage of the genome in the 7 HG. A total of 33 LG were obtained, corresponding to the full complement of the 28 strawberry chromosomes.

QTL analysis for fruit quality traits

Even if QTL mapping in strawberry and other crops have traditionally been focused on traits such as yield and disease resistance, several studies have been focused on QTL related to fruit quality characteristics. Zorrilla-Fontanesi *et al.* (2011) published the first study for quality traits in strawberry such as soluble solid content, titratable acidity, ascorbic acid content, fruit color and firmness. They used a F₁ mapping population developed in the *Instituto de Investigación y Formación Agraria y Pesquera* (IFAPA, Churriana, Malaga, Spain) during the year 2004 and which derives from the intraspecific cross between two parental lines, '232' and '1392', selected for their contrasting phenotype regarding agronomical and fruit characteristics. '232' (Sel 4-43 x 'Vilanova') is a very productive strawberry line, while '1392' ('Gaviota' x 'Camarosa') presents firm fruits with high levels of sugars, acids, anthocyanins, and ascorbic acid. A total of 33 QTL were detected in 1-3 years controlling yield, fruit size and quality traits. 36.4% of the QTL were stable over 2 or 3 years. In addition, they could identify

candidate genes related to ascorbic acid metabolism in three QTL detected for this compound. Additionally, a fruit specific expansin, *FaEXP2*, was found in a QTL for fruit firmness in LG VII-1. The volatile profile of the '232' x '1392' population was also analyzed by GC-MS, and QTL mapping allowed to identify 70 QTL related to aroma content (Zorrilla-Fontanesi *et al.*, 2012). Two genes, *FaOMT* and *FaFAD1*, were identified within QTL intervals, controlling the content of key odorant volatiles such as mesifurane and γ -decalactone, respectively (Zorrilla-Fontanesi *et al.*, 2012; Sánchez-Sevilla *et al.*, 2014). A combination of metabolomics and transcriptomics techniques validated the results obtained from the QTL analysis, and a PCR test was developed based on the two genes to predict the presence of mesifurane and γ -decalactone in strawberry cultivars (Cruz-Rus *et al.*, 2017).

Other F_1 populations of *F. x ananassa* were used to perform QTL mapping for quality traits, such as anthocyanins, soluble solid content or titratable acidity (Lerceteau-Köhler *et al.*, 2012; Castro and Lewers, 2016). Interestingly, in the three studies including similar quality traits, QTL were identified in approximately the same HG, indicating that common *loci* could be responsible of the phenotypic variation in different genotypes (Zorrilla-Fontanesi *et al.*, 2011; Lerceteau-Köhler *et al.*, 2012; Castro and Lewers, 2016; Pott *et al.*, 2018). Furthermore, clusters of QTL for correlated traits (*i.e.* total phenolics with antioxidant capacity or anthocyanins with color) were detected in the three studies. Finally, the variation of the phenotype explained by individual QTL was generally below 20%, confirming the complexity and quantitative nature of quality traits, and the influence of the environment.

A recent study using pedigree-based QTL analysis, which allows QTL evaluation in numerous genetic backgrounds, clarified the sub-genomic positions within the HG of previously identified QTL for soluble solid content and pH (Verma *et al.*, 2017).

Ring *et al.* (2013) identified *FaPRX27*, a putative peroxidase involved in lignin formation during fruit ripening, by combining transcriptomics analysis with metabolite profiling in different varieties of strawberry. QTL mapping in two different populations confirmed the role of the peroxidase, as QTL were detected

for fruit color decrease and for several phenolic compounds and flavonoids in the same region where *FaPRX27* is located. The results of this study seem to indicate a competition between lignin and anthocyanins synthesis for common precursors in the phenylpropanoid pathway.

Another study focusing in fruit texture identified a putative rhamnogalacturonate lyase gene, *FaRGlyase1*, involved in pectin degradation during ripening. The gene was mapped in a F2 population and co-localized with a QTL for fruit firmness (Molina-Hidalgo *et al.*, 2013).

QTL mapping in the wild species *F. vesca* was also performed using a near-isogenic line (NIL) collection developed by Urrutia *et al.* (2015a,b). A NIL is identical to an original genotype (*F. vesca* in this case), except for a single DNA introgressed fragment from a donor line (*F. bucharica*). Differences between the phenotypes of the NIL collection and the original genotype can be attributed to genetic factors in the introgressed fragment, and is a powerful tool for QTL identification (Monforte *et al.*, 2001). 7 QTL for nutritional traits such as sugar composition and total polyphenol content were detected (Urrutia *et al.*, 2015a). Further studies combining metabolomics techniques with QTL mapping allowed the identification of 76 and 50 QTL for polyphenols and volatiles respectively (Urrutia *et al.*, 2015b, 2017). LG5 and LG7 seem to be the most determinant regions controlling volatile synthesis, as they accumulate the largest number of QTL and some of the detected QTL were in agreement with those described in *F. x ananassa* '232' x '1392' population by Zorrilla-Fontanesi *et al.* (2012).

QTL analysis for fruit quality traits have also been conducted in other economically-important fruits, such as apple (*M. x domestica*, Ma *et al.*, 2016), peach (*P. persica*, Zeballos *et al.*, 2016), melon (*Cucumis melo*, Argyris *et al.*, 2017), sweet orange (*Citrus sinensis*, Curtolo *et al.*, 2017), tomato (*Solanum lycopersicum*, Capel *et al.*, 2017) or pepper (*Capsicum annuum*, Popovsky-Sarid *et al.*, 2017) for example.

Recent development of high throughput metabolomics techniques allows the concomitant identification of a wide range of metabolites which are directly involved in taste, aroma and nutritional characteristics of the fruit (Osorio *et al.*, 2012). This is a powerful tool for the characterization of cultivars, and, together

with QTL mapping, can provide useful knowledge about the genetic determinants of fruit quality traits.

Schauer *et al.* (2006) accurately quantified 74 primary metabolites by GC-MS in tomato introgression lines (IL) of the wild species *S. pennellii* in the commercial tomato *S. lycopersicum* (Eshed and Zamir, 1995). 889 QTL were then identified for the content of primary metabolites, which include sugars, sugar alcohols, amino, organic and fatty acids. The same IL were used to map QTL for secondary metabolite content (Alseekh *et al.*, 2015). 43 metabolites were detected by liquid chromatography-mass spectrometry (LC-MS) and 679 QTL were found to be responsible for the content of these metabolites. Other studies in tomato, pepper and apple coupled secondary metabolite profiling by LC-MS with QTL mapping (Khan *et al.*, 2012; Wahyuni *et al.*, 2014; Ballester *et al.*, 2016).

Volatiles can be detected and quantified by GC-MS coupled with headspace solid-phase microextraction (HS-SPME) and several studies took advantage of this technique to map QTL for volatile content in apple (Dunemann *et al.*, 2012; Yauk *et al.*, 2015), peach (Sánchez *et al.*, 2014), strawberry (Zorrilla-Fontanesi *et al.*, 2012; Urrutia *et al.*, 2017) or tomato (Zanor *et al.*, 2009).

Aims

1. To identify QTL for the content of primary and secondary metabolites (mQTL) and underlying candidate genes involved in the organoleptic and nutritional characteristics of the cultivated strawberry (*F. x ananassa*), using the IFAPA F₁ '232' x '1392' mapping population.
2. To identify genomics and metabolomics factors involved in the regulation and the loss of organoleptic and nutritional characteristics during the postharvest life of five commercial varieties of strawberry.

Chapter 2: Identification of Quantitative Trait Loci (QTL) and Candidate Genes for Primary Metabolite Content in Strawberry Fruit

The work presented in this chapter has been published as: **Vallarino, JG[#], Pott, DM[#], Cruz-Rus, E, Miranda, L, Medina-Minguez, JJ, Fernie, AR, Sánchez-Sevilla JF, Osorio S*, Amaya, I*** 2018. *Horticulture Research* (2019) 6:4.

DOI: 10.1038/s41438-018-0077-3.

[#]These authors contributed equally to this work. *Corresponding authors

ABSTRACT

Abstract Improvement of nutritional and organoleptic quality of fruits is a key goal in current strawberry breeding programs. The ratio of sugars to acids is a determinant factor contributing to fruit liking, although different sugars and acids contribute in varying degrees to this complex trait. A segregating F1 population of 95 individuals, previously characterized for several fruit quality characters, was used to map during 2 years quantitative trait loci (QTL) for 50 primary metabolites, L-ascorbic acid (L-AA) and other related traits such as soluble solid content (SSC), titratable acidity (TA), and pH. A total of 133 mQTL were detected above the established thresholds for 44 traits. Only 12.9% of QTL were detected in the 2 years, suggesting a large environmental influence on primary metabolite content. An objective of this study was the identification of key metabolites that were associated to the overall variation in SSC and acidity. As it was observed in previous studies, a number of QTL controlling several metabolites and traits were co-located in homoeology group V (HG V). mQTL controlling a large variance in raffinose, sucrose, succinic acid, and L-AA were detected in approximate the same chromosomal regions of different homoeologous linkage groups belonging to HG V. Candidate genes for selected mQTL are proposed based on their co-localization, on the predicted function, and their differential gene expression among contrasting F1 progeny lines. RNA-seq analysis from progeny lines contrasting in L-AA content detected 826 differentially expressed genes and identified Mannose-6-phosphate isomerase, FaM6PI1, as a candidate gene contributing to natural variation in ascorbic acid in strawberry fruit.

Chapter 3: Quantitative Trait Loci and Underlying Candidate Genes Controlling Secondary Metabolites in Strawberry Fruit

Introduction

Secondary metabolites in strawberry fruit

Strawberry, along with other fruits, has a rich composition in secondary metabolites, which are involved in several important physiological processes, such as fruit pigmentation, auxin transport regulators, male fertility and biotic and abiotic stress responses (*i.e.* defense against pathogens or UV protection) (Winkel-Shirley, 2001; Coberly and Rausher, 2003; Lepiniec *et al.*, 2006; Thompson *et al.*, 2010). Some of them are exuded by plant roots and are able to promote symbiotic association by modifying the transcriptional activity of nodulation genes (Kobayashi *et al.*, 2004; Mandal *et al.*, 2010).

Polyphenolic compounds are the most abundant class of secondary metabolites present in strawberry fruits, converting them in one of the most important dietary sources of phytochemicals, together with their high content of fat-soluble vitamins, carotenoids, vitamin C, folate and thiamin. Compared with other fruits, strawberry fruit possesses high *in vitro* antioxidant activity, which positively correlates with the content of polyphenolic compounds and vitamin C (Wang and Lin, 2000; Tulipani *et al.*, 2008). In addition, studies in animals and humans have shown that polyphenols have anti-inflammatory, antimicrobial, anti-allergy, and anti-hypertensive properties. They also have the ability to prevent oxidative stress-related diseases by inhibiting the activities of some physiological enzymes and receptors (Wang *et al.*, 1996; Parelman *et al.*, 2012; Alvarez-Suarez *et al.*, 2014; Giampieri *et al.*, 2015; Forbes-Hernandez *et al.*, 2016).

Among polyphenols, flavonoids represent the most abundant class, composed mainly by anthocyanins, and, in a lesser extent, by flavonols, flavanols and proanthocyanidins (condensed tannins) (Giampieri *et al.*, 2015). Anthocyanins play a key role in fruit quality trait, as they are responsible of the color of the mature fruit. More than 25 different anthocyanins have been described in different cultivars of strawberry, even if two common pigments seem to be found in all varieties, independently of genetic and environmental factors, named as pelargonidin 3-glucoside as the major pigment and confers an orange to red

color, and cyanidin 3-glucoside is a minor pigment, giving a darker magenta to purple color to the fruit (da Silva *et al.*, 2007). Flavonols are present in strawberry as derivatives of quercetin and kaempferol. Flavanols are commonly found in strawberry flesh and achenes in monomeric (catechin and epiafzelechin) and polymeric forms, forming proanthocyanidins (PAs) (Giampieri *et al.*, 2012, 2015).

Hydrolyzable tannins, hydroxycinnamic and hydroxybenzoic acid derivatives are other important classes of polyphenolic compounds. Hydrolyzable tannins are formed by ellagitannins and gallotannins. They are composed by different combinations of gallic acid and hexahydrodiphenic acid with glucose. They range from simple sugar conjugates to oligomers and complex polymers, which, upon acid hydrolysis, release ellagic acid. The most common ellagitannin in strawberries and raspberries is sanguin H-6 and Mullen *et al.* (2003) reported the presence of hexahydroxydiphenoyl (HHDP)-glucose, which forms the basic unit of many ellagitannins, such as sanguin H-6 or lambertianin C.

The most common hydroxycinnamic acid derivatives are *p*-coumaric, caffeic and ferulic acids, and they normally occur in foods as simple esters with quinic acid or glucose (Mattila and Kumpulainen, 2002).

Synthesis of polyphenol compounds

Polyphenols are synthesized through the phenylpropanoid pathway, which gives rise to a huge range of secondary metabolites, including lignin, suberin or condensed tannins which contribute to the robustness of angiosperms and gymnosperms. Phenylpropanoid pathway derives from the shikimate pathway, and lyases connect aromatic amino acids (phenylalanine and tyrosine) to the synthesis of phenylpropanoid compounds (Figure 1; Vogt, 2010). Phenylalanine ammonia lyase (PAL) catalyzes the deamination of phenylalanine to cinnamic acid and is the gateway enzyme to the synthesis of phenols, directing carbon flow from primary to secondary metabolism (Vogt, 2010). The three initial steps, catalyzing by PAL, cinnamate-4-hydroxylase (C4H) and 4-coumaroyl CoA-ligase (4CL), are necessary to the formation of phenylpropanoid monomers which supply the basis for all resulting phenolic compounds. The formation of 4-coumaroyl CoA represents a decisive branchpoint within the pathway, providing

a direct precursor for lignin or flavonoid synthesis. In strawberry fruit, flavonoid pathway starts with the formation of naringenin catalyzed by chalcone synthase (CHS) and chalcone isomerase (CHI), a two-step condensation of four coumaroyl CoA units with three malonyl CoA. Naringenin is a flavanone and the first molecule presenting a flavan nucleus, which is a three-ring structure shared by all flavonoids (Casañal *et al.*, 2013; Petrusa *et al.*, 2013). Dihydroflavonols, such as dihydrokaempferol and dihydroquercetin are synthesized from naringenin, which, in turn, can be converted to anthocyanidins, which are colorless and unstable pigments.

Anthocyanidins, such as leucopelargonidin and leucocyanidin, are then oxidized to the pigments cyanidin and pelargonidin, responsible of the color of the fruit (Petrussa *et al.*, 2013). The final products of anthocyanins and flavonols synthesis accumulate in the vacuole or are secreted into the apoplastic space, as *O*-glycosyl derivatives. The reduction of leucocyanidin or cyanidin by leucocyanidin reductase (LAR) or anthocyanidin reductase (ANR) yields catechin and epicatechin respectively. Formation of PAs occurs by the addition of leucocyanidin molecules to the terminal unit of catechin or epicatechin (Bogs, 2005).

Hydroxycinnamic acid derivatives are mainly formed from coumaric, caffeic and ferulic acids in strawberry fruits. C4H converts cinnamic acid to *p*-coumaric acid in the second step of the phenylpropanoid pathway, while *p*-hydroxycinnamoyl-CoA: quinate shikimate *p*-hydroxycinnamoyltransferase (HCT) catalyzes the formation of caffeic acid from coumaric acid, and caffeic acid/5-hydroxyferulic acid *O*-methyltransferase (COMT) the formation of ferulic acid from caffeic acid (Mouradov and Spangenberg, 2014). Hydroxybenzoic acid derivatives and other benzoic acids also derive from hydroxycinnamic acids (Widhalm and Dudareva, 2015).

Very little information is known about ellagitannin and gallotannin polyphenols biosynthesis (Schulenburg *et al.*, 2016). Gallic acid, which forms the core structure of this class of compounds, is likely formed by dehydrogenation of 5-dihydroshikimate (Werner *et al.*, 2004). A recent study identified two shikimate dehydrogenases in grape involved in the formation of gallic acid from 5-

dihydroshikimate (Bontpart *et al.*, 2016). Gallic acid is then esterified with a molecule of UDP-glucose to form β -glucogallin by a glucosyltransferase. β -glucogallin is the first specific metabolite in the pathway of soluble tannins. Schulenburg *et al.* (2016) identified several glycosyltransferases able to catalyze the formation of β -glucogallin in *Fragaria* and *Rubus* genera. The hydroxyl groups of the glucose can be further esterified with other galloyl residues, until obtaining a molecule of pentagalloylglucose. Complex gallotannins are formed by the addition of further galloyl residues to pentagalloylglucose. Alternatively, pentagalloylglucose can be oxidized to yield HHDP moieties and form ellagitannins, the other class of soluble tannins (Niemetz and Gross, 2005).

Changes in polyphenol content affected by fruit ripening and environmental conditions

Polyphenol content in strawberry fruits is strongly affected by genetic, developmental and environmental factors (Fait *et al.*, 2008b; Tulipani *et al.*, 2008).

During growth and ripening, the fruit exhibits important dynamic fluctuations in secondary metabolites. In unripe fruits (green fruit), large amounts of catechin, epicatechin and derived PAs are accumulated (Macheix and Fleuriet, 1993). Halbwirth *et al.* (2006) observed two activity peaks during fruit ripening for most of the enzymes involved in flavonoids synthesis. The first activity peak in immature fruit coincides with the levels of flavanols and PAs. In the later stage of fruit ripening, a redirection of flavonoid biosynthesis is observed from flavanols and PAs to flavonols and anthocyanins (Fait *et al.*, 2008).

The major accumulation of β -glucogallin peaks at the early stage of achenes and receptacle ripening, and decrease towards ripe stage of the fruit, similar to the trend observed with the condensed tannins. It is known that tannins are defense compounds against pathogens (Silva *et al.*, 1997). Moreover, astringent and antimicrobial compounds are possibly accumulated during the initial growth of the fruit to offer protection against bacteria, fungi or animals, while the decrease of tannins levels at the ripe stage (and the concomitant decrease of astringency) and the parallel increase of anthocyanins and flavonols may enhance the attractiveness of the fruit to seed dispersers (Schulenburg *et al.*, 2016).

Even if genotype is the predominant factor regarding differences in polyphenol content between strawberry cultivars, environment also affects the composition in secondary metabolites of the fruit. In particular, several studies highlighted the influence of environmental factors on the accumulation of flavonols in strawberry fruits (Carbone *et al.*, 2009; Urrutia *et al.*, 2015b). In addition, Carbone *et al.*, (2009) observed that epicatechin/catechin ratio and the degree of polymerization of PA were subject to environmental effect. Interestingly, Urrutia *et al.* (2015) noted that the balance between the different polyphenolic classes was more stable than the absolute quantification of each class separately, suggesting a tighter regulation of the relative abundance of secondary metabolites. Another study focusing on the tannin composition concluded that the ellagitannin content was modified between strawberries grown at different latitudes (Josuttis *et al.*, 2013). However, information on the environmental factors responsible of polyphenolic composition variation is still lacking, even if several studies pointed out the role of temperature (Wang and Zheng, 2001; Remberg *et al.*, 2010; Tulipani *et al.*, 2011).

Also, it is known that polyphenols are involved in abiotic stress responses, therefore it is expected that changes in the environment as consequences of global warming will affect the qualitative and/or quantitative content of these compounds in plant. For instance, it has been described that levels of these compounds change with UV radiation (Van Leeuwen *et al.*, 2017) and also with the salinity of the soil (Galli *et al.*, 2016). Other studies in grape pointed out that water deficit could modulate the expression of the genes involved in the phenylpropanoid and flavonoid pathways, leading to an increase of phenolic compounds (Deluc *et al.*, 2009; Savoi *et al.*, 2016).

As part of this study of the organoleptic and nutritional characteristics of the '232'x'1392' strawberry population, a metabolomics analysis, using Ultra Performance Liquid Chromatography coupled to tandem mass spectrometry (UPLC-Orbitrap-MS/MS), was performed to tentatively identify and semi-quantify the content of secondary metabolites of the parental and progeny lines. A QTL analysis was then carried out to map genomic regions and candidate genes involved in the synthesis and regulation of polyphenols in strawberry.

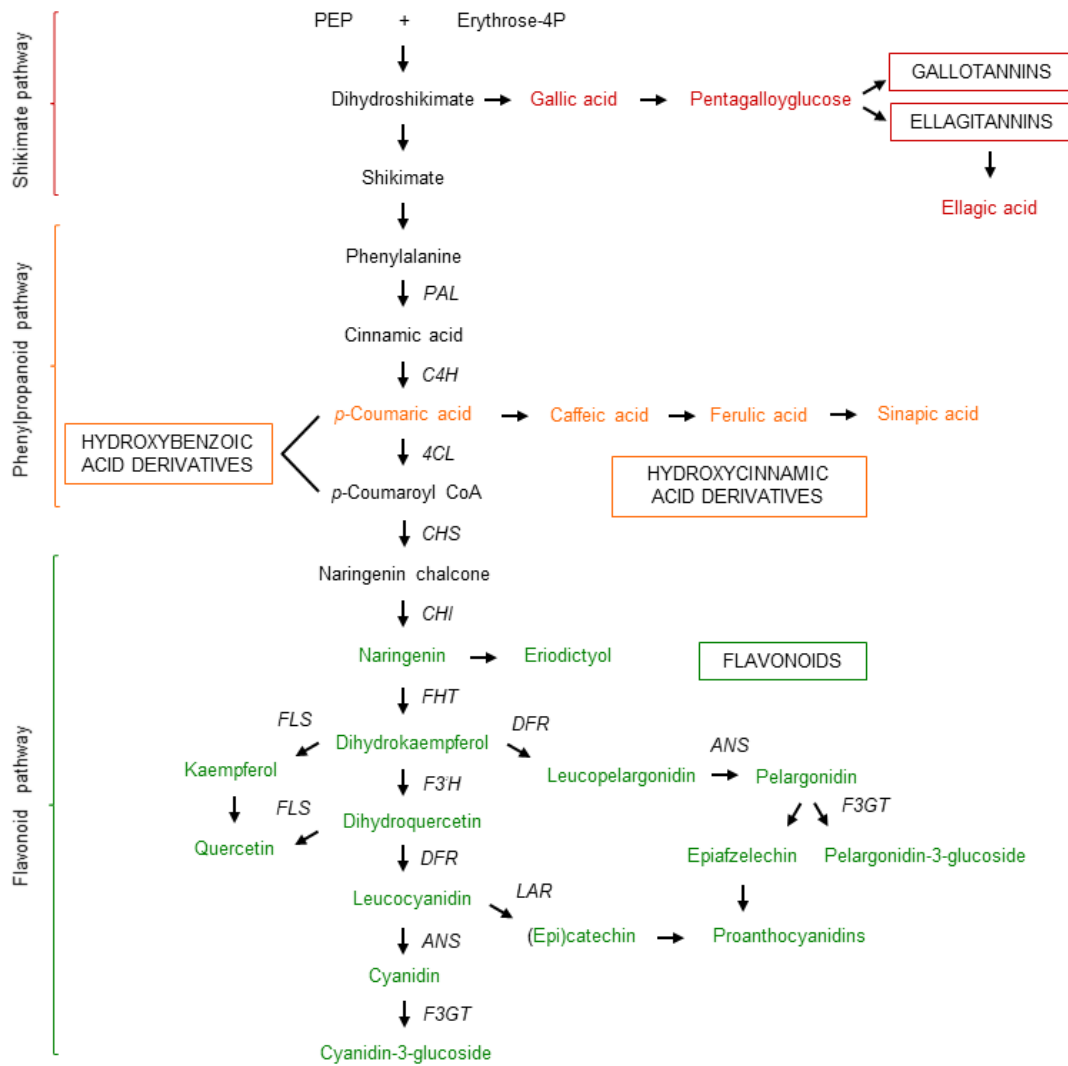


Figure 1: General scheme of shikimate, phenylpropanoid and flavonoid pathways. Some enzymes of the pathways are indicated. *PAL*: Phenylalanine lyase; *C4H*: cinnamate-4-hydroxylase, *4CL*: 4-coumaroyl CoA-ligase; *CHS*: chalcone synthase; *CHI*: chalcone isomerase; *FHT*: flavanone 3-hydroxylase; *FLS*: flavonol synthase; *DFR*: dihydroflavonol 4-reductase; *ANS*: anthocyanidin synthase; *F3H*: flavonol 3'-hydroxylase; *LAR*: leucocyanidin reductase; *F3GT*: flavonoid 3-O-glucosyltransferase.

Materials and Methods

Plant material

The *F. x ananassa* mapping population '1392' x '232' used for the metabolomics and QTL analysis was previously described in chapter 2 and was grown and harvested in 2013 and 2014 as explained in chapter 2. The same three biological replicates of the different parental and F₁ lines were used for primary (see chapter 2) and secondary metabolites analysis.

Extraction and analysis of metabolites by UPLC-Orbitrap-MS/MS measurements

50 mg of the pulverized samples were extracted during 30 minutes at room temperature with a mixture of methyl-tert-butyl ether:methanol (3:1) in an orbital shaker. To facilitate cell disruption, samples were then incubated 10 minutes in a cooled sonic bath, before adding a mixture of water:methanol (3:1), which results in the formation of two liquid phases. A fixed volume of the polar phase was transferred to a fresh Eppendorf tube before concentrating it to dryness in Speed-vac (Centrivac, Heraeus Instrument, Hanau, Germany).

Chromatographic separation was performed by Waters Acquity UPLC system using a C18 reverse-phase column (100 x 2.1 mm ID, 1.8µm particle size; Waters, Milford, MA, USA). The mass spectra were acquired using an Exactive mass spectrometer (Thermo Fisher Scientific, Waltham, MA, USA). The spectra were recorded alternating full-scan and all-ion fragmentation scan modes, covering a mass range from 100 to 1500 m/z. All data were processed using Xcalibur 2.1 software (Thermo Fisher). Processing of chromatograms, peaks detection and integration were performed using REFINER MS 7.5 (GeneData: <http://www.genedata.com>). The MS/MS fragmentation of the metabolites was compared with candidate molecules found in databases, and verified with earlier literatures on similar compounds, especially when the presence of the metabolite was reported in strawberry. Integration of the peak area of the corresponding molecular ion was used to quantify the metabolites in the different lines of the population. Data were expressed as the relative content of each metabolite compared to the '1392' parental.

Statistical analysis

The range of variation in the F₁ progeny, skewness and kurtosis were calculated, and the Shapiro-Wilk test (Shapiro and Wilk, 1965) was applied to test normality of metabolite distribution. For the metabolites deviating from normality, several transformations (Ln, Log10, Log2, inverse of square root, square, cube, reciprocal and arcsine in degrees or radians) were tested, and the transformation that gave the least skewed result was used for the following QTL mapping.

QTL mapping

The mapping of mQTL for the content of secondary metabolites in the population was performed as described in chapter 2.

Candidate genes screening

2-LOD intervals of detected mQTL and linked genetic markers were used to determine the genomic regions for the screening of candidate genes. Due to the high synteny and collinearity between *F. vesca* and *F. x ananassa* genomes, the available genome sequences of the diploid *F. vesca* species (Tenessen *et al.*, 2014; Edger *et al.*, 2018) were used to identify candidate genes within the QTL intervals. Candidate genes were first selected based on their function in *F. vesca* if described or the function of their homolog in *Arabidopsis thaliana*. Their expression in individuals of the population with contrasting levels of the metabolite(s) corresponding to the identified mQTL was measured by quantitative RT-PCR (qRT-PCR).

qRT-PCR of the candidate genes

Approximately 300 mg of fruit tissue were added to a 2ml Eppendorf tube and mixed with 900 µl of extraction buffer (2% cetyltrimethylammonium bromide, 2.5% polyvinylpyrrolidone, 2M NaCl, 100mM Tris-HCl pH 8.0, 25mM EDTA pH 8.0 and 2% β-mercaptoethanol, DEPC water), previously warmed at 65°C. The mixture was shaken at 65°C for 10 min. An equal volume of chloroform:isoamyl alcohol (24:1 v/v) was added and the samples were mixed by vortex. The upper aqueous phase was recovered after a centrifugation step of 10 min at 10,000 rpm and 4°C. A second extraction with chloroform:isoamyl alcohol was repeated, and the RNA was precipitated by the addition of LiCl 9M (with a final LiCl

concentration of 3M). After an incubation of 30 min at 4°C, RNA was pelleted by a centrifugation step of 20 min at full speed and 4°C. The pellets were resuspended in 500 µl SSE buffer (10mM Tris-HCl pH 8.0, 0.5% SDS, 1M NaCl), previously warmed at 65°C. After an extraction with an equal volume of chloroform:isoamyl alcohol and a centrifugation step of 10 min at 10,000rpm and 4°C, the upper aqueous phase was recovered, and RNA was precipitated with cold isopropanol. After a centrifugation step of 15 min at full speed, pellets were washed with ethanol 70% and finally resuspended in 30 µl of DEPC water. Contaminating DNA was removed with Turbo DNase (Ambion, Austin TX, USA), following the instructions of the manufacturer. Removal of DNA from the RNA samples was confirmed by performing PCR on 1 µl of total RNA using glyceraldehyde-3-phosphphate dehydrogenase (*GAPDH*) primers. Total RNA was quantified using micro-spectrophotometry (NanoDrop Technologies), and its integrity was checked by electrophoresis under denaturing conditions. First-strand cDNA synthesis of 500 ng of RNA in a final volume of 20 µl was performed using iScript cDNA synthesis kit (Bio-Rad), following the instructions of the manufacturer. Expression of the candidate genes was analyzed in the selected individuals of the population with the fluorescent intercalating dye SsoFast EvaGreen supermix in CFX96 detection system (Bio-Rad). Expression data were normalized to the reference genes *GAPDH* and *CHP1*. qRT-PCR primers of the candidate genes are listed in Annex 1.

Cloning of the candidate gene *FvH4_1g16310*

The full coding sequence of the candidate gene (XM_004287970.2) was PCR-amplified from strawberry (*F. x ananassa*) cDNA using specific primers (Annex 1). The sequence was introduced in *pEAQ-HT-dest1* (Sainsbury *et al.*, 2009) and *pK7WG2D* (Karimi *et al.*, 2002) plasmids with GATEWAY™ cloning technology (Invitrogen, Gaithersburg, MD, USA), for transient and stable overexpression of the candidate gene respectively. In both plasmids, the expression of the gene was under the control of the 35S promotor of *Cauliflower mosaic virus* (CaMV).

For the RNAi silencing construct, a 289pb sequence of the candidate gene mRNA was amplified by PCR using specific primers (Annex 1) and introduced in *pK7GWIWG2D(II)* (Karimi *et al.*, 2002) plasmid with GATEWAY™ cloning

technology for stable silencing. The expression of the RNAi construct was under the control of the CaMV 35S promotor.

Transient transformation of strawberry fruits

AGL0 *Agrobacterium tumefaciens* strain was transformed either with *pEAQ-HT-dest1-acetyltransferase* construct or the empty vector *pEAQ-HT-dest1*, and was used for transient transformation (agroinfiltration) on strawberry fruits grown under glasshouse conditions (IFAPA, Churriana, Malaga, Spain). Agroinfiltration with the overexpressed construct *pEAQ-HT-dest1-acetyltransferase* or the empty vector *pEAQ-HT-dest1* as a control were carried out during the months of April and May, as described by Hoffmann *et al.* (2006). Briefly, *A. tumefaciens* were grown overnight at 28°C in 50 ml liquid LB medium supplemented with rifampicin 50 µg/ml and kanamycin 50 µg/ml until reaching 0.8 O.D.₆₀₀. Cultures were then centrifuged 5 min at room temperature and at 5500 rpm and the pellets were resuspended in 40ml of MMA medium (MS salt 4.3g/l, MES 10mM and sucrose 20g/l). Two other steps of centrifugation and resuspension of the pellets in fresh MMA were repeated. Finally, pellets were resuspended in 20ml of MMA medium, and green stage fruits were injected with 100-200 µl of the *Agrobacterium* suspension. Fruits were harvested when fully ripe and directly frozen in liquid nitrogen. After removal of the achenes, frozen fruits were pulverized with the help of a TissueLyser II (Quiagen). RNA extraction, expression of the *acetyltransferase*, *phenylalanine ammonia-lyase (FaPAL)* and *FvH4_1g16840* by qRT-PCR was performed on injected fruits as described previously. Primary and secondary metabolites of the injected fruits were measured as described previously in this chapter and chapter 2.

Stable transformation of *F. x ananassa* cv. Camarosa

Camarosa explants were transformed with *A. tumefaciens* strain GV3101, harboring the overexpression *pK7WG2D-acetyltransferase* and silencing *pK7GWIWG2D(II)-acetyltransferaseRNAi* constructs respectively. Stable transformation was performed as described by Barceló *et al.* (1998). Leaf disks were used as explants and were incubated ten days in dark and in basal medium containing the macroelements of the N30K formulation (Margara, 1984), supplemented with MS microelements, vitamins (Murashige and Skoog, 1962)

and the hormones indole-3-butyric acid (0.5 mg/ml) and benzyladenine (20 mg/ml). After the induction period, explants were placed in 50ml tubes and inoculated with an overnight *A. tumefaciens* culture diluted 1/10 in sterile water and shaken during 15 min. Infected explants were dried on sterile filter paper and cultivated on the same medium for two days in dark. Explants were then transferred to selection medium, supplemented with kanamycin (50 mg/l) and carbenicillin (500 mg/l) and kept another three days in dark. After this period, explants were transferred to light conditions and kept in the same medium until shoots regenerated. Every 28 days, explants were transferred to fresh medium, and the shoots were transferred to multiplication N30K medium, supplemented with kinetin (0.47 mg/l), kanamycin (50 mg/l) and carbenicillin (500 mg/l).

Results

Variation in the secondary metabolites composition in '232'x'1392' mapping population

To focus on the nutritional aspects of strawberry fruits, the variation in secondary metabolites content in the two parental lines and its F₁ progeny was estimated in the two years (2013 and 2014) using a well-established metabolomics approach (Giavalisco *et al.*, 2011). A total of 130 secondary metabolites were tentatively identified by UPLC-Orbitrap-MS/MS, 125 being polyphenols and five belonging to the terpenoid class (Table 1; Annex 2). Within the polyphenolic compounds, the most numerous group belonged to flavonoids (55), followed by soluble tannins (49) and hydroxycinnamic and hydroxybenzoic acid derivatives (21).

Among flavonoids, the condensed tannin class comprised 12 procyanidins and 10 propelargonidins forming dimers, trimers or tetramers structures. Additionally, we identified three (epi)afzelechin hexose isomers and three (epi)catechin and (epi)catechin glucuronide isomers, which conformed the flavanol class in the mapping population. 16 flavonols, derivatives of quercetin and kaempferol, were also identified. Seven glycoside conjugates of pelargonidin, cyanidin and peonidin were detected and listed as anthocyanins, being the most abundant pelargonidin-hexose followed by cyanidin-hexose. Peonidin-3-O-glucoside,

which is formed by the methylation of cyanidin-3-*O*-glucoside, was detected at very low levels and was not present in all the individuals of the population (Annex 2). Finally, naringenin chalcone-hexose and two isomers of eriodictyol-hexose conformed the flavonone class; diosmetin acetylhexoside, an *O*-methylated flavone, were also found in the parental lines and progeny.

Eight galloyl-glucoses, 27 ellagitannin precursors, ellagitannins and ellagic acid derivatives previously described in strawberry, and 14 putative ellagitannins were classified as soluble tannins. Finally, 15 hydroxycinnamic acid derivatives, originating from caffeic, coumaric, ferulic and sinapic acids, were identified, together with six hydroxybenzoic acid derivatives. One isomer of ferulic acid conjugated with a hexose molecule was detected only in the population harvested in 2014.

By checking the metabolic changes between the two harvests and between the parental lines, we observed that 33 metabolites showed significant differences ($P < 0.05$). Indeed, the levels of five procyanidins, three flavanols, nine flavonols, three anthocyanins, three galloyl glucoses, six ellagitannin, three coumaric acid derivatives and one sinapic acid hexose derivative were significantly different in '232' and '1392' individuals over the two studied years (Table 1). Interestingly, from the two main anthocyanin pigments, only cyanidin-hexose, which is the minor pigment responsible of the fruit color (Petrucci *et al.*, 2013), showed significant lower levels in the '232' parental in both harvests, while there were no significant differences for pelargonidin-hexose (the main pigment) between the two lines. However, the content in pelargonidin-hexose is slightly lower in the '232' line for both harvests, while the content in pelargonidin rutinose is significantly lower and, in the opposite, the content in pelargonidin malonyl hexose is significantly higher.

In addition, the two parental lines presented significant differences in 43 other metabolites for one of the two harvests. Only the hydroxybenzoic acid derivatives group did not show any significant differences between '232' and '1392' lines in any of the harvests. For 40 metabolites, '232' parental displayed higher values (for both harvests) than the other parental, being the proanthocyanidins the most

representative group. Indeed, all the procyanidins and seven out of ten propelargonidins were more abundant in the '232' lines for both harvests.

Almost all identified metabolites displayed a continuous variation, indicating their polygenic origin, although their distributions were generally deviated from normality. Some metabolites, such as isomer 2 of ellagic acid-hexose, unknown ellagitannin isomer 1, tri-galloyl-glucose and kaempferol pentose hexose glucuronide isomer 2, were not detected in any harvest in a few individuals of the population. High variation for almost all the compounds was observed in the population, and transgressive segregation was found for most metabolites in both direction (Table 1), even in those with no significant differences between the two parental lines, such as hydroxybenzoic acid derivatives. Only caffeic acid-hexose showed very little variation in the segregating population (Figure 2). Interestingly, the anthocyanin profile of the F₁ progeny seemed more similar to the parental '232' than the parental '1392'. Cyanidin-hexose was dramatically decreased in the population, as it was in the '232' line, while pelargonidin-hexose profile did not show extreme differences compared to the '1392' line (Figure 2). In addition, cyanidin-hexose and pelargonidin-hexose did not exceed in the population 1.06/1.86 and 1.29/1.89 relative content in 2013/2014 harvests respectively, which are low values in comparison with the other identified compounds. Other conjugates of pelargonidin were increased in the population and in '232' when compared to '1392'.

Table 1: Tentatively identified metabolites in the UPLC-Orbitrap-MS/MS, retention time (RT), molecular ion (m/z), mode (positive/negative), mean value of the parental '232' and range in the population for 2013 and 2014 harvests. Bold values indicate significant difference between '232' and '1392' parental lines ($P < 0.05$). Data are relativized to the mean value of the '1392' parental line.

Metabolite	RT	m/z	mode (-/+)	232 parental		2013		2014	
				2013	2014	min	max	min	max
PROCYANIDINS									
Procyanidin dimer 1	4.66	577.13	-	1.47	2.02	0.43	1.78	0.62	2.81
Procyanidin dimer 2	4.89	577.13	-	1.46	1.54	0.46	1.72	0.49	3.61
Procyanidin dimer 3	5.81	577.13	-	1.65	1.80	0.47	5.13	0.63	4.70
Procyanidin dimer 4	6.23	577.13	-	1.25	1.69	0.52	1.68	0.62	2.78
Procyanidin trimer 1	3.62	865.20	-	1.44	1.99	0.45	1.90	0.61	2.87
Procyanidin trimer 2	5.01	865.20	-	1.62	1.46	0.44	2.13	0.44	3.50
Procyanidin trimer 3	5.10	865.20	-	1.29	2.03	0.44	1.84	0.60	2.75
Procyanidin trimer 4	5.20	865.20	-	1.20	1.49	0.48	1.97	0.61	2.81
Procyanidin tetramer 1	4.46	1153.26	-	1.56	2.58	0.00	2.84	0.21	5.11
Procyanidin tetramer 2	4.77	1153.26	-	1.67	2.13	0.39	2.24	0.42	3.70
Procyanidin tetramer 3	5.18	1153.26	-	1.09	1.75	0.39	1.96	0.55	2.82
Procyanidin tetramer 4	5.45	1153.26	-	1.50	1.22	0.26	2.55	0.24	4.75
PROPELARGONIDINS									
Propelargonidin dimer 1	5.24	561.13	-	1.07	1.46	0.38	2.24	0.44	2.64
Propelargonidin dimer 2	5.57	561.14	-	0.69	0.58	0.22	1.84	0.00	3.45
Propelargonidin dimer 3	6.52	561.14	-	0.82	0.84	0.00	2.08	0.00	6.24
Propelargonidin dimer 4	6.87	561.14	-	0.97	1.22	0.38	2.31	0.35	2.66
Propelargonidin trimer 1	3.99	849.20	-	1.39	1.56	0.38	1.96	0.39	2.74
Propelargonidin trimer 2	5.41	849.20	-	1.41	2.28	0.00	2.45	0.00	4.33
Propelargonidin trimer 3	5.46	849.20	-	1.63	1.27	0.00	3.34	0.00	4.32
Propelargonidin trimer 4	5.63	849.20	-	1.24	2.23	0.46	1.73	0.55	2.98
Propelargonidin trimer 5	6.50	849.20	-	1.45	2.35	0.26	2.35	0.23	3.87
Propelargonidin trimer 6	6.85	849.20	-	1.34	1.57	0.38	2.56	0.33	3.16
FLAVAN 3-OLS									
(Epi)catechin	5.06	289.07	-	1.21	1.59	0.45	1.63	0.57	3.28
(Epi)afzelechin 1	7.53	435.13	-	0.24	0.23	0.12	1.13	0.17	1.35
(Epi)afzelechin 2	8.29	435.13	-	1.18	1.01	0.24	3.20	0.32	3.25
(Epi)afzelechin 3	8.80	435.13	-	1.23	1.46	0.00	3.26	0.00	4.13
Epicatechin glucuronide 1	5.17	465.11	-	0.41	0.29	0.00	1.00	0.05	1.94
Epicatechin glucuronide 2	5.41	465.10	-	0.47	0.35	0.04	0.94	0.04	1.89
FLAVONOLS									
Kaempferol-hexose 1	5.17	447.09	-	0.48	0.32	0.06	1.00	0.08	1.86
Kaempferol-hexose 2	5.51	447.09	-	0.13	0.12	0.04	2.83	0.04	3.58
Kaempferol-hexose 3	7.72	447.09	-	1.72	1.67	0.29	2.47	0.31	2.81
Kaempferol-glucuronide	7.72	461.07	-	0.86	0.99	0.11	1.50	0.21	2.91
Quercetin-glucuronide	7.10	477.07	-	1.33	1.46	0.17	1.21	0.18	3.96
Isorhamnetin glucuronide	7.94	491.08	-	2.92	1.87	0.11	4.37	0.15	6.97
Quercetin hexose	7.14	463.09	-	0.94	0.81	0.16	1.25	0.05	2.84
Kaempferol malonylhexose	8.14	535.11	+	5.03	3.33	0.50	8.25	0.47	9.21
Kaempferol coumaroyl hexose	7.47	595.16	+	0.49	0.80	0.15	2.33	0.16	2.76
Kaempferol acetylhexose	8.65	491.12	+	1.29	1.29	0.08	2.49	0.00	5.20
Quercetin-acetylhexose	7.89	507.11	+	0.59	0.36	0.15	3.12	0.00	4.44
Rutin 1	5.59	609.15	-	1.04	0.82	0.07	1.04	0.23	2.70
Rutin 2	6.91	609.14	-	0.49	0.46	0.07	1.46	0.01	2.79
Kaempferol hexose glucuronide	5.55	623.12	-	0.76	1.06	0.07	1.46	0.24	3.85
Kaempferol pentose hexose glucuronide	9.55	593.13	-	0.40	0.54	0.00	3.25	0.00	4.35

Quercetin malonylhexose	7.45	551.10	+	1.95	1.93	0.16	6.81	0.00	5.42
FLAVANONES									
Eriodictyol hexose 1	5.50	449.11	-	1.17	0.96	0.24	1.49	0.23	3.03
Eriodictyol hexose 2	6.04	449.11	-	0.89	0.92	0.20	1.40	0.22	2.81
Naringenin chalcone hexose	6.29	433.11	-	1.03	0.94	0.15	1.89	0.33	2.18
ANTHOCYANINS									
Cyanidin hexose	5.12	449.11	+	0.50	0.45	0.05	1.06	0.06	1.86
Pelargonidin hexose	5.50	433.11	+	0.90	0.87	0.27	1.29	0.46	1.89
Pelargonidin malonyl hexose	6.37	519.11	+	2.19	1.45	0.28	7.45	0.04	8.44
Pelargonidin rutinose	5.61	579.17	+	0.42	0.55	0.26	1.28	0.29	1.44
Peonidin 3-O-glucoside	5.67	463.12	+	0.92	0.46	0.00	10.74	0.00	6.82
Pelargonidin acetyl hexoside 1	6.38	473.11	-	2.18	1.84	0.07	7.27	0.24	13.74
Pelargonidin acetyl hexoside 2	6.91	473.11	-	1.55	1.56	0.18	2.77	0.00	6.66
FLAVONE									
Diosmetin acetylhexoside	8.29	503.12	-	1.27	0.90	0.00	4.37	0.00	4.92
GALLOYL GLUCOSES									
Galloyl-hexose 1	2.57	331.07	-	0.66	0.48	0.31	2.14	0.26	3.08
Galloyl-hexose 2	2.84	331.07	-	0.89	0.72	0.49	2.23	0.32	2.48
Galloyl-hexose 3	3.24	331.07	-	1.62	1.49	0.80	5.71	0.45	3.40
Galloyl-hexose 4	3.65	331.07	-	0.90	0.66	0.33	2.29	0.15	3.13
Galloylquinic acid 1	1.85	343.07	-	0.94	0.33	0.20	2.19	0.09	4.34
Galloylquinic acid 2	3.05	343.07	-	0.70	0.39	0.23	2.23	0.16	3.95
Galloylquinic acid 3	3.35	343.07	-	0.64	0.15	0.00	2.22	0.00	4.93
Tri-galloyl-hexose	4.62	343.07	-	1.04	0.13	0.00	2.89	0.00	14.44
ELLAGITANNINS AND ELLAGIC ACID COMPOUNDS OR PRECURSOR/DERIVATIVE									
HHDP glucose 1	1.58	481.06	-	1.28	0.79	0.57	4.65	0.36	3.51
HHDP glucose 2	2.06	481.06	-	1.05	0.65	0.49	2.57	0.21	2.76
Bis(HHDP) glucose 1	3.66	783.07	-	1.16	1.00	0.35	3.81	0.27	3.74
Bis(HHDP) glucose 2	3.80	783.07	-	0.86	0.61	0.55	1.98	0.37	2.96
Bis(HHDP) glucose 3	4.52	783.07	-	0.83	0.56	0.51	1.99	0.38	2.76
Galloyl-HHDP-glucose	5.09	633.07	-	1.06	0.76	0.47	2.61	0.20	3.49
Di-galloyl HHDP glucose	5.95	785.08	-	0.51	0.44	0.27	1.88	0.00	2.86
Ellagic acid deoxyhexose 1	6.67	447.06	-	1.00	0.73	0.60	2.02	0.41	2.49
Ellagic acid deoxyhexose 2	6.79	447.06	-	1.22	0.98	0.65	4.40	0.41	3.89
Ellagic acid	7.00	301.00	-	1.05	0.69	0.30	2.60	0.22	6.42
Galloyl-bis(HHDP)-glucose 1	6.16	935.08	-	0.50	0.40	0.23	2.05	0.10	7.58
Galloyl-bis(HHDP)-glucose 2	6.29	935.08	-	0.66	0.67	0.26	2.33	0.14	5.52
Galloyl-bis(HHDP)-glucose 3	6.76	935.07	-	1.19	0.90	0.29	3.26	0.15	12.78
Galloyl-bis(HHDP)-glucose 4	6.88	935.08	-	3.21	2.18	0.57	10.91	0.25	6.72
Tri-galloyl HHDP glucose 1	6.16	937.08	-	0.45	0.45	0.15	2.05	0.17	6.83
Tri-galloyl HHDP glucose 2	6.29	937.08	-	0.64	0.58	0.25	2.45	0.14	5.55
Unknown ellagitannin 1	4.07	935.08	+	1.08	0.55	0.34	3.43	0.00	8.91
Unknown ellagitannin 2	4.48	935.08	+	0.86	0.38	0.47	2.85	0.06	3.26
Unknown ellagitannin 3	4.69	935.08	+	1.29	0.88	0.63	3.63	0.12	14.73
Unknown ellagitannin 4	5.43	935.08	+	1.17	0.86	0.55	3.74	0.00	8.30
Unknown ellagitannin 5	6.28	935.08	+	0.67	0.25	0.00	2.84	0.00	4.06
Ellagic acid hexose 1	5.76	463.05	-	0.94	0.62	0.38	2.23	0.00	3.18
Ellagic acid hexose 2	5.87	463.05	-	1.55	0.80	0.00	4.75	0.00	3.13
Ellagic acid hexose 3	6.01	463.05	-	1.02	0.71	0.53	1.96	0.31	2.69
Tris-galloyl-glucose 1	5.09	635.08	-	1.05	0.75	0.47	2.60	0.17	3.73
Tris-galloyl-glucose 2	5.69	635.09	-	0.29	0.31	0.00	1.29	0.00	2.98
Methylellagic acid methyl hexose	3.74	519.11	-	0.70	0.54	0.16	1.30	0.15	1.67
PUTATIVE ELLAGITANNINS									
Rhoipteleatin H 1	3.35	965.05	-	0.50	0.27	0.00	3.72	0.00	2.27
Rhoipteleatin H 2	3.95	965.05	-	0.55	0.73	0.00	3.72	0.00	18.60
Castalagin 1	5.62	933.06	-	0.63	0.61	0.33	2.46	0.23	3.81
Castalagin 2	5.94	933.06	-	1.24	0.63	0.37	3.05	0.17	6.23
Castalagin 3	6.28	933.06	-	0.79	0.70	0.31	2.69	0.20	4.29
Castalagin 4	6.37	933.06	-	1.50	0.85	0.42	4.22	0.00	9.78
Castalagin 5	6.87	933.06	-	0.72	0.80	0.33	3.62	0.23	6.41
Castalagin 6	7.46	933.06	-	0.77	0.85	0.37	3.77	0.18	7.44

Lagerstannin A 1	4.79	799.06	-	0.42	0.75	0.14	1.81	0.00	5.24
Lagerstannin A 2	5.77	799.06	-	0.45	0.75	0.18	1.90	0.14	3.72
Lagerstannin B 1	4.82	949.06	-	0.96	0.81	0.38	2.28	0.07	6.31
Lagerstannin B 2	7.30	949.06	-	0.47	0.65	0.14	2.23	0.10	2.77
Lagerstannin B 3	7.42	949.06	-	0.81	0.53	0.00	2.25	0.00	3.28
Lagerstannin B 4	8.25	949.06	-	0.52	0.65	0.20	2.92	0.15	2.57
HYDROXYCINNAMIC ACID AND DERIVATIVES									
Caffeic acid hexose	0.80	341.11	-	0.95	1.00	0.91	1.14	0.80	1.15
Coumaric acid hexose 1	5.18	325.09	-	0.25	0.28	0.16	1.03	0.10	1.31
Coumaric acid hexose 2	5.43	325.09	-	0.40	0.34	0.17	1.05	0.11	1.68
Ferulic acid hexose 1	5.56	355.10	-	0.82	0.75	0.48	2.51	0.34	2.80
Ferulic acid hexose 2	5.77	355.10	-	ND	0.93	ND	ND	0.45	2.65
Ferulic acid hexose 3	6.98	355.10	-	0.83	0.95	0.19	5.58	0.00	6.72
Ferulic acid hexose 4	7.39	355.10	-	0.94	0.60	0.34	5.07	0.12	3.19
Sinapic acid hexose derivative 1	8.53	385.15	-	2.07	0.88	0.18	3.97	0.05	4.76
Sinapic acid hexose derivative 2	9.78	385.15	-	0.05	0.06	0.00	1.20	0.01	1.23
Sinapic acid hexose derivative 3	9.95	385.15	-	0.52	0.91	0.10	3.05	0.13	2.28
Sinapic acid hexose derivative 4	11.27	385.15	-	0.57	1.04	0.04	2.56	0.07	3.88
m-Coumaric acid 1	5.11	163.04	-	0.69	0.57	0.29	1.12	0.20	2.76
m-Coumaric acid 2	6.43	163.04	-	0.16	0.10	0.06	1.46	0.04	1.76
Cinnamic acid- hexo 1	7.00	311.11	+	0.60	0.42	0.12	10.08	0.00	3.96
Cinnamic acid- hexo 2	7.39	311.11	+	0.76	0.45	0.19	8.79	0.00	4.43
BENZOIC ACID DERIVATIVES									
Di-hydroxybenzoic acid hexose 1	3.63	315.07	-	1.03	0.85	0.60	4.39	0.26	4.52
Di-hydroxybenzoic acid hexose 2	4.35	315.07	-	1.46	1.41	0.47	11.19	0.32	3.65
Di-hydroxy methyl benzoic acid hexose 1	3.82	329.09	-	1.12	0.81	0.41	1.82	0.52	1.93
Di-hydroxy methyl benzoic acid hexose 2	5.97	329.09	-	1.48	1.87	0.20	2.89	0.42	9.55
Di-hydroxy methyl benzoic acid hexose 3	6.04	329.09	-	0.92	0.84	0.19	1.45	0.19	3.43
1-O-protocatechuyI-beta-xylose	4.45	285.06	-	1.12	0.72	0.50	8.40	0.37	2.55
TERPENOID DERIVATIVES									
Triterpenoid-hexose 1	10.85	695.40	-	1.08	0.98	0.37	4.67	0.07	4.59
Triterpenoid-hexose 2	11.06	695.40	-	0.89	0.85	0.19	3.27	0.23	6.44
Triterpenoid-hexose 3	9.33	711.39	-	0.99	0.79	0.40	1.85	0.44	2.19
Sesquiterpenoid hexose 1	8.47	463.25	-	0.68	1.29	0.32	5.79	0.23	3.83
Sesquiterpenoid hexose 2	8.99	463.25	-	0.36	0.39	0.29	2.17	0.29	1.46

Hierarchical cluster analysis

To further investigate the relationships between both compounds and individuals of the population, hierarchical cluster analysis (HCA) using the secondary metabolite profiles of the F₁ progeny was performed (Figure 2). Mean log₂-transformed values of each metabolite, relativized to the mean value of the '1392' parental, for the two harvests and for each line of the progeny were used to group into clusters both compounds and lines, using Pearson coefficient. The analysis grouped the metabolites into three main clusters, named A, B and C. Cluster A represented the most numerous group of compounds, and could be in turn divided into several sub-clusters. The main group of metabolites found in this cluster includes ellagitannins, ellagic acid derivatives, galloyl glucoses and HHDP glucose derivatives, confirming the relationship between soluble tannins, their precursor and derivative molecules. Another sub-cluster grouped the isomers of

cinnamic, coumaric, ferulic and sinapic acid derivatives, corresponding to the majority of hydroxycinnamic acids detected in the segregating population. Two isomers of (epi)afzelechin clustered together with two propelargonidin dimers, indicating that possibly these two PAs originated from the polymerization of the flavanol epiafzelechin. The main pigment pelargonidin-hexose clustered with flavanones such as naringenin chalcone and eriodictyol derivatives and the flavanol kaempferol coumaroyl-hexose, pointing out their biosynthetic relationship in the flavonoid pathway.

Cluster B can be divided into two sub-clusters, the main one being defined by the majority of proanthocyanidin tannins (procyanidin and propelargonidin dimers, trimers and tetramers) grouped together with the flavanol (epi)catechin demonstrating once again the relationships between flavanol and PAs. The other smaller sub-cluster comprised two conjugates of the anthocyanin pelargonidin (pelargonidin acetyl hexoside and pelargonidin malonyl hexose) and the flavanol kaempferol malonyl-hexose.

Finally, cluster C grouped metabolites which content in the F₁ progeny was mainly lower than in the '1392' parental more than biosynthetically related compounds, even if an interesting sub-cluster can be observed. In this sub-cluster, cyanidin-hexose, the minor pigment in strawberry fruit, grouped together with derivatives of the flavonols quercetin and kaempferol, and epicatechin derivatives. In the flavonoid biosynthetic pathway, cyanidin-3-O-glucoside and epicatechin share cyanidin as common precursor, and dihydrokaempferol and dihydroquercetin are upstream metabolites (Figure 1).

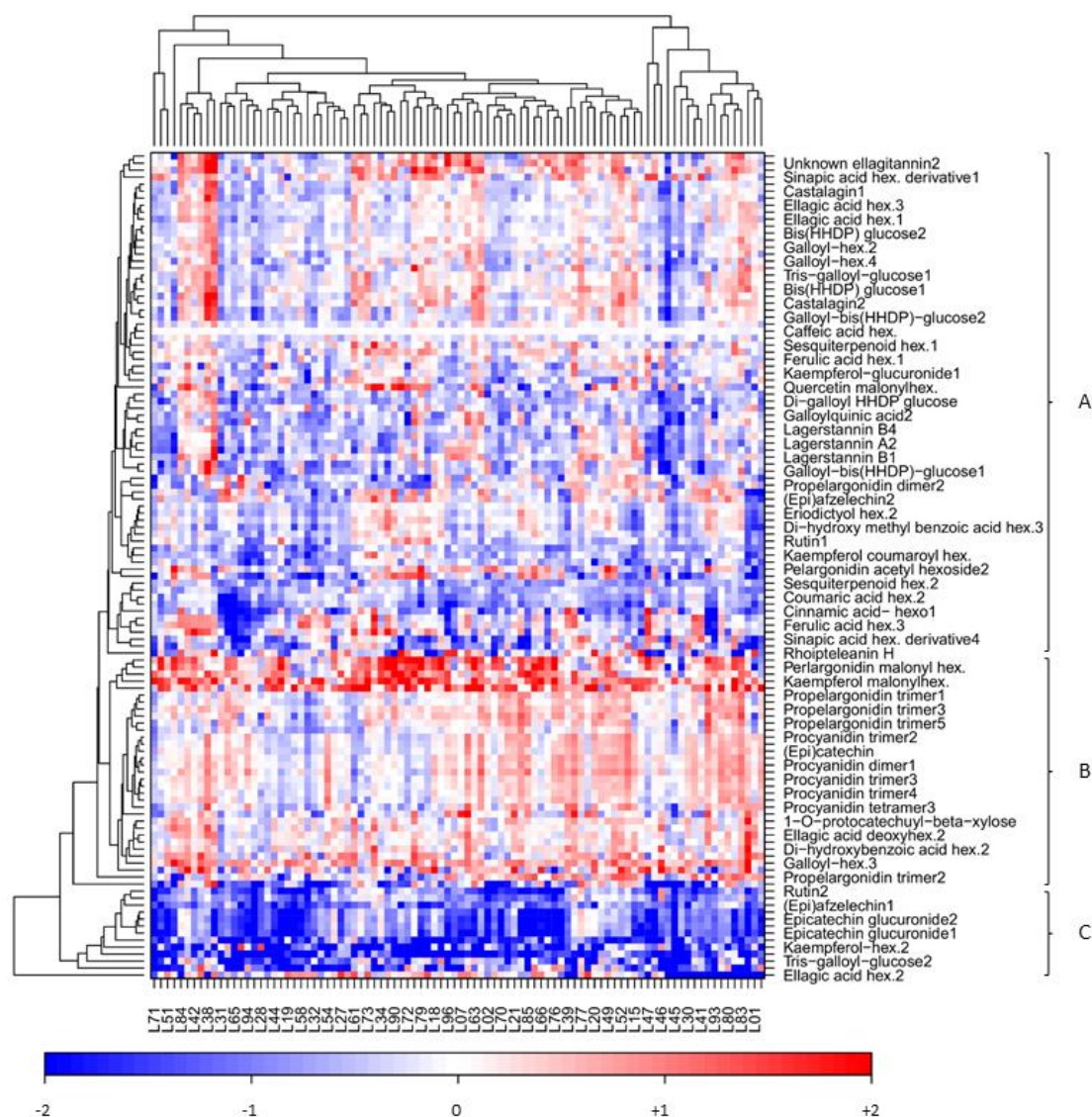


Figure 2: Hierarchical cluster analysis (HCA) and heatmap visualization of secondary metabolite profiles in the '232' × '1392' population over two successive seasons (2013–2014). F₁ lines with a relative content for a given compound similar, lower, or higher than that of the reference parent '1392' are shown in white, blue, or red, respectively.

Correlation analysis of metabolites

Mean metabolites values for the two harvests were normalized using standard scores and pair-wise Pearson's correlations were performed to point out the degree of coordination in the secondary metabolism and to facilitate the detection

of possible co-regulations among different metabolites (Figure 3). A total of 3169 significant correlations were found for 2013, and 3477 for 2014, the majority positive, except for 209 and 86 negative respectively ($P < 0.05$). As expected, strong correlations were observed between polyphenols classified in the same group, the most outstanding being for proanthocyanidins and compounds originated from ellagitannins metabolism. (Epi)catechin and (epi)afzelechin isomer 1 showed strong positive correlation with all the proanthocyanidins, while (epi)afzelechin isomers 2 and 3 only with some propelargonidins. Interestingly, negative correlations were observed between some condensed tannins and some of the flavonols/anthocyanins, indicating a possible competition for precursors between the different branches of the flavonoid pathway. Curiously, many significant positive correlations were noticed between condensed and soluble tannins, even if they do not share direct biosynthetic relationships.

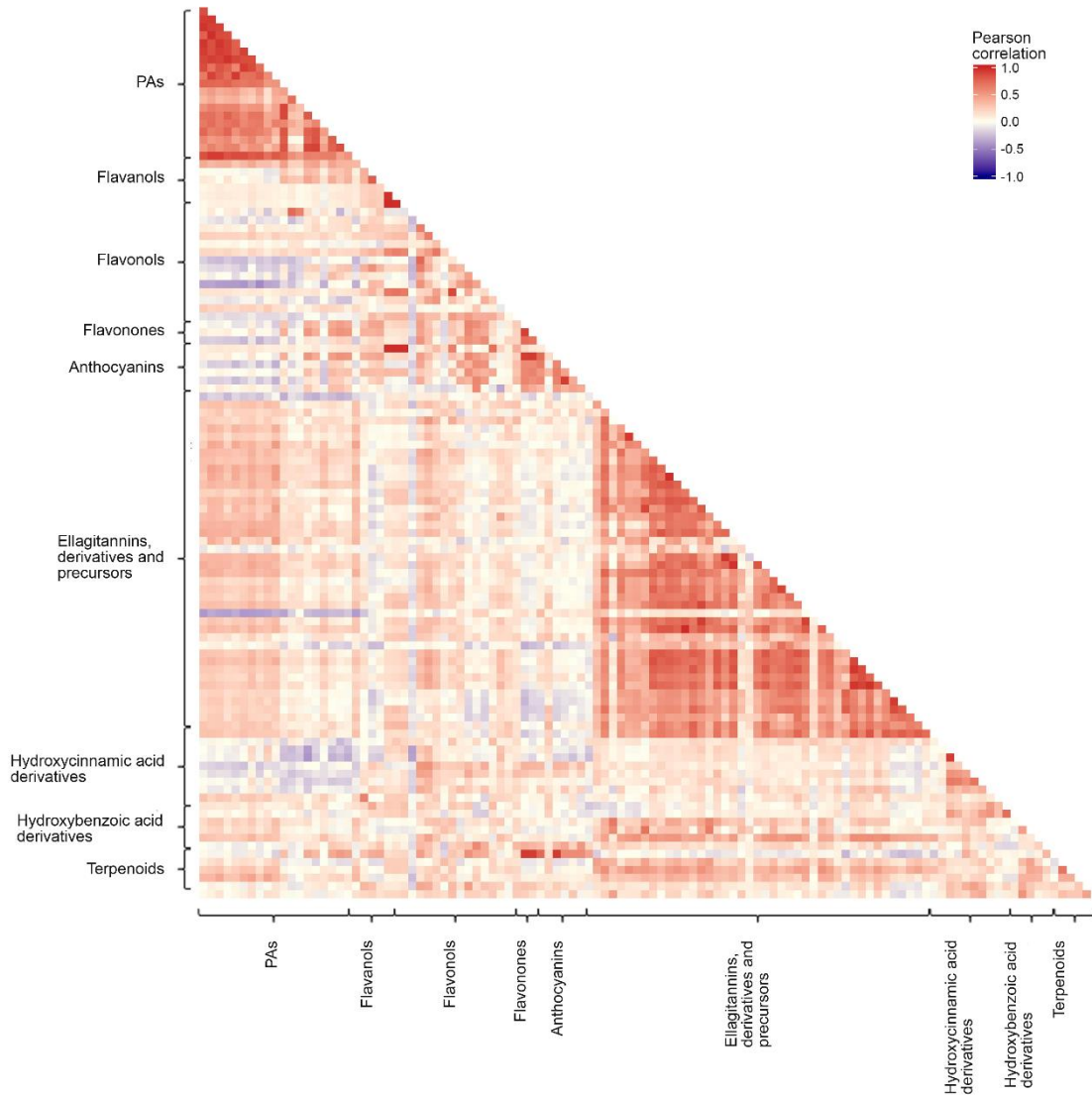


Figure 3: Heat map representation of pair-wise correlations between metabolites identified in '232' × '1392' for years 2013 and 2014. Red and blue indicate positive and negative correlations, respectively.

Identification of mQTL controlling secondary metabolites in the '232'x'1392' population

QTL analysis for the detected and semi-quantified secondary metabolites in the mapping population was performed as described in chapter 2 for the primary metabolites. The metabolites tri-galloyl hexose, unknown ellagitannins 1 and 4 and rhoipteleatin H 1 were removed from the analysis due to a high number of missing values in the F₁ population. Detected QTL under the threshold by rMQM were included only if a significant association between the marker and the trait was observed by the Kruskal-Wallis test ($P < 0.005$), or if a QTL was identified in the same genomic region for the same metabolite in the other harvest or for another related metabolite in any of the two harvests.

A total of 465 significant associations were found between markers and 116 out of the 130 identified metabolites, using the average metabolite content from each year separately (Table 2). 209 QTL (45% of the total number) were detected for flavonoids, 156 QTL (33.5%) for galloyl glucoses, ellagitannins and their precursors/derivatives, 76 QTL (16.3%) for hydroxycinnamic and benzoic acid derivatives and 24 QTL for terpenoid metabolites (5.2%).

QTL for each trait detected in the same chromosomal regions (i.e. with overlapping confidence interval) in the two different harvests were considered stable and comprised 110 (23.7%) of the total number of QTL.

QTL were detected in all the linkage groups, with the exception of LG I-4 and LG I-5. The number of QTL detected for each trait ranged from one (i.e. quercetin hexose, rutin 1 and di-hydroxy methyl benzoic acid hexose 4) to eight ((epi)afzelechin 1 and tris-galloyl-glucose 2). The phenotypic variation (R^2) explained by each QTL ranged from 3.5% (for *qK-acehex-8.56-III-1* in 2014) to 70.7% (for *qEAhex-5.87-I-2* in 2013).

Interestingly, clusters of QTL for related metabolites or for different isomers of the same compound were detected in the seven homoeology groups, indicating the presence of *loci* controlling the levels of secondary metabolites in a coordinated way (Figure 4). Clusters of QTL related to proanthocyanidin metabolites were detected in LG I-2, LG V-2 and LG V-3. In LG I-2, QTL for the flavanols catechin and (epi)afzelechin colocalized with 18 QTL for propelargonidins and

procyanidins, suggesting the presence of a *locus* involved in tannin condensation. Furthermore, several QTL for other flavonoid compounds were also located in LG V-2, including stable QTL for the anthocyanins pelargonidin-hexose (main pigment), pelargonidin malonyl hexose and pelargonidin rutinose, for derivatives of the flavanol kaempferol and for derivatives of the flavonone eriodictyol. Another cluster of QTL including different flavonoids was observed in LG V-4, with stable QTL for the two isomers of the flavanol epicatechin glucuronide, for the flavonols isorhamnetin glucuronide, kaempferol hexose 1 and rutin 2 and the flavonone naringenin chalcone hexose.

More specifically, QTL for different (epi)afzelechin isomers and kaempferol derivatives were detected in different linkage groups of HG VI (LG VI-1, LG VI-2 and LG VI-7) for (epi)afzelechin and LG VI-3 and LG VI-6 for kaempferol derivatives), suggesting the possibility of homoeo-QTL.

Clusters of QTL for hydroxycinnamic and hydroxybenzoic acid derivatives were also observed along the population map, being the most numerous ones in LG IV-2 and LG IV-3, grouping seven and ten QTL for different phenolic acid derivatives respectively (Figure 4).

Regarding soluble tannins, numerous clusters were distributed in the seven homoeology groups. LG I-3 grouped QTL for isomers of galloylquinic acids and LG II-5 for lagerstannin compounds, while clusters in LG I-2, LG II-4, LG III-3, LG IV-1, LG V-1, VI-2 and the four linkage groups of HG VII grouped QTL for different galloyl glucoses, ellagitannins and their precursors/derivatives (Figure 4).

QTL cluster detected for terpenoid metabolites were observed in LG IV-4 and LG VII-3, while a stable QTL for sesquiterpenoid hexose 2 was located in LG V-3 (Figure 4).

Two stable QTL for ellagitannin derivatives/precursors were selected for further study. In LG I-2, a QTL for ellagic acid hexose isomer 2 was detected, with a high LOD value and a 2-LOD confidence interval between 49 and 59 cM (*qEAhex-5.87-I-2*, Table 4). In addition, this mQTL explained a high percent of the observed phenotypic variation (70.7% in 2013 and 51.4%), suggesting that a key gene involved in ellagic acid hexose metabolism is located within the interval defined by the QTL (Figure 4).

Other stable QTL for two isomers of galloyl-bis(HHDP)-glucose (isomer 1 and 4) was selected in LG IV-1 for further study, explaining approximately 30% of the phenotypic variation for the isomer 1 and 45% for the isomer 4 and located between 33.9 and 44.5 cM (*G-BHglu-6.16-IV-1* and *G-BHglu-6.88-IV-1*, Table 2 and Figure 4).

Table 2: mQTL detected for secondary metabolites in the '232' x '1392' linkage map by Kruskal-Wallis (KW) and restricted multiple QTL mapping (rMQM) analysis. For the identification of the different compounds, retention time is indicated together with metabolite names (see Table 1). The position of the LOD peak (in cM), the markers used as cofactors and the 1-LOD and 2-LOD confidence intervals are indicated. The estimated mean effect (for transformed data) of the QTL (μ) associated with each of the genotypes (ac, ad, bc, bd) with phase type {00} is shown. QTL detected for the same metabolite in both harvests are indicated in bold.

Trait	Year	QTL	KW ^a	Group	Position	Locus	Thrs.	LOD	2-LOD	1-LOD interval	2-LOD	$\mu_{ac}\{00\}$	$\mu_{ad}\{00\}$	$\mu_{bc}\{00\}$	$\mu_{bd}\{00\}$	R ² (%) ^c	
(Epi)afzelechin or phloretin hexose 7.53	2013	<i>qAfzhex-7.53-IV-2</i>	-	LGIV-2	57.657	F00645-26:A>C-LG4	5.0	5.4	57.2	57.2	58.9	58.9	-0.212	-0.283	-0.535	-0.581	12
		<i>qAfzhex-7.53-VI-1</i>	-	LGVI-1	17.875	M00766-58:T>A-LG6		8.7	13.4	13.4	21.4	24.4	-0.213	-0.512	-0.535	-0.805	22.2
		<i>qAfzhex-7.53-VI-2</i>	*	LGVI-2	39.556	EMFv010-170h		10.9	36.3	38.6	43.1	49.3	-0.212	-0.607	-0.054	-0.540	27.7
		<i>qAfzhex-7.53-VI-7</i>	****	LGVI-7	19.51	EMFv010-180h		7.5	13.7	18.1	29.9	31.3	-0.212	-0.502	-0.059	-0.409	14.3
	2014	<i>qAfzhex-7.53-I-2</i>	***	LGI-2	51.742	F13347-55:C>T-LG1	5.1	8.5	47.4	50.7	52.7	53.6	-0.187	-0.261	-0.704	-0.571	17.6
		<i>qAfzhex-7.53-V-1</i>	-	LGVI-1	45.414	15736-34:A>G-LG5		6.7	40.0	44.4	51.1	51.1	-0.187	-0.160	-0.047	0.314	13.4
		<i>qAfzhex-7.53-VI-2</i>	****	LGVI-2	60.478	M14935-28:C>T-LG6		6.3	45.6	47.6	60.5	60.5	-0.286	-0.541	0.006	-0.387	15.9
		<i>qAfzhex-7.53-VI-7</i>	****	LGVI-7	23.672	M20868-26:G>A-LG6		10.4	13.7	15.6	25.5	27.5	-0.187	-0.597	0.020	-0.333	22.5
(Epi)afzelechin or phloretin hexose 8.29	2013	<i>qAfzhex-8.29-I-2</i>	****	LGI-2	84.408	11980-57:G>A-LG1	5.1	5.7	83.6	83.6	85.8	85.8	0.076	0.310	0.326	-0.100	13.2
		<i>qAfzhex-8.29-VI-1</i>	****	LGVI-1	9.962	M17235-40:A>T-LG6		13.0	7.5	7.5	17.9	17.9	0.076	-0.465	-0.406	-0.919	42
		<i>qAfzhex-8.29-VI-2</i>	*	LGVI-2	47.777	EMFn228-268		5.4	27.7	29.7	52.3	60.5	0.076	0.180	0.416	0.754	21.5
	2014	<i>qAfzhex-8.29-V-4</i>	-	LGVI-4	28.722	25825-6:G>A-	5.3	5.3	28.3	28.3	29.2	29.2	0.493	1.125	0.548	0.415	15
		<i>qAfzhex-8.29-VI-1</i>	****	LGVI-1	26.616	EMFv006-208		15.5	26.2	26.2	28.3	28.3	0.493	-0.041	-0.121	-0.493	43.2
		<i>qAfzhex-8.29-VI-2</i>	***	LGVI-2	38.625	M20098-16:G>A-LG6		8.1	36.3	36.3	45.6	45.6	0.493	0.856	0.490	1.014	18.1
(Epi)afzelechin or phloretin hexose 8.8	2013	<i>qAfzhex-8.8-VI-7</i>	*	LGVI-7	36.878	M27657-20:C>T-LG6	4.9	5.2	31.3	35.1	36.9	36.9	0.875	1.132	1.105	1.239	19.5
2014	<i>qAfzhex-8.8-VI-1</i>	****	LGVI-1	13.386	M14012-48:C>T-LG6	4.9	6.0	7.5	12.7	28.8	34.6	1.337	1.078	1.091	0.833	26.1	
(Epi)catechin	2013	<i>qCat-5.06-I-2</i>	****	LGI-2	32.342	F28830-24:C>T-LG1	5.1	5.2	31.0	31.0	37.5	42.9	-0.058	-0.061	-0.184	-0.375	16.3
		<i>qCat-5.06-III-3^b</i>	***	LGIII-3	80.559	15653-52:A>G-		4.8	77.6	79.5	81.7	85.1	-0.058	0.131	-0.156	0.103	15
		<i>qCat-5.06-V-3^b</i>	*	LGVI-3	39.456	M21814-37:G>C-LG5		4.6	25.6	25.6	45.3	50.1	-0.058	0.094	-0.244	0.015	14.3
	2014	<i>qCat-5.06-I-2</i>	***	LGI-2	34.534	F41005-30:C>T-LG1	5.2	5.22	34.2	34.2	35.6	35.6	0.325	-0.333	-0.180	-0.155	38.3
		<i>qCat-5.06-V-4</i>	-	LGVI-4	18.746	42748-25:C>T-		6.06	18.3	18.3	19.2	19.2	0.334	1.023	0.368	0.389	16.4
Epicatechin glucuronide 5.17	2013	<i>qCatgluc-5.17-V-4</i>	****	LGVI-4	28.0	37540--	5.1	12.0	26.2	27.7	28.3	28.7	0.426	0.691	0.616	0.752	47.7
		<i>qCatgluc-5.17-V-1</i>	-	LGVI-1	16.1	ChFaM106-155h	5.3	5.8	4.0	15.0	17.4	21.6	-2.111	-1.863	-2.486	-1.538	15.8
		<i>qCatgluc-5.17-V-4</i>	****	LGVI-4	34.9	29488-18:C>T-		12.7	27.7	31.0	36.2	41.1	-2.122	-1.189	-1.189	-0.744	38.1
2013	<i>qCatgluc-5.41-IV-1</i>	*	LGIV-1	47.042	F35515-42:C>T-LG4	5.2	5.48	46.3	46.3	48.6	48.6	0.426	0.277	0.170	0.379	26.2	

Epicatechin glucuronide 5.41		<i>qCatgluc-5.41-V-2</i>	-	LGV-2	17.264	M00247-47:C>G-LG5		6.74	10.0	15.6	18.5	18.5	0.426	0.593	0.517	0.609	21
		<i>qCatgluc-5.41-V-4</i>	****	LGV-4	34.12	FAC003-186/207		12.72	27.7	33.6	39.8	39.8	0.426	0.638	0.638	0.719	25.8
	2014	<i>qCatgluc-5.41-V-4</i>	***	LGV-4	34.12	FAC003-186/207	5.4	11.24	26.6	27.7	41.1	41.1	0.511	0.822	0.822	0.940	33.8
		<i>qCatgluc-5.41-VII-2^b</i>	*	LGVII-2	72.44	M16131-13:A>C-LG7		5.37	72.1	72.1	77.5	81.0	0.511	0.642	0.778	0.550	14.5
		<i>qCatgluc-5.41-VI-7</i>	-	LGVII-7	25.521	37612-45:T>C-		4.49	20.4	22.1	36.5	36.9	0.511	0.254	0.406	0.311	11.7
Cyanidin hexose 5.12	2013	<i>qCyhex-5.12-V-2</i>	***	LGV-2	29.535	M37700-41:T>G-LG4	5.0	5.4	10.0	30.3	41.9	41.9	0.338	0.485	0.455	0.500	15.3
		<i>qCyhex-5.12-V-4</i>	**	LGV-4	33.854	11693-58:C>A-LG5		12.4	23.3	33.6	38.9	39.8	0.341	0.532	0.532	0.633	41.5
	2014	<i>qCyhex-5.12-V-1</i>	-	LGV-1	16.144	ChFaM106-155h	5.2	5.85	2.0	13.8	17.4	21.6	0.373	0.529	0.327	0.603	16.1
		<i>qCyhex-5.12-V-4</i>	****	LGV-4	38.315	18898-64:A>T-		11.73	30.6	33.0	41.1	41.1	0.396	0.686	0.643	0.825	34.7
		<i>qCyhex-5.12-VI-3</i>	-	LGVII-3	16.901	M38290-44:G>A-LG1		5.4	13.7	14.7	23.3	36.7	0.397	0.622	0.397	0.529	13.2
Pelargonidin hexose 5.50	2013	<i>qPghex-5.50-II-3</i>	-	LGVII-3	9.001	13698-23:C>G-	5	5.13	0.0	5.4	18.5	23.6	-0.453	-0.551	-0.667	-0.395	11.1
		<i>qPghex-5.50-V-2</i>	****	LGV-2	17.264	M00247-47:C>G-LG5		11.11	15.6	15.6	18.5	18.5	-0.451	-0.088	-0.332	-0.113	25.9
		<i>qPghex-5.50-VII-4</i>	*	LGVII-4	22.650	24194-52:C>A-LG7		7.26	21.7	21.7	24.7	26.7	-0.451	-0.394	-0.274	-0.717	18.2
	2014	<i>qPghex-5.50-II-2^b</i>	*	LGVII-2	60.346	M37487-47:G>A-	5.2	4.55	37.5	51.8	66.0	69.8	-0.042	-0.225	0.025	-0.173	12.6
		<i>qPghex-5.50-V-2</i>	***	LGV-2	15.590	ChFaM044-226		8.08	0.0	14.2	27.0	30.3	-0.042	0.194	0.062	0.352	24.3
		<i>qPghex-5.50-V-4^b</i>	***	LGV-4	20.281	19863-20:C>T-LG4		4.91	8.6	18.7	24.2	24.6	-0.042	-0.144	-0.144	-0.323	13.5
Pelargonidin malonyl hexose 6.37	2013	<i>qPgmhex-6.37-I-2^b</i>	***	LGI-2	58.192	M31827-35:T>C-LG1	4.9	4.11	39.0	51.7	73.4	99.0	0.757	0.835	1.235	1.261	9.9
		<i>qPgmhex-6.37-VI-1</i>	**	LGVII-1	32.027	F29279-33:T>C-LG6		8.1	30.4	30.9	33.6	33.6	0.757	0.727	0.746	0.010	27
	2014	<i>qPgmhex-6.37-III-1</i>	**	LGVIII-1	28.196	F38699-57:A>G-	5.1	8.24	27.1	27.1	29.3	29.3	1.850	1.960	1.781	1.245	21.4
		<i>qPgmhex-6.37-V-1</i>	*	LGV-1	21.927	22257-11:T>C-LG5		5.66	20.7	21.6	23.7	23.7	1.842	1.916	1.745	2.465	17.1
		<i>qPgmhex-6.37-V-4</i>	***	LGV-4	20.281	19863-20:C>T-LG4		6.04	7.0	19.9	22.8	41.1	1.850	1.520	1.520	1.158	13.2
Pelargonidin rutinoside 5.61	2013	<i>qPgrut-5.61-V-2</i>	****	LGV-2	17.264	M00247-47:C>G-LG5	5.1	5.16	0.0	0.0	18.5	21.8	-0.820	-0.519	-0.699	-0.416	23.1
	2014	<i>qPgrut-5.61-V-2</i>	*	LGV-2	15.59	ChFaM044-226	5.2	6.98	3.9	6.3	18.5	18.5	0.903	0.946	0.930	1.075	18.9
		<i>qPgrut-5.61-V-3</i>	*	LGV-3	13.529	F44050-59:G>A-LG5		7.23	9.2	12.5	14.3	17.0	0.903	0.991	0.857	0.825	20.2
Procyanidin dimer 4.66	2013	<i>qProCydi-4.66-I-2</i>	****	LGI-2	32.342	F28830-24:C>T-LG1	5.2	6.32	26.7	40.0	42.9	50.7	0.140	0.065	-0.148	-0.231	22.5
		<i>qProCydi-4.66-V-3</i>	***	LGV-3	39.456	M21814-37:G>C-LG5		6.11	26.4	27.0	40.0	45.3	0.106	0.370	-0.060	0.210	21.1
Procyanidin dimer 4.89	2013	<i>qProCydi-4.89-I-2</i>	****	LGI-2	32.342	F28830-24:C>T-LG1	5.3	10.52	31.0	31.0	34.2	34.2	1.305	1.270	1.395	1.531	23
		<i>qProCydi-4.89-IV-1</i>	**	LGIV-1	101.794	F14784-64:G>A-LG5		6.18	100.3	100.3	103.2	103.2	1.245	0.953	0.877	1.140	52.5
	2014	<i>qProCydi-4.89-II-1</i>	*	LGVII-1	93.134	ChFaM126-188h	5.1	5.19	85.9	88.9	93.1	93.1	1.147	1.066	1.054	1.293	36.9
		<i>qProCydi-4.89-IV-1</i>	-	LGIV-1	101.794	F14784-64:G>A-LG5		5.62	84.6	89.4	103.2	103.2	1.147	0.884	0.775	0.987	52.2
Procyanidin dimer 6.21	2013	<i>qProCydi-6.21-III-3</i>	*	LGVIII-3	80.846	ChFaM159-262h	6	7.17	78.5	79.5	81.7	82.3	0.661	0.952	0.754	0.987	23.6
		<i>qProCydi-6.21-IV-1^b</i>	****	LGIV-1	11.263	M42707-57:A>C-LG1		5.66	9.2	9.2	13.3	13.3	0.661	0.797	0.551	0.486	19.2
		<i>qProCydi-6.21-V-3</i>	***	LGV-3	28.221	F27887-44:A>T-LG5		8.59	25.6	26.4	29.4	29.4	0.661	1.142	0.632	0.854	39.7
2014	<i>qProCydi-6.21-I-2</i>	***	LGI-2	15.406	F18760-32:G>A-LG1	5.1	6.96	14.7	14.6	16.5	16.5	0.192	0.192	-0.142	-0.142	23.8	

Chapter 3: Quantitative Trait Loci and Underlying Candidate Genes Controlling Secondary Metabolites in Strawberry Fruit

		<i>qProCydi-6.21-VI-1</i>	*	LGVI-1	9.962	M17235-40:A>T-LG6		4.04	6.5	6.5	11.0	11.0	0.192	0.138	0.165	0.466	16
Procyanidin tetramer 4.46	2013	<i>qProCytet-4.46-I-2</i>	****	LGI-2	41.304	14064-18:T>C-	5.4	6.89	32.3	39.0	42.9	42.9	1.255	1.526	0.735	0.728	25.8
		<i>qProCytet-4.46-V-3</i>	****	LGV-3	10.145	M12243-63:G>A-LG5		6.4	2.6	9.2	16.2	17.4	1.255	1.803	1.078	1.758	23.5
	2014	<i>qProCytet-4.46-II-2</i>	-	LGII-2	41.783	M13933-57:T>G-	5.3	8.5	40.4	40.4	42.2	42.2	2.576	1.176	0.546	0.988	55.5
		<i>qProCytet-4.46-VI-1</i>	**	LGVI-1	10.986	12065-68:G>A-LG6		5.79	10.0	10.0	12.7	12.7	2.655	2.949	2.785	3.507	16.2
Procyanidin tetramer 4.77	2013	<i>qProCytet-4.77-I-2</i>	****	LGI-2	32.342	F28830-24:C>T-LG1	5.6	7.34	23.2	31.0	34.3	34.3	1.370	1.038	0.870	0.789	28.4
		<i>qProCytet-4.77-IV-2</i>	-	LGIV-2	79.498	F10855-63:C>T-LG4		7.49	78.9	78.9	80.6	80.6	1.174	1.388	1.023	0.812	27.5
	2014	<i>qProCytet-4.77-V-4^b</i>	**	LGIV-4	4.054	F26824-60:A>G-LG5	5.1	5	0.0	0.0	9.7	10.1	-0.083	0.450	0.418	0.520	25.5
Procyanidin tetramer 5.18	2013	<i>qProCytet-5.18-I-2</i>	****	LGI-2	41.304	14064-18:T>C-	5.2	7.21	23.2	32.3	49.3	50.7	0.188	0.060	-0.144	-0.220	19.5
		<i>qProCytet-5.18-IV-1</i>	****	LGIV-1	11.263	M42707-57:A>C-LG1		6.32	4.9	9.2	13.3	19.4	0.188	0.206	-0.023	-0.163	18.3
		<i>qProCytet-5.18-V-3</i>	****	LGIV-3	34.128	F14913-9:A>G-LG5		5.58	4.6	29.7	40.1	45.3	0.188	0.402	0.016	0.274	14.3
	2014	<i>qProCytet-5.18-VI-5</i>	-	LGVI-5	29.739	17806-7:C>T-	5.2	5.73	23.4	25.4	32.2	38.4	1.078	1.028	1.225	1.012	24.8
Procyanidin tetramer 5.45	2013	<i>qProCytet-5.45-I-2</i>	**	LGI-2	32.342	F28830-24:C>T-LG1	5.2	5.57	31	31	34.2	35.7	-0.220	-0.295	-0.483	-0.476	3.6
		<i>qProCytet-5.45-III-4</i>	-	LGIII-4	48.538	F10928-56:A>T-LG3*		7.66	46.8	46.8	51.0	58.4	-0.249	-0.614	-0.171	-0.838	28.7
		<i>qProCytet-5.45-IV-1</i>	*	LGIV-1	101.794	F14784-64:G>A-LG5		7.33	100.3	100.3	103.2	103.2	-0.253	0.130	0.608	-0.128	31.4
	2014	<i>qProCytet-5.45-I-1</i>	-	LGI-1	16.710	F12638-50:T>C-LG1	4.9	5.8	13.8	13.8	18.8	20.3	-0.460	0.133	0.091	0.087	18.8
	<i>qProCytet-5.45-VI-1</i>	-	LGVI-1	7.523	26030-63:A>G-LG6		7.25	6.6	6.6	9.5	10	-0.460	-0.235	-0.719	0.077	27.9	
Procyanidin trimer 3.26	2013	<i>qProCytri-3.26-I-1</i>	****	LGI-2	32.342	F28830-24:C>T-LG1	5.1	6.31	23.2	31	34.2	42.9	0.068	-0.013	-0.243	-0.292	18.3
		<i>qProCytri-3.26-IV-2^b</i>	*	LGIV-2	79.498	F10855-63:C>T-LG4		4.74	78.9	78.9	81.1	94.6	0.025	0.191	-0.041	-0.172	12
		<i>qProCytri-3.26-V-3^b</i>	***	LGIV-3	28.221	F27887-44:A>T-LG5		4.57	25.6	27	40.1	45.3	0.025	0.381	0.118	0.179	15.1
Procyanidin trimer 5.01	2013	<i>qProCytri-5.01-III-3</i>	**	LGIII-3	80.846	ChFaM159-262h	5.3	6.45	78.5	79.5	81.7	82.3	1.404	1.204	1.390	1.213	24.5
		<i>qProCytri-5.01-IV-1^b</i>	*	LGIV-1	118.296	ChFvM232-188		4.48	86.6	91.4	120.3	128.3	1.404	1.404	1.260	1.260	16.4
		<i>qProCytri-5.01-V-3</i>	**	LGIV-3	28.221	F27887-44:A>T-LG5		7.39	25.6	25.6	29.4	29.4	1.404	1.096	1.338	1.200	33.2
Procyanidin trimer 5.10	2013	<i>qProCytri-5.10-I-2</i>	****	LGI-2	32.342	F28830-24:C>T-LG1	5.2	5.92	23.2	31	42.9	50.7	0.079	0.074	-0.136	-0.290	21.5
		<i>qProCytri-5.10-V-3^b</i>	***	LGIV-3	29.735	F14812-61:G>C-LG5		5.08	25.6	27	44.2	54.1	0.070	0.302	-0.087	0.102	18.6
Procyanidin trimer 5.20	2013	<i>qProCytri-5.20-I-2</i>	****	LGI-2	35.672	F32156-17:A>C-LG1	5.1	8.97	31	34.5	37.5	41	-0.364	-0.088	-0.417	-0.531	23.4
		<i>qProCytri-5.20-IV-1</i>	****	LGIV-1	101.794	F14784-64:G>A-LG5		7.5	100.3	100.3	103.2	103.2	-0.362	0.039	0.209	-0.273	37.8
		<i>qProCytri-5.20-V-3</i>	****	LGIV-3	30.614	F13243-54:C>T-LG5		7.69	27	29.4	31.7	44.2	-0.362	-0.183	-0.553	-0.218	15.6
Propelargonidin dimer 5.24	2013	<i>qProPgdi-5.24-I-2^b</i>	****	LGI-2	32.342	F28830-24:C>T-LG1	5	4.27	20.3	31	35	56.4	0.321	0.095	0.026	-0.093	16.2
		<i>qProPgdi-5.24-II-5</i>	-	LGII-5	59.178	M21394-35:A>G-LG2		5.14	47.4	47.4	60.4	68.6	0.178	0.566	0.338	0.279	14.9
		<i>qProPgdi-5.24-IV-1^b</i>	*	LGIV-1	17.609	F37395-32:C>T-LG4		4.19	7.8	17.4	28.2	28.2	0.178	0.344	0.209	0.024	11.7
		<i>qProPgdi-5.24-IV-3</i>	**	LGIV-3	76.413	F01491-66:G>A-LG5		5.78	75.1	75.1	78.4	78.4	0.177	-0.089	-0.238	-0.277	16.7
Propelargonidin dimer 5.57	2013	<i>qProPgdi-5.57-I-2^b</i>	-	LGI-2	32.342	F28830-24:C>T-LG1	5.4	4.64	31	31	58.9	60.8	-0.105	-0.033	-0.133	-0.540	18.3
		<i>qProPgdi-5.57-V-2</i>	****	LGIV-2	15.590	ChFaM044-226		8.68	10	11.2	19.3	25.8	-0.108	0.017	-0.584	-0.578	34.2
	2014	<i>qProPgdi-5.57-II-1</i>	***	LGII-1	83.577	F12978-43:G>T-LG2	4.9	6.23	81	81	92.9	92.9	0.864	1.072	1.044	0.629	20.5
	<i>qProPgdi-5.57-V-2</i>	***	LGIV-2	18.506	M30873-45:T>G-LG5		5.1	5.8	10	21.8	25.9	0.864	0.899	0.691	0.514	14.3	

Propelargonidin dimer 6.52	2013	<i>qProPgdi-6.52-VI-6</i>	***	LGVI-6	29.419	FaQR-S1	4.8	6.48	21.6	25.9	30.7	34.6	0.350	0.532	0.696	0.836	27.5
		<i>qProPgdi-6.52-VII-4^b</i>	*	LGVII-4	11.064	F10940-16:T>C-LG7		4.27	6.4	6.4	26.7	27.2	0.350	0.567	0.726	0.341	18.5
	2014	<i>qProPgdi-6.52-II-4</i>	-	LGII-4	9.033	25187-5:T>C-	5	5	7	7	14	14	1.374	0.879	1.391	1.173	18
Propelargonidin dimer 6.87		<i>qProPgdi-6.52-V-2</i>	***	LGV-2	19.784	F13908-63:A>G-LG5		6.46	0	15.6	25.9	27	1.379	1.429	1.008	0.943	20.3
	2013	<i>qProPgdi-6.87-I-2</i>	****	LGI-2	37.496	F40498-26:G>A-LG1	5.2	6	32.3	35.7	39	41	-0.334	0.129	-0.043	-0.305	31.4
		<i>qProPgdi-6.87-IV-3</i>	****	LGIV-3	76.413	F01491-66:G>A-LG5		7	75.1	75.1	78.4	78.4	-0.335	-0.524	-0.768	-0.669	19.2
		<i>qProPgdi-6.87-V-2</i>	****	LGV-2	11.221	M36394-40:C>A-LG5		7.42	0	10	18.5	18.5	-0.334	-0.009	-0.254	0.055	23.3
	2014	<i>qProPgdi-6.87-IV-3</i>	-	LGIV-3	39.736	F33888-13:A>G-LG4	5.1	8.18	38.8	38.8	40.5	40.5	-0.103	0.344	0.016	-0.416	32.8
		<i>qProPgdi-6.87-V-3</i>	*	LGV-3	46.780	M29391-61:C>T-LG5		5.93	31.7	41.1	50.1	55.9	-0.103	-0.169	-0.584	-0.107	20.9
Propelargonidin dimer 3.99	2014	<i>qProPgdi-3.99-I-2</i>	***	LGI-2	45.516	F39616-66:A>T-LG1	4.9	5.27	44.4	44.4	58	65.7	0.515	0.674	0.393	0.203	18.2
		<i>qProPgdi-3.99-II-2</i>	-	LGII-2	68.30	M33690-38:C>G-LG2		4.58	67.2	67.9	69.1	69.1	0.515	0.091	0.188	0.308	15.2
Propelargonidin trimer 5.41	2013	<i>qProPgtri-5.41-I-2</i>	****	LGI-2	28.179	F00721-39:G>A-LG1	5.1	6.77	26.7	26.7	29.9	29.9	1.024	1.024	0.518	0.518	21.4
		<i>qProPgtri-5.41-III-2^b</i>	**	LGIII-2	81.931	M22246-19:T>G-		4.64	74.8	75.9	93.8	104.5	1.038	1.450	0.983	1.067	14
		<i>qProPgtri-5.41-VII-1</i>	*	LGVII-1	43.311	M35119-35:A>G-LG7		5.1	36.6	40.8	53.4	58.4	1.024	0.660	1.249	1.153	15.3
	2014	<i>qProPgtri-5.41-V-1</i>	-	LGV-1	41.304	F15028-27:G>T-LG5	5.1	6.22	34.7	40.9	41.3	51.1	3.037	4.038	3.494	3.260	15.2
	<i>qProPgtri-5.41-V-3</i>	-	LGV-3	28.221	F27887-44:A>T-LG5		8.88	27	27	29.4	29.4	3.037	1.608	1.566	2.271	41.9	
Propelargonidin trimer 5.46	2013	<i>qProPgtri-5.46-I-2</i>	****	LGI-2	41.304	14064-18:T>C-	5.4	5.5	31	39	42.9	48.4	1.400	1.457	0.838	0.943	16.5
Propelargonidin trimer 5.63	2013	<i>qProPgtri-5.63-I-2</i>	****	LGI-2	14.611	F11045-38:C>T-LG1	5.1	7.14	13.1	13.1	23.2	23.2	0.254	0.254	-0.032	-0.032	22.3
		<i>qProPgtri-5.63-V-2^b</i>	****	LGV-2	11.221	M36394-40:C>A-LG5		4.7	0	10	17.3	29.5	0.254	0.480	0.225	0.406	9.3
		<i>qProPgtri-5.63-VII-2</i>	****	LGVII-2	37.205	M26148-15:G>A-LG7		5.18	20.5	35.9	39.2	44.8	0.247	0.007	0.005	-0.163	21.1
Propelargonidin trimer 6.50	2013	<i>qProPgtri-6.50-I-2</i>	****	LGI-2	14.611	F11045-38:C>T-LG1	5	6.28	13.1	13.1	15.4	20.3	0.972	0.972	0.779	0.779	21.1
		<i>qProPgtri-6.50-V-2</i>	*	LGV-2	15.590	ChFaM044-226		5.67	0	0	17.3	21.8	0.972	1.156	1.128	1.210	18.8
Propelargonidin trimer 6.85	2013	<i>qProPgtri-6.85-IV-3</i>	***	LGIV-3	76.413	F01491-66:G>A-LG5	5.1	5.71	59.2	62.7	78.4	85.9	-0.256	-0.613	-0.712	-0.792	17.6
		<i>qProPgtri-6.85-IV-4</i>	-	LGIV-4	17.403	F14526-66:T>A-LG4		5.26	3.4	15.2	20.2	20.2	-0.259	0.027	-0.027	0.188	17.5
		<i>qProPgtri-6.85-V-2</i>	****	LGV-2	11.221	M36394-40:C>A-LG5		7.4	0	10	14.2	17.3	-0.259	0.148	-0.090	0.280	23.7
	2014	<i>qProPgtri-6.85-II-5</i>	-	LGII-5	56.418	M43853-58:C>A-LG2	5.1	5.46	55.7	55.7	56.9	56.9	0.071	-0.350	-0.300	0.189	19.4
		<i>qProPgtri-6.85-IV-3</i>	*	LGIV-3	60.903	M14557-31:C>A-*		5.66	58.4	59.2	61.7	66.3	0.071	0.327	0.035	-0.155	19.2
		<i>qProPgtri-6.85-VII-3</i>	*	LGVII-3	47.581	F39028-48:A>C-LG7		5.45	32.9	37	50	54.8	0.082	0.370	0.441	0.564	17.2
Pelargonidin acetyl hexoside 6.38	2013	<i>Pgacehex-6.38-V-1^b</i>	*	LGV-1	31.78	M11633-54:T>A-	5	4.7	29.8	31.2	33.7	35.1	1.147	1.268	0.997	0.752	15.6
		<i>Pgacehex-6.38-V-2</i>	*	LGV-2	18.26	M30873-45:T>G-LG5		6.11	15.6	17.3	27.8	30.3	1.128	1.641	1.399	1.665	22.0
		<i>Pgacehex-6.38-V-4</i>	***	LGV-4	38.93	40256-25:T>G-LG5		5.79	26.7	27.3	40.8	42.1	1.146	1.243	1.224	0.772	18.9
	2014	<i>Pgacehex-6.38-V-2</i>	***	LGV-2	8.99	F32504-65:T>G-LG5	5.1	5.34	0	2	16.6	21.7	0.944	1.516	1.197	1.823	17.5

		<i>Pgacehex-6.38-V-4</i>	***	LGIV-4	20.28	19863-20:C>T-LG4		7.48	18.3	18.4	22.6	23.3	0.983	0.536	0.536	-0.042	23.8
Pelargonidin acetyl hexoside 6.91	2013	<i>Pgacehex-6.91-IV-3</i>	***	LGIV-3	35.02	CFVCT005-100	5.2	5.85	32.2	33.2	36.3	36.7	-0.768	-1.547	-0.981	-1.289	23.1
		<i>Pgacehex-6.91-V-2</i>	***	LGIV-2	28.84	M37700-41:T>G-LG4		9.8	27	27	30.3	30.3	-0.784	0.116	-0.394	-0.215	42.8
		<i>Pgacehex-6.91-VI-6</i>	*	LGVI-6	30.10	F11188-48:A>G-LG6		7.03	27.7	29.4	30.7	30.7	-0.768	0.101	-0.383	-0.411	32.5
	2014	<i>Pgacehex-6.91-V-2</i>	***	LGIV-2	23.85	ChFaM120-184	5.2	6.49	14.2	18.5	27.8	35.6	1.184	1.520	1.466	1.928	29.4
Quercetin-acetylhexose 7.89	2013	<i>Querahex-7.89-V-4</i>	****	LGIV-4	28.03	37540--	5.5	11.15	26.2	27.7	38.7	38.7	0.370	0.816	0.659	0.782	44.0
Quercetin-glucuronide 7.10	2013	<i>QuerGn-7.10-VII-1</i>	**	LGVII-1	34.46	21227-23:G>T-LG7	5.1	5.31	31.8	32.9	41.8	42.2	0.645	0.555	0.764	0.667	21.7
	2014	<i>QuerGn-7.10-III-3</i>	**	LGIII-3	70.89	37665--	5.2	5.68	70.1	70.1	72.1	72.1	1.568	1.299	1.144	1.349	17.1
		<i>QuerGn-7.10-III-4^b</i>	*	LGIII-4	49.58	F29568-22:A>G-LG3		4.65	44.1	48.5	50.6	51	1.574	1.466	1.809	1.754	12.5
		<i>QuerGn-7.10-VI-1</i>	-	LGVI-1	3.04	39018-54:A>G-LG6		6.08	0	0	5	6.6	1.569	1.164	1.333	1.507	17.3
Quercetin malonylhexose 7.45	2013	<i>Quermhex-7.45-IV-3</i>	**	LGIV-3 C2		F35038-25:T>C-	4.9	5.33	39.7	40.7	41.6	41.6	-0.189	-0.802	0.000	-0.065	15.9
		<i>Quermhex-7.45-V-2</i>	***	LGIV-2	17.26	M00247-47:C>G-LG5		5.13	0	15.6	36.6	49.1	-0.189	0.195	0.109	0.476	13.7
	2014	<i>Quermhex-7.45-II-1</i>	*	LGII-1	21.25	16799-47:A>G-LG2	5.2	5.36	19	20	24.6	30.8	1.738	1.096	1.504	1.367	15.7
		<i>Quermhex-7.45-II-5^b</i>	-	LGII-5	47.21	34721-32:C>A-LG2		4.7	35.7	46.8	48.3	59.1	1.746	1.561	1.561	2.127	14.0
		<i>Quermhex-7.45-V-3</i>	*	LGIV-3	51.45	M38469-17:A>C-LG5		6.49	31.7	50.6	52.5	57.7	1.746	1.645	1.898	1.158	18.1
		<i>Quermhex-7.45-VI-3</i>	*	LGVI-3	41.97	F34354-6:C>T-LG6		5.76	38.9	38.9	45	46	1.746	1.227	1.032	1.050	16.9
Quercetin hexose 7.14	2013	<i>Querhex-7.14-VI-4</i>	-	LGVI-4	41.51	F11777-36:G>A-LG6	5	6.76	33	35	44.3	44.3	-0.581	-1.366	-0.790	-0.902	53.0
Rutin 5.59	2014	<i>Rutin-5.59-III-2</i>	***	LGIII-2	37.86	M11179-32:C>T-LG3	5	5.06	18.8	27.7	39.9	40.1	-0.596	-0.072	-0.321	-0.255	16.6
Rutin 6.91	2013	<i>Rutin-6.91-V-4</i>	****	LGIV-4	37.81	17685-25:A>G-LG5	5.3	6.12	20.8	23.3	39.8	39.8	0.508	0.658	0.687	0.735	26.9
	2014	<i>Rutin-6.91-V-4</i>	****	LGIV-4	28.28	23801-15:G>A-LG5	5	5.41	22.8	24.2	28.7	28.7	0.371	0.651	0.627	0.611	11.4
		<i>Rutin-6.91-VII-2</i>	*	LGVII-2	46.80	21145-30:G>A-LG7		6.22	43.5	44.5	50.9	58.5	0.371	0.502	0.739	0.352	21.1
Diosmetin acetylhexoside 8.29	2013	<i>qDmacehex-8.29-I-2</i>	****	LGI-2	84.41	11980-57:G>A-LG1	5.3	4.25	83.6	83.6	85.4	92.6	1.603	1.885	1.549	1.242	6.8
		<i>qDmacehex-8.29-III-1</i>	*	LGIII-1	37.11	M33766-39:C>T-LG3*		4.42	33.7	34.7	39.6	42.9	1.603	1.865	1.688	1.236	8.5
		<i>qDmacehex-8.29-VI-1</i>	****	LGVI-1	9.96	M17235-40:A>T-LG6		13.28	7.5	8.5	10.9	16.7	1.603	0.700	0.717	0.116	33.6
		<i>qDmacehex-8.29-VI-2</i>	-	LGVI-2	31.81	M13555-65:A>T-LG6		4.48	27.7	29.7	32.8	35.6	1.603	2.305	2.049	1.770	7.0
	2014	<i>qDmacehex-8.29-III-1</i>	****	LGIII-1	27.13	BFACT043-202**	5.5	5.68	5.1	17.2	29.2	36.5	1.754	1.456	1.704	1.065	21.5
	<i>qDmacehex-8.29-VI-1</i>	****	LGVI-1	17.88	M00766-58:T>A-LG6		6.63	14.1	15.1	18.9	26.1	1.755	1.139	0.894	1.036	28.3	
Eriodictyol hexose 5.50	2013	<i>qEriodhex-5.50-V-2</i>	****	LGIV-2	17.26	M00247-47:C>G-LG5	5.2	6.34	0	15.6	18.3	34.7	0.811	1.120	0.961	1.151	23.9
	2014	<i>qEriodhex-5.50-V-2</i>	****	LGIV-2	17.26	M00247-47:C>G-LG5	5	5.82	0	15.2	25.9	30.3	1.032	1.201	1.145	1.327	21.0

		<i>qEriodhex-5.50-V-4</i>	**	LGV-4	20.28	19863-20:C>T-LG4		5.35	13.1	19.9	23.3	34.1	1.032	0.900	0.900	0.768	18.4
	2013	<i>qEriodhex-6.04-II-3</i>	-	LGII-3	17.41	M14564-7:A>G-LG2	5.2	6.9	8.2	16.9	18.5	19.5	-0.367	-0.598	-0.857	-0.526	18.8
		<i>qEriodhex-6.04-V-2</i>	****	LGV-2	17.26	M00247-47:C>G-LG5		6.32	0	0	18.5	30.3	-0.367	0.029	-0.250	-0.051	16.7
		<i>qEriodhex-6.04-VI-1^b</i>	*	LGVI-1	19.57	M43680-36:G>A-LG6		5.1	17.9	17.9	20.6	23.3	-0.367	-0.223	-0.385	-0.598	13.7
Eriodictyol hexose 6.04	2014	<i>qEriodhex-6.04-II-2</i>	-	LGII-2	67.87	M37172-64:T>A-LG2	5	7.01	67.2	67.2	68.1	68.3	0.355	-0.171	0.103	0.078	16.3
		<i>qEriodhex-6.04-IV-4</i>	-	LGIV-4	60.22	F21176-51:G>A-LG4		5.8	58.8	58.8	62.2	62.2	0.355	0.355	0.005	0.005	11.9
		<i>qEriodhex-6.04-V-2</i>	**	LGV-2	17.26	M00247-47:C>G-LG5		10.53	15.2	15.3	18.3	21.8	0.355	0.838	0.465	0.999	26.2
		<i>qEriodhex-6.04-V-4</i>	***	LGV-4	23.29	M05642-52:G>A-LG5		9.45	18.3	18.3	24.2	24.2	0.356	0.338	0.205	-0.198	23.5
	2013	<i>qlrh-Gn-7.94-II-2</i>	****	LGII-2	71.55	29030-61:T>C-	5	7.83	63.9	63.9	73.8	74.8	-0.664	-0.178	-1.135	-0.452	20.7
		<i>qlrh-Gn-7.94-V-4</i>	****	LGV-4	55.49	SVP-445		7.34	46.8	47.8	56.5	60.1	-0.664	0.052	-0.200	0.443	27.2
Isorhamnetin glucuronide 7.94	2014	<i>qlrh-Gn-7.94-II-2</i>	****	LGII-2	75.76	12317-55:A>G-LG2	5.2	10.1	65.1	75.2	84.7	96.5	-0.421	-0.166	-1.472	-0.834	37.7
		<i>qlrh-Gn-7.94-II-3</i>	**	LGII-3	56.61	M32484-68:C>T-LG2		5.86	28.9	53.2	57.6	57.6	-0.421	-0.827	0.024	0.339	26.1
		<i>qlrh-Gn-7.94-V-4</i>	**	LGV-4	51.07	M35315-25:A>G-LG1		5.26	45.33	46.8	53.7	55.5	-0.421	0.313	-0.005	0.426	19.4
						ChFaM009- 590/598/600											
Kaempferol acetylhexose 8.65	2014	<i>qK-acehex-8.65-III-1</i>	***	LGIII-1	39.27	M28178-10:T>G-	5.2	5.21	35.5	38	39.4	42.5	0.353	0.146	-0.020	0.112	3.5
		<i>qK-acehex-8.65-V-1</i>	*	LGV-1	52.70			8.91	50.2	52.6	54.1	54.1	0.361	0.425	1.233	1.112	53.1
		<i>qK-acehex-8.65-VII-4</i>	*	LGVII-4	68.59	F17544-23:C>T-LG7		9.67	63.6	65.6	68.6	68.6	0.353	1.129	0.337	1.097	40.3
	2013	<i>K-couhex.7.47-III-1</i>	***	LGIII-1 LGVII-4	47.82	M32014-34:A>G-LG2*	4.8	5.84	26.1	44	49.5	50.6	-0.765	-0.453	-0.864	-0.984	24.8
		<i>K-couhex.7.47-VII-4</i>	*		25.65	F45819-16:G>T-LG7		5.95	21.7	22.7	28.2	29	-0.772	-0.503	-0.255	-0.925	27.3
Kaempferol coumaroyl hexose 7.47	2014	<i>K-couhex.7.47-I-2</i>	-	LGI-2	84.41	11980-57:G>A-LG1	5	5.09	80.4	83.6	97.4	99	-0.357	-0.403	-0.669	-0.781	10.6
		<i>K-couhex.7.47-V-2</i>	**	LGV-2	0.00	22161-13:G>T-LG5		6.76	0	0	7	10	-0.357	0.030	0.179	0.212	19.0
		<i>K-couhex.7.47-V-4</i>	*	LGV-4 LGVII-2	33.61	17622-5:A>T-		5.67	19.9	32.3	34.1	43.2	-0.357	-0.489	-0.489	-0.854	14.6
		<i>K-couhex.7.47-VII-2</i>	*		46.80	21145-30:G>A-LG7		5.91	44.8	44.8	50.9	53.6	-0.357	-0.047	0.125	-0.410	17.8
	2013	<i>K-Gn-7.72-V-4</i>	**	LGV-4	18.18	12897-32:T>C-LG4	5.1	5.07	16.7	17.4	18.4	27.7	0.940	0.735	0.789	0.874	20.4
Kaempferol- glucuronide 7.72	2014	<i>K-Gn-7.72-IV-1</i>	*	LGIV-1	19.44	M42810-48:T>C-LG4	5.1	5.13	17.7	17.7	21.5	23.5	1.069	0.786	0.994	0.928	17.0
		<i>K-Gn-7.72-V-1^b</i>	*	LGV-1 LGVII-1	21.93	22257-11:T>C-LG5		5.04	15.7	21.6	28.7	30.8	1.068	1.113	0.986	1.369	20.0
		<i>K-Gn-7.72-VII-1</i>	-		43.20	F25909-50:T>C-LG7		5.45	34.5	36.6	48	48	1.069	1.282	1.232	0.981	19.5
	2013	<i>K-hex-5.17-V-4</i>	****	LGV-4	38.72	39476-17:C>T-	5.1	9.81	27.7	33.6	39.8	41.1	0.476	0.641	0.654	0.758	40.1
Kaempferol- hexose 5.17	2014	<i>K-hex-5.17-V-1</i>	-	LGV-1	16.14	ChFaM106-155h	5.4	8.14	13.7	15	17.4	17.6	0.363	0.501	0.281	0.604	23.5
		<i>K-hex-5.17-V-4</i>	****	LGV-4	34.92	29488-18:C>T-		10.98	33.9	34.1	35.9	42.7	0.388	0.589	0.589	0.755	30.4
		<i>K-hex-5.17-VI-3</i>	-	LGVI-3	16.90	M38290-44:G>A-LG1		6.18	14.7	15.7	22.9	24.2	0.388	0.637	0.414	0.501	15.1
Kaempferol- hexose 5.51	2013	<i>K-hex-5.51-II-2</i>	-	LGII-2	15.90	BFACT002-184	5.4	6.35	13.7	13.7	17.8	18.8	0.472	-0.740	-0.647	-0.450	15.8
		<i>K-hex-5.51-IV-1</i>	-	LGIV-1	44.83	F36234-63:C>T-		6.16	42.5	43.5	45.8	45.8	0.460	-0.136	-0.328	0.145	7.5

		<i>K-hex-5.51-V-2</i>	****	LGVI-2	17.26	M00247-47:C>G-LG5		28.1	15.3	15.6	18.3	19.8	0.460	0.869	-1.020	-0.886	51.9
	2014	<i>K-hex-5.51-V-2</i>	****	LGVI-2	16.59	ChFaM044-226	5.5	20.84	12.2	14.2	18.5	19.3	-0.468	-0.057	-2.034	-1.854	66.6
Kaempferol-hexose 7.72	2013	<i>K-hex-7.72-V-4</i>	****	LGVI-4	39.77	12138-40:A>G-LG5	5	7.18	33.6	38.9	40.8	41.1	-0.071	-0.500	-0.464	-0.464	26.8
		<i>K-hex-7.72-VII-4</i>	-	LGVII-4	24.65	F45819-16:G>T-LG7		8.46	22.7	23.6	27.2	27.2	-0.229	-0.069	0.269	-0.395	31.4
	2014	<i>K-hex-7.72-VI-3</i>	***	LGVI-3	26.74	M27561-10:A>T-	5.2	5.29	19.6	19.6	34.1	46.5	0.996	1.242	1.096	0.976	25.6
Kaempferol hexose glucuronide 5.55	2013	<i>K-hexGn-5.55-II-5</i>	*	LGII-5	53.73	M11100-59:C>T-LG5	5.2	6.03	51.8	53	54.7	54.7	0.550	0.443	0.747	0.393	29.6
		<i>K-hexGn-5.55-V-2</i>	*	LGVI-2	34.43	34923--LG5		5.79	18.5	24.9	35.6	39.4	0.636	0.418	0.778	0.620	20.5
	2014	<i>K-hexGn-5.55-III-3</i>	*	LGIII-3	80.56	15653-52:A>G-	5.3	4.68	69.8	70.9	81.7	81.7	0.434	0.129	-0.251	-0.001	15.0
		<i>K-hexGn-5.55-V-2</i>	**	LGVI-2	25.85	ChFaM120-184		7.12	18.5	21.9	28.8	34.4	0.417	-0.227	0.562	0.439	25.9
Kaempferol malonylhexose 8.14	2013	<i>K-malhex-8.14-I-1</i>	-	LGI-1	56.30	12230-15:A>C-	5	5.04	37.9	51	61.5	70.7	-0.173	-0.080	0.033	0.433	24.1
		<i>K-malhex-8.14-VI-3</i>	****	LGVI-3	24.20	10796-19:G>C-LG6		5.63	21.9	23.3	32.9	33.1	-0.176	0.395	-0.011	0.166	20.8
		<i>K-malhex-8.14-VI-6</i>	****	LGVI-6	0.00	M40412-33:T>C-LG6		5.83	0	0	1.6	17.4	0.493	0.050	0.762	0.251	20.2
Kaempferol pentose hexose glucuronide 9.55	2013	<i>K-phGn-9.55-I-1</i>	***	LGI-1	41.61	F13621-28:T>C-LG1	5.6	5.29	37.9	40.1	57.5	61.5	0.262	0.307	0.299	0.677	19.0
		<i>K-phGn-9.55-VI-6</i>	****	LGVI-6	0.00	M40412-33:T>C-LG6		10.25	0	0	8.9	9.6	0.236	0.492	0.461	0.795	33.7
	2014	<i>K-phGn-9.55-VI-6</i>	****	LGVI-6	10.70	BFFv11-05-02-210	5	8.56	0	9.2	12.4	13.6	0.271	0.879	0.470	0.935	31.7
Naringenin chalcone hexose 6.29	2013	<i>NarChhex-6.29-IV-3</i>	****	LGIV-3	61.70	M11824-57:T>A-LG4*	5.1	5.27	45.9	61.1	77.4	98.8	1.040	0.878	1.012	0.879	17.0
		<i>NarChhex-6.29-V-4</i>	****	LGVI-4	37.38	13279-66:G>C-		6.66	34.1	37	42.1	46.3	1.040	1.024	1.024	0.844	22.3
	2014	<i>NarChhex-6.29-III-2</i>	*	LGIII-2	31.35	M27101-53:A>C-	5.1	8.05	28.7	29.6	32.3	32.4	-0.571	-0.034	-0.289	-0.146	20.7
		<i>NarChhex-6.29-III-3</i>	-	LGIII-3	11.60	M23500-33:G>T-		5.27	6.7	9.2	13.8	16.7	-0.571	-0.162	-0.181	-0.305	15.1
		<i>NarChhex-6.29-V-1</i>	*	LGVI-1	21.62	F27289-27:C>G-		4.9	13.8	13.8	34.7	51.1	-0.576	-0.589	-0.698	-0.260	14.5
		<i>NarChhex-6.29-V-4</i>	*	LGVI-4	13.13	28585-19:A>G-		5.9	2.6	11.2	14.2	21.6	-0.571	-0.740	-0.740	-1.065	15.2
Galloyl hexose 2.57	2013	<i>qGallhex-2.57-II-1</i>	***	LGII-1	33.508	F01921-50:C>T-LG2	5	6.12	25.3	32.3	34.2	45.4	0.010	0.076	-0.452	0.046	17.4
		<i>qGallhex-2.57-II-2</i>	****	LGII-2	65.085	M13317-50:C>T-LG2		6.94	58.4	63.5	69.8	96.5	0.010	0.396	-0.011	0.114	15.6
		<i>qGallhex-2.57-VII-1</i>	****	LGVII-1	11.039	F25393-13:C>A-LG7		5.97	9.7	9.7	12.3	30.4	0.010	-0.365	-0.490	-0.488	24.1
	2014	<i>qGallhex-2.57-II-1</i>	***	LGII-1	36.608	F34512-41:C>A-LG2	5	7.15	30.8	33.5	38.9	40.9	0.952	0.655	0.940	0.757	15.3
		<i>qGallhex-2.57-III-2</i>	-	LGIII-2	51.019	F11594-58:G>T-LG2		5.36	47.2	50.2	51.9	59	0.952	1.217	1.099	1.033	10.4
		<i>qGallhex-2.57-V-1</i>	-	LGVI-1	44.420	M33503-35:A>T-LG5		6.78	41.3	42.2	45.4	45.4	0.952	0.799	1.098	0.845	12.4
	<i>qGallhex-2.57-VI-4</i>	-	LGVI-4	54.400	F37041-56:C>A-LG6		6.16	46	52.9	55.8	56.8	0.952	1.193	1.232	1.173	11.5	
		<i>qGallhex-2.57-VII-1</i>	****	LGVII-1	23.344	F10992-38:T>A-LG7		9.12	11	21.7	25.1	27.1	0.952	0.861	1.189	1.186	17.5
Galloyl hexose 2.84	2013	<i>qGallhex-2.84-VI-5</i>	-	LGVI-5	38.364	37297-9:A>T-	5	7.13	33.9	36.6	40.6	44.2	-0.384	-0.197	-0.405	-0.081	19.6
		<i>qGallhex-2.84-VII-3</i>	***	LGVII-3	42.277	27124-23:A>G-		10.78	41.6	41.6	43.9	44.9	-0.382	-0.358	-0.108	-0.579	30.5
		<i>qGallhex-2.84-VII-4</i>	-	LGVII-4	21.678	M44107-31:T>A-LG7		8.56	19.8	19.8	22.7	22.7	-0.384	-0.066	-0.215	-0.620	29.6

Galloyl hexose 3.24	2013	<i>qGallhex-3.24-III-3</i>	**	LGIII-3	80.846	ChFaM159-262h	5	5.94	62.1	78.5	81.7	82.3	0.610	0.666	0.777	0.713	17.6
		<i>qGallhex-3.24-IV-1</i>	*	LGIV-1	31.463	BFACT008-128		5.68	2.9	26.2	33.5	36.6	0.610	0.642	0.770	0.610	18.7
		<i>qGallhex-3.24-V-3</i>	****	LGV-3	6.945	M24308-10:T>G-LG5		9.46	4.6	4.6	8.3	8.3	0.610	0.423	0.621	0.522	29.7
Galloyl hexose 3.65	2014	<i>qGallhex-3.24-II-2</i>	-	LGII-2	93.669	M12424-34:T>C-LG6	5	5.03	77.9	85.1	96.5	96.5	1.419	1.184	1.157	1.148	20.5
		<i>qGallhex-3.24-II-4</i>	***	LGII-4	10.230	42663-7:G>A-		6.74	5.6	9	11.6	14.1	1.419	1.618	1.602	1.341	27
	2013	<i>qGallhex-3.65-I-1^b</i>	*	LGI-1	53.417	23869-49:C>T-	5	4.73	50	51	56.3	56.3	-0.372	-0.657	-0.266	-0.309	13.8
Galloyl hexose 3.65		<i>qGallhex-3.65-IV-4^b</i>	****	LGIV-4	7.677	M12275-49:A>G-		4.9	4.8	4.8	9.6	14.5	-0.372	0.043	-0.320	-0.160	14.4
		<i>qGallhex-3.65-VII-1</i>	***	LGVII-1	15.452	31995-12:G>C-LG7		5.42	8.3	14.3	25.1	28.7	-0.372	-0.187	-0.409	-0.643	15.9
	2014	<i>qGallhex-3.65-II-4</i>	-	LGII-4	31.441	F13323-21:G>T-LG2	5	5.98	30.7	31.2	33.8	33.8	-1.204	-0.783	-0.690	-1.365	22.3
		<i>qGallhex-3.65-V-1</i>	*	LGV-1	40.029	14975-59:A>G-		7.85	34.7	38.6	40.6	42.2	-1.209	-0.714	-1.066	-0.471	25.3
Galloylquinic acid 1.85		<i>qGallhex-3.65-VII-2</i>	*	LGVII-2	51.522	M31664-22:C>T-LG7		7.38	44.8	46.8	53.1	54.1	-1.210	-0.800	-0.424	-0.970	25.9
	2013	<i>qGallquin-1.85-I-3</i>	****	LGI-3	15.730	M23448-51:G>T-	5	18.14	0	14.4	17.2	17.2	0.845	1.069	0.845	1.069	19.8
		<i>qGallquin-1.85-III-2</i>	*	LGIII-2	40.123	M12093-45:C>T-LG3		12.45	37.9	37.9	41.6	41.6	0.845	0.769	0.592	0.826	21.0
		<i>qGallquin-1.85-VI-3</i>	-	LGVI-3	34.875	CTCA-146		8.56	33.1	33.1	36.7	36.7	0.845	1.049	0.993	0.979	16.9
		<i>qGallquin-1.85-VII-3</i>	****	LGVII-3	55.981	F22420-31:A>T-LG7		12.89	54.8	54.8	56.7	56.7	0.845	0.522	0.877	0.581	35.4
Galloylquinic acid 3.05	2014	<i>qGallquin-1.85-I-2^b</i>	*	LGI-2	35.672	F32156-17:A>C-LG1	4.9	4.69	17.2	34.5	37.5	39	0.093	-0.957	-0.639	-1.082	38.9
		<i>qGallquin-1.85-VII-1</i>	-	LGVII-1	32.928	M31995-46:T>A-LG7		6.11	30.8	30.8	34.5	34.5	0.096	0.583	-0.009	-0.280	32.0
Galloylquinic acid 3.35	2013	<i>qGallquin-3.05-I-3</i>	****	LGI-3	15.730	M23448-51:G>T-	4.9	10.42	11.3	14.4	31.8	31.8	-0.653	-0.092	-0.653	-0.092	32.5
		<i>qGallquin-3.05-II-2</i>	*	LGII-2	93.669	M12424-34:T>C-LG6		5.05	65.1	80.2	96.5	96.5	-0.653	-0.483	-1.018	-0.893	20.0
Ellagic acid 7.00	2013	<i>qGallquin-3.35-I-3</i>	****	LGI-3	15.730	M23448-51:G>T-	4.8	7.09	0	14.4	31.8	33.8	0.647	0.921	0.647	0.921	29.9
	2014	<i>qGallquin-3.35-II-4</i>	*	LGII-4	3.479	28117-67:T>C-LG2	5.6	6.88	0	0	4	5.8	0.769	0.511	0.461	1.604	53
Ellagic acid deoxyhexose 6.67		<i>qEA-7.00-VII-2</i>	***	LGVII-2	44.82	SAAT-S2	4.9	5.61	39.2	39.4	51.2	53.1	-0.362	0.003	0.208	0.326	20.6
		<i>qEA-7.00-III-3</i>	**	LGIII-3	95.07	F11907-10:C>T-LG3		5.53	92.44	92.44	96.11	98.11	-0.363	-0.212	-0.871	-0.538	18.1
Ellagic acid deoxyhexose 6.79	2014	<i>qEAdhex-6.67-II-4</i>	***	LGII-4	13.57	11775-27:A>G-LG2	5	7.18	8.38	12.8	14.1	14.1	0.116	-0.157	-0.177	-0.332	25.6
		<i>qEAdhex-6.67-VII-4^b</i>	-	LGVII-4	13.05	F11347-65:C>A-LG7**		4.86	6.44	8.7	17.8	19.8	0.116	0.339	0.277	0.602	17.8
	2013	<i>qEAdhex-6.79-II-4</i>	****	LGII-4	9.03	25187-5:T>C-	5.1	6.57	5.57	8.39	10.23	10.23	0.741	0.931	0.953	0.860	28.0
Ellagic acid deoxyhexose 6.79		<i>qEAdhex-6.79-III-3^b</i>	*	LGIII-3	76.14	M41100-38:G>A-LG3		4.19	70.12	74.1	77.12	105	0.733	0.742	0.877	0.810	16.2
	2014	<i>qEAdhex-6.79-II-4^b</i>	**	LGII-4	13.57	11775-27:A>G-LG2	5.1	3.44	8.38	11.79	14.1	23.66	0.871	0.901	0.931	1.030	9.6
		<i>qEAdhex-6.79-III-3^b</i>	*	LGIII-3	71.16	F23153-22:C>T-LG3		4.91	70.12	70.88	72.13	73.45	0.871	0.870	1.079	0.926	14.3
		<i>qEAdhex-6.79-V-4</i>	-	LGV-4	21.62	ChFaM196-122h		5.05	20.5	20.83	21.9	24.16	0.877	1.077	0.831	0.851	19.4
Ellagic acid hexose 5.87	2013	<i>qEAhex-5.87-I-2</i>	****	LGI-2	54.72	M10828-43:T>G-	6.1	23.34	49.3	54.14	56.25	58.9	0.114	0.925	1.120	1.394	70.7
	2014	<i>qEAhex-5.87-I-2</i>	****	LGI-2	55.38	30785-64:G>T-LG1	5.6	21.31	53.6	54.14	56.25	56.36	0.080	0.819	0.990	1.058	51.4

		<i>qEAhex-5.87-II-4</i>	-	LGII-4	11.79	24012-50:A>G-		6.27	9.03	10.23	12.05	13.57	0.080	0.028	-0.572	0.013	10.3
		<i>qEAhex-5.87-IV-1</i>	-	LGIV-1	33.92	F13436-30:A>G-LG4		7.31	31.46	31.46	35.5	35.5	0.080	0.175	0.650	0.212	11.1
Ellagic acid hexose 6.01	2013	<i>qEAhex-6.01-II-4</i>	****	LGII-4	9.03	25187-5:T>C-	5.2	7.27	8.38	8.38	10.23	10.23	0.395	-0.014	0.049	0.106	29.5
		<i>qEAhex-6.01-III-3^b</i>	-	LGIII-3	86.81	BFACT045-162		4	70.9	75.8	105.2	105.2	0.396	0.347	0.189	0.107	14.8
Galloyl-bis(HHDP)-glucose 6.16	2014	<i>qEAhex-6.01-II-4^b</i>	****	LGII-4	13.57	11775-27:A>G-LG2	5	4.51	11.79	12.1	14.1	14.1	0.137	-0.131	-0.216	-0.317	20.4
	2013	<i>G-BHglu-6.16-IV-1</i>	****	LGIV-1	35.50	ChFaM017-136	5.1	13.99	33.92	33.92	35.8	36.6	-0.621	-0.548	-1.100	-1.154	31.5
		<i>G-BHglu-6.16-V-1^b</i>	-	LGVI-1	18.09	38845--LG5		4.42	2	17.55	18.37	20.56	-0.580	-0.368	-0.506	-0.143	10.8
		<i>G-BHglu-6.16-VI-2</i>	*	LGVI-2	16.03	M31478-44:T>A-LG6		5.55	13.74	13.74	18.8	29.7	-0.620	-0.231	-0.520	-0.300	10.3
		<i>G-BHglu-6.16-VII-3</i>	*	LGVII-3	47.58	F39028-48:A>C-LG7		5.51	42.28	45.11	54.78	55.98	-0.590	-0.541	-0.166	-0.465	10.7
	2014	<i>G-BHglu-6.16-IV-1</i>	***	LGIV-1	41.18	F20883-65:G>T-LG4	4.9	8.16	36.6	36.6	42.16	44.5	0.289	0.711	-0.103	-0.053	28.6
		<i>G-BHglu-6.16-V-1</i>	-	LGVI-1	0.00	M13799-15:T>G-LG5		6.11	0	0	6.9	8.9	0.289	-0.110	-0.661	-0.305	23.3
Galloyl-bis(HHDP)-glucose 6.88	2013	<i>G-BHglu-6.88-II-2</i>	-	LGII-2	71.55	29030-61:T>C-	5	7.15	67.18	68.15	72.8	74.8	-0.088	0.309	-0.052	0.021	7.8
		<i>G-BHglu-6.88-II-4</i>	*	LGII-4	30.53	ChFaM004-147		8.65	29.1	29.8	31.21	31.21	-0.088	0.089	-0.278	-0.486	12.7
		<i>G-BHglu-6.88-IV-1</i>	****	LGIV-1	35.50	ChFaM017-136		27.17	33.92	33.92	35.83	35.83	-0.098	-0.186	0.672	0.830	42.4
		<i>G-BHglu-6.88-IV-4</i>	***	LGIV-4	19.31	21004-37:C>T-LG4		7.66	1.4	18.55	20.82	20.82	-0.088	0.298	-0.150	0.151	7.7
		<i>G-BHglu-6.88-VI-2</i>	*	LGVI-2	13.74	M18650-56:C>T-		9.39	4	10.95	22.9	24.5	-0.089	0.394	0.283	0.439	11.6
	2014	<i>G-BHglu-6.88-IV-1</i>	****	LGIV-1	35.50	ChFaM017-136	5.2	13.63	33.92	33.92	35.83	35.83	0.143	-0.114	1.087	0.842	49.7
Galloyl-HHDP-glucose 5.09	2013	<i>G-Hglu-5.09-VI-2</i>	*	LGVI-2	18.80	M25388-24:A>G-	5.1	7.89	10.95	13.74	29.73	29.73	-0.491	-0.018	-0.084	-0.121	34.3
	2014	<i>G-Hglu-5.09-I-2</i>	*	LGI-2	8.46	F12694-18:A>T-LG1	4.8	7.67	6.49	6.49	10.46	11.76	0.057	0.057	-0.389	-0.389	22.0
		<i>G-Hglu-5.09-III-1</i>	*	LGIII-1	22.68	25437-34:C>T-		5.08	19.67	22.5	23.1	23.1	0.057	0.488	0.382	0.100	15.7
		<i>G-Hglu-5.09-VI-4</i>	-	LGVI-4	55.82	F00421-66:G>C-LG6		8.93	52.91	55.31	56.81	56.81	0.057	-0.638	-0.338	-0.368	29.5
		<i>G-Hglu-5.09-VII-2</i>	***	LGVII-2	46.80	21145-30:G>A-LG7		7.59	44.82	44.82	48.8	50.35	0.057	0.568	0.650	0.239	23.5
HHDP glucose 1.58	2013	<i>HHDPglu-1.58-I-2^b</i>	-	LGI-2	35.67	F32156-17:A>C-LG1	4.7	4.54	34.5	34.5	37.5	37.5	0.893	0.685	0.785	0.864	33.0
		<i>HHDPglu-1.58-II-4</i>	*	LGII-4	9.03	25187-5:T>C-		7.13	8.39	8.39	10.23	10.23	0.892	1.077	1.093	0.975	32.9
		<i>HHDPglu-1.58-III-3^b</i>	-	LGIII-3	86.01	ChFvM140-104		4.51	75.82	76.14	104.3	105.2	0.894	0.843	0.952	0.982	17.8
	2014	<i>HHDPglu-1.58-I-2</i>	-	LGI-2	97.36	F30543-16:T>G-LG5	5.1	5.07	84.4	93.66	99.04	99.04	1.164	0.801	0.955	0.950	41.8
		<i>HHDPglu-1.58-III-3</i>	***	LGIII-3	71.16	F23153-22:C>T-LG3		5.92	70.9	70.9	72.13	72.13	1.164	1.226	1.429	1.293	20.9
HHDP glucose 2.06	2013	<i>HHDPglu-2.06-IV-1</i>	****	LGIV-1	62.98	F33514-56:C>A-LG4	5.1	5.59	44.8	62	63.9	72.5	0.100	0.100	-0.172	-0.172	18.8
		<i>HHDPglu-2.06-IV-3^b</i>	*	LGIV-3	38.51	LOX-S2		4.22	32.2	35	52.5	53.2	0.100	0.116	0.292	0.360	14.3
Lagerstannin A 4.79	2013	<i>LagtA-4.79-II-5</i>	***	LGII-5	56.42	M43853-58:C>A-LG2	5.1	9.2	55.7	55.7	56.9	58.1	-0.624	-1.264	-0.151	-0.969	42.2
		<i>LagtA-4.79-VI-5</i>	-	LGVI-5	5.87	M31649-53:A>G-LG6		5.21	0	1.8	19.4	19.4	-0.624	-0.926	-1.039	-0.334	25.9
	2014	<i>LagtA-4.79-I-2</i>	*	LGI-2	35.67	F32156-17:A>C-LG1	5	5.48	34.5	34.5	37.5	37.5	0.688	1.092	0.516	0.721	29.9
		<i>LagtA-4.79-II-5^b</i>	-	LGII-5	58.09	F46332-44:A>C-LG2		4.95	54.8	54.8	59.2	59.2	0.720	0.567	0.970	0.414	36.6
		<i>LagtA-4.79-VI-1</i>	*	LGVI-1	9.96	M17235-40:A>T-LG6		5.32	0	7.5	11	38.1	0.690	0.846	0.874	1.186	18.8

Chapter 3: Quantitative Trait Loci and Underlying Candidate Genes Controlling Secondary Metabolites in Strawberry Fruit

Lagerstannin A 5.77	2013	<i>LagtA-5.77-II-5</i>	***	LGII-5	56.93	15703-58:G>A-LG2	5	8.72	55.7	56.4	58.1	58.1	-0.576	-1.257	-0.187	-0.778	31.0
		<i>LagtA-5.77-IV-3</i>	*	LGIV-3	44.78	F21099-40:A>G-		6.87	32.2	43.4	52.5	53.2	-0.632	-0.418	-0.405	-0.053	23.8
	2014	<i>LagtA-5.77-I-2^b</i>	*	LGI-2	35.67	F32156-17:A>C-LG1	4.9	4.49	32.3	34.2	44.4	52.7	-0.412	0.420	-0.444	0.001	30.2
		<i>LagtA-5.77-V-1</i>	***	LGV-1	26.06	F34200-22:T>A-LG5		5.62	13.8	25.7	29.8	31.3	-0.409	-0.105	-0.689	-0.945	24.7
Lagerstannin B 4.82	2013	<i>LagtB-4.82-II-4</i>	*	LGII-4	9.03	25187-5:T>C-	5.2	5.33	8.4	8.4	10.2	11.6	0.059	-0.512	-0.198	-0.110	26.7
		<i>LagtB-4.82-IV-2^b</i>	-	LGIV-2	86.59	F14153-28:C>A-LG4		4.32	85.6	85.6	87	87	0.051	0.351	0.523	-0.123	36.9
	2014	<i>LagtB-4.82-I-2</i>	**	LGI-2	35.67	F32156-17:A>C-LG1	5	6.52	34.5	34.5	37.5	37.5	-0.979	-0.087	-1.146	-0.848	30.7
		<i>LagtB-4.82-IV-2</i>	-	LGIV-2	67.88	M22341-63:T>G-LG4		5.98	66.4	66.4	68.8	69.7	-0.978	-1.271	-0.389	-0.920	19.6
	<i>LagtB-4.82-VI-1</i>	*	LGVI-1	35.86	F37091-34:C>A-LG6		7.35	34.6	34.8	37.4	38.1	-0.978	-0.686	-0.432	0.057	20.9	
Lagerstannin B 7.30	2013	<i>LagtB-7.30-II-5</i>	*	LGII-5	56.42	M43853-58:C>A-LG2	5	8.46	55.7	55.7	56.9	58.1	-0.384	-0.996	-0.175	-0.795	36.6
		<i>LagtB-7.30-VI-5</i>	-	LGVI-5	15.75	25637-41:A>T-LG6		5.49	1.8	3.8	19.4	19.4	-0.384	-0.766	-0.780	-0.161	24.7
		<i>LagtB-7.30-VII-4</i>	-	4	30.79	F45059-8:T>C-LG7		6.65	29	29	32.8	34.2	-0.377	-0.164	0.242	0.192	26.8
Lagerstannin B 7.42	2013	<i>LagtB-7.42-II-5</i>	-	LGII-5	56.42	M43853-58:C>A-LG2	5	5.75	55.7	55.7	56.9	56.9	-0.766	-1.071	-0.654	-1.097	12.1
		<i>LagtB-7.42-III-2</i>	-	LGIII-2	56.23	M13708-26:A>G-LG2		5.43	41.6	43	57.6	59	-0.766	-0.896	-0.449	-0.960	13.3
		<i>LagtB-7.42-IV-1</i>	*	LGIV-1	46.29	F20746-41:A>T-LG4		6.37	44.8	44.8	47	47	-0.766	-0.406	-0.879	-0.848	16.5
		<i>LagtB-7.42-IV-3</i>	*	LGIV-3	43.37	F23458-34:A>C-LG4		8.17	42.2	42.8	46.7	46.7	-0.767	-0.746	-0.550	-0.226	21.9
		<i>LagtB-7.42-V-4</i>	**	LGV-4	42.71	M16560-9:T>A-		6.96	41.1	41.1	45.2	46.8	-0.766	-0.315	-0.340	-0.267	17.2
	2014	<i>LagtB-7.42-III-3^b</i>	*	LGIII-3	40.40	16712-44:C>A-	5	4.83	31.6	36.6	45.5	47.5	-0.388	-0.983	-1.127	-0.683	23.2
	<i>LagtB-7.42-VII-1</i>	-	1	23.34	F10992-38:T>A-LG7		5.01	21.7	21.7	25.1	32.8	-0.387	0.115	-0.482	-0.614	15.8	
Lagerstannin B 8.25	2014	<i>LagtB-8.25-III-2</i>	-	LGIII-2	49.53	CTCA-227	4.9	4.9	41.6	48.8	51	60.9	-0.373	-0.557	-0.989	-0.308	15.4
		<i>LagtB-8.25-VII-4</i>	-	4	17.78	F12044-26:G>C-LG7*		6.25	6.4	6.4	19.8	21.7	-0.373	-0.453	-0.289	0.347	23.4
Rhoipteleatin H 3.95	2013	<i>RhoH-3.95-V-4</i>	***	LGV-4	33.61	17622-5:A>T-	5	5.02	19.2	33	41.1	42.7	-0.992	-0.446	-0.446	0.156	20.7
	2014	<i>RhoH-3.95-VI-1</i>	***	LGVI-1	35.86	F37091-34:C>A-LG6	5	5.72	25.1	33.6	37.4	37.4	-0.176	0.043	0.334	0.982	18.0
		<i>RhoH-3.95-VII-2^b</i>	*	2	56.27	20385-29:A>C-		4.66	31.4	53.6	58.5	62.8	-0.176	0.632	-0.135	0.568	14.9
Tris-galloyl- glucose 5.09	2013	<i>TGalglu-5.09-III-2</i>	-	LGIII-2	68.70	F34855-10:G>A-LG3	4.9	5.03	66.5	66.5	70.6	71	-0.381	-0.518	-0.511	-0.744	13.8
		<i>TGalglu-5.09-V-1</i>	-	LGV-1	19.35	21665-44:T>C-LG5		5.74	18.1	18.4	20.6	20.6	-0.381	-0.069	0.007	0.121	21.2
		<i>TGalglu-5.09-VI-2</i>	*	LGVI-2	18.80	M25388-24:A>G-		8.96	13.7	16	24.5	27.7	-0.381	0.094	0.037	-0.049	28.2
		<i>TGalglu-5.09-VII-3^b</i>	*	3	47.80	14529-36:G>A-LG7		3.79	40.7	45.1	62.2	62.2	-0.377	-0.528	-0.199	-0.434	9.2
	2014	<i>TGalglu-5.09-I-1</i>	*	LGI-2	8.46	F12694-18:A>T-LG1	4.9	5.64	5.1	6.5	17.2	24.4	0.189	0.189	-0.215	-0.215	15.7
		<i>TGalglu-5.09-V-2^b</i>	-	LGV-2	3.85	F21563-13:A>G-LG5		4.25	0	0	7	17.3	0.189	0.144	0.000	0.532	11.4
	<i>TGalglu-5.09-VI-4</i>	-	LGVI-4	55.82	F00421-66:G>C-LG6		8.05	48.9	52.9	56.8	56.8	0.189	-0.499	-0.241	-0.269	26.3	
	<i>TGalglu-5.09-VII-2^b</i>	**	2	46.80	21145-30:G>A-LG7		4.41	37.2	44.8	50.3	53.6	0.189	0.648	0.575	0.543	12.6	

Chapter 3: Quantitative Trait Loci and Underlying Candidate Genes Controlling Secondary Metabolites in Strawberry Fruit

Tris-galloyl-glucose 5.69	2013	<i>TGalglu-5.69-II-1</i>	-	LGII-1	59.64	M43400--LG2	5	5.21	49.1	59	65.4	73.4	0.579	0.498	0.365	0.586	14.5
		<i>TGalglu-5.69-III-1</i>	****	LGIII-1	46.19	F18418-49:A>C-LG3		6.96	43	45.1	47.2	47.8	0.579	0.641	0.418	0.395	19.6
		<i>TGalglu-5.69-V-3^b</i>	**	LGVI-3	47.95	M12353-41:C>T-		4.25	25.6	29.4	50.1	54.1	0.579	0.696	0.819	0.737	11.5
Tri-galloyl HHDP glucose 6.16	2013	<i>TGalHglu-6.16-IV-1</i>	****	LGIV-1	35.50	ChFaM017-136	5	10.01	28.2	33.9	35.8	36.6	-0.465	-0.417	-1.029	-1.090	31.1
		<i>TGalHglu-6.16-VI-2</i>	-	LGVI-2	16.03	M31478-44:T>A-LG6		5.16	0	13.7	20.5	24.5	-0.453	0.114	-0.059	0.059	15.6
	2014	<i>TGalHglu-6.16-IV-1</i>	****	LGIV-1	42.50	11205-28:A>G-LG4	5	5.85	26.2	33.9	44.5	49.9	0.966	0.855	1.107	1.298	21.6
	<i>TGalHglu-6.16-V-1</i>	*	LGVI-1	13.77	M11115-55:G>A-LG5		4.74	4.9	12.8	15	16.1	0.966	1.207	1.430	1.168	19.5	
Unknown ellagitannin 4.48	2013	<i>UnkET-4.48-II-2</i>	-	LGII-2	72.80	M35511-30:G>A-LG2	5	5.28	63.9	63.9	74.8	90.9	-0.237	-0.247	-0.319	-0.524	11.4
		<i>UnkET-4.48-III-3</i>	*	LGIII-3	79.80	F40029-28:G>A-LG3		6.22	77.6	79.5	80.6	81.7	-0.237	0.037	-0.296	-0.172	15.1
		<i>UnkET-4.48-V-1</i>	-	LGVI-1	18.09	38845--LG5		6.57	17.1	17.5	19.4	20.6	-0.206	-0.081	-0.271	0.090	16.0
	2014	<i>UnkET-4.48-II-5</i>	*	LGII-5	37.00	11687-58:T>A-LG2	5	6.19	34.7	36.1	37.8	37.8	0.585	0.914	0.567	0.847	22.9
		<i>UnkET-4.48-VII-1^b</i>	-	1	32.93	M31995-46:T>A-LG7		4.3	12.3	18.7	34.4	34.4	0.585	0.772	0.615	0.430	14.8
	<i>UnkET-4.48-VII-2^b</i>	-	2	33.00	M26503-7:A>G-LG7		4.12	13.9	18.4	33.9	46.8	0.585	0.810	0.585	0.810	12.3	
Unknown ellagitannin 4.69	2013	<i>UnkET-4.69-V-1</i>	-	1	18.09	38845--LG5	5.1	6.18	17.6	17.6	18.4	18.4	-0.033	0.173	0.107	0.447	21.3
		<i>UnkET-4.69-VII-1^b</i>	**	1	23.34	F10992-38:T>A-LG7		4.8	9.7	18.7	25.1	32.8	-0.085	0.038	-0.211	-0.357	10.5
	2014	<i>UnkET-4.69-III-1</i>	-	1	19.99	17951-41:T>C-LG3	5.1	5.66	19.7	19.7	21.6	21.6	-0.561	0.292	0.424	-0.431	20.3
	<i>UnkET-4.69-VII-1^b</i>	*	1	45.87	F14673-22:C>G-LG7		5.01	40.8	43.3	48	49.8	-0.561	-0.275	-0.739	-1.278	17.0	
Bis(HHDP) glucose 3.80	2013	<i>BHHDPglu-3.80-II-4</i>	*	LGII-4	9.03	25187-5:T>C-	4.9	6.45	8.4	8.4	10.2	14.1	0.236	-0.084	-0.017	0.107	26.4
		<i>BHHDPglu-3.80-III-3^b</i>	*	LGIII-3	98.26	F13596-62:A>G-LG3		4.81	96.1	96.1	104.2	105.2	0.235	0.072	-0.061	-0.011	18.8
	2014	<i>BHHDPglu-3.80-II-4</i>	-	LGII-4	13.57	11775-27:A>G-LG2	5.1	5.93	11.8	12.1	14.1	25.3	0.974	1.037	1.205	1.201	19.7
Bis(HHDP) glucose 4.52	2013	<i>BHHDPglu-4.52-IV-2</i>	-	LGIV-2	66.44	37872--LG4	5	5.11	59.6	65.5	67.2	67.9	0.946	0.930	1.064	1.045	17.2
		<i>BHHDPglu-4.52-VII-3</i>	***	3	42.28	27124-23:A>G-		6.48	40.7	41.6	47.1	54.8	0.948	0.983	0.887	1.068	21.4
Castalagin 5.62	2014	<i>Cast-5.62-VII-4</i>	*	4	13.05	F11347-65:C>A-LG7**	5	5.53	6.4	6.5	19.8	21.7	-0.294	-0.021	0.056	0.532	25.7
Castalagin 5.94	2014	<i>Cast-5.94-III-2</i>	-	2	41.57	F12288-30:C>G-	4.9	6.04	40.1	40.1	43	43	0.557	1.130	0.152	0.958	33.4
		<i>Cast-5.94-III-3</i>	*	3	74.06	34601--		5.67	70.9	73.4	75.8	79.8	0.557	0.385	-0.026	0.519	19.9
Castalagin 6.28	2013	<i>Cast-5.28-IV-4</i>	*	4	107.85	ChFaM023-151h	4.9	4.92	104	104	119.5	124.2	-0.759	-0.737	-0.457	-0.721	13.0
		<i>Cast-5.28-V-1</i>	-	1	18.09	38845--LG5		7.3	17.1	17.6	18.4	19.4	-0.720	-0.521	-0.561	-0.181	25.0
		<i>Cast-5.28-VI-2</i>	*	2	24.48	M14618-24:C>T-LG6		6.22	2	16	27.7	33.3	-0.759	-0.650	-0.417	-0.757	15.2
		<i>Cast-5.28-VI-3</i>	*	3	24.20	10796-19:G>C-LG6		5.31	21.9	21.9	24.6	24.6	-0.759	-0.414	-0.535	-0.504	12.4
	2014	<i>Cast-5.28-VII-4</i>	*	4	8.73	F03318-60:G>C-LG7	4.8	4.93	6.4	6.5	19.8	21.7	-0.350	-0.516	-0.363	0.222	21.2
Castalagin 6.37	2013	<i>Cast-6.37-IV-4^b</i>	-	4	106.88	ChFaM138-305	5.1	4.48	102.2	104	119.4	123.6	0.651	0.357	0.946	0.602	18.2

Chapter 3: Quantitative Trait Loci and Underlying Candidate Genes Controlling Secondary Metabolites in Strawberry Fruit

	2014	<i>Cast-6.37-II-5^b</i>	-	LGII-5	51.26	16595-56:A>T-	4.9	4.1	47.2	49.8	51.8	55.7	0.129	0.302	-0.372	0.505	15.9
		<i>Cast-6.37-VII-1</i>	-	LGVII-1	32.93	M31995-46:T>A-LG7		7.32	27.1	28.7	34.4	34.4	0.129	0.970	0.471	-0.130	26.8
		<i>Cast-6.37-VII-3</i>	*	LGVII-3	21.02	F34133-39:T>C-LG7		6.25	19.1	19.9	21.3	22.3	0.129	0.016	-0.835	0.020	19.7
Castalagin 6.87	2013	<i>Cast-6.87-II-2^b</i>	*	LGII-2	65.96	M28484-36:G>T-	5.1	4.96	63.5	65.1	76.6	81.8	0.036	0.295	0.197	-0.087	10.3
		<i>Cast-6.87-IV-4</i>	*	LGIV-4	114.77	ChFaM148-156/158		9.14	111.6	111.6	124.2	124.2	0.036	0.262	0.498	0.016	22.9
		<i>Cast-6.87-V-1</i>	-	LGV-1	18.09	38845--LG5		5.39	17.6	17.6	18.4	19.4	0.053	0.173	0.103	0.503	9.6
		<i>Cast-6.87-VII-3</i>	-	LGVII-3	56.73	40926--LG7		7.91	54.8	56	59.6	61.6	0.036	-0.728	-0.328	-0.411	38.3
Castalagin 7.46	2013	<i>Cast-7.46-VI-3</i>	***	LGVI-3	26.74	M27561-10:A>T-	5	5.72	4.2	24.6	31.1	33.1	-0.615	-0.120	-0.533	-0.212	23.2
		<i>Cast-7.46-VI-5</i>	*	LGVI-5	38.36	37297-9:A>T-		6.92	30.2	36.1	40.4	46.2	-0.615	-0.340	-0.285	0.081	30.7
Di-galloyl HHPD glucose 5.95	2013	<i>DG-Hglu_5.95-IV-1</i>	***	LGIV-1	62.98	F33514-56:C>A-LG4	5.1	5.09	40.2	62	63.9	67.7	-0.666	-0.666	-0.975	-0.975	16.8
		<i>DG-Hglu_5.95-VI-5</i>	*	LGVI-5	40.61	M33723-47:A>T-LG6		5.05	28.2	36.6	46.2	48.2	-0.666	-0.447	-0.494	-0.240	17.6
Methylellagic acid methyl hexose 3.74	2014	<i>DG-Hglu_5.95-III-3</i>	*	LGIII-3	40.40	16712-44:C>A-	5.1	6.57	36.6	36.6	42.4	48.3	0.819	1.314	1.258	1.067	34.3
	2013	<i>MEANhex-3.74-II-3^b</i>	*	LGII-3	1.22	15829-7:A>G-	5.1	4.36	0	0	11.5	38.2	0.777	0.849	0.759	0.905	14.0
		MEANhex-3.74-V-4	****	LGIV-4	45.22	25929-8:T>G-LG5		7.09	43.2	43.2	46.3	61.1	0.779	0.710	0.832	0.630	23.7
	2014	MEANhex-3.74-V-4	**	LGIV-4	53.73	M32104-46:A>C-	5	5.99	43.2	46.8	64.2	65.2	1.060	0.835	0.976	0.844	19.7
		<i>MEANhex-3.74-VII-1</i>	***	LGVII-1	45.87	F14673-22:C>G-LG7		5.87	41.8	43.3	49.7	56.5	1.058	1.211	1.039	0.956	13.9
1-O-protocatechuy-beta-xylose 4.45	2013	<i>PCBX-4.45-VI-3</i>	*	LGVI-3	4.20	M13581-68:T>A-LG6	5.1	5.69	0	2	8.3	8.3	0.647	0.679	1.001	0.783	47.5
		<i>PCBX-4.45-VI-4^b</i>	-	LGVI-4	24.32	11675-64:G>A-LG2		4.21	17.1	20.1	44.3	44.3	0.647	0.860	0.747	0.806	24.0
	2014	<i>PCBX-4.45-II-5</i>	-	LGII-5	36.09	31968-37:T>A-LG2	5	8.18	34.7	34.7	37	37	0.180	0.304	0.075	0.666	25.4
		<i>PCBX-4.45-III-2</i>	-	LGIII-2	88.61	ChFaM080-219*		6.04	78.3	81.9	90.4	98.2	0.180	-0.165	0.164	0.237	15.0
		<i>PCBX-4.45-III-3</i>	**	LGIII-3	72.13	11000-51:G>A-LG3		5.55	66.2	67.2	73.1	74.1	0.180	-0.171	-0.308	-0.216	16.8
		<i>PCBX-4.45-VI-4^b</i>	**	LGVI-4	70.74	35068--LG6		4.54	43.5	68.1	76.1	78.4	0.180	0.162	0.223	-0.137	9.9
Cinnamic acid-hexo 7.00	2013	<i>qCinnhex-7.00-I-1</i>	-	LG I-1	9.147	F13002-34:A>T-LG1	4.8	4.9	0	4.5	13.5	20.3	0.545	-0.190	-0.018	-0.103	19.4
		<i>qCinnhex-7.00-IV-2</i>	***	LGIV-2	94.562	16233-40:G>A-		5.5	72.1	93.1	94.6	94.6	0.524	-0.166	-0.348	-0.325	20
		<i>qCinnhex-7.00-VII-4</i>	*	4	11.064	F10940-16:T>C-LG7		5.68	6.4	8.7	15	17.8	0.545	1.456	0.834	0.952	26.2
	2014	<i>qCinnhex-7.00-II-1</i>	*	LGII-1	9.809	F32536-66:A>C-LG2	5.5	5.35	0	0	20	21.6	0.935	1.020	1.355	1.457	16.7
	<i>qCinnhex-7.00-III-3^b</i>	*	LGIII-3	77.605	14214-20:G>A-		5.33	70.1	77.1	78.5	80.8	0.935	0.560	0.499	0.961	18.5	
		<i>qCinnhex-7.00-IV-2^b</i>	-	LGIV-2	90.471	F13974-36:G>C-LG4		4.33	78.9	89.4	93.1	95.6	0.935	0.550	0.341	0.539	14.1
Cinnamic acid-hexo 7.39	2013	<i>qCinnhex-7.39-II-2</i>	**	LGII-2	67.175	M20515-30:C>A-LG2	4.7	4.99	62.6	66	68.3	69.1	0.000	0.318	-0.490	-0.044	22.6
		<i>qCinnhex-7.39-VII-4</i>	*	4	6.450	BFACT029-227*		5.3	6.4	6.4	16.3	17.8	-0.560	0.230	-0.215	0.273	27.6
	2014	<i>qCinnhex-7.39-IV-2</i>	****	LGIV-2	73.454	EmFv136-138	6.4	7.43	72.3	72.3	74.6	85	0.968	1.103	0.738	0.584	23.3
		<i>qCinnhex-7.39-IV-3^b</i>	**	LGIV-3	36.669	F19219-47:G>A-LG4		5.17	36.3	36.3	52.5	52.5	0.970	1.036	1.377	1.256	15.5

		<i>qCinnhex-7.39-V-3^b</i>	-	LGIV-3	10.145	M12243-63:G>A-LG5		5.07	0	4.6	10.7	26.4	0.968	0.735	0.745	0.493	15.4
Coumaric acid hexose 5.18	2013	<i>qCouhex-5.18-III-1^b</i>	****	LGIII-1	13.867	ChFvM233-218	5.1	5.07	0	0	22.5	29.3	0.596	0.678	0.728	0.761	18.3
		<i>qCouhex-5.18-IV-3</i>	****	LGIV-3	38.508	LOX-S2		5.15	37.7	37.7	44.8	45.1	0.596	0.598	0.735	0.685	17.2
	2014	<i>qCouhex-5.18-IV-2</i>	****	LGIV-2	73.454	EmFv136-138	5.2	6.95	72.3	72.3	74.6	85.6	0.457	0.626	0.409	0.288	22.6
		<i>qCouhex-5.18-IV-3</i>	****	LGIV-3	45.050	ChFaM161-209		9.43	41.6	41.6	45.9	45.9	0.457	0.500	0.802	0.704	30.4
Coumaric acid hexose 5.43	2013	<i>qCouhex-5.43-IV-3</i>	****	LGIV-3	38.508	LOX-S2	5.1	6.02	32.2	37.7	44.8	52.5	0.562	0.522	0.748	0.744	26
		<i>qCouhex-5.43-III-1^b</i>	**	LGIII-1	80.223	M35756-31:T>C-LG3	5.1	4.43	73	78	82.9	82.9	0.807	0.688	0.855	0.786	10
	2014	<i>qCouhex-5.43-IV-2</i>	***	LGIV-2	73.454	EmFv136-138		6.15	72.3	72.3	75.4	85.6	0.807	0.861	0.734	0.677	16.6
		<i>qCouhex-5.43-IV-3</i>	****	LGIV-3	42.155	F11831-65:C>T-		11.33	72.3	78	82.9	82.9	0.807	0.766	0.999	0.964	33.8
Di-hydroxybenzoic acid hexose 3.63	2014	<i>qDHBAhex-3.63-III-3</i>	*	LGIII-3	71.164	F23153-22:C>T-LG3	5	5.74	68.8	70.1	72.1	73.4	1.182	1.212	1.453	1.362	17.7
		<i>qDHBAhex-3.63-V-4</i>	-	LGIV-4	24.162	30182-42:G>A-LG5		5.59	22.6	23.3	25.6	26.6	1.182	1.360	0.999	1.268	20.7
		<i>qDHBAhex-3.63-VI-1</i>	****	LGVI-1	35.861	F37091-34:C>A-LG6		6.9	23.9	24.4	38.5	43.8	1.182	0.854	1.113	0.903	27.2
Di-hydroxybenzoic acid hexose 4.35	2014	<i>qDHBAhex-4.35-II-2</i>	-	LGII-2	67.175	M20515-30:C>A-LG2	4.9	5.89	66	66	67.9	67.9	1.029	0.524	0.617	0.647	18.4
		<i>qDHBAhex-4.35-VI-3</i>	-	LGVI-3	4.198	M13581-68:T>A-LG6		5.79	0	2	6.5	6.5	1.029	0.468	0.206	0.478	36.4
		<i>qDHBAhex-4.35-VII-1</i>	*	LGVII-1	45.657	M21972-10:G>A-LG7		7.2	42.2	43.3	46.8	46.8	1.029	0.961	0.969	0.508	21.9
Di-hydroxy methyl benzoic acid hexose 3.82	2013	<i>qDHMBAhex-3.82-I-1</i>	-	LGI-1	38.404	F13255-48:C>T-LG1	4.8	8.17	37.9	37.9	39.3	43.6	1.016	1.253	1.142	1.027	57.9
		<i>qDHMBAhex-3.82-II-1</i>	-	LGII-1	59.033	ChFvM201-264		8.55	58.3	58.6	59.6	61.4	0.990	0.910	0.873	0.960	58.4
		<i>qDHMBAhex-3.82-V-3</i>	*	LGIV-3	23.702	F23321-10:G>A-		5.51	23.6	23.6	24.5	26.4	0.990	0.840	0.927	0.985	50.3
Di-hydroxy methyl benzoic acid hexose 5.97	2014	<i>qDHMBAhex-3.82-VII-1</i>	****	LGVII-1	44.188	ChFaM208-229h	5	5.73	32.9	43.3	46.8	48.7	0.732	0.911	0.491	1.178	14.5
Di-hydroxy methyl benzoic acid hexose 6.04	2013	<i>qDHMBAhex-6.04-V-2</i>	****	LGIV-2	17.264	M00247-47:C>G-LG5	5.2	8.15	10	10	18.5	30.3	-0.403	0.122	-0.342	0.041	21.9
		<i>qDHMBAhex-6.04-VII-4^b</i>	*	LGVII-4	27.205	13346-42:A>C-		5.17	16.4	21.7	29	29	-0.403	-0.520	-0.361	-1.079	19.6
	2014	<i>qDHMBAhex-6.04-V-2^b</i>	***	LGIV-2	6.992	ChFaM106-144	5	4.76	0	0	29.5	30.3	-0.063	0.304	0.145	0.559	18.3
		<i>qDHMBAhex-6.04-V-4</i>	***	LGIV-4	20.498	25656-39:C>T-		5.37	8.6	19.9	23.3	34.9	-0.051	-0.326	-0.508	-0.697	21.3
Ferulic acid hexose 5.56	2013	<i>qFerhex-5.56-III-2</i>	***	LGIII-2	57.614	M30011-30:A>G-LG3	5	5.27	56.3	56.8	59	59	0.848	0.984	0.935	1.020	16.0
		<i>qFerhex-5.56-V-4</i>	****	LGIV-4	9.746	15001-41:C>G-LG5		9.12	0	2.6	12.3	16.7	0.848	0.924	0.968	1.106	32.8
	2014	<i>qFerhex-5.56-III-2</i>	-	LGIII-2	29.610	ChFvM271-AAT-S1	5	6.05	21.4	26.7	31.3	39.9	-0.003	0.423	0.139	-0.005	19.4
		<i>qFerhex-5.56-V-4</i>	****	LGIV-4	11.212	17095-51:C>G-LG5		11.1	2.6	8.6	12.3	16.7	-0.003	-0.268	-0.268	-0.791	39.6

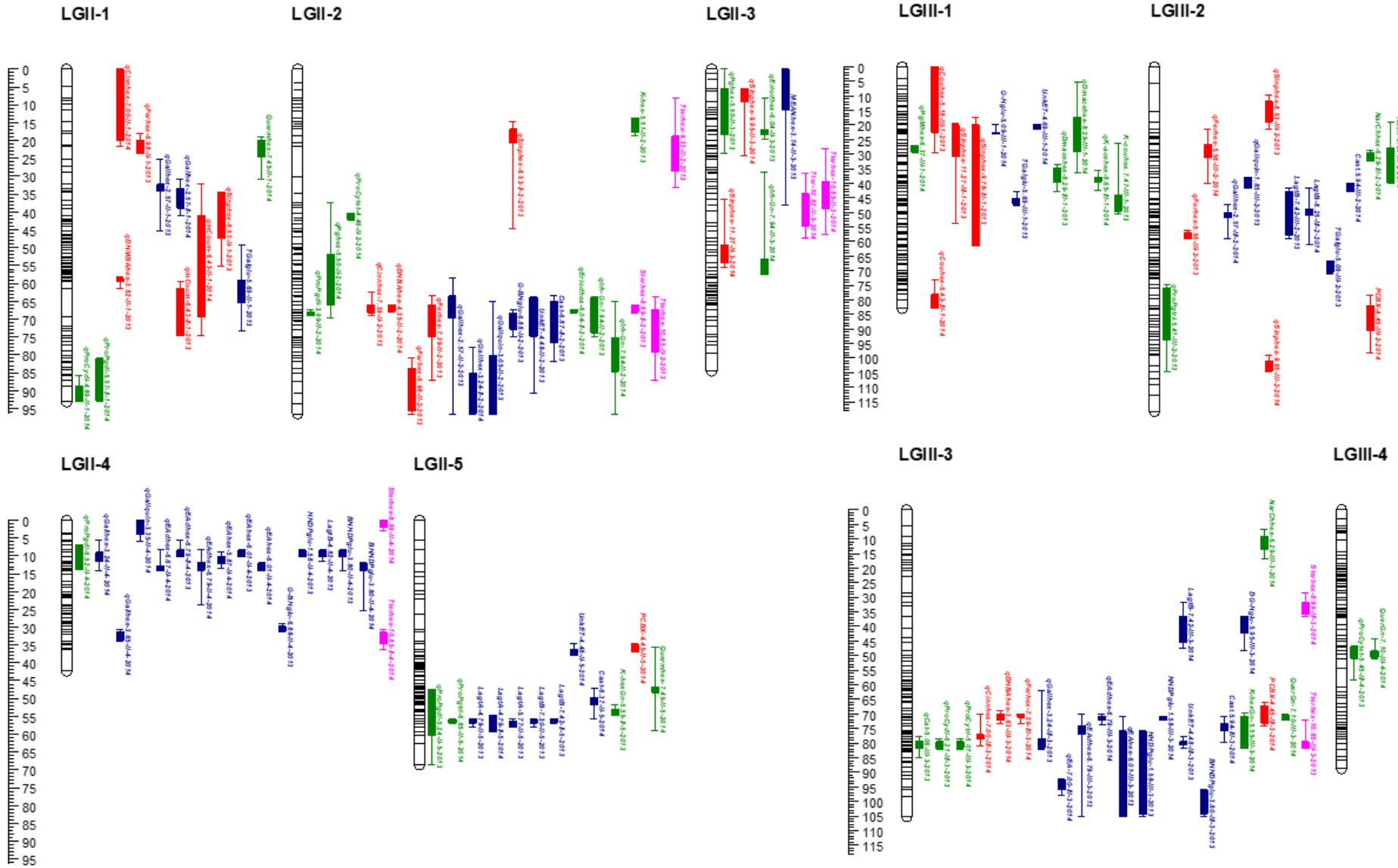
Ferulic acid hexose 6.98	2013	<i>qFerhex-6.98-II-1</i>	-	LGII-1	21.254	16799-47:A>G-LG2	5	8.02	18	20	23.6	23.6	-0.495	-0.403	-0.020	-1.201	35.6
		<i>qFerhex-6.98-II-2</i>	***	LGII-2	93.669	M12424-34:T>C-LG6		9.17	80.8	83.7	95.7	96.5	-0.491	0.286	-0.554	-0.588	35.7
		<i>qFerhex-6.98-IV-3</i>	***	LGIV-3	33.169	F30867-46:A>G-LG4		6.39	22.8	28.3	32	36.3	-0.467	-1.107	-0.363	-0.355	23.4
	2014	<i>qFerhex-6.98-V-2^b</i>	-	LGV-2	46.601	F27403-27:G>T-LG5	4.8	4.06	45.4	45.4	47.1	47.1	0.845	0.721	0.671	1.210	14.0
		<i>qFerhex-6.98-VII-4</i>	***	LGVII-4	49.571	17949-21:C>G-LG7		6.73	46.6	48.5	50.7	50.7	0.845	1.480	1.005	0.906	25.0
Ferulic acid hexose 7.39	2013	<i>qFerhex-7.39-II-2</i>	****	LGII-2	67.175	M20515-30:C>A-LG2	4.9	5.11	63.5	66	74.9	87	0.135	0.457	-0.262	0.055	23.1
		<i>qFerhex-7.39-VII-4^b</i>	*	LGVII-4	6.450	BFACT029-227*		4.77	6.4	6.4	17.8	19.8	-0.384	0.359	-0.071	0.271	27.2
	2014	<i>qFerhex-7.39-III-3</i>	-	LGIII-3	70.886	37665--	5.2	5.77	70.1	70.1	71.2	73.4	-0.075	-0.736	-0.793	-0.363	17.1
		<i>qFerhex-7.39-IV-2</i>	****	LGIV-2	73.454	EmFv136-138		7.84	72.3	72.3	74.6	75.4	-0.093	0.244	-0.397	-0.631	24.1
		<i>qFerhex-7.39-IV-3</i>	****	LGIV-3	49.290	F32402-40:C>G-LG4*		5.76	36.3	41.6	52.5	52.5	-0.093	-0.239	0.523	0.224	16.5
m-Coumaric acid 5.11	2013	<i>qmCoum-5.11-I-2</i>	*	LGI-2	99.044	F32377-39:C>G-LG1	5	8.58	97.4	97.4	99.04	99.04	-0.683	-0.213	-0.538	-0.478	49.9
		<i>qmCoum-5.11-IV-2</i>	-	LGIV-2	63.757	F19191-13:C>T-LG4		5.73	62.4	63.1	64	64	-0.683	-0.964	-0.890	-0.765	17.8
		<i>qmCoum-5.11-V-2</i>	-	LGV-2	53.977	M34072-12:T>G-LG5		6.69	51.4	53.2	59.2	60.3	-0.683	-0.700	-0.663	-0.358	21.5
m-Coumaric acid 6.43	2013	<i>qmCoum-6.43-II-1</i>	****	LGII-1	69.537	F18967-58:A>G-LG2	5.2	15.16	59.6	61.4	74.6	74.6	-0.971	-1.866	-0.954	-1.801	36.9
		<i>qmCoum-6.43-IV-3</i>	*	LGIV-3	45.050	ChFaM161-209		9.33	42.8	44.8	45.9	45.9	-0.971	-0.262	-0.245	-0.464	22
		<i>qmCoum-6.43-VI-1</i>	*	LGVI-1	35.861	F37091-34:C>A-LG6		10.81	34.8	34.8	37.4	37.4	-0.971	-0.905	-1.263	-0.548	19.1
		<i>qmCoum-6.43-VI-2</i>	-	LGVI-2	49.312	M28969-22:C>T-		6.36	47.6	47.8	51.3	54.3	-0.971	-0.721	-0.892	-1.417	14.5
	2014	<i>qmCoum-6.43-II-1</i>	****	LGII-1	61.372	F13047-43:G>T-LG2	5	10.13	32.3	41	69.4	74.6	-0.825	-1.899	-0.997	-1.623	29
		<i>qmCoum-6.43-IV-3</i>	***	LGIV-3	53.773	M14305-21:G>A-LG4*		5.01	29.9	32.2	55.5	79.4	-0.825	-0.787	-0.470	-0.156	13.6
		<i>qmCoum-6.43-V-2</i>	-	LGV-2	27.027	ChFaM120-184		5.07	21.9	23.9	34.4	49.1	-0.825	-1.411	-0.706	-1.056	12.4
Sinapic acid hexose 11.27	2013	<i>qSinphex-11.27-III-1</i>	***	LGIII-1	29.267	ChFaM040-198*	5.1	5.57	19.5	20	30.9	53.7	0.556	0.819	0.886	0.914	24.4
	2014	<i>qSinphex-11.27-II-3</i>	***	LGII-3	50.519	F21588-31:G>C-LG2	5.2	6.45	36.5	49.2	54.1	55.4	0.301	-0.981	-0.127	-0.137	24.4
		<i>qSinphex-11.27-IV-3^b</i>	***	LGIV-3	43.762	F33942-27:A>C-LG4		5.04	41	41.6	45.5	46.7	0.330	-0.621	0.528	0.436	24.3
Sinapic acid hexose 8.53	2013	<i>qSinphex-8.53-II-1</i>	****	LGII-1	46.190	F41484-47:C>G-LG2	5	9.19	34.5	34.5	47.3	55.2	0.675	1.050	0.783	0.987	37
		<i>qSinphex-8.53-II-2^b</i>	***	LGII-2	18.771	F35670-57:G>C-		4.84	14.7	16.8	20.6	44.6	0.669	1.000	1.010	0.776	27
		<i>qSinphex-8.53-III-2</i>	-	LGIII-2	15.435	13356-7:G>A-		5.56	9.8	11.8	18.8	21.4	0.673	0.764	0.796	1.109	28.9
Sinapic acid hexose 9.78	2013	<i>qSinphex-9.78-III-1^b</i>	****	LGIII-1	29.267	ChFaM040-198*	5.1	4.09	17.2	20	61.4	61.4	0.426	0.608	0.597	0.592	12.4
		<i>qSinphex-9.78-VI-2</i>	*	LGVI-2	39.556	EMFv010-170h		10.18	35.6	36.3	49.3	55.1	0.426	0.208	0.493	0.214	35.8
	2014	<i>qSinphex-9.78-VI-2</i>	****	LGVI-2	47.777	EMFn228-268	5.3	8.17	38.6	45.6	49.3	54.3	0.803	0.544	0.781	0.515	26
	<i>qSinphex-9.78-VI-7</i>	***	LGVI-7	23.672	M20868-26:G>A-LG6		6.02	13.7	22.1	25.5	27.5	0.803	0.553	0.756	0.595	18.1	
Sinapic acid hexose 9.95	2014	<i>qSinphex-9.95-II-3</i>	-	LGII-3	6.223	F45818-39:G>A-LG6	5.3	5.52	5.4	5.4	9	24.2	0.019	0.483	0.706	-0.052	19.3
		<i>qSinphex-9.95-III-2</i>	****	LGIII-2	102.783	F24406-46:G>A-LG3		8.03	99.1	101.1	104.5	104.5	0.010	0.044	-0.814	-0.587	25.9
		<i>qSinphex-9.95-VI-1</i>	*	LGVI-1	23.477	M29946-61:G>A-LG6		5.98	22.3	22.3	38.5	42.5	0.010	-0.761	-0.490	-0.768	17.8
	2013	<i>Sterhex-8.47-IV-3^b</i>	-	LGIV-3	43.76	F33942-27:A>C-LG4	5.2	3.61	38.2	43.4	46.7	55.5	1.427	1.132	1.258	1.098	24.1

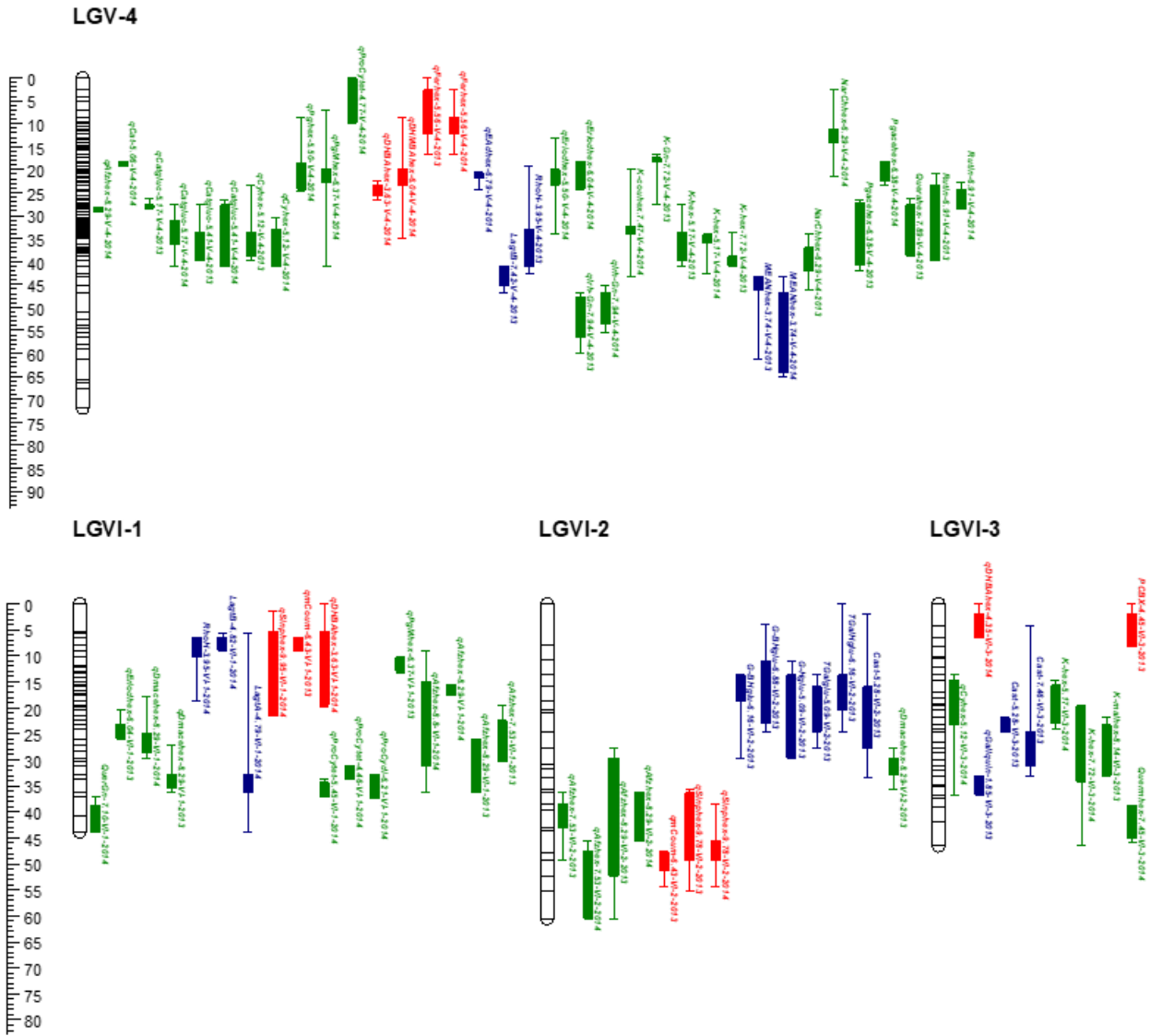
		<i>Sterhex-8.47-IV-4</i>	****	LGIV-4	4.85	M37566-36:A>T-LG4		6.94	2.4	3.4	7.7	31.9	1.424	1.452	1.410	1.111	30.6
Sesquiterpenoid hexose 8.47	2014	<i>Sterhex-8.47-IV-3</i>	-	LGIV-3	42.16	F11831-65:C>T-	5	5.13	28.3	41	43.8	52.5	-0.459	-0.586	-0.133	-0.156	15.0
		<i>Sterhex-8.47-IV-4</i>	****	LGIV-4	20.17	F38270-41:T>C-LG4		7.4	18.6	19.3	21.8	22.5	-0.459	-0.371	0.050	0.035	21.0
		<i>Sterhex-8.47-VII-1</i>	*	LGVII-1	42.16	F21065-31:C>G-		5.35	36.6	37.8	43.2	44.2	-0.459	-0.184	-0.143	-0.631	14.6
Sesquiterpenoid hexose 8.99	2013	<i>Sterhex-8.99-II-2^b</i>	*	LGII-2	67.18	M20515-30:C>A-LG2	5	4.6	66	66	67.9	68.3	1.372	1.187	1.360	1.359	14.1
		<i>Sterhex-8.99-V-3</i>	***	LGIV-3	19.65	F25448-32:T>C-LG5		6.12	17	18.8	20.6	20.6	1.368	1.207	1.370	1.487	19.7
		<i>Sterhex-8.99-VII-2</i>	****	LGVII-2	55.42	M18777-63:C>A-LG7		5.23	43.5	44.8	56.3	57.2	1.372	1.531	1.372	1.568	15.3
	2014	<i>Sterhex-8.99-II-4</i>	*	LGII-4	0.00	16373-44:T>C-	5	7.91	0	0	2	3	-0.368	-0.377	-0.065	-0.670	37.3
		<i>Sterhex-8.99-III-3</i>	-	LGIII-3	32.84	ChFaM021-212		11.98	28.7	31.6	35.8	36.6	-0.368	-0.193	-0.105	-0.658	43.0
Triterpenoid- hexose 10.85		<i>Sterhex-8.99-IV-3</i>	-	LGIV-3	42.16	F11831-65:C>T-		11.06	35	35	42.8	42.8	-0.368	-0.019	0.016	0.118	22.4
		<i>Sterhex-8.99-V-3</i>	****	LGIV-3	31.72	F43700-18:T>G-LG5		16.68	31.2	31.2	33.7	33.7	-0.368	-0.584	-0.878	-1.012	41.1
	2013	<i>Tterhex-10.85-II-2</i>	**	LGII-2	72.84	ChFaM026-092	5.1	5.32	63.9	67.2	79.3	87	1.184	1.049	1.273	1.226	12.8
		<i>Tterhex-10.85-III-2^b</i>	-	LGIII-2	21.40	29115-28:T>A-		4.19	18.4	19.8	25.7	36.8	1.184	1.171	1.062	0.938	14.0
		<i>Tterhex-10.85-III-3</i>	*	LGIII-3	80.56	15653-52:A>G-		5.3	72.1	79.5	81.7	81.7	1.184	1.112	1.324	1.102	13.9
		<i>Tterhex-10.85-VII-3</i>	*	LGVII-3	51.69	F26803-31:C>T-LG7		7.27	50	50	53.5	56	1.184	0.979	1.069	1.283	21.9
	2014	<i>Tterhex-10.85-II-3</i>	*	LGII-3	34.75	F20779-21:A>G-LG2	5.1	5.2	22.3	31.4	39.2	46.2	1.816	1.738	1.902	1.534	13.7
Triterpenoid- hexose 11.06		<i>Tterhex-10.85-II-4</i>	*	LGII-4	33.09	25222-45:T>A-LG6		6.01	30.7	31.4	34.6	36.3	1.840	2.056	1.644	1.636	15.5
		<i>Tterhex-10.85-V-1</i>	*	LGIV-1	63.13	M00709-36:T>A-LG5		6.46	58.8	60.3	65.5	65.5	1.816	1.365	1.127	1.124	41.7
	2013	<i>Tterhex-11.06-II-2^b</i>	***	LGII-2	41.78	M13933-57:T>G-	5.1	4.47	38.1	38.1	50.3	67	-0.648	-0.399	-0.790	-0.345	15.6
		<i>Tterhex-11.06-VII-3</i>	*	LGVII-3	52.80	ChFaM170-S1		6.39	49.3	49.3	54.5	54.5	-0.648	-0.320	-0.120	-0.647	24.6
	2014	<i>Tterhex-11.06-VII-1</i>	*	LGVII-1	23.34	F10992-38:T>A-LG7	5	5.82	21.7	21.7	30.8	33.9	-0.500	0.170	-0.257	-0.447	20.6
Triterpenoid- hexose 9.33	2013	<i>Tterhex-9.33-II-2</i>	****	LGII-2	20.61	F20695-10:A>C-LG2	5	6.27	8	18.8	28.7	33.2	1.279	1.108	1.035	1.055	28.2
		<i>Tterhex-9.33-VII-3^b</i>	***	LGVII-3	4.51	20483-26:C>G-		4.38	0	0.8	17.7	21	1.279	1.239	1.424	1.342	17.0

^a Significance level of Kruskal-Wallis test. *, P<0.005; **, P<0.001; ***, P<0.0005; ****, P<0.0001.

^b QTL detected below the threshold

^c Percentage of the variance explained by the QTL.





Association of QTL, mQTL and genic-markers controlling the variation of ellagic acid-hexose

Next, a screening for candidate genes involved in ellagitannin metabolism underlying the two stable mQTL for ellagic acid-hexose isomer 2 and galloyl-bis(HHDP)-glucose isomers 1 and 4 was performed. 2-LOD interval was taken as the confidence interval for mQTL location, and the corresponding genomic regions in the integrated map of the '232' and '1392' population were extrapolated with the help of the DNA markers developed by Sanchez-Sevilla *et al.* (2015). The 2-LOD interval for *qEAhex-5.87-I-2* was established between 49.3 and 58.9 cM (3942780-10160211 bp on *F. vesca* chromosome 1), and *G-BHglu-6.16-IV-1* and *G-BHglu-6.88-IV-1* spanned the interval 33.92-44.5 cM (2955040-17118782 bp on *F. vesca* chromosome 4). The high macrosynteny between *F. x ananassa* and *F. vesca* allowed to use *F. vesca* genome annotation (Tennessen *et al.*, 2014; Edger *et al.*, 2018, www.rosaceae.org) to look for possible candidate genes, and gene function was always confirmed with Nucleotide BLAST (NCBI; blast.ncbi.nlm.nih.gov). Candidates were selected based on available information about phenylpropanoids and soluble tannins pathways (KEGG; www.kegg.jp) and previous publications about ellagitannins synthesis and metabolism (Vogt, 2010; Mittasch *et al.*, 2014; Bontpart *et al.*, 2016; Schulenburg *et al.*, 2016). In addition, expression pattern of the candidates in *F. x ananassa* cv. 'Camarosa' published RNASeq data (Sánchez-Sevilla *et al.*, 2017) was verified, to select only the ones with expression in mature (red stage) achenes and receptacle. Selected candidate genes for the two mQTL are showed in Table 3.

Table 3: candidate genes within 2-LOD confidence interval of mQTL for ellagic acid hexose isomer 2 (*qEAhex-I-2*) and galloyl-bis(HHDP)-glucose isomers 1 and 4 (*G-BHglu-IV-1*). The position in *F. vesca* is indicated (in bp) and gene identifiers from Genome database for Rosaceae and NCBI are indicated, together with gene function according to NCBI Blast.

	Gene identifier v2	Gene identifier v4	Chr	Start (pb)	End (pb)	NCBI annotation	gene identifier (NCBI)
<i>qEAhex-I-2</i>	gene14782	FvH4_1g13410	Fvb1	7351159	7356569	succinate dehydrogenase [ubiquinone] flavo subunit mitochondrial	LOC101295629
	gene14783	FvH4_1g13420	Fvb1	7360792	7365888	Cytochrome P450 90B1 (Dwarf4) (putative)	LOC101304220
	gene23807	FvH4_1g16310	Fvb1	9370732	9399786	uncharacterized acetyltransferase at3g50280-like	LOC101313936
	gene23808	FvH4_1g16300	Fvb1	9368603	9370555	uncharacterized acetyltransferase At3g50280-like	LOC101314213
	gene23864	FvH4_1g16460	Fvb1	9491397	9494265	probable 2-oxoglutarate-dependent dioxygenase At3g49630	LOC101311031
	gene23879	-	Fvb1	-	-	uncharacterized acetyltransferase At3g50280-like	LOC101313067
	gene24014	FvH4_1g16870	Fvb1	9767840	9775186	cytochrome family subfamily polypeptide	LOC101306382
	gene24019	FvH4_1g16840	Fvb1	9751153	9755033	UDP-glycosyltransferase 84B2-like	LOC101307255
<i>G-BHglu-IV-1</i>	gene11466	FvH4_4g03650	Fvb4	3252001	3253967	kaempferol 3-O-beta-D-galactosyltransferase-like	LOC101293776
	gene12222	FvH4_4g06180	Fvb4	5532764	5534741	cytochrome P450 CYP73A100-like	LOC101306528
	gene12026	FvH4_4g06480	Fvb4	5766151	5770057	serine carboxypeptidase-like 13	LOC101310318
	gene12010	FvH4_4g06510	Fvb4	5791111	5794928	serine carboxypeptidase-like 13	LOC101311192
	gene36574	FvH4_4g06040	Fvb4	5456898	5463462	3-oxo-Delta(4,5)-steroid 5-beta-reductase-like	LOC101305374
	gene16984	FvH4_4g08180	Fvb4	7987871	7993429	NADPH--cytochrome P450 reductase 2	LOC101300898
	gene36596	FvH4_4g07930	Fvb4	7485556	7489882	serine carboxypeptidase-like 18	LOC101305358

Expression analysis of the candidate genes

The basal expression of the candidate genes was measured by quantitative RT-PCR (qRT-PCR) in ripe fruits from F₁ lines showing contrasting content in ellagitannins and derivatives and parental lines. The primers sequences used for each candidate are listed in Annex 1, and the relative content of ellagic acid hexose (isomer 2) and galloyl bis(HHDP) glucose (isomers 1 and 4) in the selected F₁ lines are showed in Figure 5.

The expression of the *gene FvH4_1g16310* presented a significant 3.6-fold increase ($P < 0.01$) in the selected F₁ lines with high content of ellagic acid hexose isomer 2, when compared to the F₁ lines where the metabolite was undetectable (Figure 6). No significant differences in the expression of the selected candidate genes for the mQTL of the two isomers of galloyl-bis(HHDP)-glucose were found between the two F₁ lines groups. *Genes FvH4_4g07930*, *FvH4_1g16300*, *FvH4_4g03650*, *FvH4_4g06180*, *FvH4_4g08180* and *FvH4_4g07930* did not show expression in the fruits of the '1392' parental line nor the tested F₁ lines, or the obtained Ct value were too high (Ct > 35) to quantify expression.

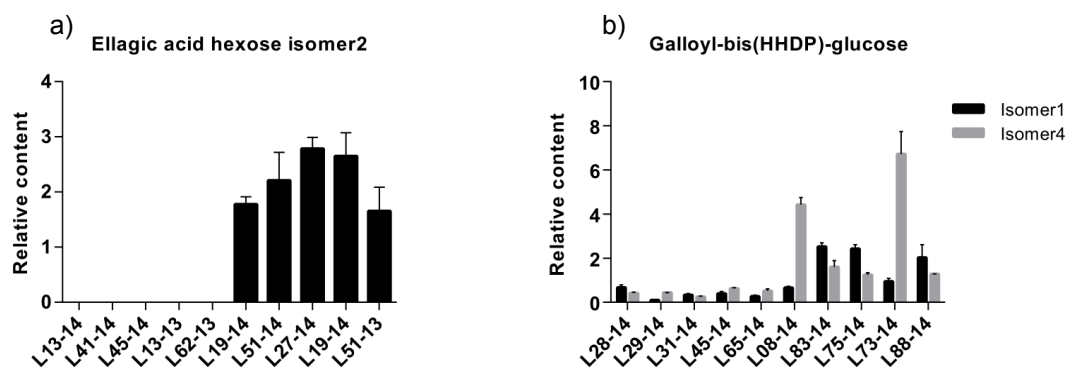


Figure 5: a) Mean metabolite content in the F₁ lines selected for their contrasting content in ellagic acid hexose isomer 2 in the two years. b) Mean metabolite content in the F₁ lines selected for their contrasting content in galloyl-bis(HHDP)-glucose isomers 1 and 4 in the two years

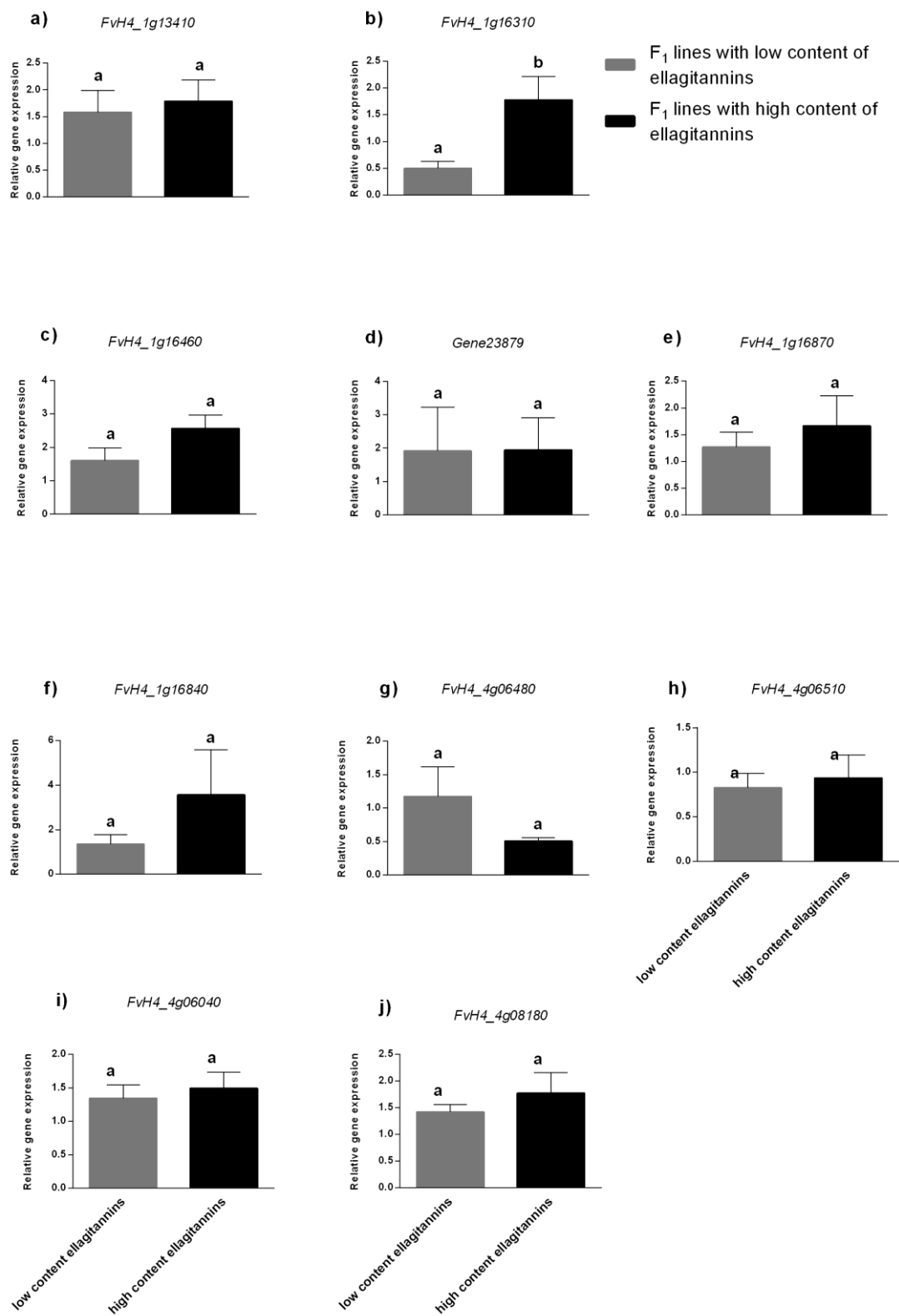


Figure 6: Relative expression by qRT-PCR of candidate genes *FvH4_1g13410* (a), *FvH4_1g16310* (b), *FvH4_1g16460* (c), *gene23879* (d), *FvH4_1g16870* (e), *FvH4_1g16840* (f), *FvH4_4g06480* (g), *FvH4_4g06510* (h), *FvH4_4g06040* (i) and *FvH4_4g08180* (j). Grey columns indicate mean relative expression of the genes in the five selected F₁ lines with low content of the metabolites corresponding to the mQTL and black column relative mean expression in the five selected F₁ lines with high content of the metabolites. Error bars indicate \pm SE. Different letters indicate significant differences between pool of lines using *t*-Student significant difference test adjusted to 95% significance.

The gene *FvH4_1g16310* (*Fragaria vesca* v4.0.a1 genome annotation, Edger *et al.*, 2018) encodes an uncharacterized acetyltransferase. Gene ontology annotation and BLAST analysis showed that this enzyme belongs to the same family than β -glucogallin *O*-galloyltransferases (EC.2.3.1.90). These enzymes are classified as acyltransferases, which transfer groups other than aminoacyl groups. They use β -glucogallin as donor and acceptor, forming di-galloylglucose (Figure 7), which, in turn, can act as acceptor, with the consequent formation of trigalloylglucose. In a previous study, β -glucogallin *O*-galloyltransferases proteins have been classified as enzymes involved in the synthesis of pentagalloylglucoses, precursors for ellagitannins and gallotannins (Denzel *et al.*, 1988).

For these reasons, and in order to characterize functionally the role of the acetyltransferase protein in strawberry, the gene *FvH4_1g16310* was chosen as a candidate for transient and stable silencing/overexpression in *F. x ananassa*.

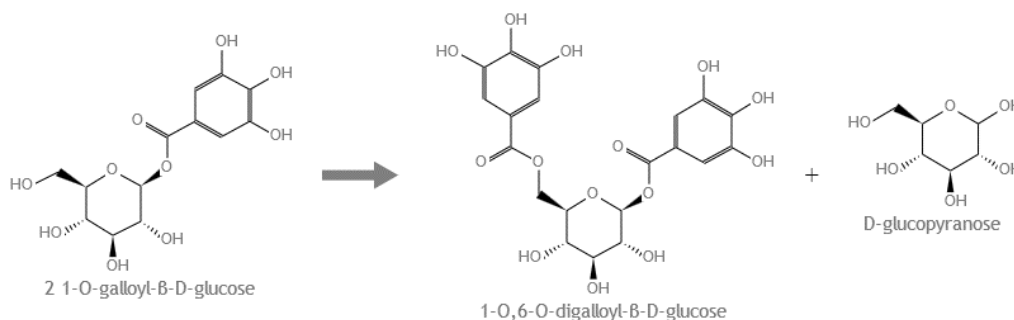


Figure 7: reaction catalyzed by β -glucogallin *O*-galloyltransferase. Two molecules of 1-O-galloyl- β -D-glucose (β -glucogallin) are converted to one molecule of 1-O,6-O-digalloyl- β -D-glucose and D-glucopyranose

Transient overexpression of *acetyltransferase* gene in strawberry fruits

In previous studies, transient overexpression of candidate genes by agroinfiltration has been successfully used to investigate gene functions in strawberry fruit (Jia *et al.*, 2013; Han *et al.*, 2015; Vallarino *et al.*, 2015). Injection of green fruits with a solution containing *A. tumefaciens* strain AGL0 harboring *35S::acetyltransferase gene* construct to overexpress the candidate gene was performed in fruits of different varieties of *F. x ananassa* (cv. 'Camarosa', 'Candongga', 'Fortuna', 'Nieve', 'Primoris', 'Rabida', 'Sabrina' and 'Splendor'). In parallel, fruits were also injected with the empty vector (*pEAQ-HT-dest1*) to serve as control. The fruits were harvested at ripe stage and immediately frozen in liquid nitrogen. No phenotype was observed in the overexpressed fruits, and only seven fruits showed overexpression by qRT-PCR when compared to their respective control (Figure 8).

Next, a deeper genetic and metabolic study of the overexpressed fruits was undertaken. To figure out if the overexpression of the *acetyltransferase* has an effect on the expression of other genes involved in ellagitannin/polyphenol metabolism, expression of *FaPAL* and the gene *FvH4_1g16840* was measured by qRT-PCR in the overexpressed and control fruits. *FaPAL* was chosen for being the central gene in the general phenylpropanoid pathway (Figure 1), while *FvH4_1g16840* gene was selected for its homology with a glycosyltransferase which catalyzes the formation of β -glucogallin in oak (Mittash *et al.*, 2014). Different isoforms of *FaPAL* are described in *F. vesca* genome; the selected isoform (*FvH4_7g19130*) was chosen for its high expression in *F. x ananassa* 'Camarosa' receptacle and achenes (Sánchez-Sevilla *et al.*, 2017).

However, neither of the selected genes showed a clear expression pattern in the overexpressed fruits, when compared to their control (Figure 9). Indeed, *FaPAL* expression was significantly increased in two fruits ('Rabida1 and 2') and decreased in another two (Sabrina and Camarosa) (Figure 9a). *FvH4_1g16840* gene expression was greatly enhanced in two fruits ('Rabida1' and 'Camarosa'), but did not show any significant differences with control fruits in the other five (Figure 9b).

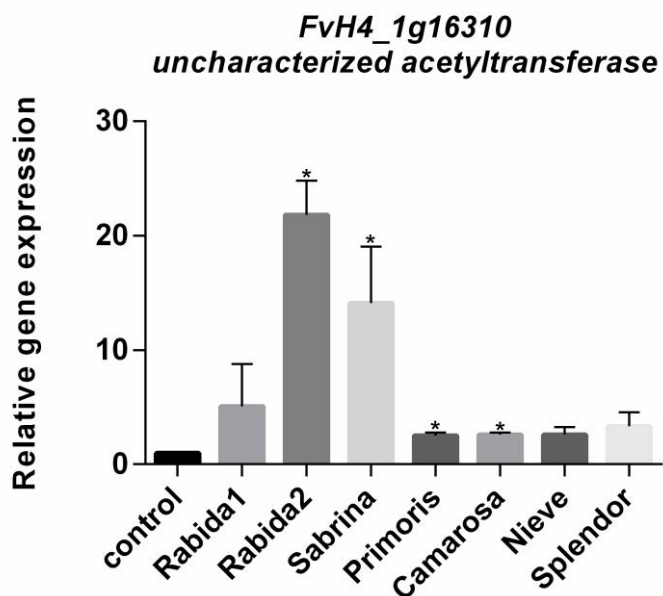


Figure 8: Relative expression of the *acetyltransferase* gene in *A.tumefaciens* injected fruits, compared to their control (empty vector). For reason of simplification, only one control is represented in the graph. The bars represent the relative mean expression value of three technical replicates. Error bars indicate \pm SE. Asterisks indicate significant difference between overexpressed fruit and its control by t-test analysis: *, $P<0.05$.

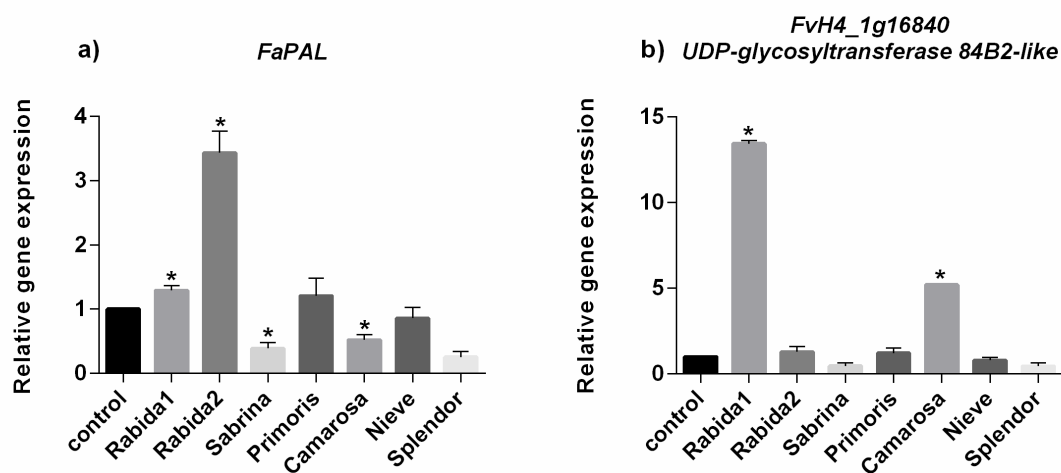


Figure 9: Relative expression of *FaPAL* (a) and *FvH4_1g16840* (b) in *overexpressed* fruits, compared to their control (empty vector). For reason of simplification, only one control is represented in the graph. The bars represent the relative mean expression value of three technical replicates. Error bars indicate \pm SE. Asterisks indicate significant difference between overexpressed fruit and its control by t-test analysis: *, $P < 0.05$.

Metabolomics studies, including primary, secondary and volatiles, are ongoing. Preliminary analysis for secondary and primary metabolites by UPLC-Orbitrap-MS/MS and GC-TOF-MS respectively are presented in Tables 4 and 5.

Regarding secondary metabolism, a deeper look was taken in possible changes of ellagitannins and derivatives relative content (Figure 10). Ellagic acid hexose isomer 2 was increased (up to 50% in 'Rabida1' fruit) in four overexpressed fruits, but was decreased in the other three. Furthermore, 'Rabida1' overexpressed fruit showed a general enhancement of ellagitannin relative content, and of the other class of tannins (PAs, Table 4). Besides, 'Rabida2', 'Sabrina', 'Primoris' and 'Camarosa' fruits presented an increase of the levels of some ellagitannin compounds, but almost no change or a decrease in others. Finally, for 'Nieve' and 'Splendor' overexpressed fruits a general decrease of ellagitannin content was observed (Figure 10), making difficult to draw any conclusions.

Interestingly, tyrosine relative content in all the injected fruits with the construct harboring the *35S::acetyltransferase* and phenylalanine relative content in five of these fruits were decreased when compared to their respective control. In addition, there was also a decrease in the levels of fructose-6-phosphate in the overexpressed fruits, with the exception of 'Sabrina' fruit (Table 5).

Table 4: Changes in secondary metabolites in *35S::acetyltransferase*-overexpressed strawberry receptacle relative to the control. Missing values indicate that the metabolite was detected in the injected fruit but not in its corresponding control.

	Metabolite	Rabida1	Rabida2	Sabrina	Primoris	Camarosa	Nieve	Splendor
Condensed tannins	Procyanidin dimer1	3.493	1.199	1.095	0.561	0.673	0.896	1.127
	Procyanidin dimer2	3.286	0.918	1.061	0.463	0.712	0.870	1.129
	Procyanidin dimer3	3.134	0.829	1.090	0.567	0.677	0.896	1.231
	Procyanidin dimer4	3.638	1.089	1.052	0.562	0.614	0.972	1.070
	Procyanidin trimer1	2.845	1.192	1.070	0.525	0.701	0.805	1.304
	Procyanidin trimer2	3.770	0.870	1.083	0.421	0.713	0.802	1.189
	Procyanidin trimer3	4.526	1.307	1.144	0.571	0.578	1.134	1.159
	Procyanidin trimer4	2.914	1.417	1.154	0.520	0.743	1.206	1.136
	Procyanidin tetramer1	3.514	1.271	1.045	0.534	0.953	0.884	1.392
	Procyanidin tetramer2	3.574	1.267	1.044	0.438	0.701	0.918	1.326
	Procyanidin tetramer3	5.013	1.433	1.110	0.566	0.578	1.134	1.053
	Procyanidin tetramer4	6.122	1.090	1.065	0.343	0.654	0.650	2.355
	Propelargonidin dimer1	1.990	0.696	1.152	0.524	0.634	0.905	1.040
	Propelargonidin dimer2	4.002	0.525	0.961	0.813	0.818	0.571	0.582
	Propelargonidin dimer3	3.528	0.667	1.240	0.707	0.536	0.535	1.004
	Propelargonidin dimer4	1.614	0.798	1.286	0.453	0.592	0.963	1.198
	Propelargonidin trimer1	1.305	0.726	1.050	0.615	0.712	0.676	1.146
	Propelargonidin trimer2	3.028	0.717	1.107	0.691	0.621	0.864	0.825
	Propelargonidin trimer3	1.841	0.533	1.042	0.899	0.483	0.843	0.947
	Propelargonidin trimer4	1.630	0.832	1.043	0.570	0.621	0.965	1.268
	Propelargonidin trimer5	2.475	0.553	1.027	0.709	0.439	0.608	1.518
	Propelargonidin trimer6	2.052	0.765	1.360	0.760	0.524	1.324	0.881
	Propelargonidin trimer7	1.357	0.683	0.811	0.542	0.632	0.828	1.349
Propelargonidin trimer8	1.700	1.100	1.234	1.218	0.557	0.669	1.254	
Flavanols	(Epi)catechin	3.060	0.936	1.103	0.566	0.657	1.158	1.059
	(Epi)afzelechin1	1.389	0.544	1.144	0.657	0.685	0.740	1.007
	(Epi)afzelechin2	0.638	0.855	1.114	0.883	0.757	0.257	0.805
	(Epi)afzelechin3	1.091	1.400	0.956	0.687	0.462	0.264	0.726
Flavonols	Kaempferol-hexose1	0.473	0.821	1.150	0.104	0.641	0.520	0.534
	Kaempferol-hexose2	0.546	0.797	1.018	2.479	0.141	1.354	0.861
	Kaempferol-hexose3	1.015	0.457	1.312	1.221	1.324	0.405	1.225
	Kaempferol-glucuronide	0.922	0.868	1.108	1.049	0.642	2.041	1.158
	Quercetin-glucuronide	1.425	0.888	1.239	0.905	0.846	1.569	0.781
	Isorhamnetin glucuronide	0.863	0.779	0.510	1.354	0.541	1.120	1.260
	Quercetin hexose	0.672	0.701	1.078	0.381	1.278	0.368	0.736
	Kaempferol malonylhexose	0.471	0.629	2.123	1.088	2.057	0.347	1.656
	Kaempferol coumaroyl hexose	0.240	0.649	1.135	1.254	0.819	1.090	1.401
	Kaempferol acetylhexose	4.803	0.511	1.263	0.710	2.263	0.751	1.693
	Quercetin-acetylhexose	9.683	0.608	0.897	0.205	3.665	0.168	1.003
	Rutin1	0.190	0.621	1.050	1.514	1.458	0.482	1.103
	Rutin2	0.891	0.592	0.969	0.415	0.972	0.240	0.854
	Kaempferol hexose glucuronide	2.464	0.709	4.236	1.350	2.150	0.276	1.192
	Kaempferol pentose hexose glucuronide	9.589	0.125	2.586	1.359	0.774	0.049	0.299
Quercetin malonylhexose	0.417	0.774	1.390	0.226	6.792	0.110	1.056	
Flavonones	Eriodictyol hexose1	0.630	0.726	1.079	0.663	1.059	0.895	0.977
	Eriodictyol hexose2	0.637	0.672	1.162	0.643	1.209	0.712	0.973
	Naringenin chalcone hexose	0.224	0.805	1.174	1.037	1.205	0.990	1.173
Anthocyanins	Cyanidin hexose	0.452	0.931	0.967	0.170	1.136	0.438	0.561
	Pelargonidin hexose	0.615	0.745	1.038	0.743	1.116	0.805	0.981
	Pelargonidin malonyl hexose	0.335	0.743	1.119	0.792	5.024	0.518	1.317

	Pelargonidin rutinose	0.371	0.983	1.104	0.852	0.489	1.228	1.069
Galloyl glucoses	Galloyl-hexose1	1.654	1.017	1.103	2.355	0.507	0.674	0.873
	Galloyl-hexose2	3.062	0.961	1.111	0.832	0.801	0.677	0.923
	Galloyl-hexose3	2.584	1.231	1.105	0.490	0.993	1.539	0.537
	Galloyl-hexose4	2.514	0.514	1.137	1.023	1.010	0.617	0.642
	Galloyl-hexose5	2.016	1.503	1.149	0.598	1.003	1.420	0.488
	Galloylquinic acid1			0.000	0.000	1.313	0.000	1.281
	Galloylquinic acid2	2.342	3.439	1.315	0.954	0.810	0.267	0.863
	Galloylquinic acid3	1.863	3.303	0.783	0.757	0.618	0.200	1.318
Ellagitannins and ellagic acid	HHDP glucose1	2.961	1.114	1.071	0.901	1.051	0.631	0.746
	HHDP glucose2	2.503	0.785	2.283	0.000	1.414	0.486	0.666
	Bis(HHDP) glucose1	2.234	0.752	1.842	1.942	2.175	0.400	0.292
	Bis(HHDP) glucose2	2.585	1.175	1.242	0.834	0.961	0.659	0.806
	Bis(HHDP) glucose3	2.526	1.194	1.208	0.870	0.973	0.671	0.828
	Galloyl-HHDP-glucose	2.665	0.639	1.337	0.992	1.486	0.369	0.763
	Di-galloyl HHDP glucose	3.751	0.592	1.656		1.732	0.266	0.685
	Ellagic acid deoxyhexose1	2.210	0.784	1.341	0.873	1.004	0.450	0.728
	Ellagic acid deoxyhexose2	3.345	1.314	1.168	0.854	0.757	0.629	0.593
	Ellagic acid	1.510	0.302	1.341	2.238	4.675	0.179	0.468
	Galloyl-bis(HHDP)-glucose1	4.351	0.706	1.461	1.471	1.719	0.312	1.032
	Galloyl-bis(HHDP)-glucose2	3.780	0.808	1.313	1.029	1.448	0.370	0.724
	Galloyl-bis(HHDP)-glucose3	5.375	1.602	1.240	0.787	0.543	0.730	0.796
	Galloyl-bis(HHDP)-glucose4	3.593	3.790	1.305	0.839	0.731	0.726	0.566
	Unknown ellagitannin1	2.481	1.790	1.646	0.671	1.385	0.819	0.689
	Unknown ellagitannin2	2.982	0.312	2.282		4.342	0.198	0.000
	Ellagic acid hexose1	3.630	0.674	1.689	3.243	3.245	0.318	0.824
	Ellagic acid hexose2	1.516	0.757	1.103	1.408	1.240	0.816	0.686
	Ellagic acid hexose3	2.889	0.716	1.427	0.941	1.560	0.400	0.575
	Tris-galloyl-glucose1	3.419	0.653	1.357	0.963	1.315	0.458	0.697
Tris-galloyl-glucose2	2.940	0.814	2.003	1.727	0.851	0.253	0.000	
Putative ellagitannins	Rhoipteleatin H	4.162	0.561	0.873	1.905	3.122	0.391	0.532
	Castalagin1	1.288	0.718	1.322	1.535	1.769	0.445	0.304
	Castalagin2	2.424	1.141	0.859	0.708	1.158	0.748	0.974
	Castalagin3	3.351	0.790	1.067	0.738	1.072	0.473	1.039
	Castalagin4	1.929	0.517	1.931	0.722	1.574	0.717	0.788
	Castalagin5	1.470	0.476	1.573	0	3.186	0.450	0.267
	Lagerstannin A1	2.406	0.743	1.687		4.290	0.178	0
	Lagerstannin A2	2.450	0.723	1.001		2.569	0.251	0.092
	Lagerstannin B1	2.520	0.515	1.148		5.255	0.250	0.453
	Lagerstannin B2	1.976	0.543	1.018		3.165	0.338	0.000
	Lagerstannin B3	2.006	0.442	1.183		6.101	0.264	0.000
	Lagerstannin B4	1.561	0.499	1.434		4.781	0.278	0.000
Benzoic acids	Di-hydroxybenzoic acid hexose1	2.406	1.412	1.090	0.527	1.036	1.385	0.376
	Di-hydroxybenzoic acid hexose2	2.416	1.024	1.073	1.084	0.606	1.377	0.716
	Di-hydroxy methyl benzoic acid hexose3	2.644	0.828	0.928	0.696	0.734	0.729	0.741
	Di-hydroxy methyl benzoic acid hexose4	1.165	0.713	1.017	0.989	1.061	0.507	1.061
	Di-hydroxy methyl benzoic acid hexose5	0.346	0.612	1.045	0.689	1.485	0.656	0.884
Hydroxycinnamic acids derivatives	Caffeic acid hexose	0.697	1.128	1.116	1.358	0.375	0.744	1.338
	Coumaric acid hexose1	0.080	1.802	1.071	2.748	0.405	0.924	0.687
	Coumaric acid hexose2	0.093	1.936	1.077	2.790	0.566	1.258	0.755
	Ferulic acid hexose1	0.689	1.407	1.104	1.439	0.171	1.649	1.208
	Ferulic acid hexose2	0.944	1.203	1.105	1.159	0.316	1.574	1.313
	Ferulic acid hexose3	0.064	2.868	1.059	5.696	0.209	0.325	0.739
	Sinapic acid hexose derivative1	0.017	1.371	1.015	1.240	0.562	0.050	0.645

	Sinapic acid hexose derivative2	0.007	1.748	1.089	1.922	0.653	0.111	0.629
	Sinapic acid hexose derivative3	0.020	1.395	1.153	1.252	0.518	0.056	0.680
	Cinnamic acid- hexo	0.041	3.814	1.096	7.995	0.175	0.289	0.769
Terpenoids	Triterpenoid-hexose1	6.287	0.982	1.149	0.449	0.025	0.879	0.682
	Triterpenoid-hexose2	4.772	0.729	1.191	0.294	0.102	0.853	0.388
	Sesquiterpenoid hexose1	0.157	1.112	1.042	1.050	1.299	0.589	0.707
	Sesquiterpenoid hexose2	0.253	1.206	1.032	0.987	0.755	0.513	0.944

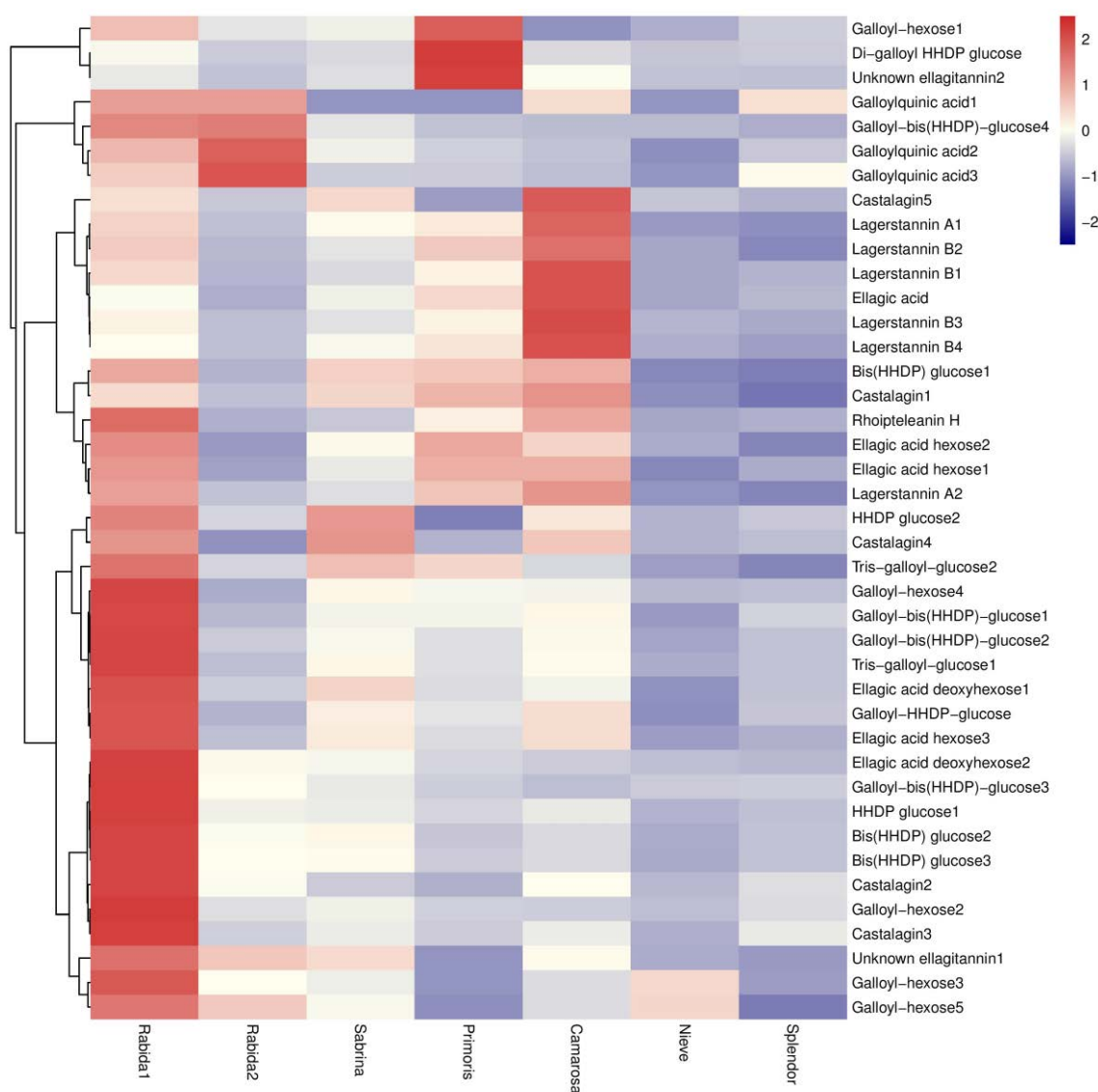


Figure 10: heatmap visualization of relative ellagitannin profiles in the overexpressed fruits. Overexpressed fruit with a relative content for a given compound similar, lower, or higher than that of its control are shown in white, blue, or red, respectively.

Table 5: Changes in primary metabolites in *35S::acetyltransferase*-overexpressed strawberry receptacle relative to the control.

	Name Analyte	Rabida1	Rabida2	Sabrina	Primoris	Camarosa	Nieve	Splendor
Amino acids	Alanine	2.589	2.459	0.752	0.999	0.739	1.063	1.620
	Valine	2.558	2.625	0.873	0.742	0.399	1.590	1.507
	Isoleucine	2.230	2.849	0.808	0.442	0.349	1.090	1.780
	Glycine	0.821	1.558	0.939	1.261	1.056	1.229	1.293
	Proline	0.125	1.697	0.688	2.281	0.171	1.841	2.366
	Serine	0.644	1.920	0.731	1.304	0.790	1.978	1.408
	Threonine	1.507	2.358	0.772	0.586	0.619	1.457	1.315
	beta-Alanine	0.118	0.768	0.677	2.772	0.990	1.797	1.304
	Aspartic acid	1.010	0.877	0.898	1.279	0.725	1.405	1.154
	Methionine	0.184	0.792	0.644	2.093	0.701	3.032	1.551
	Asparagine	13.438	1.618	0.977	0.620	0.709	2.225	1.048
	Pyroglutamic acid	1.263	1.222	0.784	1.556	0.676	1.167	1.067
	Glutamic acid	0.944	0.893	1.026	1.318	0.582	1.269	0.850
	Phenylalanine	0.637	0.807	1.241	0.368	0.346	0.721	1.531
	Tyrosine	0.813	0.000	0.928	0.355	0.459	0.139	0.452
	Tryptophan	0.665	1.216	0.637	1.508	0.944	2.242	1.471
GABA	0.574	1.093	0.839	1.229	0.940	1.051	0.990	
Organic acids	Phosphoric acid	1.109	1.490	0.843	1.631	0.932	1.545	1.167
	Glyceric acid	0.428	0.808	1.253	1.920	0.697	0.657	1.250
	Fumaric acid	0.512	0.725	1.204	0.997	1.025	0.662	0.772
	Malic acid	1.041	0.924	1.395	1.273	1.094	0.560	0.995
	Threonic acid	1.190	0.925	1.019	1.088	0.859	0.515	1.897
	Quinic acid	1.510	0.833	1.325	0.693	1.278	1.062	0.587
	Glucuronic acid	0.270	0.773	0.654	1.166	0.178	1.265	1.271
	DHA_dimer	0.531	0.840	0.957	1.418	0.470	1.132	0.981
	Citric acid	1.088	1.021	0.510	0.637	0.502	1.419	1.162
Sugars and sugar alcohols	Erythritol	0.649	1.365	1.874	1.719	0.835	1.141	0.904
	Xylose	1.497	1.324	0.819	1.391	1.245	1.358	0.948
	Rhamnose	0.782	1.150	0.985	1.146	1.742	1.026	0.978
	Fucose	0.639	1.028	1.036	1.290	0.842	1.101	1.067
	Glucopyranoside	8.382	1.748	1.193	2.238	0.558	0.531	0.893
	myo-Inositol	0.134	0.223	1.438	4.358	0.086	1.794	2.069
	Fructose-6-phosphate	0.455	0.970	1.355	0.970	0.651	0.527	0.786
	Glucose-6-phosphate	0.596	0.857	1.903	1.388	0.606	0.726	1.226
	Maltose	0.055	0.210	0.827	3.993	0.000	1.726	1.148
	Galactinol	0.904	1.018	1.047	1.139	1.584	0.902	1.035
	Raffinose	0.146	0.674	0.872	3.402	1.100	2.823	1.144
	1-Kestose	0.062	0.322	0.848	3.352	0.000	2.912	1.171
	Maltotriose	0.287	1.019	1.266	1.043	2.035	1.429	0.752
	Fructose	1.285	0.187	1.159	2.715	1.191	0.889	0.862
	Glucose	1.200	0.118	1.362	3.380	1.337	0.863	0.828
Sucrose	0.388	0.066	2.725	6.730	17.490	0.331	2.067	

Stable overexpression and silencing of the *acetyltransferase* gene in *F. x ananassa* cv. Camarosa

Stable transformation of the cultivar ‘Camarosa’ was undertaken to overexpress and silence the acetyltransferase respectively, in order to get a deeper knowledge of the function of the gene *in planta*. *A. tumefaciens* strain GV3101 harboring *pK7WG2D-35S::acetyltransferase* and *pK7GWIWG2D(II)-35S::acetyltransferaseRNAi* were used to transform leaf disks explants. Regenerated shoots were grown in N30K multiplication medium, under the selection of kanamycin. PCR using a combination of primers amplifying part of the *35S::acetyltransferase* construct (Annex 1) was performed to select transgenic lines, and to confirm that the *acetyltransferase* gene was overexpressed or silenced in the regenerated plants, expression will be measured by qRT-PCR and compared to ‘Camarosa’ control plants, once the plants will be transferred into soil and acclimated.

Discussion

Variation in secondary metabolites in ‘232’ x ‘1392’ population

The relative content of 130 compounds belonging to secondary metabolism was identified in the fruits of the mapping population, over two successive harvests. As expected, the overwhelming majority of metabolites derived from phenylpropanoid and flavonoid pathways (Hanhineva, 2011). Indeed, strawberry fruit is known for its high content in polyphenols, which are essential constituents of human diet for their strong antioxidant and anti-inflammatory activities (Tulipani *et al.*, 2009; Mazzoni *et al.*, 2016). Within identified polyphenolic compounds and in agreement with their quantitative contribution, 44% were flavonoids, 39% soluble tannins and 17% hydroxycinnamic and benzoic acid derivatives.

Dissimilarities in each line between the two harvests are probably due to environmental conditions, even if important differences between genotypes are also observed. Indeed, both environment and genetic factors have been previously associated with the qualitative and quantitative content of polyphenols in strawberry fruits (Carbone *et al.*, 2009; Diamanti *et al.*, 2012; Josuttis *et al.*,

2013; Urrutia *et al.*, 2015b; Galli *et al.*, 2016). Effect of the genotype can be observed for example in the content of secondary metabolites in the parental lines of the population; even if absolute differences exist between the two years, the relative content of secondary metabolites and their proportion between the two parental lines are almost always consistent (Table 1). As expected, several metabolites showed significant differences in the parental lines, confirming their contrasting metabolic composition previously reported by Zorrilla-Fontanesi *et al.* (2011).

Distribution of most metabolites showed typical polygenic inheritance, and, in addition, transgressive behaviour was observed in the F₁ progeny for most compounds. Transgressive variation results from positive interaction between parental genotypes and by crossing genetically divergent parents, the range of phenotypic variation in the progeny is expected to be more extensive, with individuals presenting unexpected phenotypes based on the attributes of the parents (Moose and Mumm, 2008). As a consequence, the observed transgressive segregation for almost all the secondary metabolite in the F₁ progeny can be explained by the high number of significantly different metabolite levels in the parental lines.

Generally speaking, the variation in metabolite abundance across the population was greater for secondary metabolites than for primary metabolites, even if some exceptions could be observed (i.e. 98-fold and 29-fold increase in aspartic acid in some F₁ lines when compared to the '1392' parental, see chapter 2). Alseekh *et al.* (2015) also made this observation by comparing primary and secondary metabolites in tomato, and suggested that the less intricate control of secondary metabolite abundance, which is dominated by transcriptional regulation, could explain it.

HCA and metabolite-metabolite correlations indicated co-regulation of metabolites based on their biochemical relationships. As expected, strong positive correlations were obtained within common metabolic classes, such as proanthocyanidins or soluble tannins. More surprisingly, very few negative correlations were obtained between different classes. Indeed, it could be expected that different branches of the phenylpropanoid pathway compete for the

use of common precursors. Indeed, competition between flavonoid and lignin biosynthesis for a common substrate (coumaroyl-CoA) have been observed (Hoffmann *et al.*, 2006, 2011; Ring *et al.*, 2013). However, no competition has been described between flavonoid and ellagitannin synthesis, even if they share a common precursor.

mQTL controlling secondary metabolite content

mQTL for 116 out of 130 of the identified compounds were detected by the non-parametric Kruskal-Wallis test and restrictive multiple QTL mapping, and 23.7% of them were stable in the two harvests, indicating that secondary metabolite content is also affected by the environment to a large extent. Analysis of the genomic location of the QTL for secondary metabolism revealed that they are well spread across the genome in all the chromosomes, even if a few hotspots are noticeable, particularly in HG V (LG V-2 and LG V-4). It is also striking that the same linkage groups were harboring important clusters of QTL for primary metabolites (see chapter 2). This unequal distribution of mQTL over the genome has been previously reported in *Arabidopsis* populations and can be explained by an uneven localization of biosynthetic genes or the existence of master regulators, controlling metabolite accumulation in a higher hierarchical order (Keurentjes *et al.*, 2006; Wentzell *et al.*, 2007; Lisec *et al.*, 2008; Rowe *et al.*, 2008).

Previous QTL analysis in strawberry (Zorrilla-Fontanesi *et al.*, 2011; Lerceteau-Köhler *et al.*, 2012), peach (Zeballos *et al.*, 2016), raspberry (Dobson *et al.*, 2012), apple (Khan *et al.*, 2012) or grape (Fournier-Level *et al.*, 2009) identified genomic regions responsible of anthocyanin and polyphenols variation. Furthermore, Alseekh *et al.* (2015), in tomato fruits, reported a QTL mapping for 43 secondary metabolites and Urrutia *et al.* (2015b) mapped 76 stable mQTL for 22 polyphenols in *F. vesca*. However, to our knowledge, this study represents the first attempt to combine QTL detection with a so large array of secondary metabolites in the *Rosaceae* family. As a result, the vast majority of QTL reported here were previously unknown, even if QTL for related traits could be connected with the previous mentioned studies. Zorrilla-Fontanesi *et al.* (2011) described a large cluster of QTL in LG V-2, which included the collocation of QTL for titratable

acidity, pH, anthocyanin content and color parameters. Interestingly, a stable QTL for pelargonidin-hexose, the most abundant anthocyanin pigment, was located in the same linkage group in this study, with a 2-LOD confidence interval spanning from 8 cM to 30 cM. In addition, the QTL could explain around 25% of total phenotypic variation in pelargonidin-hexose content, being the major detected QTL for this metabolite in the two harvests. Moreover, a QTL for cyanidin-hexose, the minor pigment in strawberry fruit, was detected in 2013 in LG V-2 with a 2-LOD interval coinciding with pelargonidin-hexose QTL. Stable QTL for other derivatives of pelargonidin (pelargonidin rutinose and pelargonidin acetyl hexoside) were also detected in the same region of LG V-2. Taken together, these results indicate the presence in LG V-2 of a *locus* involved in anthocyanin content, which in turn influence the color phenotype of the fruit. However, the presence of several QTL detected for other flavonoid compounds in the same genomic region of LG V-2, such as PAs, flavanols and flavonols, cannot rule out that the *locus* responsible of anthocyanin and color variation in the F₁ mapping population is acting upon the flavonoid pathway upstream anthocyanin synthesis. Stable QTL for cyanidin-hexose and pelargonidin acetyl hexoside, and a QTL for pelargonidin-hexose and pelargonidin malonyl hexose only detected in 2014, among other QTL related to flavonoid metabolites, were located at the beginning of LG V-4, suggesting the possible presence of a homoeo-QTL.

Castro and Lewers (2016) and Lerceteau-Köhler *et al.* (2012) also mapped in different strawberry populations QTL for anthocyanin content, antioxidant capacity, total phenols and color parameter in HG V, confirming the presence of a *locus* related to flavonoid content in this chromosome. QTL mapping in *F. vesca* introgression lines also pointed out chromosome 5 as harboring *locus* or *loci* involved in polyphenol metabolism (Urrutia *et al.*, 2015b,a). Candidate genes located on chromosome 5 were proposed by the authors of the latter study, and included genes encoding for an anthocyanidin synthase (*FaANS*), an anthocyanidin reductase (*FaANR*) and a flavonoid 3'hydroxylase which was shown to be related to anthocyanin balance (Thill *et al.*, 2013). In addition, the transcription factor *FaMYB1*, involved in flavonols and anthocyanins production during ripening, has been localized in chromosome 5 (Almeida *et al.*, 2007).

QTL mapping in peach also found *loci* related to anthocyanin content in chromosome 5, which is syntenic with chromosome 5 in *F. vesca* (Zeballos *et al.*, 2016). In apple, a mQTL hotspot for phenolic compounds was identified on linkage group 16, which is syntenic with *F. vesca* chromosome 5, and several candidate genes were proposed, i.e. *LAR1* and two *MYB* transcription factors (Khan *et al.*, 2012). In *Rubus* genus, which genome shows high synteny with *F. vesca* genome, QTL for total phenol content and antioxidant capacity were detected in LG 5 (Dobson *et al.*, 2012).

Another cluster of QTL was observed in LG I-2 for flavonoids, mainly for proanthocyanidins and flavanols. In *F. vesca*, Urrutia *et al.* (2015b) found several candidate genes in chromosome 1 which could be involved in the levels of these metabolites, such as *FaF3'H* or *FaFHT* (Figure 1). Furthermore, *FaMYB10*, one of the key transcription factors in the regulation of the phenylpropanoid/flavonoid pathways, is located on chromosome 1, and could co-localize with some QTL detected in this HG in the '232' x'1392' population (Medina-Puche *et al.*, 2014; Zhang *et al.*, 2017).

Concerning hydroxycinnamic and benzoic acid derivatives, main clusters of QTL were observed in HG IV (LG IV-2 and LG IV-3). Urrutia *et al.* (2015b) also mapped major stable QTL for the content of hydroxycinnamic acid derivatives on *F. vesca* chromosomes 2 and 4. In the '232' x'1392' population, stable QTL for coumaric acid isomer 2 was detected in LG II-1, together with other QTL for sinapic, ferulic and cinnamic acid derivatives (Figure 4). Possible candidate genes such as coumarate-CoA ligase, *CHS* and *CHI*, which are implicated in the early steps of the phenylpropanoid pathway, are located on chromosome 2. Chromosome 4 harbours *Fra a* genes which are regulators of the flavonoid pathway and pigment accumulation during ripening (Casañal *et al.*, 2013; Urrutia *et al.*, 2015b).

Candidate gene screening in LG I-2 and LG IV-1 related to ellagitannin metabolism

Notably very little is known about the biosynthesis and metabolism of gallo- and ellagitannins, even if increasing interest for these compounds has been shown due to their antioxidant and anti-inflammatory properties (Giampieri *et al.*, 2012). Gallic acid, which represents the core structure in soluble tannin molecules, is

likely formed via dehydrogenation of 5-dihydroshikimate, and thus shares a common origin with the phenylpropanoid/flavonoid pathway (Vogt, 2010, Figure 1). QTL mapping for *loci* involved in ellagitannin content can be a useful tool to shed light on their synthesis or regulation.

To our knowledge, the only study which identified QTL related to ellagic acid, which is released by ellagitannins by hydrolysis at the end of the biosynthetic pathway (Niehaus and Gross, 1997), was performed in *F. vesca* introgression lines by Urrutia *et al.* (2015b). Lines harboring introgressions in LG1 and LG4 showed significant increase in ellagic acid content. Interestingly, clusters of QTL for ellagitannin metabolites were also detected in the '232' x '1392' map in LG I-2 and LG IV-1, even if other clusters could be observed in LG II-4, LG V-1 and LG VII-1.

Position of ellagitannin QTL cluster in LG I-2 was approximately the same than the QTL cluster for flavonoids described above. Thus, it cannot be ruled out that a common *locus* regulates the levels of both phenol classes, and would act upstream the shikimate pathway. However, a stable QTL for ellagic acid hexose isomer 2, located between 49 and 59 cM approximately in LG I-2, was appealing due to its high LOD score, its clear position in both harvests and the percentage of phenotypic variation explained by it (between 51 and 71% in 2014 and 2013 respectively), suggesting the presence of a key *locus* involved in ellagic acid hexose metabolism. In addition, it is striking that ellagic acid hexose isomer 2 was not detected in 14 lines of the mapping population in any of the two harvests. A deeper analysis of the genomic region corresponding to the stable detected QTL, using *F. vesca* genome annotation (Tennessen *et al.*, 2014; Edger *et al.*, 2018), allowed the selection of eight candidate genes (Table 3). Genes *FvH4_1g13410* (succinate dehydrogenase), *FvH4_1g13420* (cytochrome P450), *FvH4_1g16460* (2-oxoglutarate-dependent dioxygenase) and *FvH4_1g16870* (cytochrome family polypeptide) were selected as candidates due to the hypothesis existing about soluble tannins synthesis. Indeed, as reviewed in Vogt (2010), it is most likely that gallic acid formed via dehydrogenation of 5-dihydroshikimate (Bontpart *et al.*, 2016) even if a dehydration step via protocatechuic acid and subsequent monooxygenation cannot be ruled out. Evidence for the existence of a specific cytochrome P450 monooxygenase or a 2-oxoglutarate dependent dioxygenase

as shown in coumarin formation would resolve the contribution of both hypotheses.

Three genes (only two in the new annotation of Edger *et al.*, (2018)) were annotated as uncharacterized acetyltransferase (*FvH4_1g16310*, *FvH4_1g6300* and *gene23879*). They are classified as acyltransferases, which transfer groups other than aminoacyl groups, and interestingly, belong to the same enzyme category than β -glucogallin O-galloyltransferase (EC 2.3.1.90). β -glucogallin O-galloyltransferase catalyzes the formation of digalloylglucose from β -glucogallin, where β -glucogallin acts as donor and acceptor. Digalloylglucose can also acts as acceptor, with the formation of trigalloylglucose (Denzel *et al.*, 1988). As a consequence, these enzymes are involved in the synthesis of pentagalloylglucose, which is the central precursor for gallo- and ellagitannin synthesis. Previous studies characterized the activity of galloyltransferases in *Rhus typhina* leaf extracts (Denzel *et al.*, 1988; Niemetz and Gross, 2001).

In addition, BLAST of the protein sequences of the uncharacterized acetyltransferases showed the presence of a hydroxycinnamoyl-CoA:shikimate/quinic acid hydroxycinnamoyltransferase (HCT) domain. HCT enzymes synthesize coumaroyl/caffeoyl shikimate and quinate from coumaroyl CoA precursor, and are involved in hydroxycinnamic acids and lignin biosynthesis (Hoffmann, 2004; Mouradov and Spangenberg, 2014).

Last candidate gene, a UDP-glycosyltransferase 84B2-like (*FvH4_1g16840*), was selected based on its homology with UGT84A13, an enzyme isolated from pedunculate oak. This enzyme is able to catalyze the formation of β -glucogallin from UDP-glucose and gallic acid, which is the first committed step of gallotannin biosynthesis (Mittasch *et al.*, 2014). Another recent study described the formation of β -glucogallin in strawberry and raspberry (Schulenburg *et al.*, 2016). They identified *FaGT2*, a glycosyltransferase, which contributes to the production of ellagic acid and ellagitannins, by catalyzing the formation of β -glucogallin from gallic acid. This gene is located on *F. vesca* chromosome 2, and interestingly a stable QTL for ellagic acid hexose isomer 3 was detected in LG II-4 in the same position than a QTL for isomer 2 in 2014. In addition, QTL for ellagic acid deoxyhexose isomers were mapped in similar location in LG II-4. Thus, it would

be interesting to further investigate this genomic region for *locus* related to ellagitannin metabolism, and to figure out if *FaGT2* is located within 2-LOD interval of QTL detected for ellagitannin metabolites.

Another hotspot for QTL related to ellagitannin and gallotannin was located on LG IV-1 of the '232' x '1392' mapping population. More specifically, two stable and major QTL for galloyl-bis(HHDP)-glucose isomers 1 and 4, which are two ellagitannins, were located on LG IV-1, explaining 30% of the phenotypic variation for the isomer 1 and 45% for the isomer 4. Additionally, 7 QTL were detected for different compounds, including another QTL for ellagic acid hexose isomer 2 detected in 2014 and a stable QTL for the ellagitannin tri-galloyl HHDP glucose. Screening for genes in the 2-LOD interval delimited by galloyl-bis(HHDP)-glucose isomers 1 and 4 stable QTL (between 33.9 and 44.5 cM in LG IV-1) allowed the identification of seven possible candidates. Gene *FvH4_4g03650* (kaempferol 3-galactosyltransferase) was selected because of its role in the flavonoid pathway. Three genes were annotated as serine carboxypeptidases (*FvH4_4g06480*, *FvH4_4g06510*, *FvH4_4g07930*) and were selected based on the hypothesis that serine carboxypeptidase-like acyltransferases could be involved in further step of galloylation, using β -glucogallin. Indeed, it has been shown that the transacylation reaction from glucose esters which leads to the formation of gallotannins is carried out by enzymes homologous to serine carboxypeptidases (Liu *et al.*, 2012; Bontpart *et al.*, 2015, 2016). Finally, gene *FvH4_4g06040*, which encodes a 3-oxo-delta (4,5)-steroid 5-beta-reductase-like, was selected because it belongs to a subfamily of short-chain dehydrogenase/reductase enzymes which include phenylcoumaran benzylic ether, phenylpropene synthase, eugenol synthase and isoflavone reductases, which are involved in the phenylpropanoid pathway.

Gene *FvH4_1g16310*: uncharacterized acetyltransferase

qRT-PCR analysis of the selected candidate genes for both ellagic acid hexose isomer 2 and galloyl-bis(HHDP)-glucose isomers 1 and 4 showed that gene *FvH4_1g16310* was clearly differentially expressed between F₁ lines with high content of ellagic acid isomer 2 and lines where the metabolite was not detected in any of the two harvests ($P < 0.01$). Expression analysis of candidate genes is an approach to decipher if the gene can be involved in metabolite content, and

was previously used successfully to identify *FaOMT*, a gene implicated in mesifurane synthesis in strawberry (Zorrilla-Fontanesi *et al.*, 2012). Indeed, it can be expected that the unbalance of a determined metabolite between lines of a population is consequence of the differential expression of one or more gene(s) implicated in its metabolism. However, it exists the possibility that the expression is unchanged, and that the difference in metabolite content is consequence of changes in the nucleotide sequence of the candidate gene. Allelic variation analysis, combined with QTL mapping, was successfully used for the identification genes related to apple and peach aroma (Dunemann *et al.*, 2012; Eduardo *et al.*, 2013; Farneti *et al.*, 2017). Thus, it would be interesting in the future to perform an allelic variation study of the selected genes for the different mapped QTL. In addition, it is important to realize that the strategy we followed to identify candidates only allowed to select genes which have been annotated as a putative function in *F. vesca* or *A. thaliana*. The presence of genes with unknown function within the QTL interval hinders their selection as possible candidates.

The gene *FvH4_1g16310* encodes an uncharacterized acetyltransferase, with a HCT domain, suggesting a possible role in the phenylpropanoid metabolism. In addition, the relation with the enzyme family β -glucogallin O-galloyltransferase could point out a connection with gallotannins and ellagitannins synthesis. In addition, a correlation between ellagic acid levels during fruit ripening and expression of the acetyltransferase in *Fragaria x ananassa* cv. 'Camarosa' receptacle and achenes was observed (Sánchez-Sevilla *et al.*, 2017). Indeed, transcripts corresponding to the *acetyltransferase* were more abundant in green tissues and were decreasing along ripening, consistent with the reduced levels of ellagic acid towards later stages of ripening (Schulenburg *et al.*, 2016; Sánchez-Sevilla *et al.*, 2017).

However, this enzyme would be implicated in the first steps of the pathway, as catalyzing part of the reactions involved in the formation of the pentagalloylglucose precursor. Ellagic acid, which is the result of ellagitannin hydrolysis, is formed at the end of the pathway. Interestingly, a QTL for lagerstannin A isomer 1 shares 2-LOD confidence interval with the stable QTL detected in LGI-2 for ellagic acid hexose isomer 2. Thus, the acetyltransferase

could influence the levels of several metabolites belonging to the soluble tannin class.

Preliminary primary metabolites analysis in transient overexpressed fruits showed a decrease in tyrosine, phenylalanine and fructose-6-phosphate relative content.

Ellagitannins precursor, gallic acid, is thought to be formed by the dehydrogenation of 3-dihydroshikimate (Bontpart *et al.*, 2016). This could explain the decrease in shikimate pathway products (tyrosine and phenylalanine) and precursor (fructose-6-phosphate, Table 5), as the overexpression of the *acetyltransferase* is expected to enhance ellagitannin synthesis and could cause a decrease of the metabolites belonging to the shikimate pathway. However, secondary metabolites analysis of the overexpressed fruits by UPLC-Orbitrap-MS/MS did not show any clear increase of ellagic acid hexose isomer2 nor ellagitannins (Figure 10).

Future metabolomics and biochemical characterization of stable strawberry plants overexpressing and silencing the *acetyltransferase* gene will shed light on the role of the candidate gene in phenol compounds synthesis.

Likewise, a deeper analysis of QTL-delimited genomic regions will surely allow the identification of new candidate genes associated with strawberry fruit secondary metabolism.

Chapter 4: Metabolomic Profiling of Postharvest Senescence in Different Strawberry Cultivars

Introduction

Fruit ripening and senescence are complex processes, which are controlled by multiple developmental and environmental signals (Qin *et al.*, 2009), even if the molecular mechanisms underlying them remains unclear. Ripening involves changes in metabolism, including chlorophyll degradation, anthocyanin accumulation, cell wall breakdown, sugars and volatiles synthesis (Ornelas-Paz *et al.*, 2013), while senescence, being the final step of fruit development, leads to the degradation of proteins, lipids and nucleic acids, resulting in cell dysfunction, disintegration and cell death (Yun *et al.*, 2012). During postharvest storage, senescence is an inevitable and negative biological process, leading to a rapid deterioration of fruit quality attributes (Tietel *et al.*, 2011). Fruit respiration, which provides the energy necessary for biochemical reactions, water loss, fungal and bacterial pathogens and physiological disorders result in the senescence acceleration of the fruit (Aked, 2002; Yang *et al.*, 2014). In addition, previous studies showed that fruit maturity and senescence are the critical factors regarding the abundance of volatiles (Lester, 2006), and that degradative processes also influence aroma compounds such as aldehydes, alcohols and esters (Tietel *et al.*, 2011).

Phytohormones, such as ethylene, abscisic acid (ABA) and auxin regulate both ripening and senescence (McAtee *et al.*, 2013). Fruits are classified as climacteric (e.g. apple, tomato, pear or peach) or non-climacteric (e.g. grape, citrus, cherry or strawberry) according to the type of ripening they present. Climacteric fruits exhibit a concomitant peak of ethylene and a sudden rise in respiration at the onset of fruit ripening (Giovannoni, 2004). Even if non-climacteric fruits do not present a peak in ethylene production previous to ripening, this phytohormone, together with ABA and auxin, is the most important regulatory factor involved in ripening and senescence of both climacteric and non-climacteric fruits (Sun *et al.*, 2010; Klee and Giovannoni, 2011). As an example, Ding *et al.* (2015) showed that the expression of ethylene-related genes can influence the senescence process in two non-climacteric fruits (grape and citrus). Jia *et al.* (2011) demonstrated that ABA accelerates the ripening processes in strawberry. Interestingly, Chen *et al.* (2016) found that in harvested strawberry fruits the increase of ABA levels during

fruit ripening is accelerated, when compared with *in planta* fruits, which could explain the intensifying senescence during postharvest shelf life. Auxin, on the opposite, has been described as a repressor of ripening in non-climacteric fruits such as strawberry (Liu *et al.*, 2011).

Postharvest treatments

Nowadays, the principal postharvest technologies commercially used to delay fruit senescence and to prolong shelf life include controlled atmosphere storage combined with the supplementation of optimal temperature. Refrigerated storage is the most common method used to reduce postharvest decay, as cold decreases enzymatic activity and respiration (Lauxmann *et al.*, 2012). In addition, low temperatures slow down the development of pathogen infections. However, limited information is available about cold signaling pathway and expression of cold-induced fruit-specific genes. Exposure of crops to temperatures below to 12°C can induce the development of a physiological disorder known as chilling injury, which has a negative impact on fruit quality and consumer acceptance (Cruz-Mendivil *et al.*, 2015). Indeed, in climacteric fruits such as tomato, storage temperature can influence negatively the expression of genes related to the synthesis of volatiles, pointing out that recommended cold treatments are not ideal to maintain aroma quality (Zou *et al.*, 2018). Transcriptional expression analysis on tomato showed that chilling treatments block ethylene biosynthesis and alters also sugars metabolism (Cruz-Mendivil *et al.* 2015).

Commercially speaking, the combination of modified atmospheres and low temperature is used to reduce the chilling injury symptoms and prolong the postharvest period of the fruit (Meir *et al.*, 1997; Pesis *et al.*, 2000; Luengwilai *et al.*, 2014; Sanhueza *et al.*, 2015). In this sense, climacteric fruits stored in controlled atmosphere show a reduction in ethylene levels, which prevent fruit ripening and senescence (Gorny and Kader, 1996; Mangaraj and Goswami, 2009). Also, complementary technologies, such as the application of the ethylene antagonist 1-methylcyclopropene, are commonly used to increase the shelf-life of climacteric fruits (Serek *et al.*, 1995). However, in the case of non-climacteric fruits, such as strawberry, no clear technology is available to prolong fruit quality during postharvest life.

Elevated CO₂ atmosphere has been suggested to improve strawberry quality during storage, as a consequence of the decrease in the respiration rate (Mitcham, 2004; Feliziani and Romanazzi, 2016). Nevertheless, adverse effects on fruit color and flavor have been described after exposure to low oxygen and high CO₂ levels (Shamaila *et al.*, 1992; Ke *et al.*, 1994). Other types of atmosphere have been successfully tested in order to improve postharvest life of strawberry, such as nitric acid, hydrogen sulfide or ozone (Pérez *et al.*, 1999; Soegiarto and Wills, 2004; Hu *et al.*, 2012). For example, Pérez *et al.* (1999) compared strawberry fruits stored at 2°C in normal and O₃-enriched atmosphere, showing three times more ascorbic acid in the enriched atmosphere. On the other hand, a negative effect of ozone treatment was observed on esters emission, with a 40% reduced emission of these volatiles in ozone-treated fruits.

‘Omic’ techniques to study fruit postharvest

Recent development of ‘omic’ techniques, such as metabolomics, can be used to cover the comprehensive analysis of plant physiology, including fruit ripening and senescence during postharvest. Several studies aimed to clarify the mechanisms underlying fruit senescence with the help of “omic” techniques (metabolomics, proteomics and/or transcriptomics). These analysis have been done in apple (Mellidou *et al.*, 2014; Sun *et al.*, 2017), tomato (Oms-Oliu *et al.*, 2011; Cruz-Mendivil *et al.*, 2015; Zou *et al.*, 2018), citrus (Sun *et al.*, 2013; Ding *et al.*, 2015; Tang *et al.*, 2016), grape (Zamboni *et al.*, 2010; Zenoni *et al.*, 2016), banana (Yuan *et al.*, 2017) and strawberry (Li *et al.*, 2015). Some examples of metabolomics analysis of postharvest related processes are shown below.

Metabolomics characterization during postharvest in banana showed important metabolic changes. The major changes were detected in the levels of dopamine, major sugars (glucose, fructose, sucrose), some amino acids (valine, alanine, aspartate) and a couple of organic acids (malic and gallic acids). Interestingly, dopamine was proposed as a key marker which defines fruit quality and senescence, due to its degradation along postharvest (Yuan *et al.*, 2017). In tomato, a metabolic characterization of the fruit during development, ripening and senescence pointed out the presence of some metabolites, such as citramalic

acid, gluconic acid and mannose, which were strongly correlated with the postharvest stage (Oms-Oliu *et al.*, 2011). In previous study, citramalic acid was also associated with storage stage in apple (Rudell *et al.*, 2008). Interestingly, citramalic acid can be metabolically converted to acetone, one of the main volatiles produced during apple postharvest (Heigh, 1956). Gluconic acid can be produced as a consequence of ascorbic acid degradation during postharvest (DeBolt *et al.*, 2006), while mannose is possibly generated due to cell wall disassembly. Additionally, Sun *et al.* (2017) applied LC-MS methods to quantify the phenolic content of different accessions of apple to confirm the relationship between some polyphenols and resistance to blue mold during postharvest.

Zamboni *et al.* (2010) coupled transcriptomic, proteomic and metabolomic characterization of the postharvest dehydration, known as withering, in some varieties of grapes. They observed that withering is characterized mainly by the induction of stress responses, to dehydration and eventual pathogen attack. Indeed, secondary metabolites, such as acylated anthocyanins, stilbenes and flavanones, and transcripts encoding enzymes involved in their synthesis were predominantly accumulated during postharvest withering. Interestingly, these metabolites are known to be involved in stress responses (Dercks and Creasy, 1989; Adrian *et al.*, 1997; Versari *et al.*, 2001) and, in addition, had a positive impact on wine quality.

In tomato and citrus, combination of metabolomics and transcriptomics showed that levels of organic acids correlated with postharvest (Centeno *et al.*, 2011; Sun *et al.*, 2013; López *et al.*, 2015). Indeed, Sun *et al.* (2013) pointed out a possible role of organic acids in reactive oxygen species (ROS) scavenging since a positive correlation with enzymatic activities of superoxide dismutase and peroxidase were also observed. Centeno *et al.* (2011) identified malic acid as a potentially regulatory metabolite involved in postharvest physiology. Taken together, these results could indicate a possible role for the organic acids in the regulation of fruit senescence.

Other studies focused on understanding the global responses of the fruit to the common postharvest treatments used to prolong shelf life. For example, in citrus, transcriptomic and proteomic studies showed that low temperature up-regulated

stress-responsive genes, and interestingly, arrested primary and secondary metabolism and the transportation of metabolites, which maintain fruit quality (Yun *et al.*, 2012). Another study in citrus, combining RNA-Seq data with GC-MS metabolite profiling, also concluded that low temperature storage delayed fruit senescence and maintain fruit quality by accelerating auxin signal (Tang *et al.*, 2016). Indeed, no remarkable changes in metabolite profiles were observed in low temperature storage, while nine key metabolites, including sugars, acids and γ -aminobutyric acid (GABA) involved in quality traits were significantly altered during room temperature storage. Expression levels of transcripts encoding enzymes involved in primary metabolism were in agreement with metabolome data. On the opposite, Yun *et al.* (2016) showed by comparative transcriptomic and metabolomic analysis in litchi fruit that senescence was accelerated by cold storage, followed by ambient conditions.

Li *et al.* (2015) linked proteomic profiles with physiological parameters in response to cold treatment and controlled atmosphere during the postharvest of strawberry. They confirmed that firmness, total soluble solids and acidity were improved with cold treatment and controlled atmosphere, even if a decrease of these quality attributes during postharvest was observed. However, CO₂-atmosphere induced a loss in ascorbic acid content when compared to normal atmosphere, as reported in other fruits and vegetables (Agar *et al.*, 1997; Shin *et al.*, 2008). In addition, strawberries stored at low temperature exhibited the lowest levels of volatiles, while the highest content was observed in postharvest fruits maintained at room temperature. This pattern correlated with the content of a quinone oxidoreductase (*FaQR*), involved in the synthesis of key odorant volatile mesifurane. The decrease of soluble solids and acidity during postharvest could be correlated with the decrease in abundance of some proteins involved in carbohydrate and energy production metabolism (Li *et al.*, 2015).

In this study a combination of metabolomic techniques was used to cover the largest range of metabolites involved in strawberry fruit quality, including volatiles, primary and secondary metabolites. Their content in five different commercial cultivars of strawberry was monitored during ten-day postharvest treatments,

consisting in a combination of cold storage (4°C) with CO₂-enriched atmosphere, O₃-enriched atmosphere and normal atmosphere. This study will allow a better biochemical characterization of the postharvest life of strawberry by comparisons at different levels (genotype, time stage and postharvest treatments).

Materials and Methods

Plant material and postharvest treatments

Between 40-50 plants of each strawberry cultivar (*F. x ananassa*, Duch. cv 'Amiga', 'Camarosa', 'Candongá', 'Fortuna' and 'Santa Clara', Figure 1) were grown under commercial conditions in Moguer (Huelva, Spain). Fully mature fruits were harvested and transported in refrigerated conditions. The following day after harvest, control fruits (referred as T0 fruits from now on) of each cultivar were frozen in liquid nitrogen, while the rest of the fruits were sorted into the different postharvest treatments: (i) non-modified atmosphere (referred as normal atmosphere from now on), (ii) CO₂-enriched atmosphere and (iii) O₃-enriched atmosphere, all treatments kept at 4°C and 90% relative humidity. For ozone treatment, fruits were kept in 0.35 ppm as described in Pérez *et al.* (1999). For CO₂ treatment, fruits were stored in atmosphere of 10% CO₂ and 11% O₂ as reported in Almenar *et al.* (2006). After three, six and ten days of the different treatments, as a biological replicate, a pools of 15-20 fruits by treatment and cultivar were frozen in liquid nitrogen, ground into powder using a TissueLyser II (Qiagen) and stored at -80°C until analysis. Table 1 summarizes the different cultivars and treatments used in the following experiments.

Table 1: Cultivars and treatments used to characterize strawberry postharvest shelf life.

		Control fruits	Normal atm.	CO ₂ -enriched atm.	O ₃ -enriched atm.
Cultivars	Amiga	T0	3 days	3 days	3 days
	Camarosa		6 days	6 days	6 days
	Candongga		10 days	10 days	10 days
	Fortuna				
	Santa Clara				



Figure 1: Ripe fruits of 'Amiga', 'Camarosa', 'Candongga', 'Fortuna' and 'Santa Clara' cultivars

Physiological parameters during postharvest: firmness, soluble solids content and pH

Strawberry fruit firmness (in g mm⁻¹) of T0 fruits and after the different treatments were measured at the equatorial zone using a penetrometer with a 3-mm probe (Effegi FDP500).

Soluble solids content (SSC, in °Brix) was evaluated with a refractometer (Atago PR32) by adding a few drops onto the lens. For each measure, a pool of ten fruits was used.

Primary metabolites analysis: GC-TOF-MS

Relative levels of primary metabolites were determined from frozen samples following the protocol established by Osorio *et al.* (2012). For sample extraction, 250 mg of frozen powdered material was extracted in 3000 µl of cold methanol

and 120 μl of internal standard (0.2 mg/ml ribitol in water) was added for quantification. The mixture was incubated for 15 min at 70 °C, mixed vigorously with 1500 μl of water and centrifuged at 2200 g. The methanol/water supernatant was reduced to dryness under vacuum. Samples were stored at -80 °C until GC-MS analysis. The dried extract was re-dissolved and derivatised for 120 min at 37 °C (in 60 μl of 30 mg/ml methoxyamine hydrochloride in pyridine) followed by a 30 min treatment at 37 °C with a mixture of 100 μl of N-methyl-N-[trimethylsilyl] trifluoroacetamide and 20 μl of retention time standard mixture composed by 0.4 ml·ml⁻¹ of the 13 fatty acid methyl esters (FAMES). Sample volumes of 1 μl were then injected in the GC-MS using a splitless or split mode and a hot needle technique.

The GC-TOF-MS system was composed of a GC 6890 N gas chromatographer (Agilent Technologies, Böblingen, Germany), and a Pegasus III time-of-flight mass spectrometer (LECO Instruments, St. Joseph, MI, USA), provided with an Electron Impact ionization source. GC was performed on a MDN-35 capillary column, 30 m in length, and 0.32 mm in inner diameter, 0.25 mm in film thickness (Macherey-Nagel). The injection temperature was set at 230°C, the interface at 250°C, and the ion source adjusted to 200°C. Helium 5.0 was used as the carrier gas at a flow rate of 2 ml/min. The analysis was performed under the following temperature program: 2 min of isothermal heating at 80°C, followed by a 15°C per min ramp to 330°C, and holding at this temperature for 6 min. Mass spectra were recorded at 20 scans/s with a scanning range of 70 to 600 m/z. The experimental set was composed by 150 samples: 5 cultivars, 10 different treatments were measured (T0 fruits, fruits kept in normal atmosphere after 3, 6 and 10 days, in CO₂-enriched atmosphere after 3, 6 and 10 days and in O₃-enriched atmosphere after 3, 6 and 10 days) × 3 replicates each. They were separated in five runs of 30 samples each one, including 'Camarosa' T0 fruits in each run to relativize metabolite intensities between runs. Both chromatograms and mass spectra were evaluated using ChromaTOF software, version 3.00 (LECO Instruments, St. Joseph, MI, USA), and .peg files were exported to .cdf using a baseline off set of 1 ('just above the noise'), an average of 5 points for smoothing, a peak width of 10 and a signal to noise ratio of 10. Identification and semi-quantitation of the compounds detected in the GC-TOF-MS metabolite

profiling experiment were performed with TagFinder software (Luedemann *et al.*, 2008). Metabolites were identified by comparison to database entries of authentic standards and spectral data from the public library GMD@CSB.DB (The Golm Metabolome Database; Kopka *et al.* (2005).

Secondary metabolites analysis: UPLC-Orbitrap-MS/MS

For each biological replicate, 50 mg were extracted during 30 minutes at room temperature with a mixture of methyl-tert-butyl ether:methanol (3:1) in an orbital shaker. To facilitate cell disruption, samples were then incubated 10 minutes in a cooled sonic bath, before adding a mixture of water:methanol (3:1), which results in the formation of two liquid phases. A fixed volume of polar phase was transferred to a fresh Eppendorf tube before concentrating it to dryness in Speed-vac (Centrivac, Heraeus Instrument, Hanau, Germany).

Chromatographic separation was performed by Waters Acquity UPLC system using a C18 reverse-phase column (100 x 2.1 mm ID, 1.8 μ m particle size; Waters, Milford, MA, USA). The mass spectra were acquired using an Exactive mass spectrometer (Thermo Fisher Scientific, Waltham, MA, USA). The spectra were recorded alternating full-scan and all-ion fragmentation scan modes, covering a mass range from 100 to 1500 m/z. All data were processed using Xcalibur 2.1 software (Thermo Fisher). Processing of chromatograms, peaks detection and integration were performed using REFINER MS 7.5 (GeneData: <http://www.genedata.com>). The MS/MS fragmentation of the metabolites was compared with candidate molecules found in databases, and verified with earlier literatures on similar compounds, especially when the presence of the metabolite was reported in strawberry. Integration of the peak area of the corresponding molecular ion was used to quantify the metabolites in all the samples. The same replicates were used as for primary metabolites and 'Camarosa' T0 fruits were also included in each run to relativize metabolite intensity.

Volatile compound analysis: HS-SPME-GC-MS

Volatile analysis was performed as described in Rambla *et al.* (2015). Briefly, 1g of each frozen sample was weighed in a 7-ml vial, closed, and incubated at 30°C for 5 min. 300 µl of NaCl saturated solution were added, and 900 µl of the homogenized mixture were transferred to a 10-ml screw cap headspace vial, from where the volatiles were immediately collected. Collection of the volatiles was performed by HS-SPME with a 65 µm-polydimethylsiloxane/divinyl-benzene fiber (Supelco). Vials were first tempered at 50°C for 10 min, and then extracted by exposing the fiber to the vial headspace for 30 min under continuous agitation and heating at 50°C. Extracted volatiles were desorbed in the GC injection port for 1 min at 250°C in splitless mode. A CombiPAL autosampler (CTC Analytics) performed the automatic incubation of the vials, extraction and desorption of the volatiles. Gas chromatography was performed on a DB-5ms (60 m x 0.25 m x 1µm) column (J&W Scientific) with helium as carrier gas at a constant flow of 1.2 ml/min. GC interface and MS source temperatures were 260°C and 230°C respectively. Oven temperature conditions were 40°C for 3 min, 5°C/min ramp until 250°C, and then held at 250°C for 5 min. Mass spectra were recorded in scan mode in the 35 to 220 mass-to-charge ratio range by a 5975B mass spectrometer (Agilent Technologies) at an ionization energy of 70 eV and a scanning speed of 7 scans/s. Chromatograms and spectra were recorded and processed using Enhanced Chemstation software (Agilent Technologies).

Statistical analysis

After analysis of the metabolomic data, R software, with pheatmap (Kolde, 2015), mixOmics (Le Cao *et al.*, 2017) and ggplot2 (Wickham, 2009) packages, was used to perform hierarchical cluster analysis (HCA), partial least squares discriminant analysis (PLS-DA) and K-means clustering (RStudio Team, 2016; Team, 2017).

Results

Fruit phenotype, firmness and soluble solids content during postharvest treatments

Mature fruits of *F. x ananassa* cv. 'Amiga', 'Camarosa', 'Candongga', 'Fortuna' and 'Santa Clara' were harvested and kept at 4°C during three, six and ten days in different atmospheres (CO₂-enriched, O₃-enriched and normal atmospheres). As an example, Figure 2 shows 'Camarosa' fruits along the different postharvest treatments. Indeed, no differences in fruit aspect was observed between cultivars (data no shown). In general, we observed that fruits were softer after 6 days of postharvest treatments as shown for 'Camarosa' fruits in Figure 2. The softening was more apparent in the fruits kept in normal atmosphere. However, after 10 days, the fruits were equally damaged in the three treatments (Figure 2).

In addition, the ripening status of the strawberry cultivars was evaluated by measuring their fruit firmness and SSC during storage in different atmospheres. One-way ANOVA and post hoc tests showed that there were significant differences in both firmness and SSC between fruits of the different cultivars in T0 (Figures 3 and 4). We observed that 'Amiga' and 'Santa Clara' fruits were firmer than 'Camarosa', 'Candongga' and 'Fortuna' fruits (Figure 3), while 'Fortuna' and 'Santa Clara' had the lowest SSC in comparison with the other cultivars (Figure 4).

Next, two-way ANOVA and Tukey's HSD post-hoc tests were performed for the different cultivars to see if both the different treatments and their duration significantly changed fruit firmness and SSC (Annex 3).

Fruit firmness was significantly decreased along postharvest, except for 'Candongga' fruits, where this decrease was not significant (Figure 3). Interestingly, an increase in firmness was observed after six days in all the treatments for 'Amiga' cultivar, after three and six days in normal and CO₂-enriched atmospheres for 'Candongga' and after three days in normal and CO₂-enriched atmospheres and six days in O₃ treatment for 'Fortuna' fruits. In 'Camarosa' and 'Candongga' fruits, O₃-enriched atmosphere treatment was significantly different from the other two treatments. However, in 'Camarosa' this

difference resulted in a less accentuated decrease in firmness for fruits kept in ozone-enriched atmosphere during the postharvest, while in 'Candongga' an opposite effect was observed. On the other hand, in 'Santa Clara' fruits, firmness was significantly increased in CO₂-enriched atmosphere when compared to the other treatments.

Regarding SSC, it was more complicated to discern a common trend, even if a general decrease could also be observed in the different cultivars and treatments (Figure 4). In 'Amiga', significant differences were observed between the two modified atmospheres and the normal one, mainly due to their contrasting behavior between the sixth and the tenth days of the postharvest period. Indeed, during the first six days, a general decrease of SSC was observed in all the treatments, while in the second part of the postharvest, SSC increased again only in the fruits kept in modified atmospheres, although this increase did not allow to recover initial levels (Figure 4). In 'Camarosa', 'Fortuna' and 'Santa Clara' no significant differences were observed between the treatments, while in 'Candongga', fruits kept in ozone-enriched atmosphere showed opposite trends that the fruits kept in CO₂-enriched and normal atmospheres. Indeed, at the beginning of the postharvest, fruits kept in O₃-enriched atmosphere presented a decrease in SSC, while the fruits kept in the two other atmospheres increased their SSC. After three days, SSC started to increase in fruits kept in O₃-enriched atmosphere, until reaching a slightly higher value than T0 fruits. On the opposite, SSC content in fruits kept in CO₂-enriched and normal atmospheres decreased at the end of the postharvest.

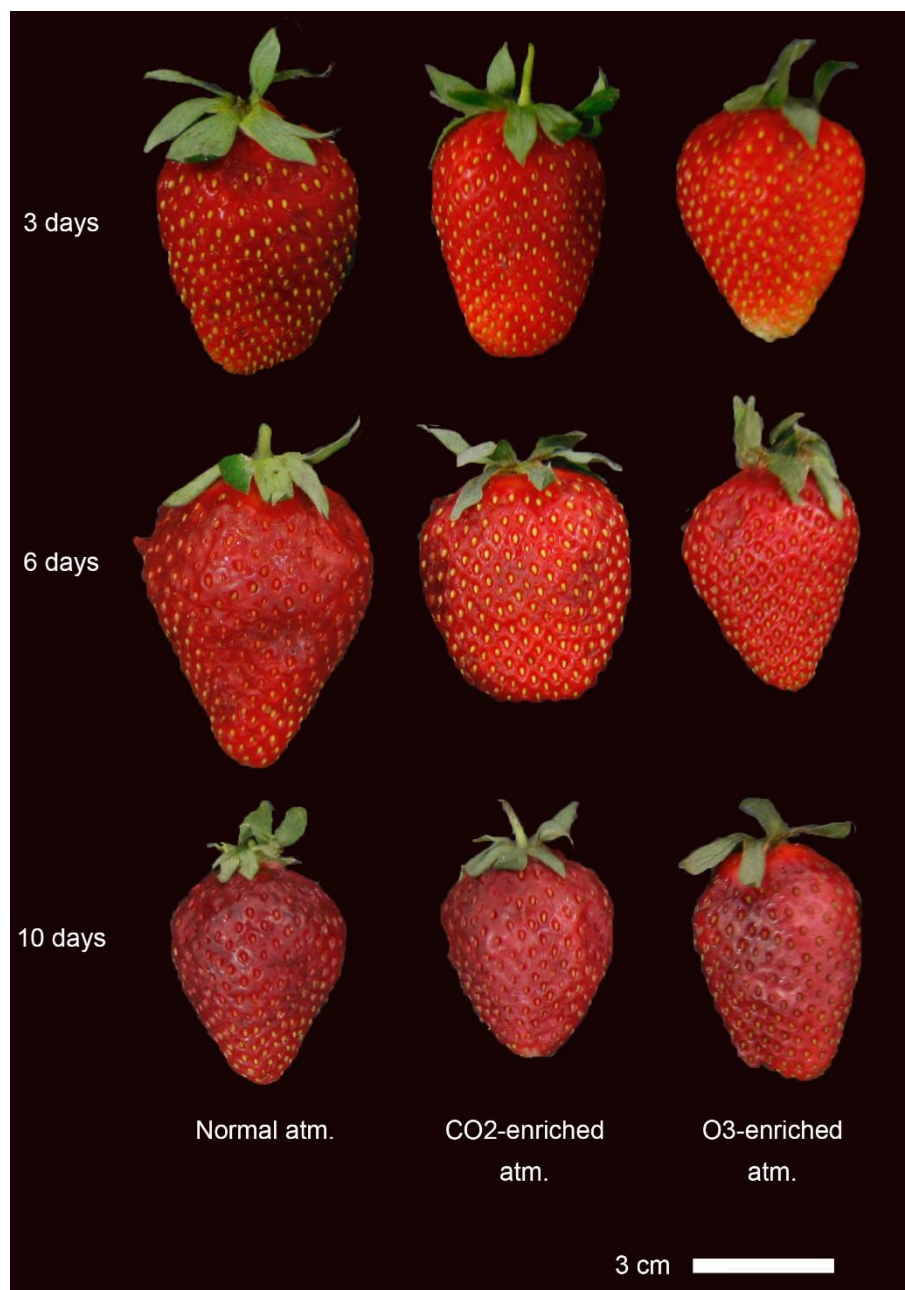


Figure 2: Evolution of 'Camarosa' fruits during the three postharvest treatments.

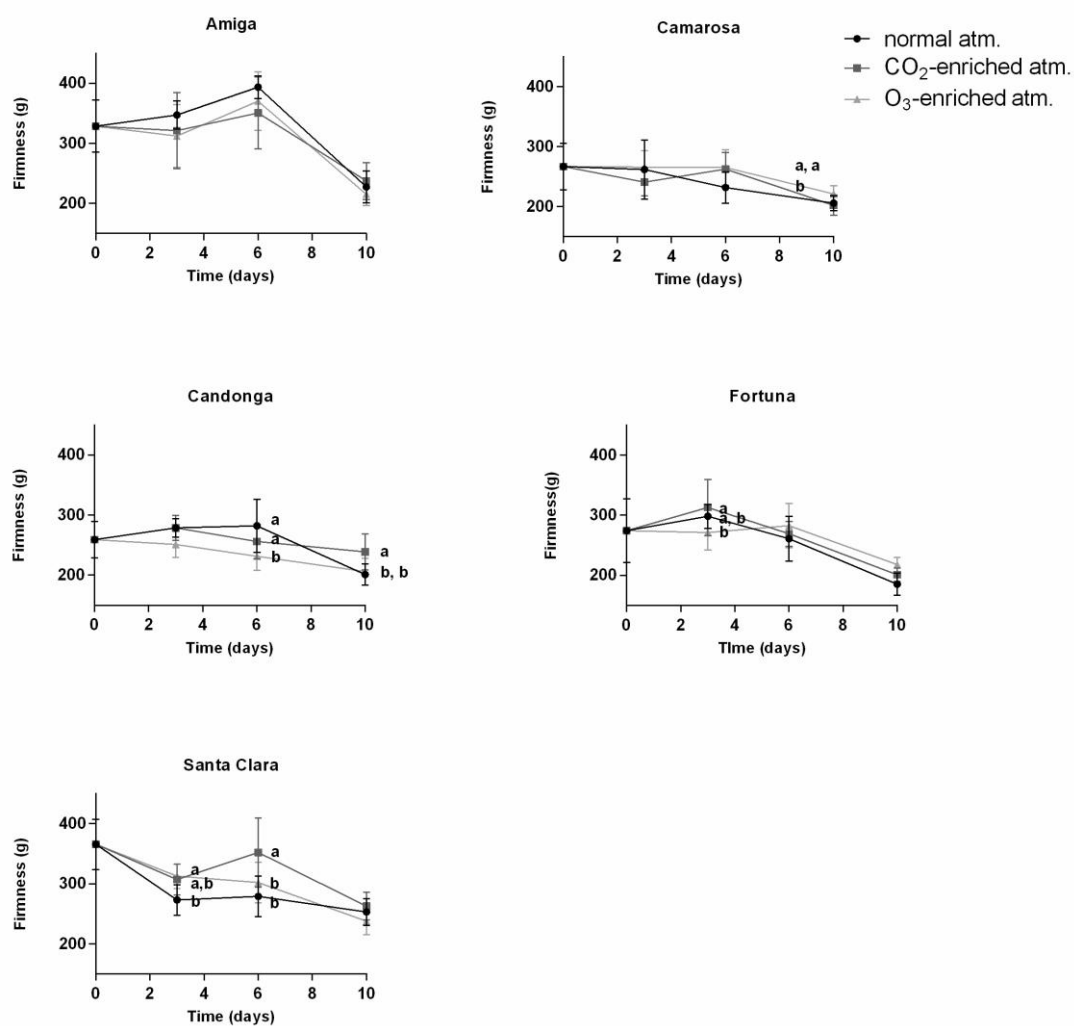


Figure 3: Changes in firmness during the postharvest treatments in the five cultivars. Letters indicate significant differences between treatments at determined time points according to ANOVA and Tukey's HSD post-hoc tests (P < 0.05).

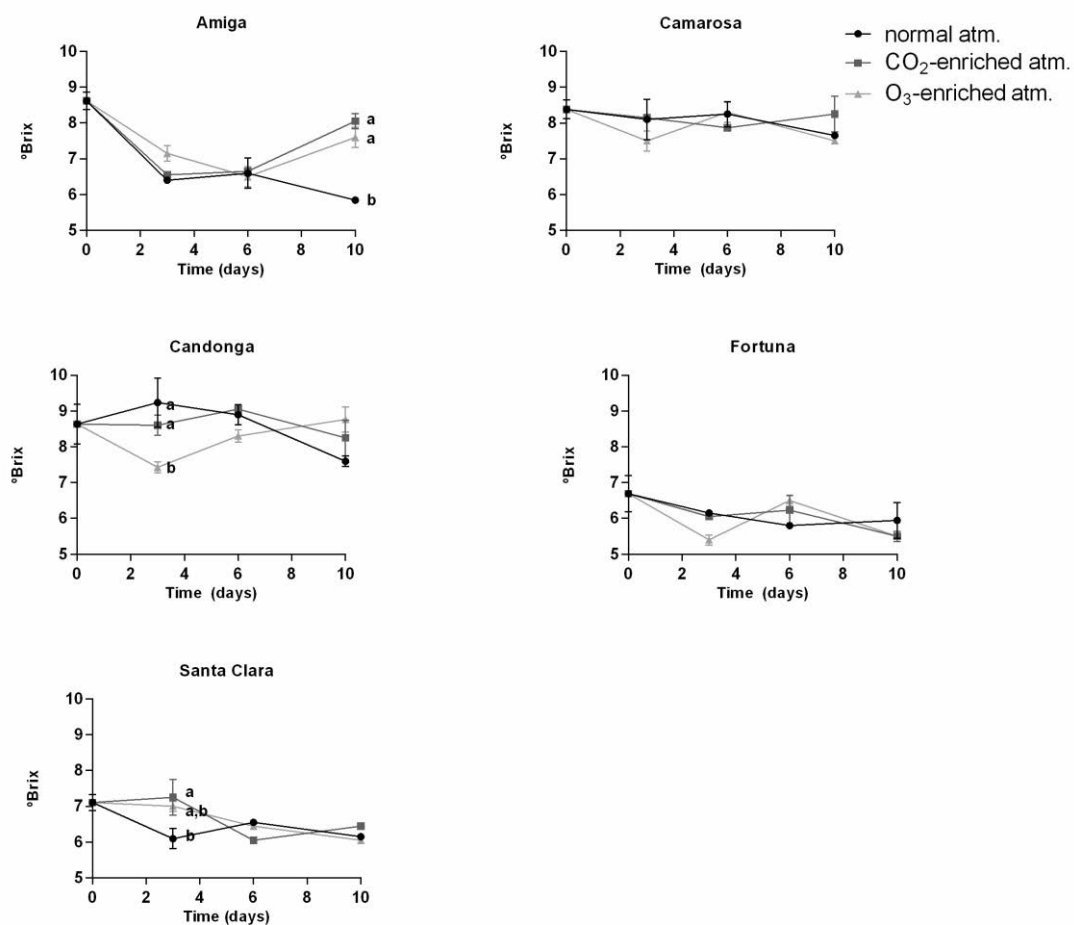


Figure 4: Changes in SSC (indicated in °Brix) during the postharvest treatments in the five cultivars. Letters indicate significant differences between treatments at determined time points according to ANOVA and Tukey's HSD post-hoc tests ($P < 0.05$).

Metabolic profiling of the five strawberry cultivars

Metabolite profiling of the postharvest treated fruits and T0 fruits was performed, using (i) gas chromatography-(TOF) mass spectrometry to identify and semi-quantify 49 primary metabolites, (ii) UPLC-Orbitrap MS/MS which allowed the identification and semi-quantification of 132 secondary metabolites and (iii) automated headspace solid phase micro-extraction (HS-SPME) sampling coupled to GC-MS for the detection of 70 volatiles. Annexes 4, 5 and 6 list the identified primary, secondary metabolites and volatiles with their relative content in the different samples. Each value represents the mean between the three replicates, and is relativized to sample dry weight and 'Camarosa' T0 fruits.

The analysis for primary metabolites included 19 amino and 11 organic acids, 13 soluble sugars, 3 sugar alcohols, 2 phosphorylated intermediates and 1 polyamine (putrescine). Maltose was detected in some samples, but not in 'Camarosa' T0 fruits. For this reason, this sugar was not included in the further analysis.

Detected secondary metabolites comprised 1 flavone, 6 flavonones, 19 flavonols, 7 anthocyanins, 4 flavanols, 22 condensed tannins, 38 ellagitannins (including precursors and derivatives), 9 galloyl glucoses, 14 hydroxycinnamic acid derivatives, 7 benzoic acid derivatives and 5 terpenoids.

The normalized levels of primary, secondary metabolites and volatiles in the T0 samples for the five cultivars used in this study are shown in Figures 5, 6 and 7 respectively. Both cultivars and metabolites were grouped by hierarchical cluster analysis (HCA), using Pearson's correlation. Interestingly, for the three datasets, 'Camarosa' and 'Candongga' clustered together, indicating their major similarity. Generally speaking, the relative content of the different metabolites was higher in 'Camarosa' and 'Candongga' cultivars. Indeed, 'Candongga' showed a relative high content of many sugars, organic acids and a series of flavonoids and hydroxycinnamic and benzoic acid derivatives (Figures 5 and 6). 'Santa Clara' presented relative high levels of several amino acids, including phenylalanine and methionine (Figure 5). Interestingly, this cultivar also showed a relative high content in secondary metabolites, which are mainly phenylpropanoids and derive from phenylalanine (Figure 6). In addition, the levels of some volatiles belonging

to the aldehyde class (pentenal, (E)-2-hexenal, (E)-2-heptenal, (E)-2-octenal), were relatively higher in 'Santa Clara' (Figure 7). Aldehydes and alcohols derived from the degradation of methionine or branched-chain and aromatic amino acids (Schwab *et al.*, 2008). 'Amiga' showed relatively low levels of metabolites, with the notable exception of mesifurane, a key aroma volatile (Figure 7).

Among the identified volatiles, which have been previously shown to play an important role in the contribution of strawberry aroma, the most abundant detected class was esters (38), followed by aldehydes (13), ketones (6), furans (5), alcohols (4) and terpenes (4). Pearson's correlation separated the cultivars into two clusters, 'Amiga' and 'Santa Clara' grouping together, while 'Fortuna', 'Camarosa' and 'Candongga' formed the other cluster (Figure 7). Key ester aroma compounds such as methyl and ethyl butanoates, methyl and ethyl hexanoates and hexyl acetate were higher in 'Camarosa' and 'Candongga' when compared to the other cultivars, while (E)-2-hexenyl acetate was higher in 'Santa Clara'. Other volatiles considered important for strawberry aroma perception are the aldehydes hexanal and (Z)-3-hexenal, which were also more abundant in 'Santa Clara' cultivar. Terpenes, such as linalool and nerolidol, provide citrus and spicy notes to the aroma, and were detected in higher concentration in 'Fortuna' cultivar. Other important compounds are 2-heptanone, which was more abundant in 'Camarosa' and 'Candongga', mesifurane, γ -decalactone, and furaneol (Figure 7). The last one was not detected, possibly due to its water-soluble nature and thermal instability (Pérez *et al.*, 1996). The furan γ -decalactone confers a peachy note to the fruit aroma, and is known to be cultivar-specific (Ulrich *et al.*, 1997). 'Candongga' and 'Fortuna' content of this volatile was more than 700 and 400 times higher than in 'Camarosa' (Figure 7).

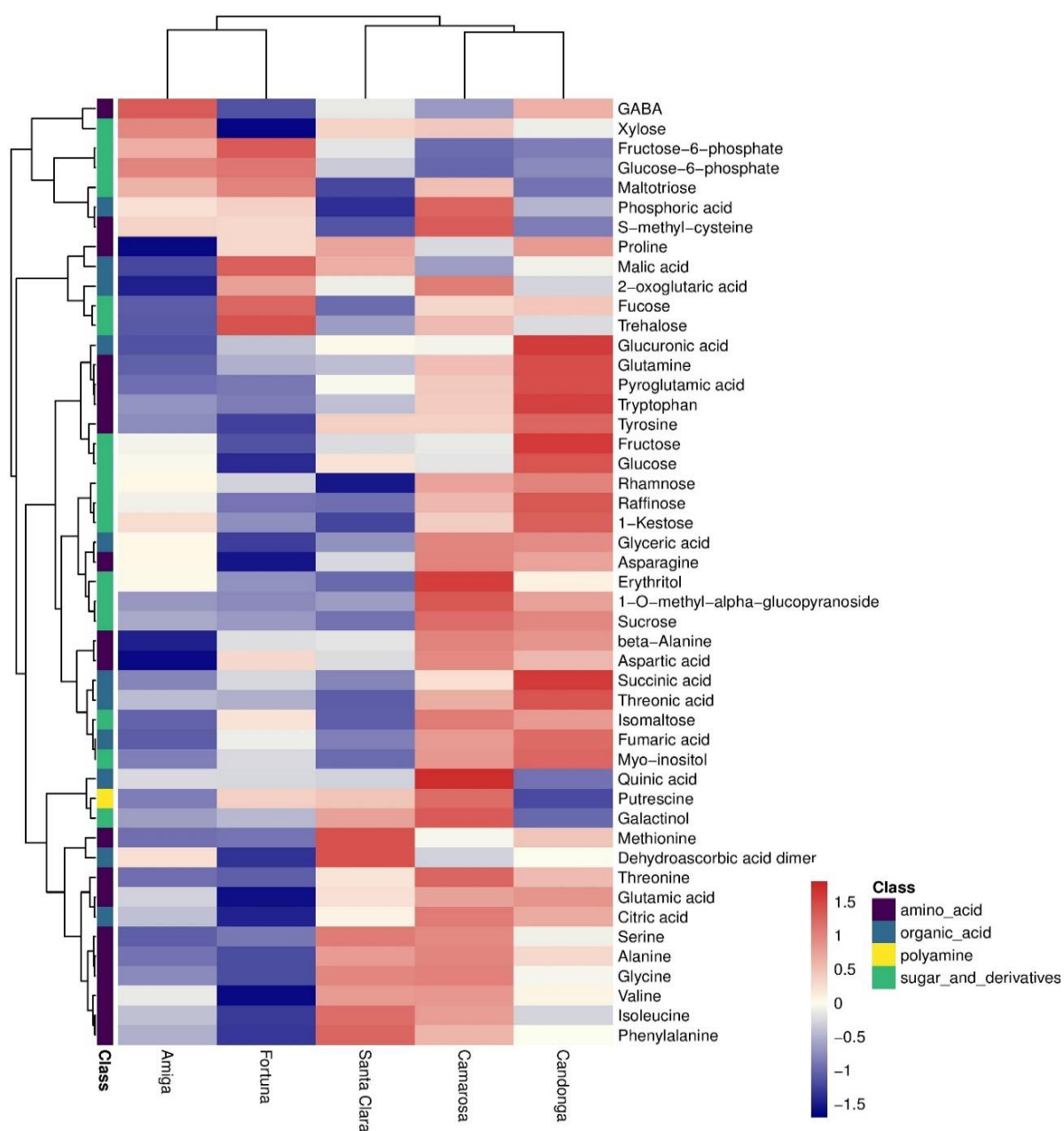


Figure 5: HCA representing normalized primary metabolite content in ‘Amiga’, ‘Camarosa’, ‘Candonga’, ‘Fortuna’ and ‘Santa Clara’ cultivars. Normalized metabolite contents were expressed as z-scores (the number of standard deviations the value is different from the mean of all values), resulting in mean centered values. Both cultivars and metabolites are grouped by Pearson’s correlation. High and low relative values are indicated in red and blue colors respectively (see color bar on the right).

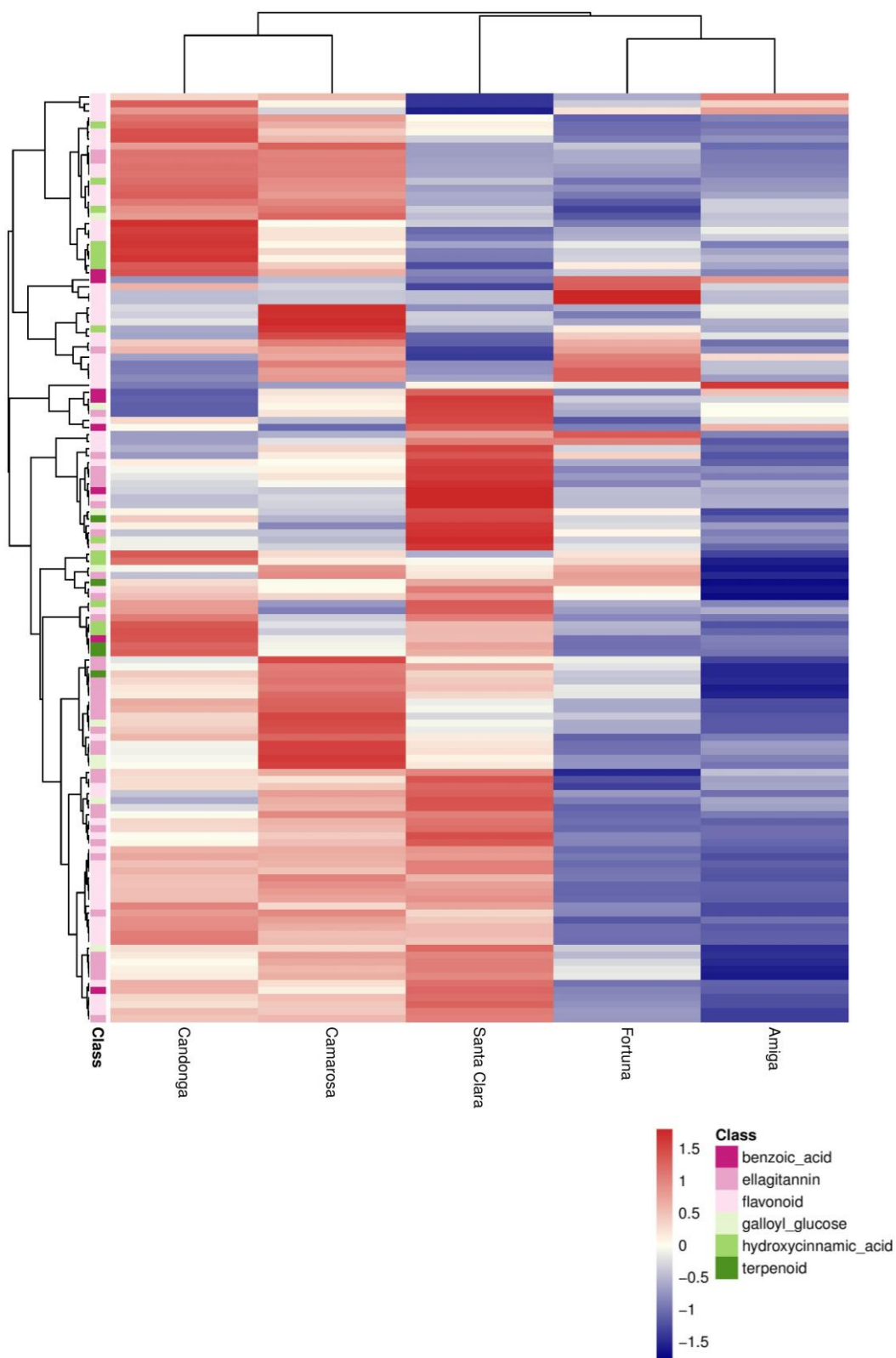


Figure 6: HCA representing normalized secondary metabolite content in ‘Amiga’, ‘Camarosa’, ‘Candonga’, ‘Fortuna’ and ‘Santa Clara’ cultivars. Normalized metabolite contents were expressed as z-scores. Both cultivars and metabolites are grouped by Pearson’s correlation. High and low relative values are indicated in red and blue colors respectively (see color bar on the right).

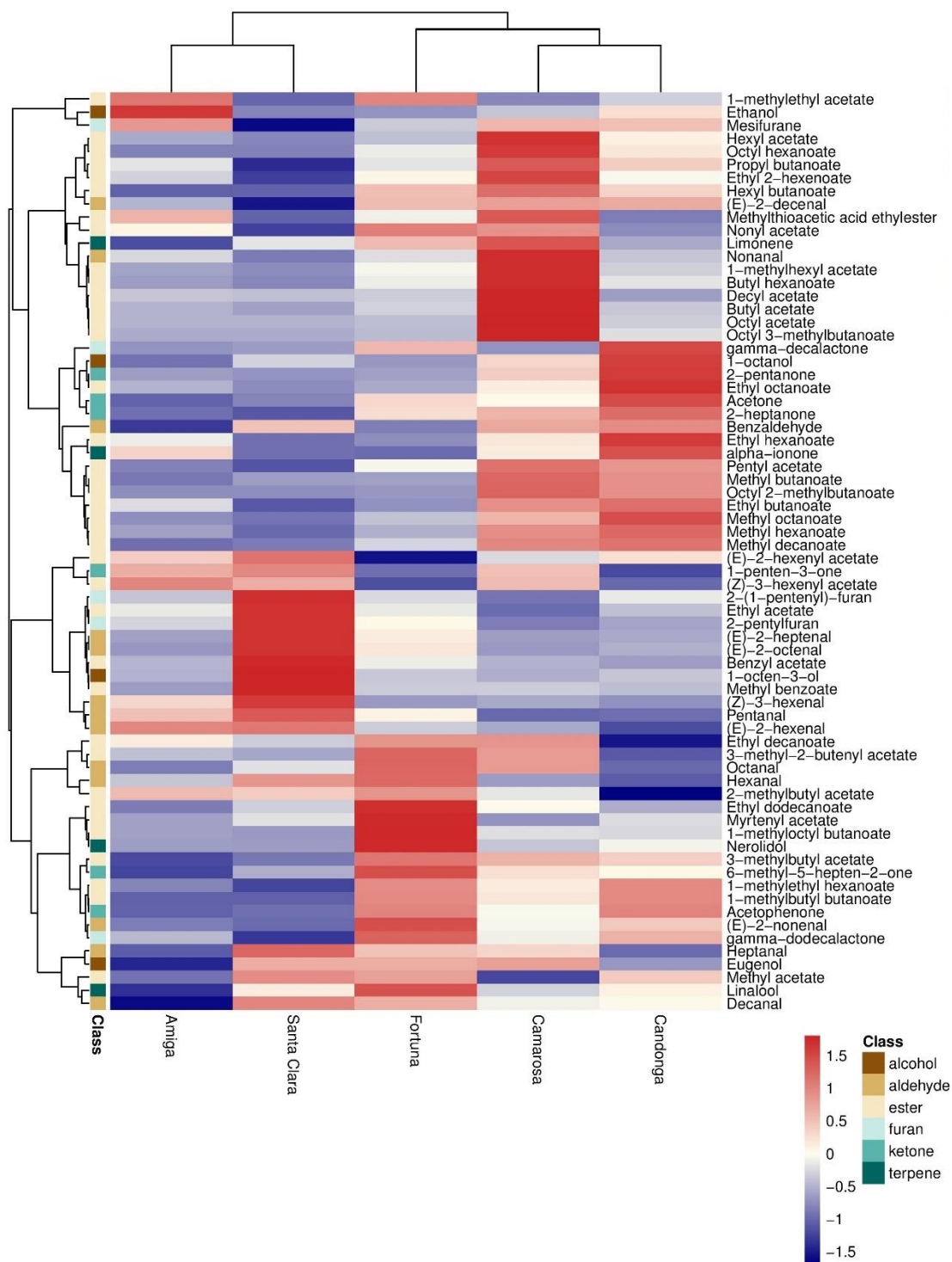


Figure 7: HCA representing normalized volatile content in ‘Amiga’, ‘Camarosa’, ‘Candonga’, ‘Fortuna’ and ‘Santa Clara’ cultivars. Normalized metabolite contents were expressed as z-scores. Both cultivars and metabolites are grouped by Pearson’s correlation. High and low relative values are indicated in red and blue colors respectively (see color bar on the right).

Metabolic changes in strawberry fruit during postharvest

Next, multivariate statistical approaches, including HCA, partial least squares regression discriminant analysis (PLS-DA) and *K*-means clustering, were used to shed light on the metabolic changes occurring during strawberry postharvest in the different tested conditions.

1) HCA of the postharvest samples

General heatmaps representing the whole set of T0 and postharvest samples are presented in Figures 8, 9 and 10 for primary, secondary metabolites and volatiles, respectively. Normalized metabolites (z-scores) were grouped by HCA, while the different samples are ordered by cultivars ('Amiga', 'Camarosa', 'Candongga', 'Fortuna' and 'Santa Clara') and by treatments and their duration (T0 fruits, ctr_3, ctr_6 and ctr_10 for the samples kept at 4°C in normal atmosphere and harvested after 3, 6 and 10 days, CO2_3, CO2_6, CO2_10 for the samples kept at 4°C and in CO₂-enriched atmosphere and harvested after 3, 6 and 10 days, O3_3, O3_6, O_10 for the samples kept at 4°C and in O₃-enriched atmosphere and harvested after 3, 6 and 10 days). Even if these representations of the data are not the more indicated to draw conclusions about the behavior of the samples, it is useful as a first approximation to group metabolites showing similar trend along postharvest of strawberry fruits. In addition, general metabolite profiles of the five cultivars along postharvest confirmed the highest similarity between 'Camarosa' and 'Candongga' cultivars for the three datasets (Figures 8-10).

Primary metabolites were divided into three main clusters A, B and C. Almost all amino acids, with the exception of glutamic acid and S-methyl-cysteine, grouped in cluster A and B, while organic acids and sugars were distributed between clusters B and C (Figure 8). Sucrose grouped together with glucopyranoside in cluster B, while fructose and glucose were located with the majority of sugars in clusters C. Malic and citric acids, the two main organic acids in strawberry fruits, clustered together with the majority of amino acids in A and B respectively (Figure 8).

For secondary metabolites, four main clusters (A, B, C and D) were observed in the HCA, each one being enriched with specific classes (Figure 9). Some ellagitannins, mainly lagerstannins, and some flavonols (mainly kaempferol

derivatives) were the main metabolite classes located in cluster A. In cluster B, ellagitannins (including precursor and derivative metabolites) and the majority of proanthocyanidins were overrepresented. Hydroxycinnamic acid derivatives, together with some flavonoids (mainly flavonols), were grouped in cluster C. Finally, flavonoids such as anthocyanins derivatives and flavonones clustered in D, together with benzoic acid derivatives (Figure 9).

Volatiles were divided into two main clusters (A and B) by HCA (Figure 10). Cluster A was enriched in aldehydes and terpenes (nerolidol, limonene and linalool), while the majority of esters was located in cluster B, which comprised most volatiles. In general, a reduction of the levels of volatiles in cluster A was observed during postharvest. A clear decrease in the level of esters and ketones in a sub-cluster from cluster B (located at the bottom of the tree) was also observed during postharvest in 'Amiga', 'Fortuna' and 'Santa Clara' cultivars, even if it seemed less accentuated in fruits kept in ozone-enriched atmosphere (Figure 10).

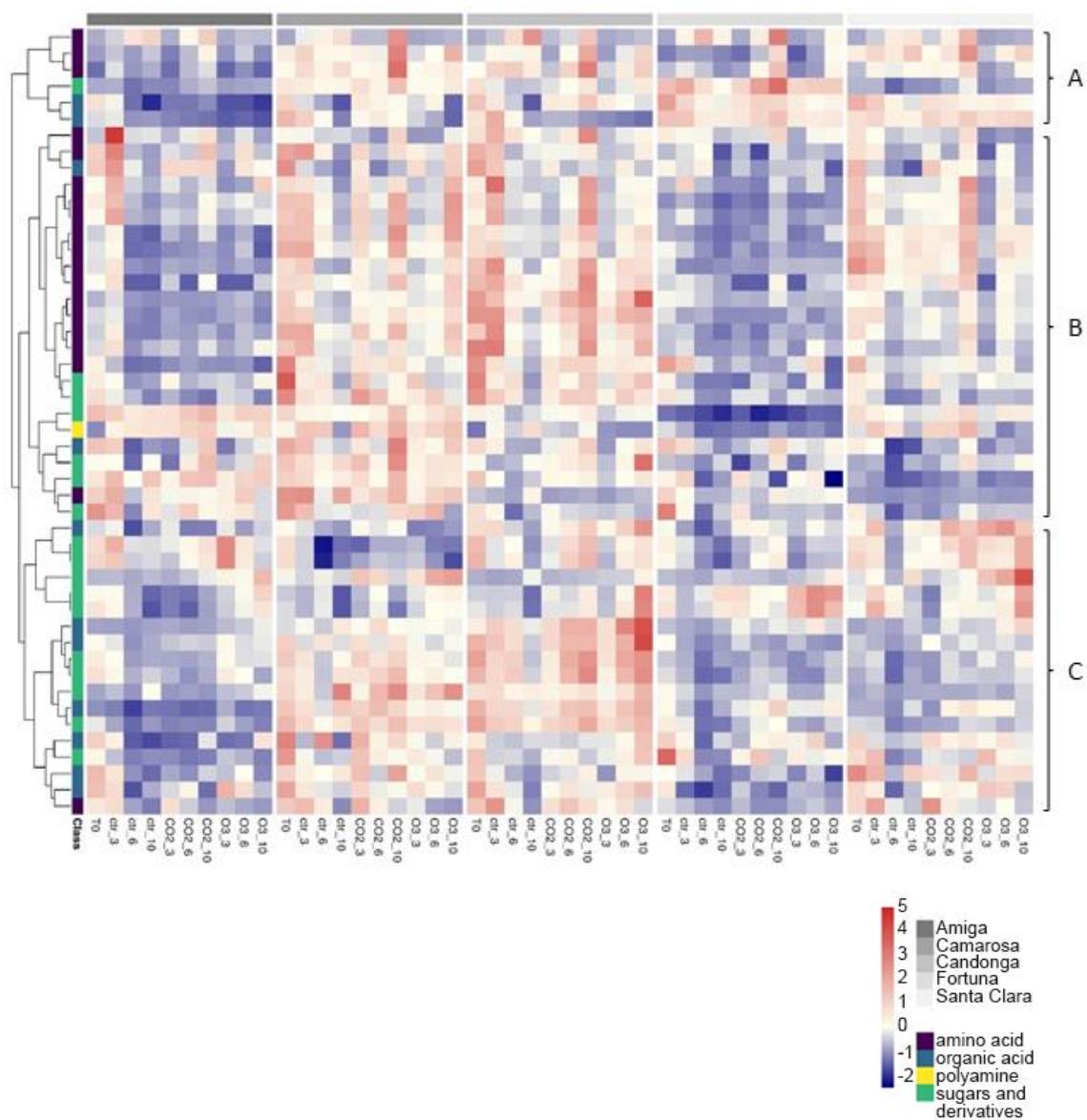


Figure 8: HCA representing normalized primary metabolite content in T0 and postharvest samples. Normalized metabolite contents were expressed as z-scores. Metabolites are grouped by Pearson's correlation, while samples are grouped by cultivars and treatment. Main metabolite clusters are indicated on the right of the plot. High and low relative values are indicated in red and blue colors respectively (see color bar on the right).

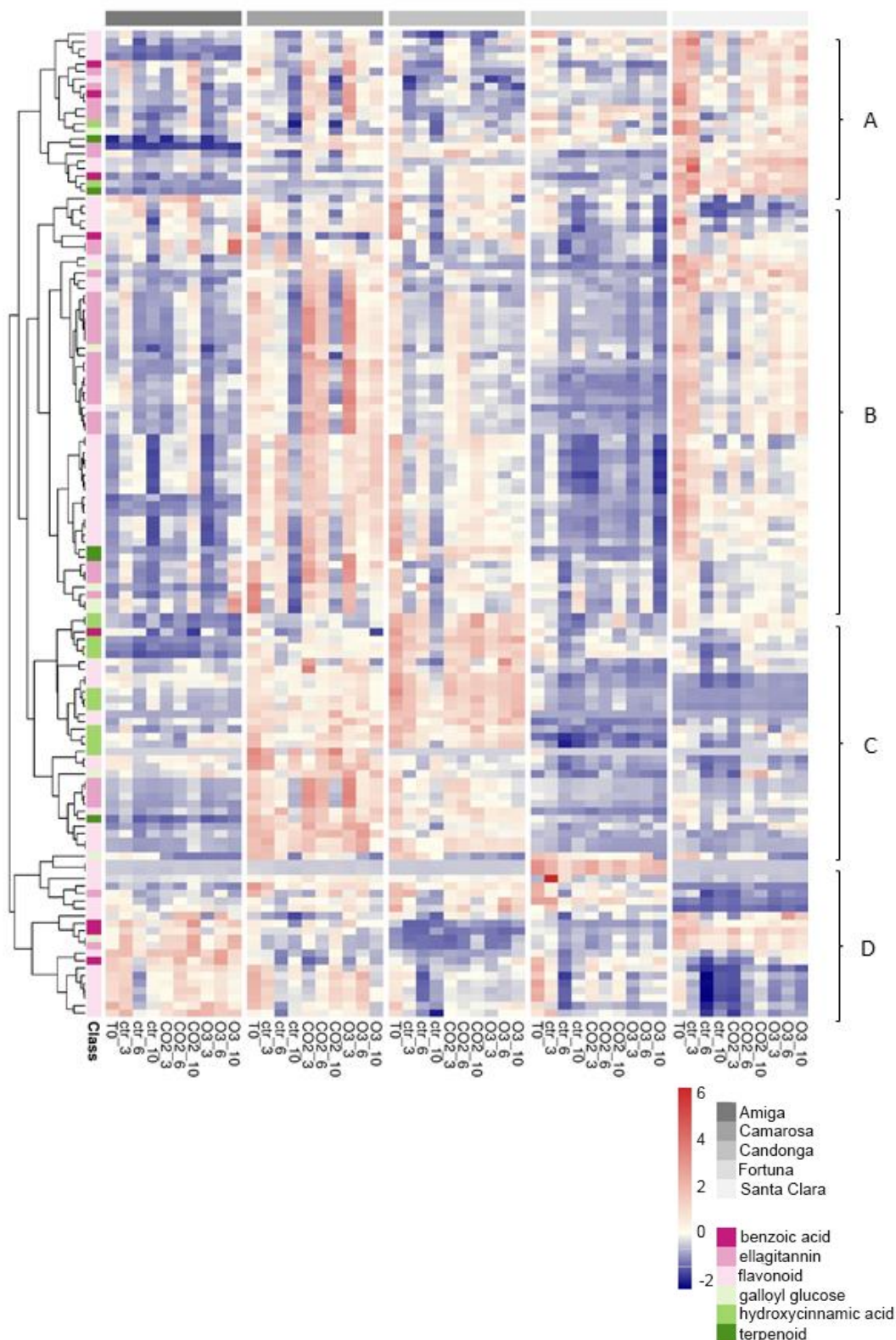


Figure 9: HCA representing normalized secondary metabolite content in T0 and postharvest samples. Normalized metabolite contents were expressed as z-scores. Metabolites are grouped by Pearson's correlation, while samples are grouped by cultivars and treatment. Main metabolite clusters are indicated on the right of the plot. High and low relative values are indicated in red and blue colors respectively (see color bar on the right).

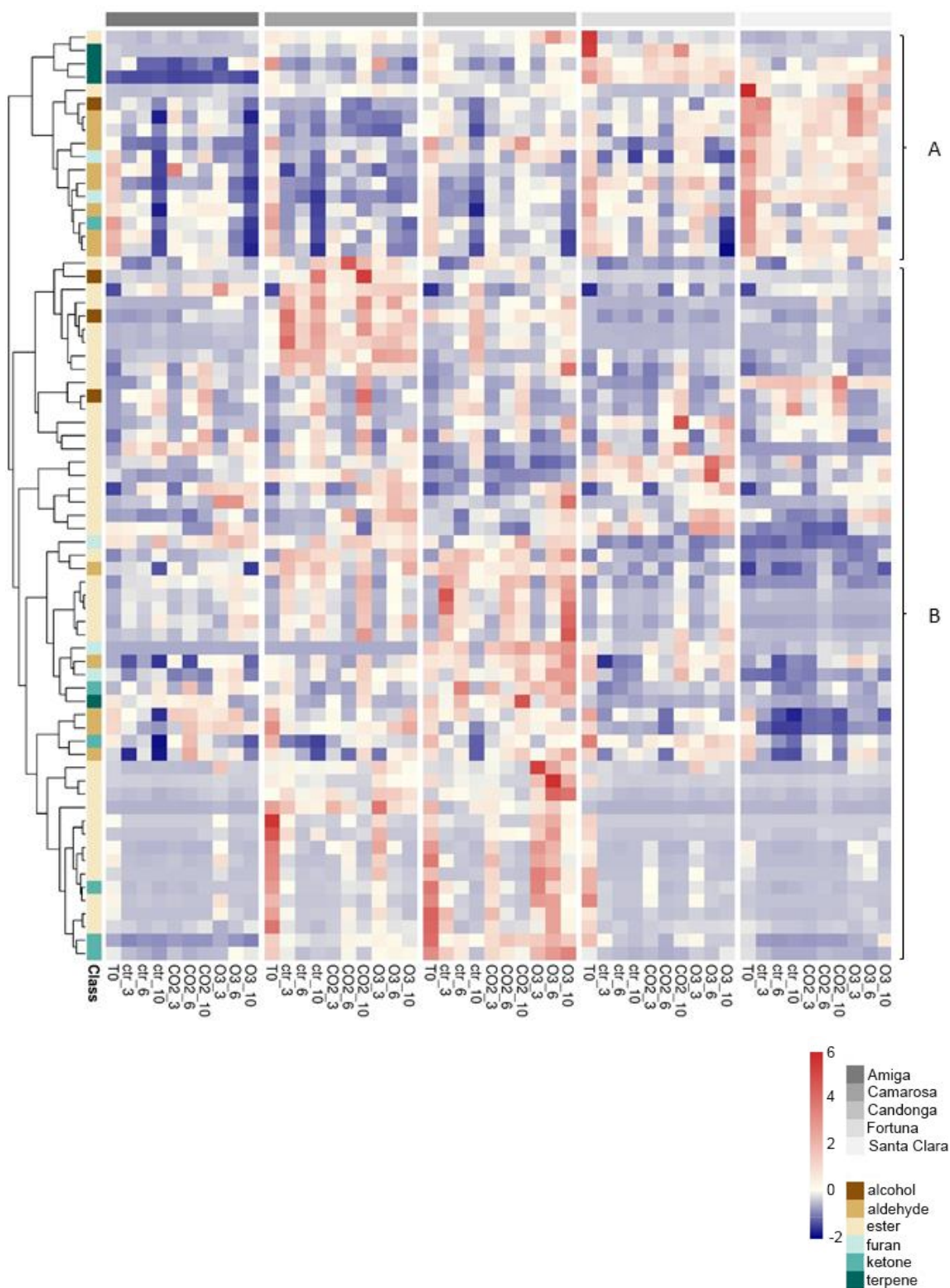


Figure 10: HCA representing normalized volatile content in T0 and postharvest samples. Normalized metabolite contents were expressed as z-scores. Metabolites are grouped by Pearson's correlation, while samples are grouped by cultivars and treatment. Main metabolite clusters are indicated on the right of the plot. High and low relative values are indicated in red and blue colors respectively (see color bar on the right).

2) PLS-DA

PLS-DA is a linear classification model used to optimize separation between different groups of samples, which is accomplished by linking two data matrices, the raw data, which include the variable values (matrix X) and the groups (or classes, matrix Y). It provides a visual interpretation of complex datasets through low-dimensional, easily interpretable scores plot. In addition, it gives several statistics, such as loading weight, that can be used to identify the most important variables (e.g. metabolites) (Gromski *et al.*, 2015).

PLS-DA model, with three components, was performed for primary, secondary metabolites and volatiles, using as Y matrix genotype (i.e. cultivar) (Figures 11, 1), postharvest treatment (Figures 12) and days for postharvest treatment (Figures 13). Loadings plots for the three components of each PLS-DA analysis are also shown in Annex 7, indicating the weight of the metabolites in the separation of the different classes.

PLS-DA model: separation according to genotype

PLS-DA model with three components was able to separate samples based on their genotype, even if the separation was not complete in the case of 'Camarosa' and 'Candongga' for primary metabolites and volatiles and for 'Amiga' and 'Santa Clara' for volatiles (Figures 11).

The percentage of explained variance for the three components was 37% (component 1), 11% (component 2) and 10% (component 3) for primary metabolites (Figure 11a). Separation of 'Candongga' and 'Camarosa' from the other three cultivars was mainly achieved by component 1, which situated the two first mentioned varieties in the positive range of the axis. Metabolites with higher loading score for the first component were 5 sugars (myo-inositol, 1-kestose, isomaltose and sucrose), 3 organic acids (fumaric, threonic and succinic acids) and 4 amino acids (pyroglutamic acid, glutamine, tyrosine and tryptophan). Component 2 roughly divided cultivars into two groups: 'Amiga' and 'Camarosa' were situated in the negative range (with xylose, rhamnose, putrescine and S-methyl-cysteine with higher negative scores), while 'Candongga', 'Fortuna' and 'Santa Clara' were in the positive range (with malic acid, 2-oxoglutaric acid,

fucose, glucose-6-phosphate and fructose 6-phosphate with higher positive scores). Component 3 clearly separated 'Santa Clara', which was located on the most positive range of the axis, from the other four cultivars, with glucuronic acid, fructose, glucose, dehydroascorbic acid dimer, xylose, methionine and serine showing highest positive loading scores (Figure 11a).

For secondary metabolites, the three first components explained 40% (component 1), 17% (component 2) and 10% (component 3) of the variance (Figure 11b). Component 1 separated 'Amiga' and 'Fortuna' (negative range) from 'Camarosa', 'Candongga' and 'Santa Clara' (positive range). Metabolites with higher positive loading scores for the first component were the flavonoids epicatechin glucuronide, cyanidin-hexose and propelargonidin trimer isomer 4, and the triterpenoid hexose isomer 3. 'Santa Clara' (negative range) was separated from the other four cultivars (positive range) by component 2, with kaempferol hexose isomer 3, di-hydroxybenzoic acid hexose 1, (epi)afzelechin hexose 1 with highest loading negative scores and sinapic acid hexose derivatives and isorhamnetin rutinose with highest loading positive scores. Finally, component 3 separated 'Amiga' and 'Camarosa' (negative range, with di-hydroxy methyl benzoic acid hexose, kaempferol coumaroyl hexose and naringenin chalcone hexose 3 as main loadings) from 'Candongga', 'Fortuna' and 'Santa Clara' (positive range, with coumaric acid hexose 2, cinnamic acid hexose 2, ferulic acid hexose 3, sesquiterpenoid hexose 1 and 2 as main loadings) (Figure 11b).

The percentage of explained variance for volatiles was 23%, 19% and 7% for components 1, 2 and 3 respectively (Figure 11c). Only component 1 clearly separated 'Camarosa' and 'Candongga' (in the positive range, with (E)-2-decenal, ethyl butanoate, 1-octanol, octyl 2-methylbutanoate as main positive loading scores) from the three remaining cultivars (in the negative range, with 2-pentylfuran, (E)-2-octenal, 1-octen-3-ol and (E)-2-heptanal as main negative loadings scores) (Figure 11c).

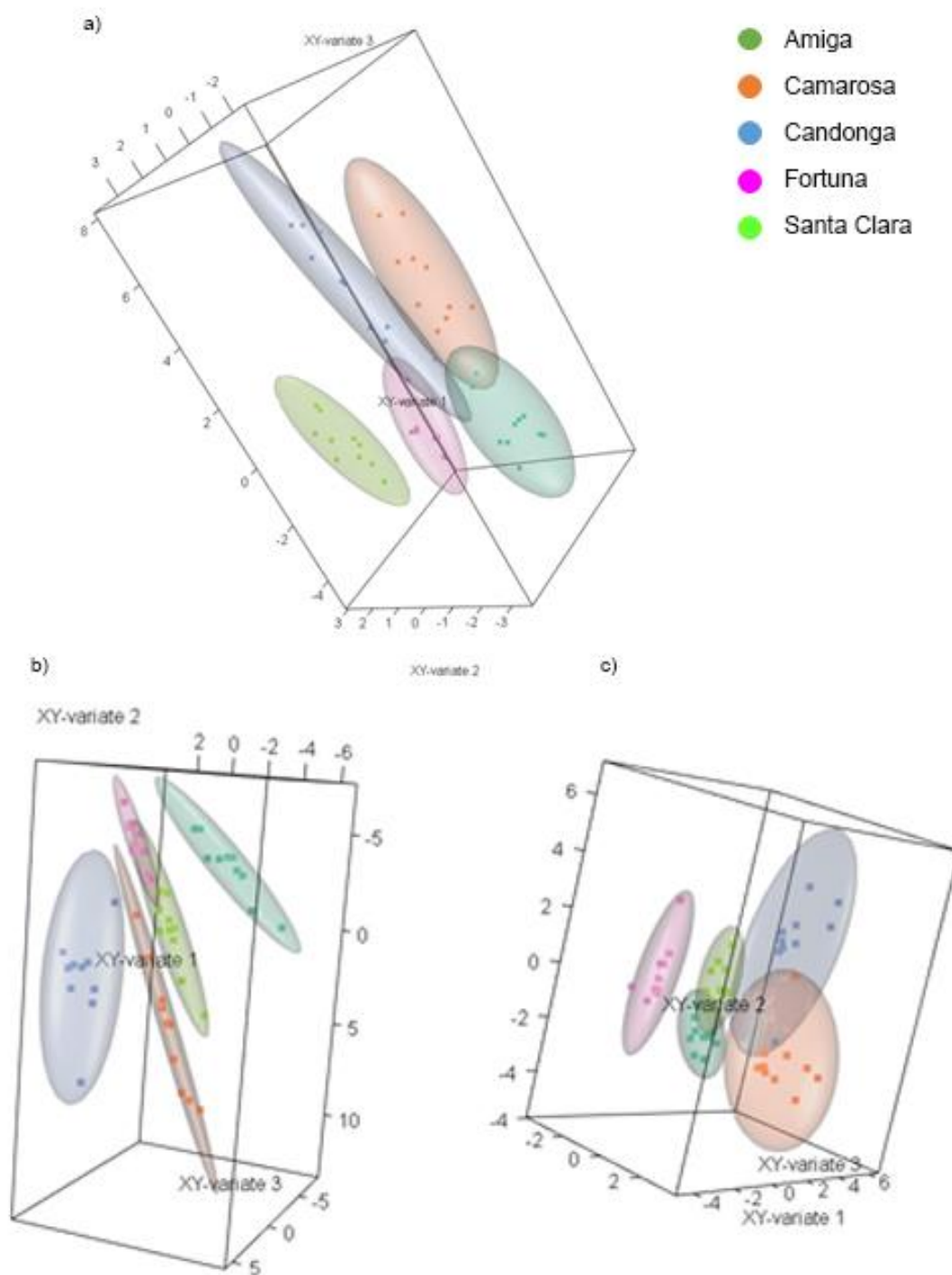


Figure 11: PLS-DA analysis for primary (a), secondary (b) metabolites and volatiles (c), with samples separation based on genotype (cultivars).

PLS-DA model: separation according to postharvest treatment

PLS-DA model with three components was also able to separate the samples according to their postharvest treatments (T0 fruits, fruits kept at 4°C, fruits kept in CO₂-enriched atmosphere and fruits kept in O₃-enriched atmosphere). As expected the separation between T0 samples and the postharvest ones was more obvious than between the different postharvest treatments, for primary, secondary metabolites and volatiles (Figures 12).

Regarding primary metabolites, components 1 (34% of explained variance) and 3 (11%) separated T0 fruits from postharvest samples, while component 2 (11%) grouped together T0 and fruits kept in O₃-enriched atmosphere (located in the positive values of the axis, being glucose-6-phosphate, fructose-6-phosphate and galactinol the main loadings) and samples kept in normal and CO₂-enriched atmospheres (distributed towards more negative values of the axis, with GABA and proline being the main loadings, Figure 12a). For component 1, metabolites which weighed more were sucrose, malic acid, citric acid, glucopyranoside, trehalose and aspartic acid for positive values (where T0 samples were located) and GABA for negative value of the axis (where postharvest samples were situated). For component 3, T0 samples were located in the negative part of the axis, being maltotriose the metabolite with the main weight, and postharvest samples in the positive range, with erythritol, glycine, β-alanine, galactinol and succinic acid as main loadings (Figure 12a).

The percentage of explained variance for secondary metabolites was 39%, 11% and 4% for the three components (Figure 12b). Component 2 separated postharvest samples (towards positive values) from T0 fruits (in the negative range). Metabolites which weighed more were naringenin chalcone hexose 2, hydroxybenzoic acid hexose 1, eriodictyol hexose 2, kaempferol hexose 1, propelargonidin trimer 3 and pelargonidin-hexose (the main anthocyanin pigment in ripe fruit) for the negative values of the axis, and quercetin acetylhexose, lagerstannin B3 and ellagic acid for the positive values. Component 1 was also partially able to separate T0 samples (in the negative range) from the postharvest fruits, with almost all the metabolites with negative loadings (Figure 12b).

Regarding volatiles, the three components of the PLS-DA model defining the postharvest treatments as Y classes explained 23%, 15% and 14% of explained variance (Figure 12c). Component 1 separated T0 fruits (located in the negative part of the axis) from postharvest samples, while component 2 isolated most of the samples kept in O₃-enriched atmosphere (in the positive range of the axis) from the remaining ones. No clear separation was achieved with component 3. Main negative loadings for component 1 were heptanal and the ketones 1-penten-3-one and 6-methyl-5-hepten-2-one and main positive loadings were (Z)-3-hexenyl, ethyl and 3-methylbutyl acetates. Propyl butanoate, 1-methylethyl, pentyl, methyl and nonyl acetates were the most important loadings for the positive range of component 2, while ethanol and 3-methylbutyl acetate were the most important for the negative range (Figure 12c).

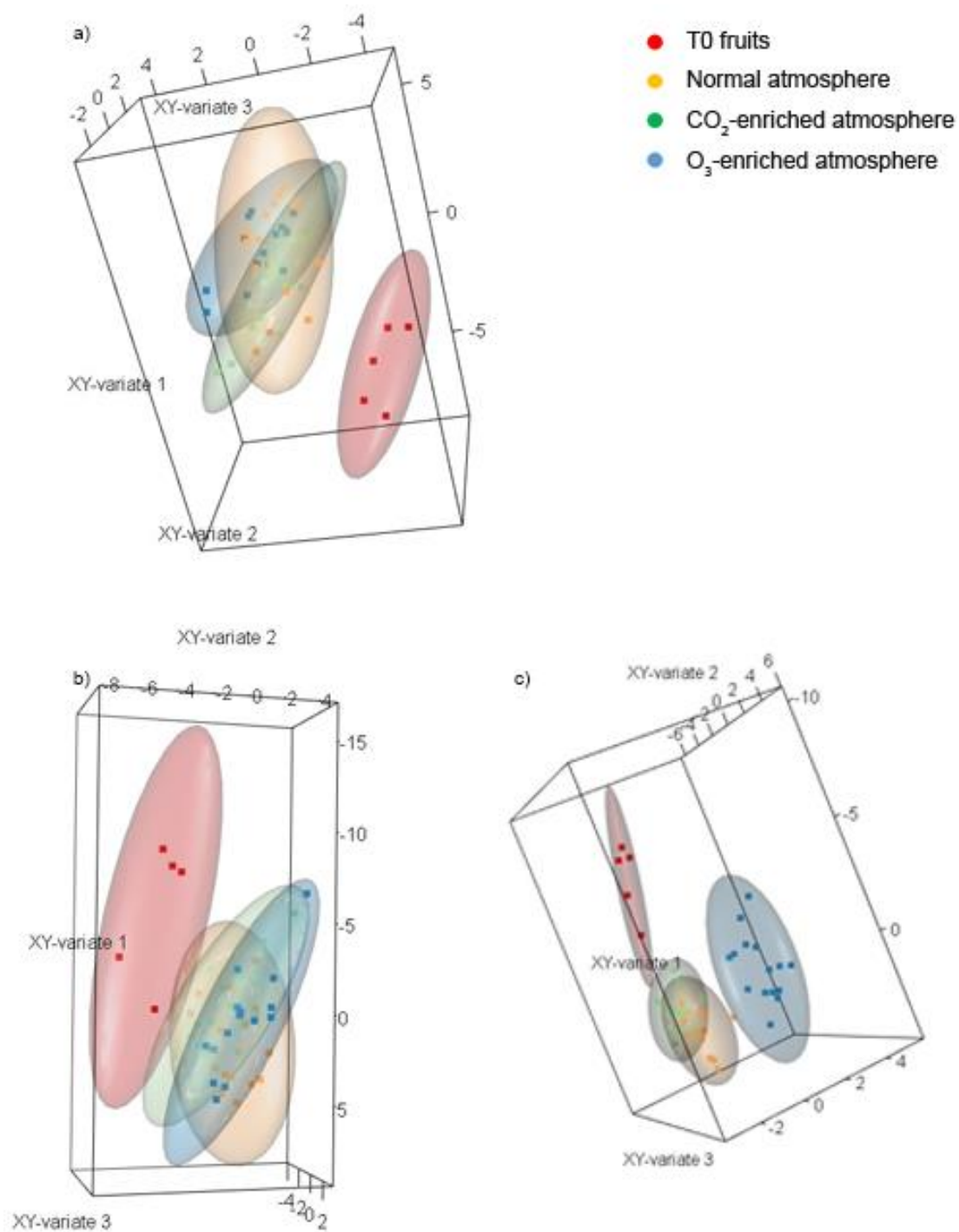


Figure 12: PLS-DA analysis for primary (a), secondary (b) metabolites and volatiles (c), with samples separation based on postharvest treatments.

PLS-DA model: separation according to the duration of postharvest treatments

Duration of postharvest treatments (0, 3, 6 and 10d for T0 fruits and samples stored during 3, 6 and 10 days) was also well separated by the three first components of PLS-DA model, for primary, secondary metabolites and volatiles (Figures 13).

For primary metabolites, component 1 (30% of explained variance) ordered samples based on the time after harvest (0, 3, 6 and 10 days after harvest, from negative to positive values), while component 2 (17% of explained variance) distinguished some samples stored 10 days in CO₂- and O₃-enriched atmospheres, which located in the positive part of the axis (Figure 13a). Primary metabolites with positive weight for component 1 were GABA, glycine, β -alanine, galactinol, succinic acid, putrescine, fructose-6-phosphate, isomaltose and glucose-6-phosphate. Regarding component 2, loadings which weighed more (with positive values) were glycine, erythritol, β -alanine, tyrosine, isomaltose, alanine and GABA. Component 3 (6% of explained variance) did not show a clear separation based on postharvest duration (Figure 13a).

Regarding secondary metabolites, the three components explained 39%, 10% and 6% of the explained variance, respectively (Figure 13b). Component 1 roughly separated samples kept during 6 and 10 days in the different postharvest treatments (located in the positive range) from the remaining ones, while component 2 distinguished T0 samples (negative range) from the postharvest ones. Galloyl-hexose 4, propelargonidin dimers 4 and 1, unknown ellagitannin 1 and galloylquinic acid 1 were the metabolites which weighed more for component 1, with negative values. For component 2, the main negative loadings weights were naringenin chalcone hexose 2, eriodictyol hexose 2, kaempferol-hexose 1, hydroxybenzoic acid-hexose 1 and galloylquinic acid 1, and the main positive loadings quercetin-acetylhexose, lagerstannin B3 and ellagic acid. Once again, no clear separation was observed with component 3 (Figure 13b).

For volatiles, PLS-DA model, using time as class, explained 24% (component 1), 13% (component 2) and 15% (component 3) of the variance (Figure 13c). Component 1 ordered the samples according to the time after harvest, from 0d (negative) to 10d (positive). Volatiles with major weights for this component were

1-penten-3-one and the aldehydes (Z)-3-hexenal, (E)-2-hexenal and heptanal with negative values, and pentyl and ethyl acetates for positive values. 3d samples were located in the positive part of the axis defined by component 2, in which ethyl acetate, nonanal, decanal, ethanol and myrtenyl acetate weighed more. No separation was obtained with component 3 (Figure 13c).

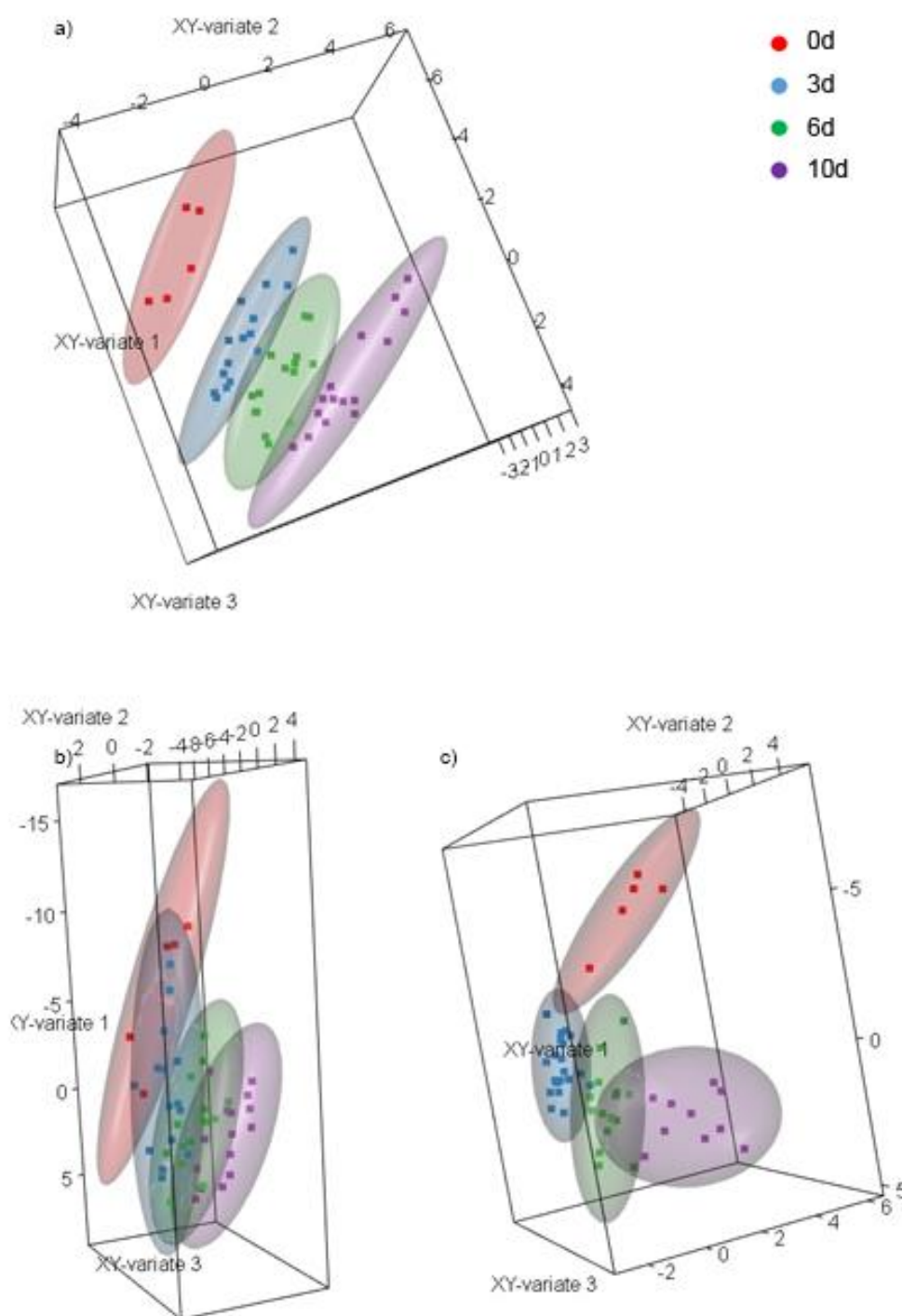


Figure 13: PLS-DA analysis for primary (a), secondary (b) metabolites and volatiles (c) with samples separation based on time after harvest (0d for T0 fruits, 3d, 6d and 10d for fruits frozen after three, six and ten days of the different postharvest treatments).

3) Metabolic changes in strawberry fruits during postharvest

To further investigate the behavior of the different groups of metabolites during postharvest life of strawberry, heatmaps showing each cultivar separately were drawn (Figures 14, 15 and 16 for primary metabolites, secondary metabolites and volatiles respectively). In addition, heatmaps showing the three treatments separately were also represented (Figures 17, 18 and 19 for primary metabolites, secondary metabolites and volatiles respectively). First, relative metabolite levels were normalized (median normalization) and then fold change of each metabolite in the postharvest samples was calculated comparing to the value in the T0 samples. Annexes 8, 9 and 10 list the fold change values for primary metabolites, secondary metabolites and volatiles, respectively. Finally, log₂ was applied to the fold change, in order to set the value of each metabolite in the T0 samples to zero. Positive values (in red in the heatmaps) indicate metabolite increased in the postharvest sample compared to the T0 sample and negative values (in blue in the heatmaps) indicate a decrease of the metabolite during postharvest.

Primary metabolites

Some general trends could be discerned in the metabolite profiles of the samples along postharvest, when compared to T0 fruits. Concerning amino acids, an increase in their levels, more obvious in 'Amiga' and 'Candonga' samples, were observed in the samples kept 3 days in normal atmosphere, following by a decrease after 6 and 10 days, with the exception of glycine, β -alanine and GABA, which were induced during postharvest in the three tested treatments. On the opposite, amino acids were at their lowest levels after 3 days of ozone treatment, and then slightly increased after 6 and 10 days, even if their values did not reach T0 fruits, with the exception of the three mentioned metabolites. In fruits kept in CO₂-enriched atmosphere, a general decrease was observed after 3 and 6 days, while amino acid levels were higher after 10 days, with some of them exceeded T0 values. A general decrease of organic acids along postharvest was also observed, with the exception of succinic acid which levels increased, being this increase enhanced in CO₂- and O₃-enriched atmosphere treatments (Figures 14 and 17). These dissimilarities in sample behavior between treatments could

indicate that biosynthetic pathways were differently regulated under normal or controlled atmospheres.

Regarding soluble sugars and their alcohol derivatives, one common feature was the increase of galactinol during postharvest, being this increase more obvious in the samples kept in O₃-enriched atmosphere. Furthermore, an increase of phosphorylated hexose intermediates (glucose- and fructose-6-phosphate) was also observed in fruits kept in O₃-enriched atmosphere, after 6 and 10 days, indicating a possible role of these compounds in oxidative stress responses. The main sugars, fructose, glucose and sucrose, were generally decreased during postharvest treatments, even if a slight increase was observed after 3 days in normal atmosphere (Figures 14 and 17).

Finally, the polyamine putrescine was induced during postharvest, being the increase more obvious in CO₂-enriched and normal atmosphere, while in O₃-enriched atmosphere it was limited to 'Amiga', 'Camarosa' and 'Candongá' cultivars (Figure 14a-c).

Secondary metabolites

Regarding secondary metabolites, trend in their evolution along postharvest seemed more cultivar-specific (Figures 15 and 18). The majority of flavonoids was increased in normal atmosphere after 3 days in 'Amiga' and 'Fortuna' cultivars. After 6 days of the same treatment, this increase was maintained for almost all proanthocyanidins in 'Amiga' and only for rutin and quercetin acetylhexose in 'Fortuna'. In fact, the levels of quercetin acetylhexose was especially enhanced in 'Fortuna' in all the postharvest samples compared to the T0 samples. After 10 days, a general decrease of flavonoids was evident for all cultivars, even if this decrease was less accentuated in 'Amiga' and 'Fortuna'. In fruits kept in CO₂-enriched atmosphere, the increase of proanthocyanidins was maintained during the whole duration of the experiment in 'Amiga', being the levels of most flavonoids even higher after 10 days. Most flavonols in 'Camarosa' was increased in fruits kept 3 days in O₃-enriched atmosphere, while proanthocyanidins levels in 'Amiga' showed an intensification along time in this treatment.

Pelargonidin-3-*O*-glucoside and cyanidin-3-*O*-glucoside, the main pigments in ripe strawberry fruits, were not accumulated in any of the sample, with the exception of a 2-fold increase in 'Amiga' fruits kept 10 days in CO₂-enriched atmosphere when compared to T0 fruits (Figures 15a, 18c).

Regarding ellagitannins and galloyl glucoses, a general decrease in their levels was noticed in the samples kept in normal atmosphere, with the exception of 'Amiga' fruits after 3 days of storage. In 'Amiga' fruits kept in CO₂-enriched atmosphere, main soluble tannins were first decreased after 3 days, and then increased after 6 and 10 days. They were also increased in 'Camarosa' fruits after 3 and 6 days, even if their level was strongly decreased after 10 days. In 'Candonga', 'Fortuna' and 'Santa Clara' cultivars, a general decrease of soluble tannins was observed after CO₂ storage. Ozone treatment caused a general decrease in the levels of ellagitannins and galloyl glucoses, except for 'Camarosa' fruits after 3 days and 'Amiga' after 10 days.

Phenolic acids (hydroxycinnamic and benzoic acid derivatives) were predominantly decreased during storage in the three treatments, with the exception of a few of them in 'Amiga' cultivar. Finally, terpenoids were also decreased, with the exception of 'Amiga' cultivar in the three treatments, and in a lesser extent in some 'Camarosa', 'Candonga' and 'Fortuna' samples (Figures 15 and 18).

Volatiles

More drastic changes, in comparison with primary and secondary metabolites, could be observed in the levels of many volatiles after storage, in the three tested conditions. Some of them were considerably increased, while other were decreased during postharvest, and these changes were consistent in the three different treatments. However, less appreciable changes were noticed in the samples kept 3 days in O₃-enriched atmosphere, when compared to CO₂-enriched atmosphere and especially to normal conditions (Figures 16 and 19).

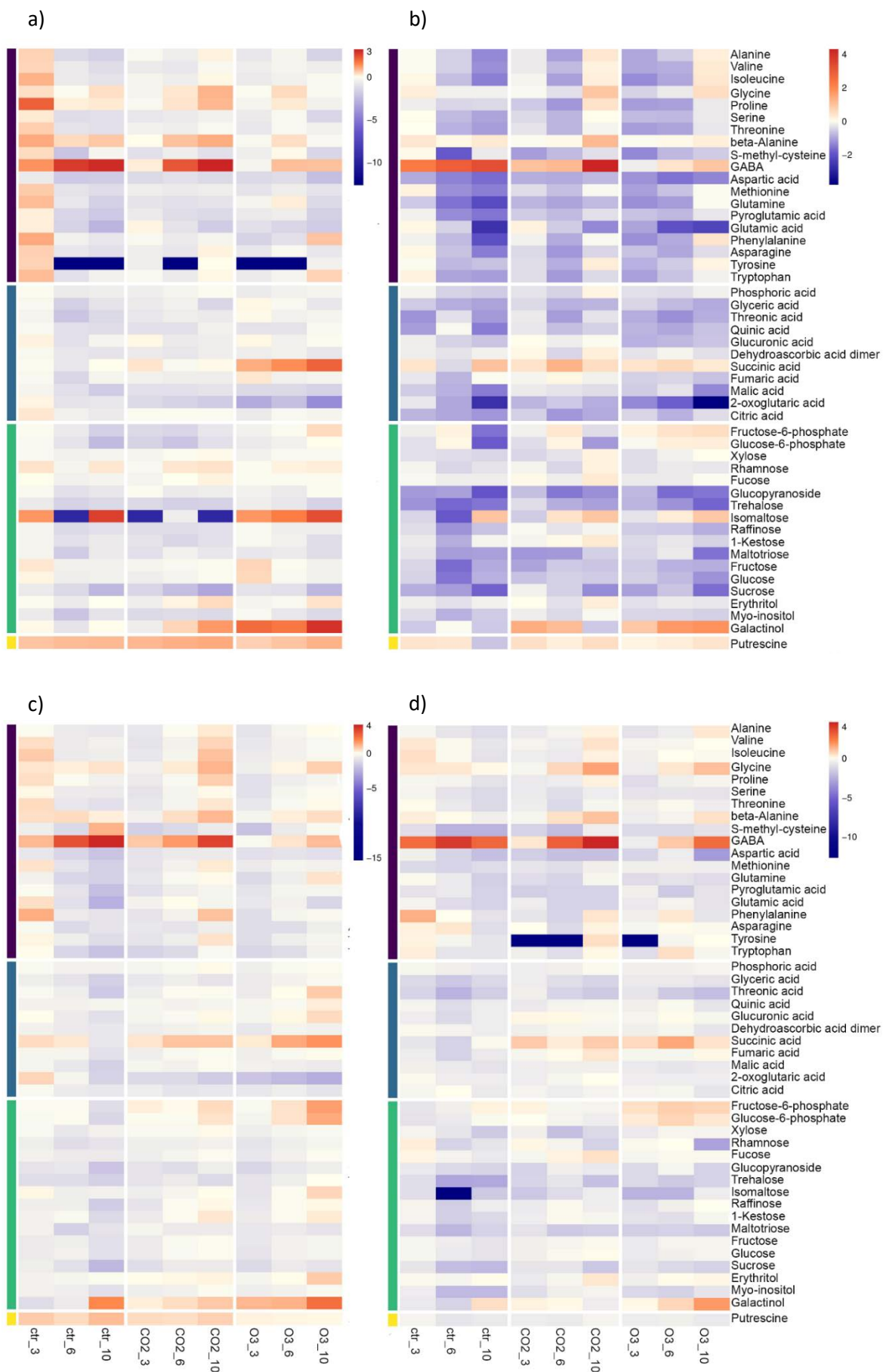
Aldehydes, furans, ketones and terpenes were generally decreased in the different treatments, except some of them, including key odorant mesifurane and γ -decalactone, in 'Santa Clara' cultivar.

Among alcohols, ethanol levels were strongly enhanced in all the postharvest samples even if the increase was slower in the fruits which were kept in ozone-enriched atmosphere. 1-octanol and eugenol were also increased along postharvest samples in 'Amiga', 'Camarosa' and 'Candonga' cultivars.

Esters are the main class of volatiles in ripe strawberry fruit, covering up to 90% of the total number. The major esters are methyl and ethyl butanoates, and methyl and ethyl hexanoates. Ethyl butanoate and hexanoate were enhanced along postharvest in all the samples, except after 3 days of O₃-enriched atmosphere treatment in 'Candonga', 'Fortuna' and 'Santa Clara' cultivars. On the opposite, methyl butanoate and hexanoate were strongly diminished in all samples, indicating different regulation in senescent fruit.

Concordant with the main ester changes in the five cultivars during postharvest, ester behavior could be divided into two, according if they suffered an important decrease or increase along storage. (Z)-3-hexenyl acetate, 2-methylbutyl acetate, 3-methylbutyl acetate, ethyl 2-hexenoate, ethyl acetate, ethyl octanoate, hexyl acetate, butyl acetate, methylthioacetic acid ethylester, myrtenyl acetate and pentyl acetate were increased in all the treatments. Propyl butanoate was increased in fruits kept in ozone-enriched atmosphere, being the increase more accentuated at the beginning of storage.

1-methylethyl hexanoate, butyl hexanoate, hexyl hexanoate, methyl benzoate and methyl octanoate were decreased, being the decrease stronger in normal and CO₂-enriched atmospheres (Figures 16 and 19).



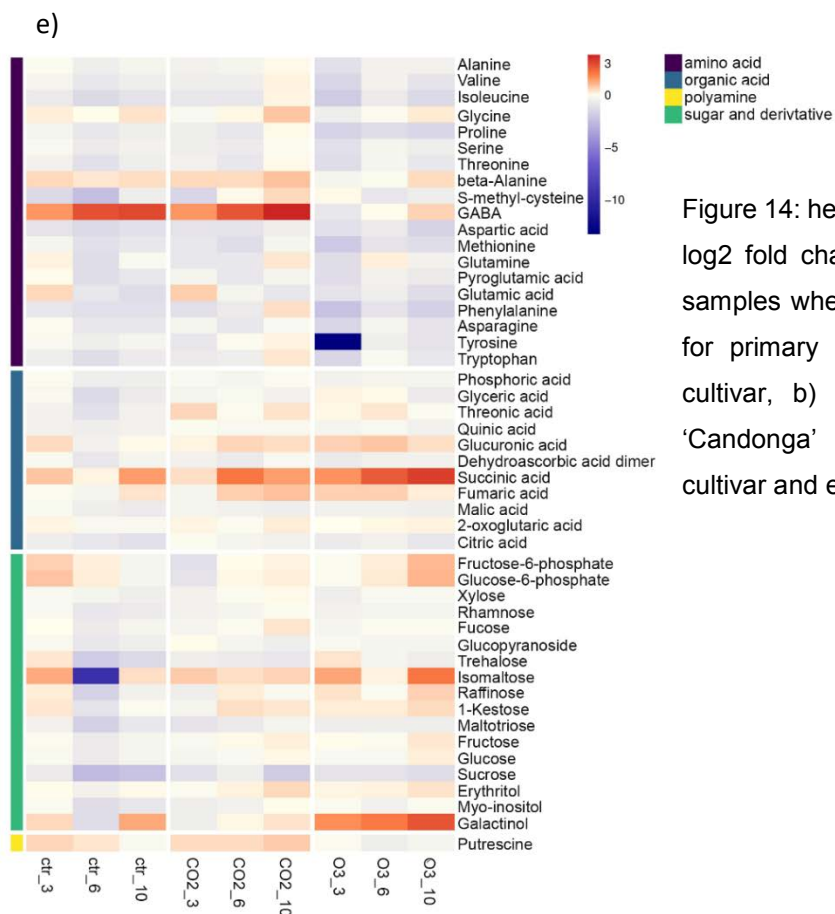
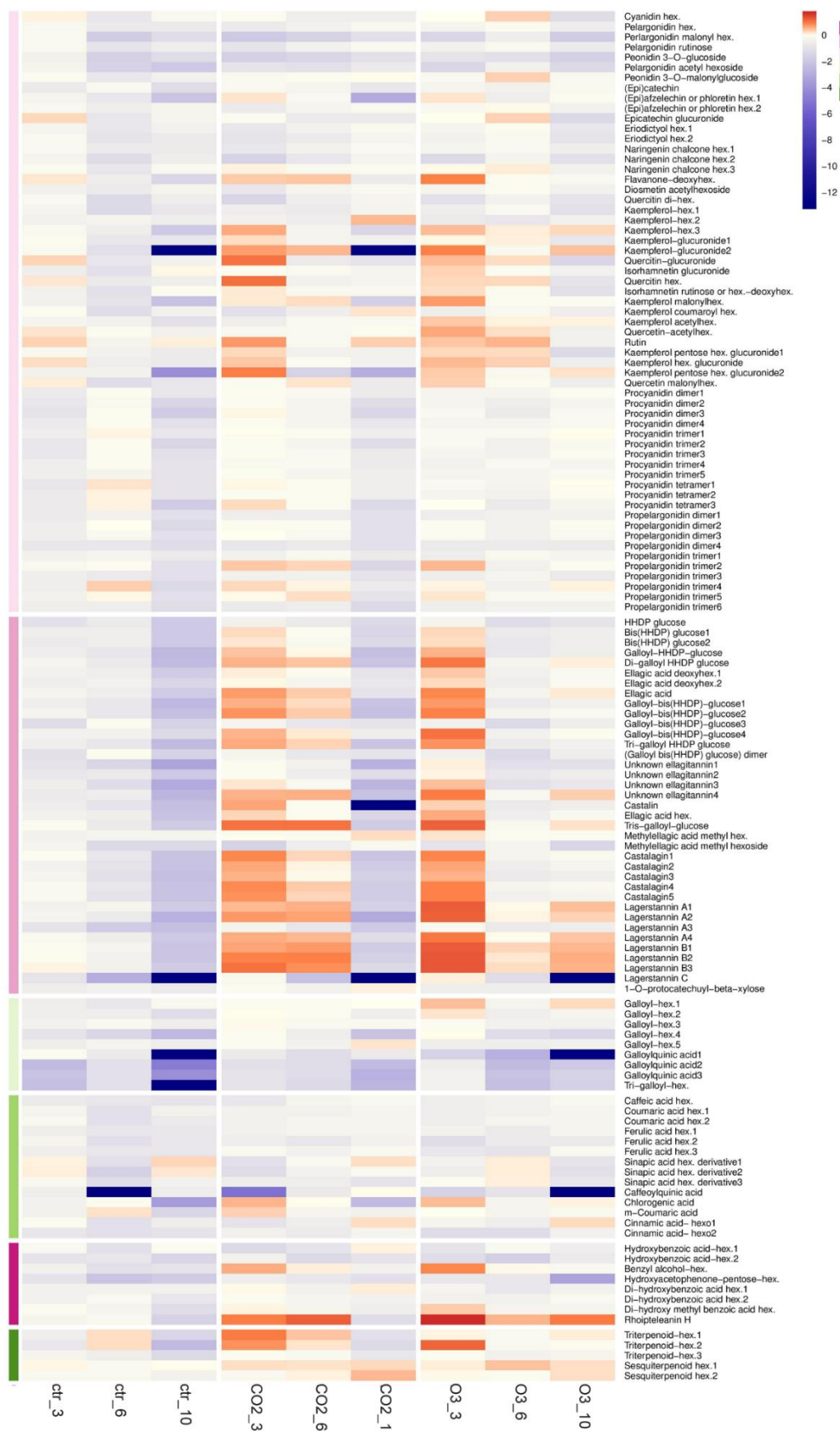
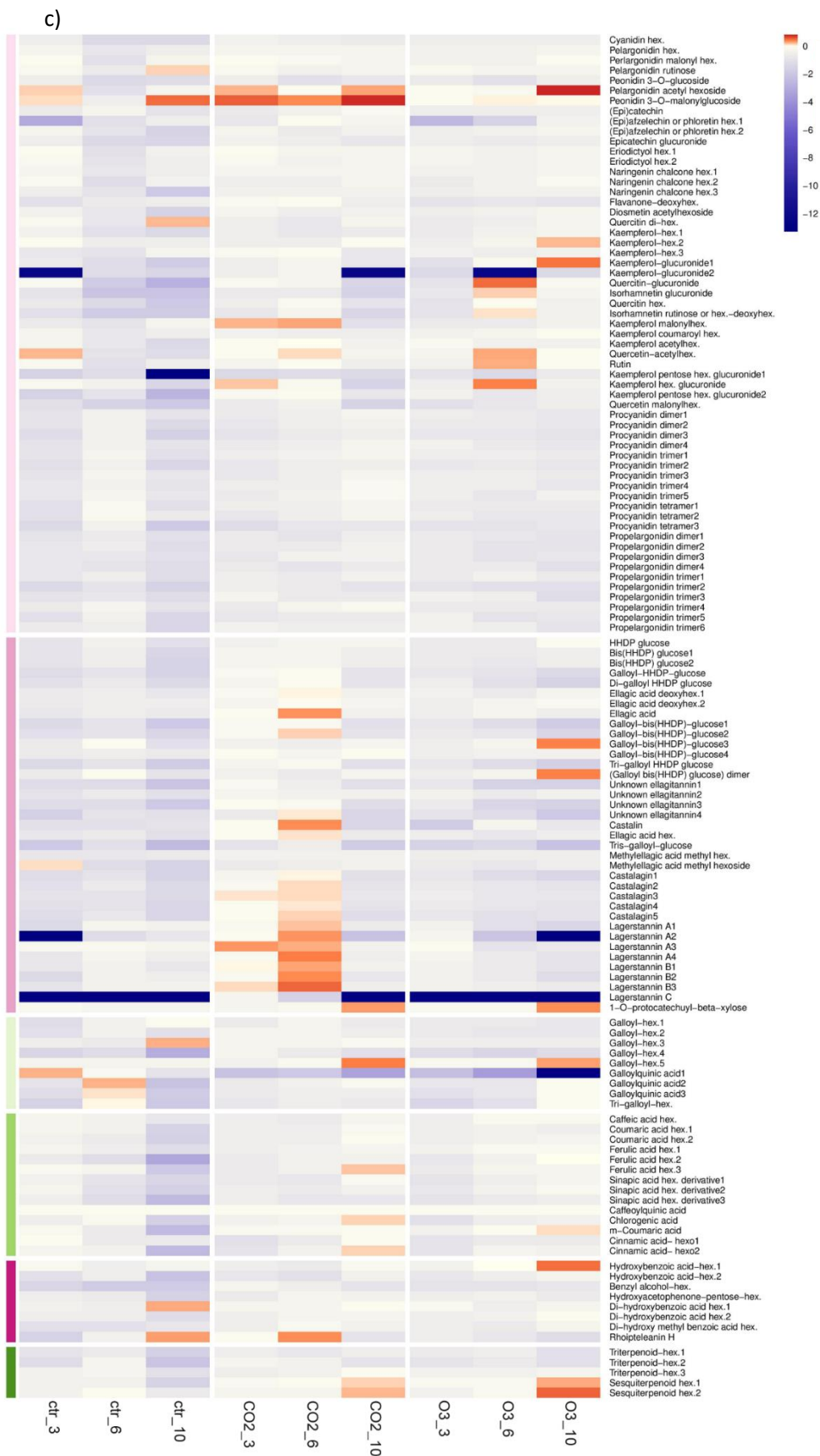


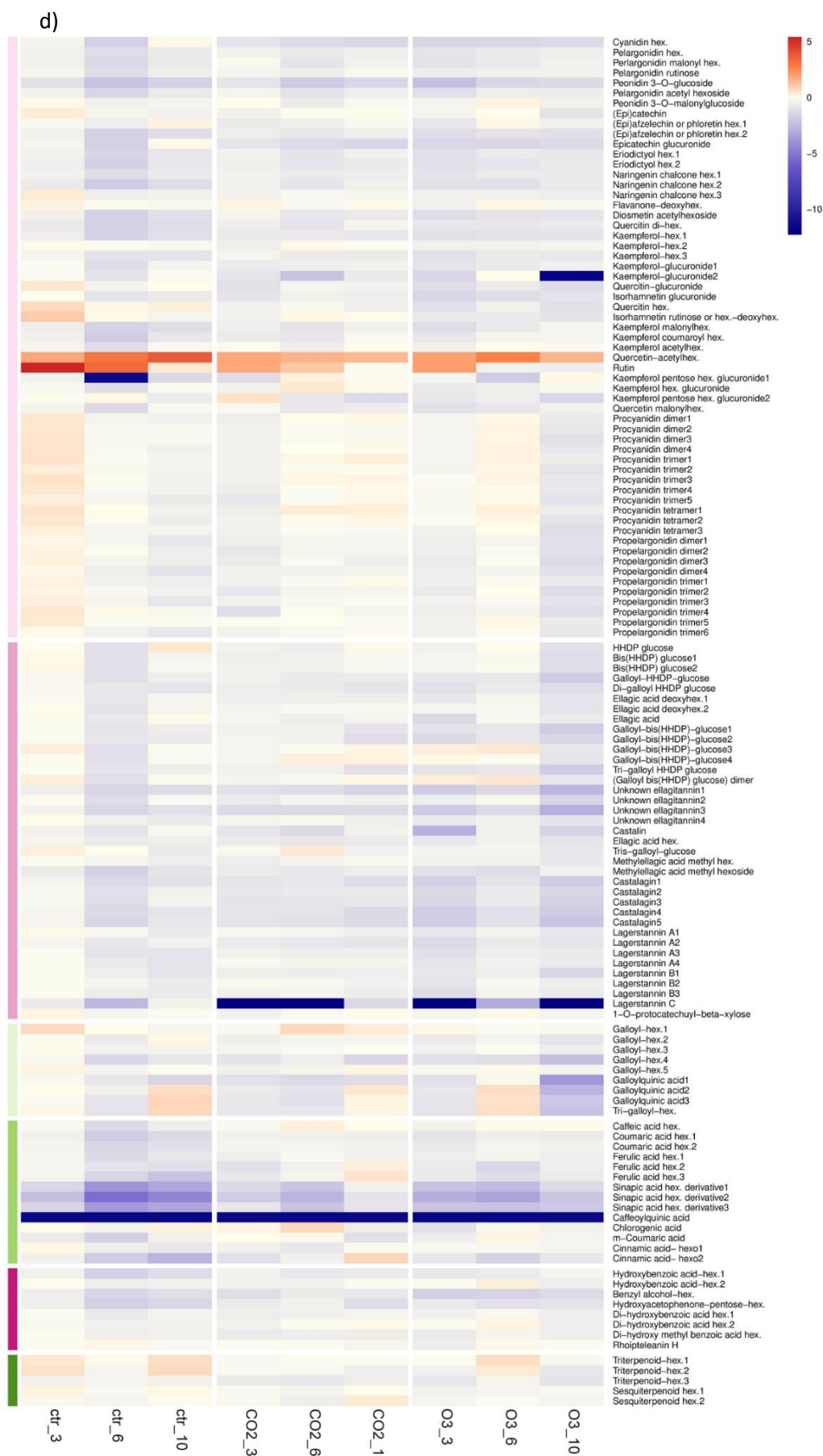
Figure 14: heatmaps representing the log₂ fold change in the postharvest samples when compared to T0 fruits for primary metabolites. a) 'Amiga' cultivar, b) 'Camarosa' cultivar, c) 'Candongra' cultivar, d) 'Fortuna' cultivar and e) 'Santa Clara' cultivar.



b)







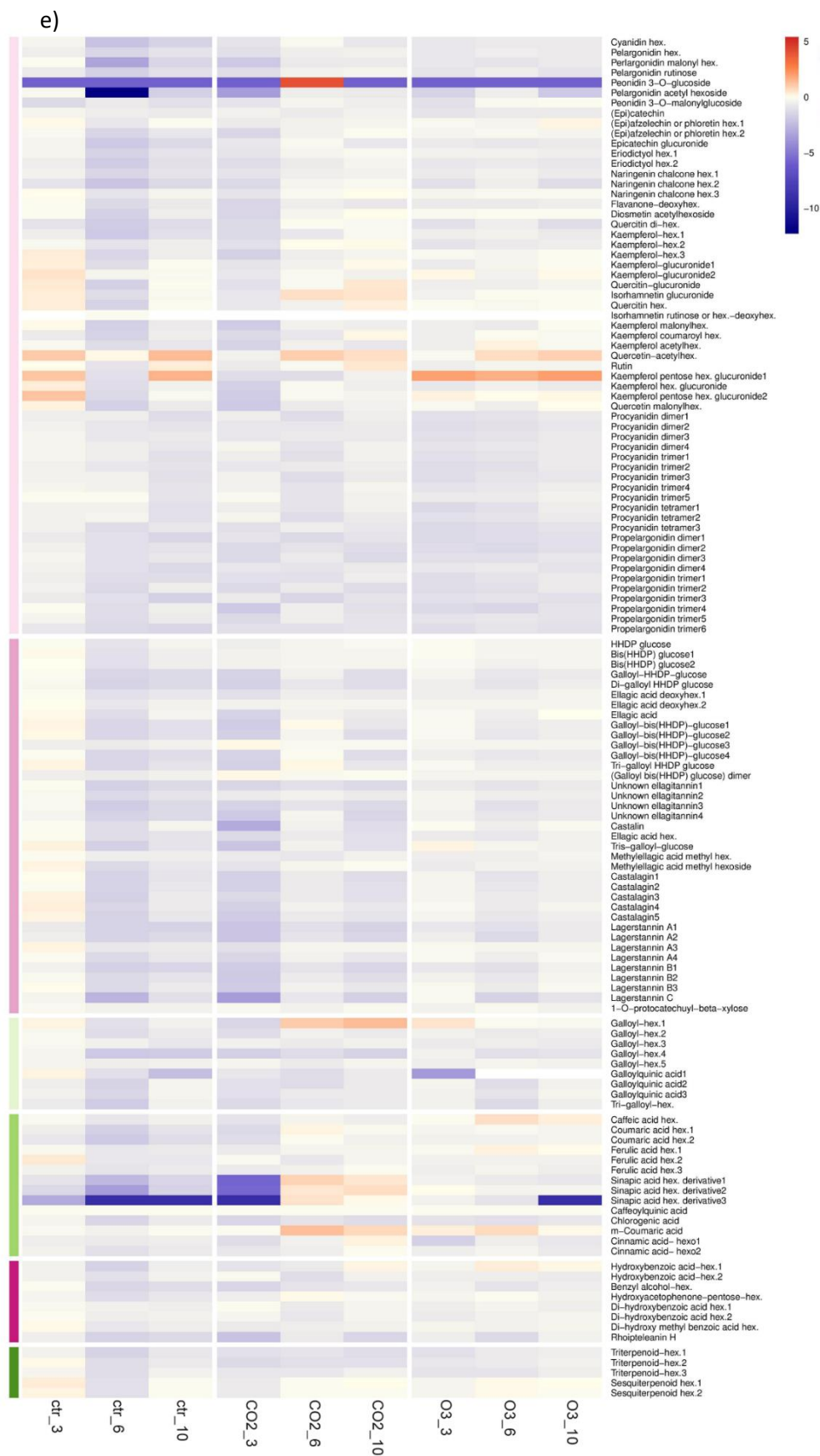
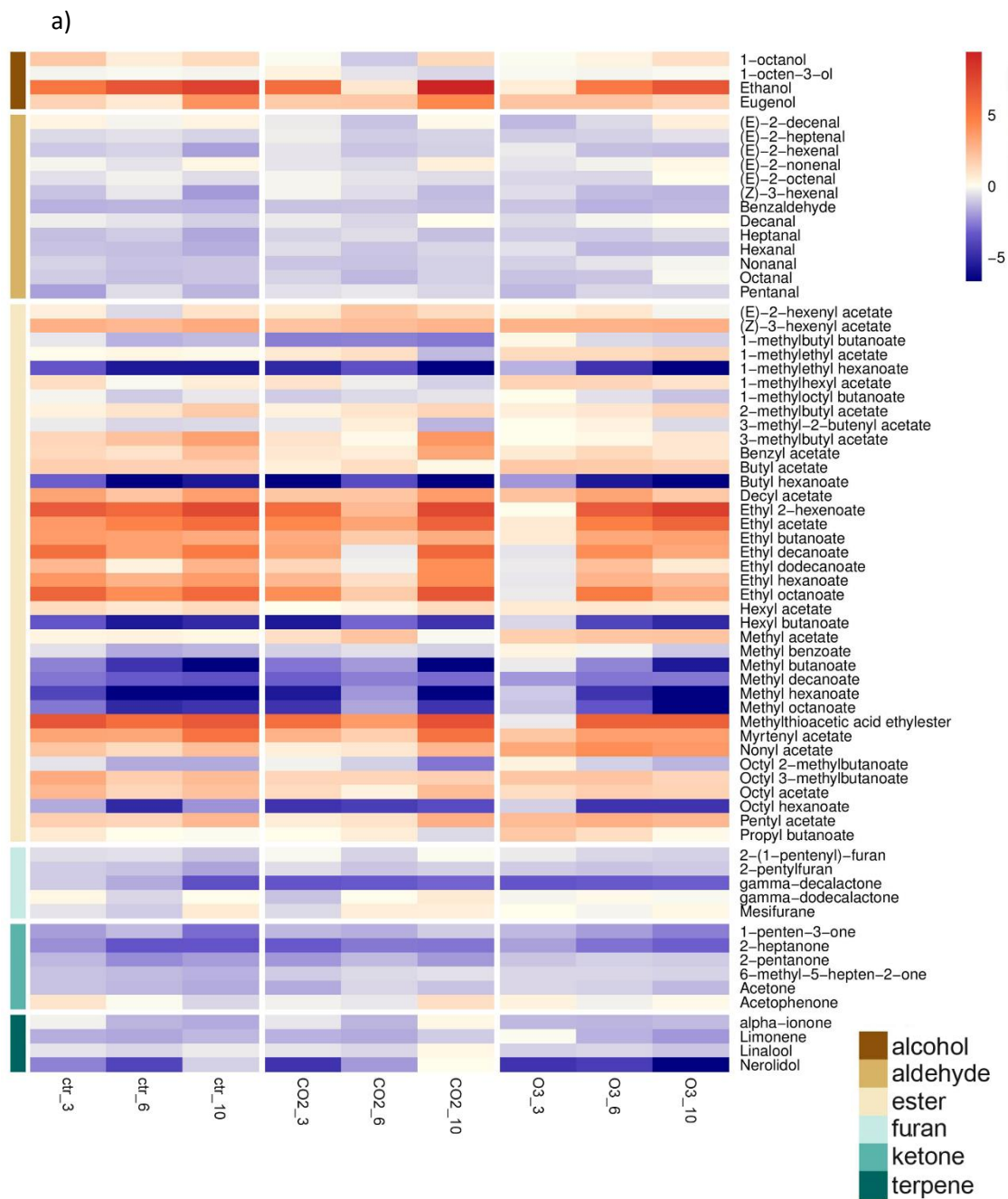
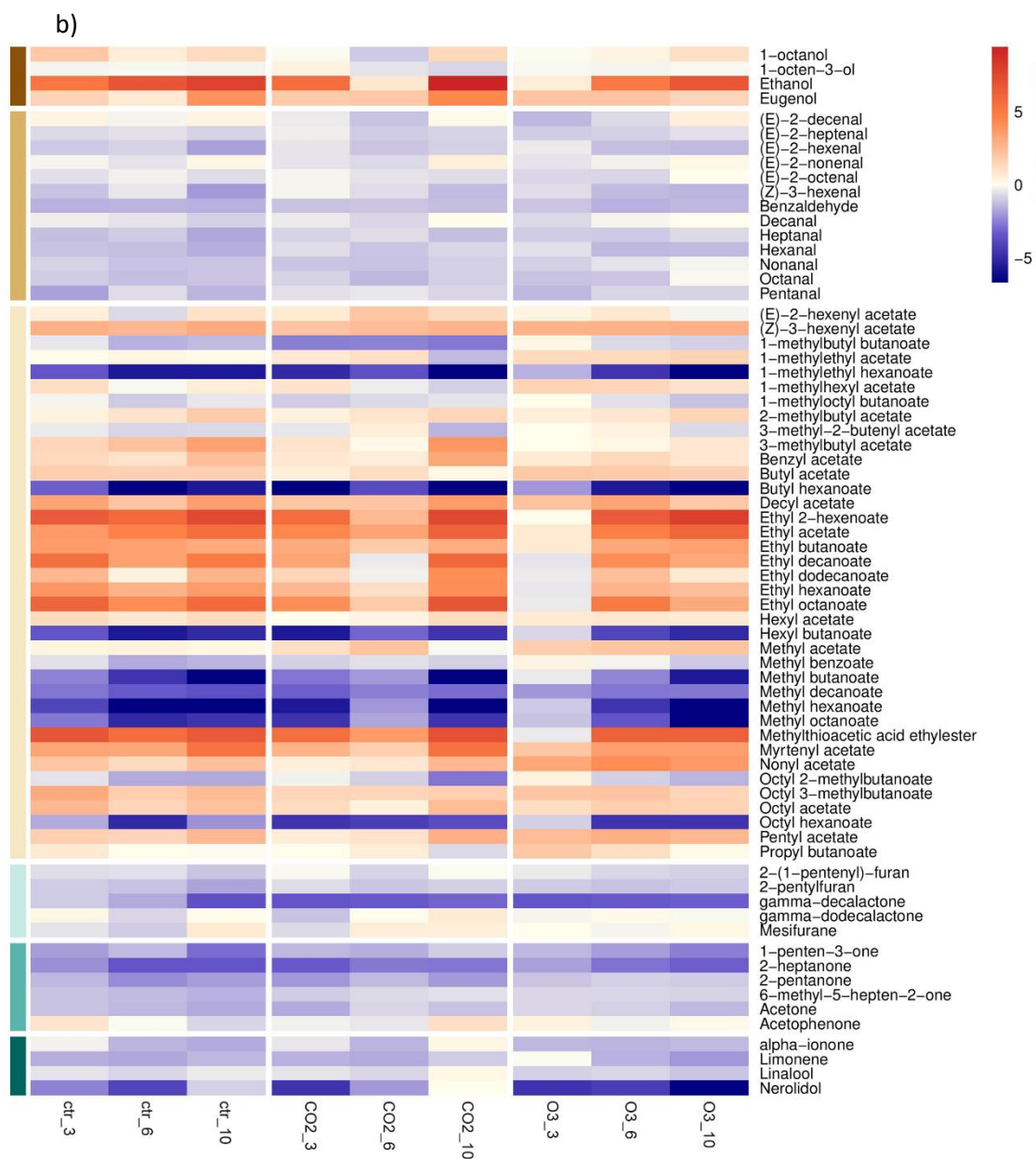
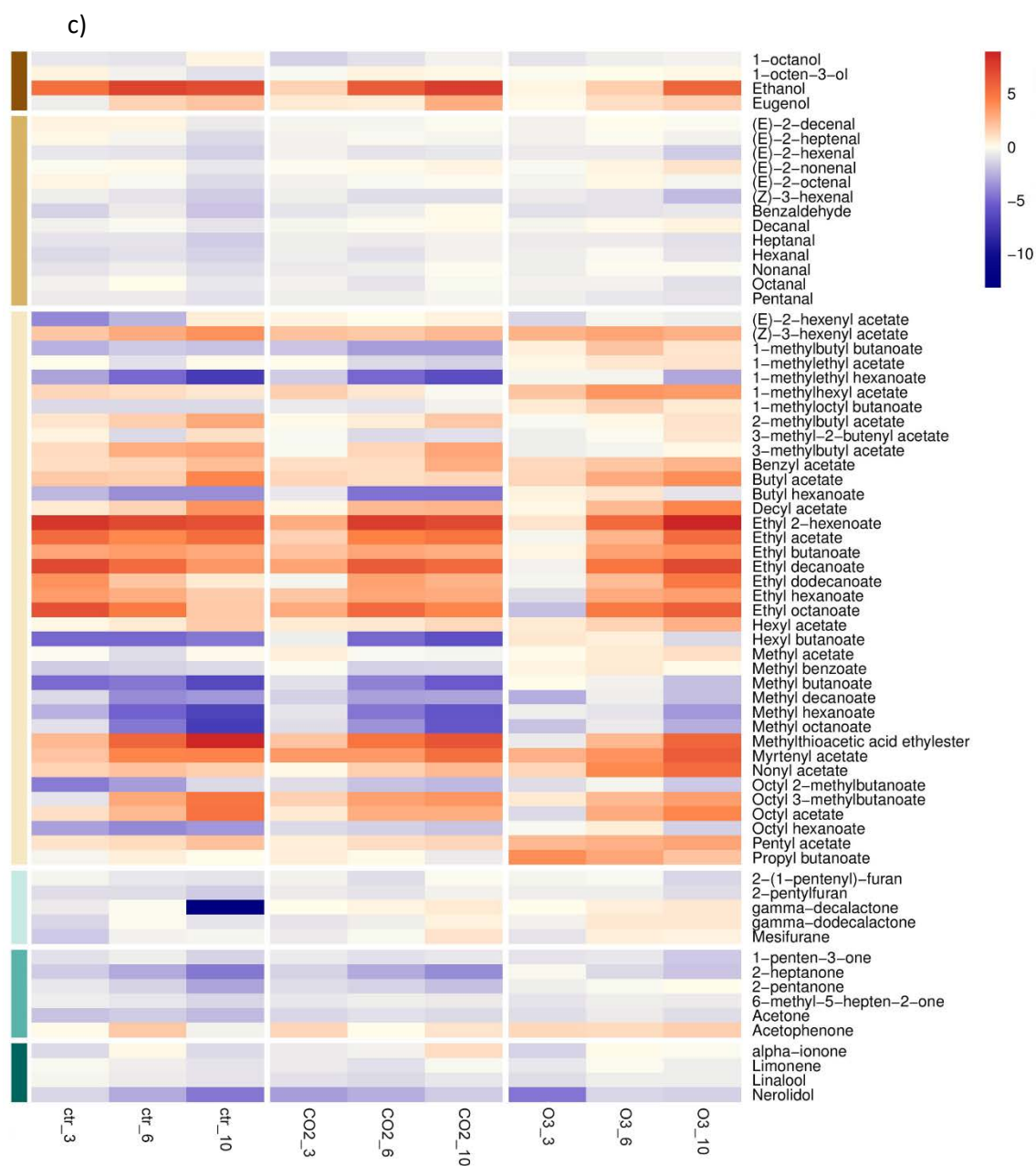
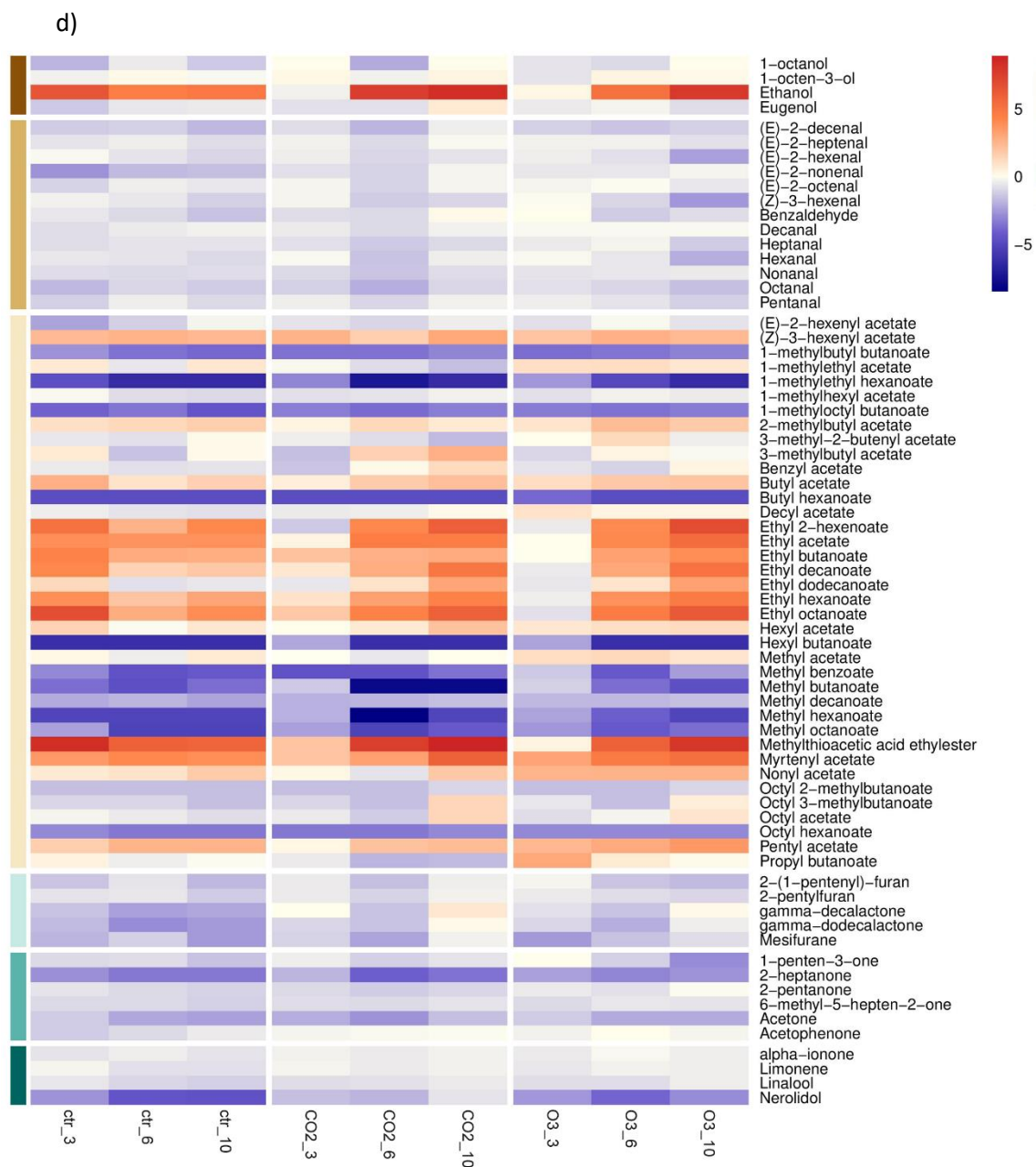


Figure 15: heatmaps representing the log₂ fold change in the postharvest samples when compared to T0 fruits for secondary metabolites. a) 'Amiga' cultivar, b) 'Camarosa' cultivar, c) 'Candongga' cultivar, d) 'Fortuna' cultivar and e) 'Santa Clara' cultivar.









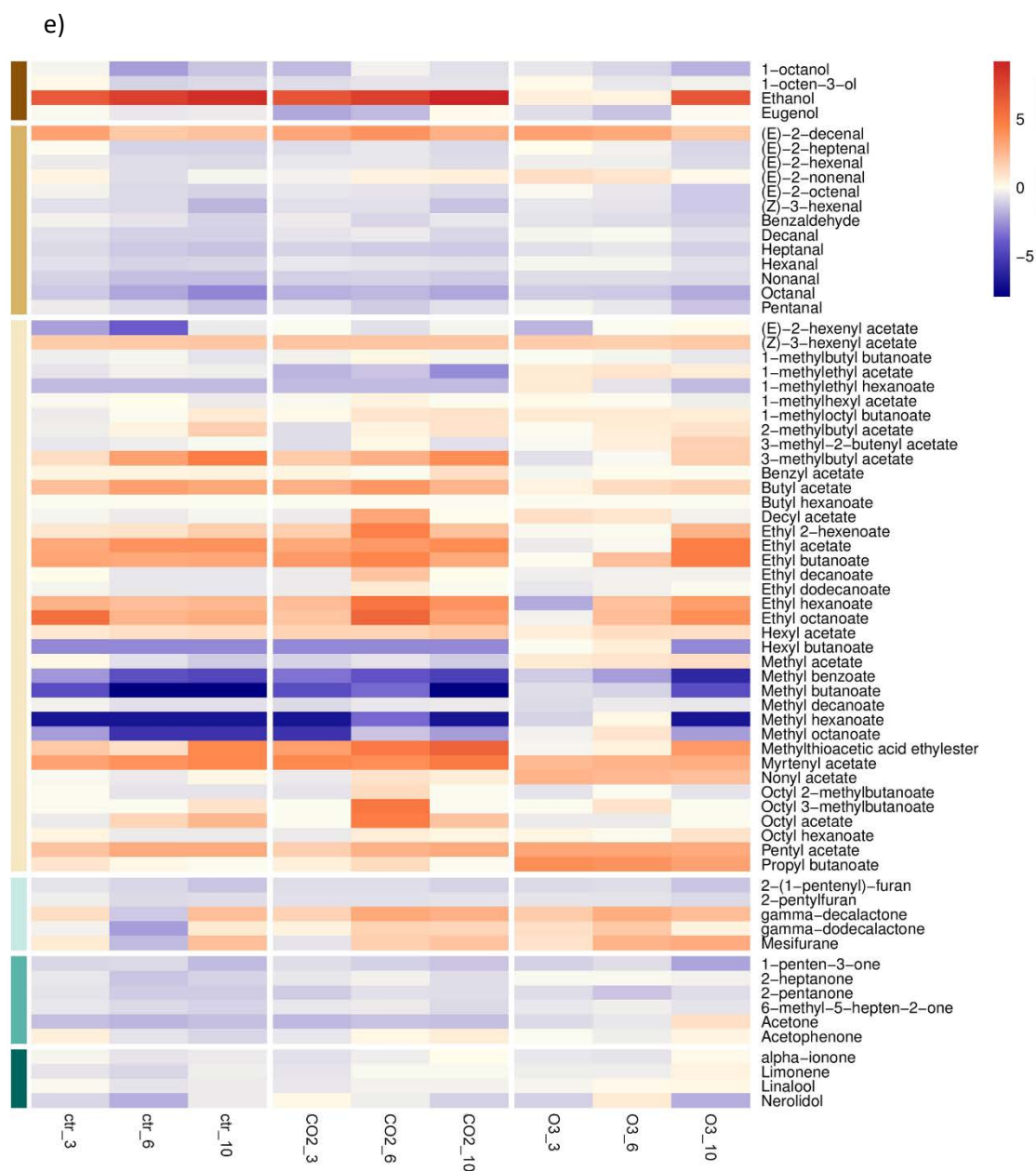


Figure 16: heatmaps representing the log₂ fold change in the postharvest samples when compared to T0 fruits for volatiles. a) 'Amiga' cultivar, b) 'Camarosa' cultivar, c) 'Candonga' cultivar, d) 'Fortuna' cultivar and e) 'Santa Clara' cultivar.

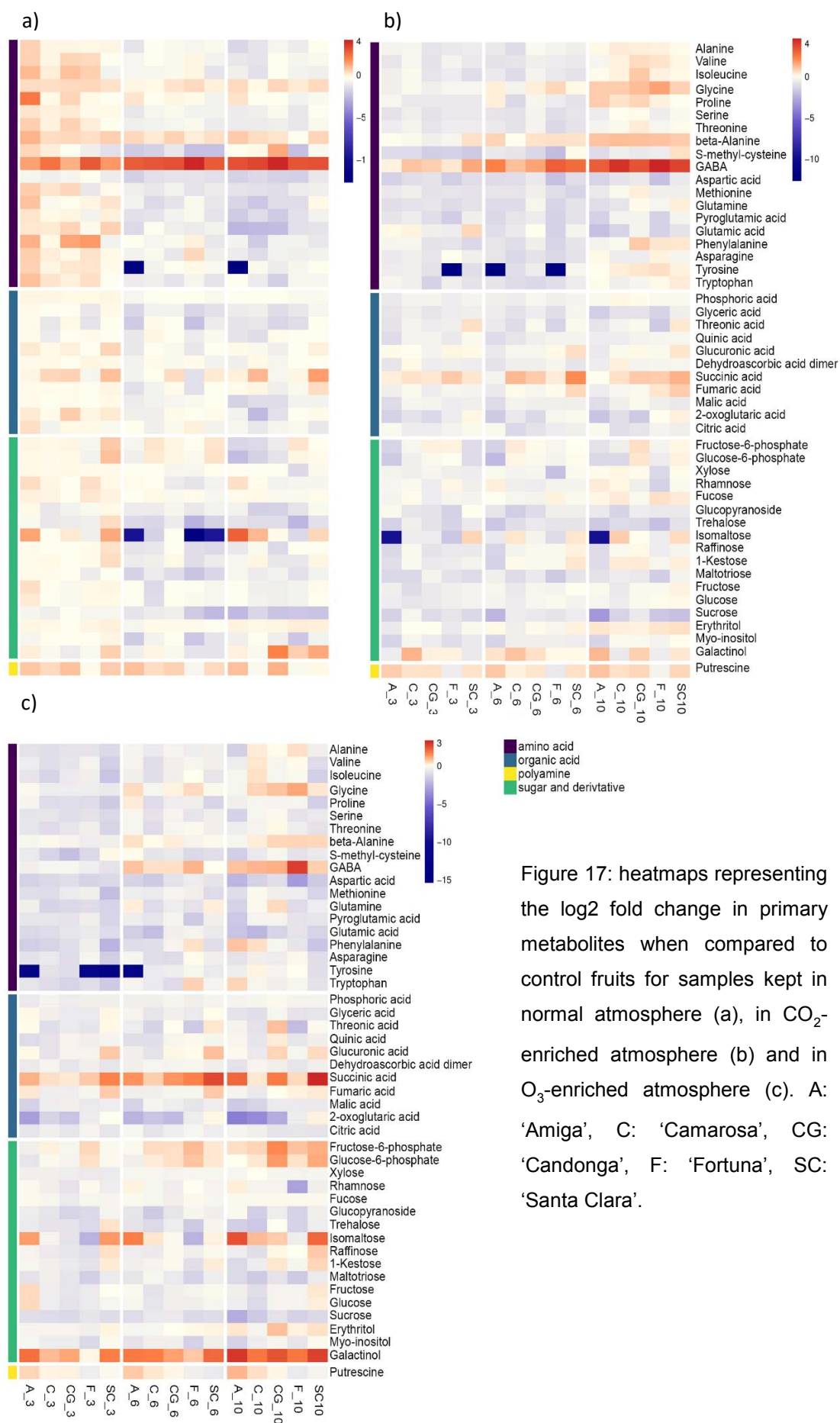
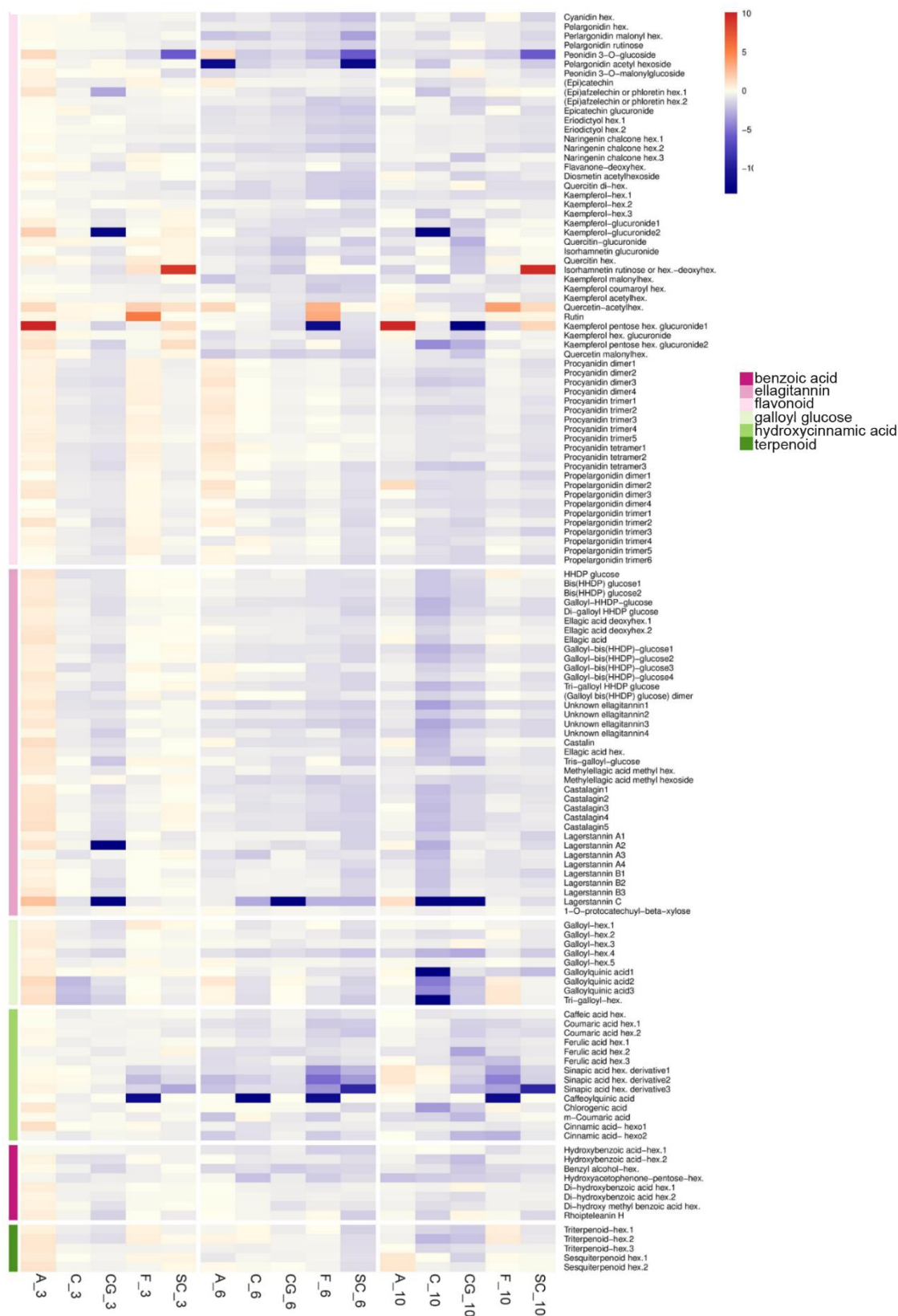
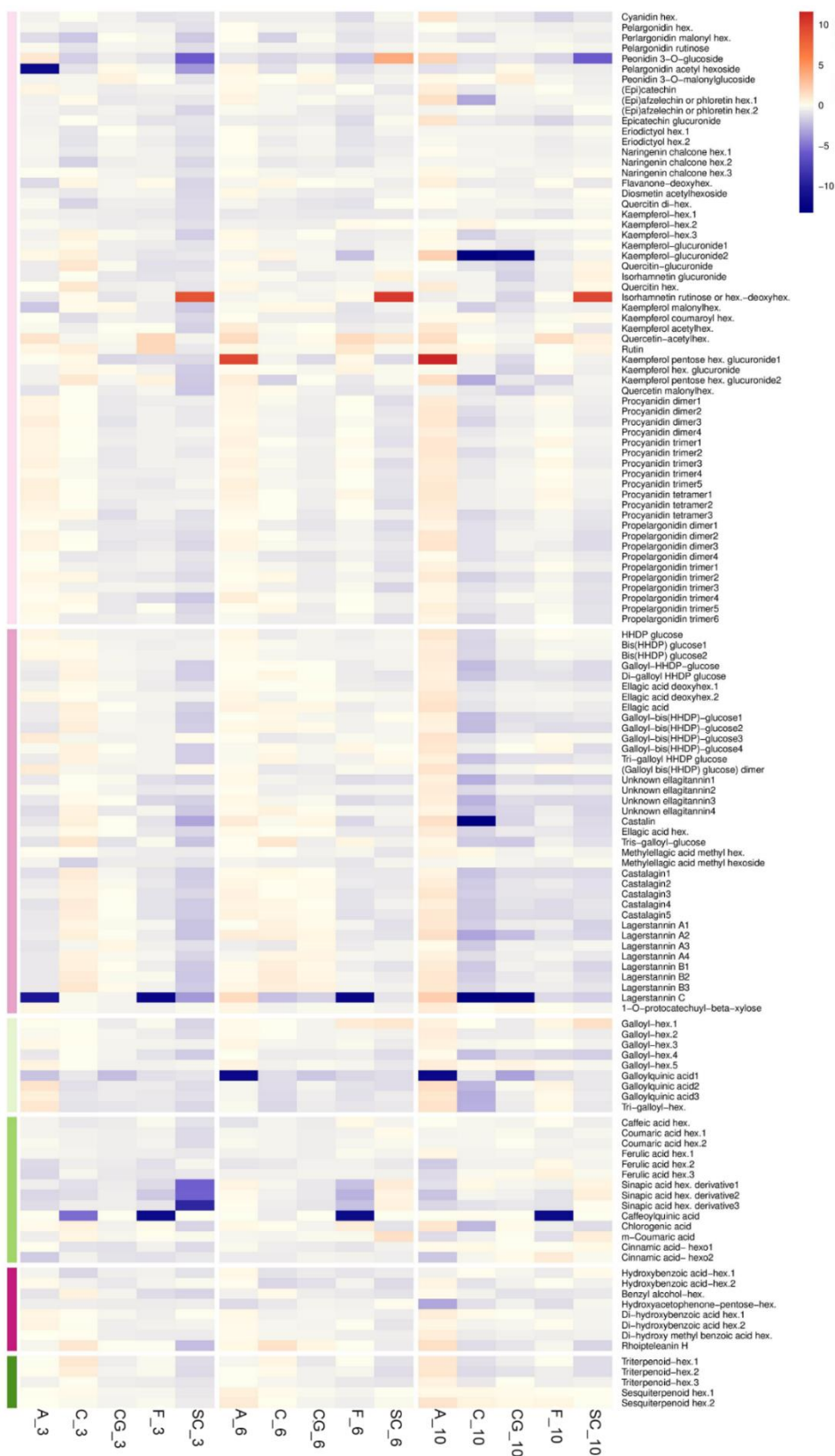


Figure 17: heatmaps representing the log₂ fold change in primary metabolites when compared to control fruits for samples kept in normal atmosphere (a), in CO₂-enriched atmosphere (b) and in O₃-enriched atmosphere (c). A: 'Amiga', C: 'Camarosa', CG: 'Candongga', F: 'Fortuna', SC: 'Santa Clara'.

a)



b)



c)

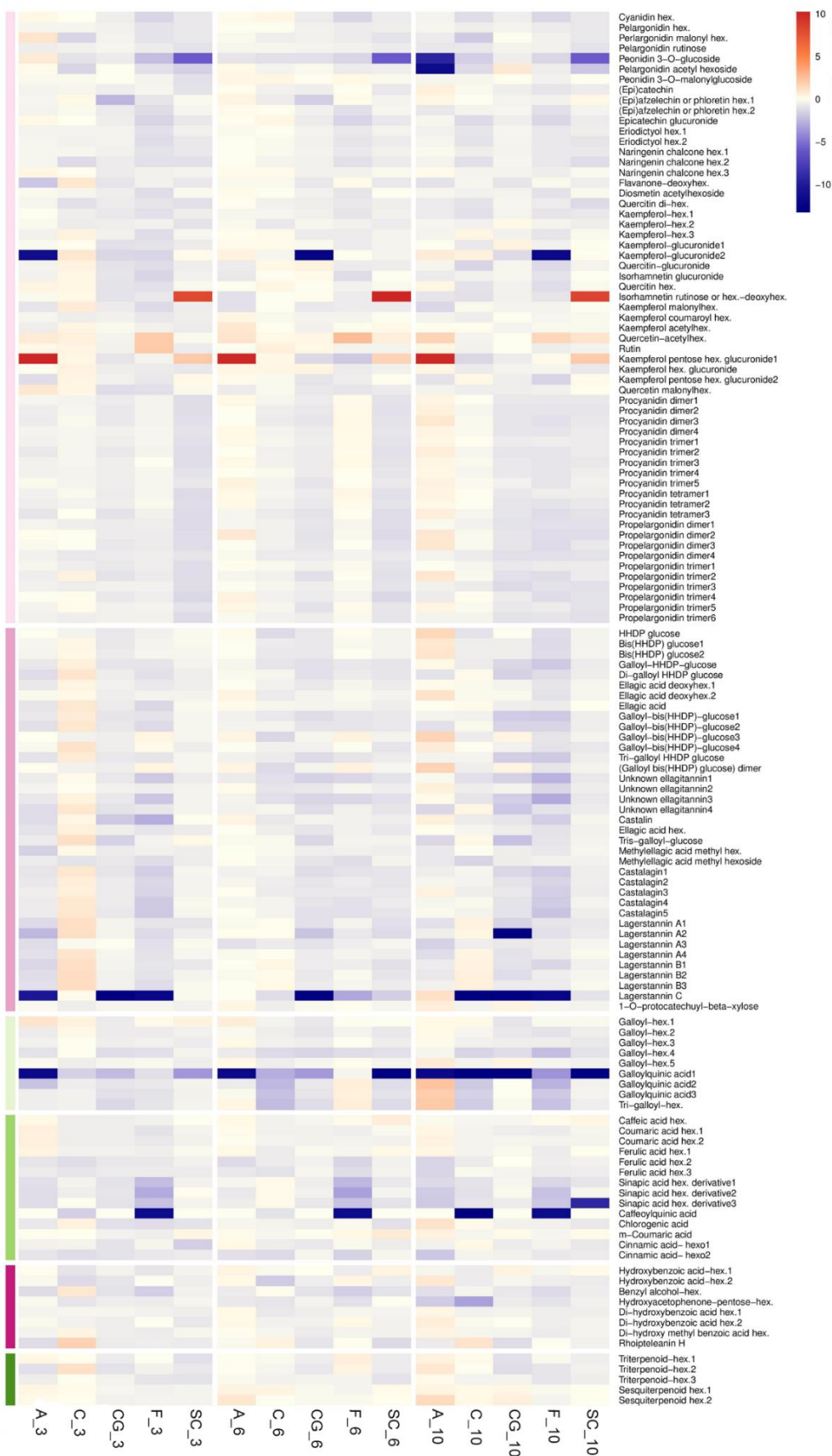
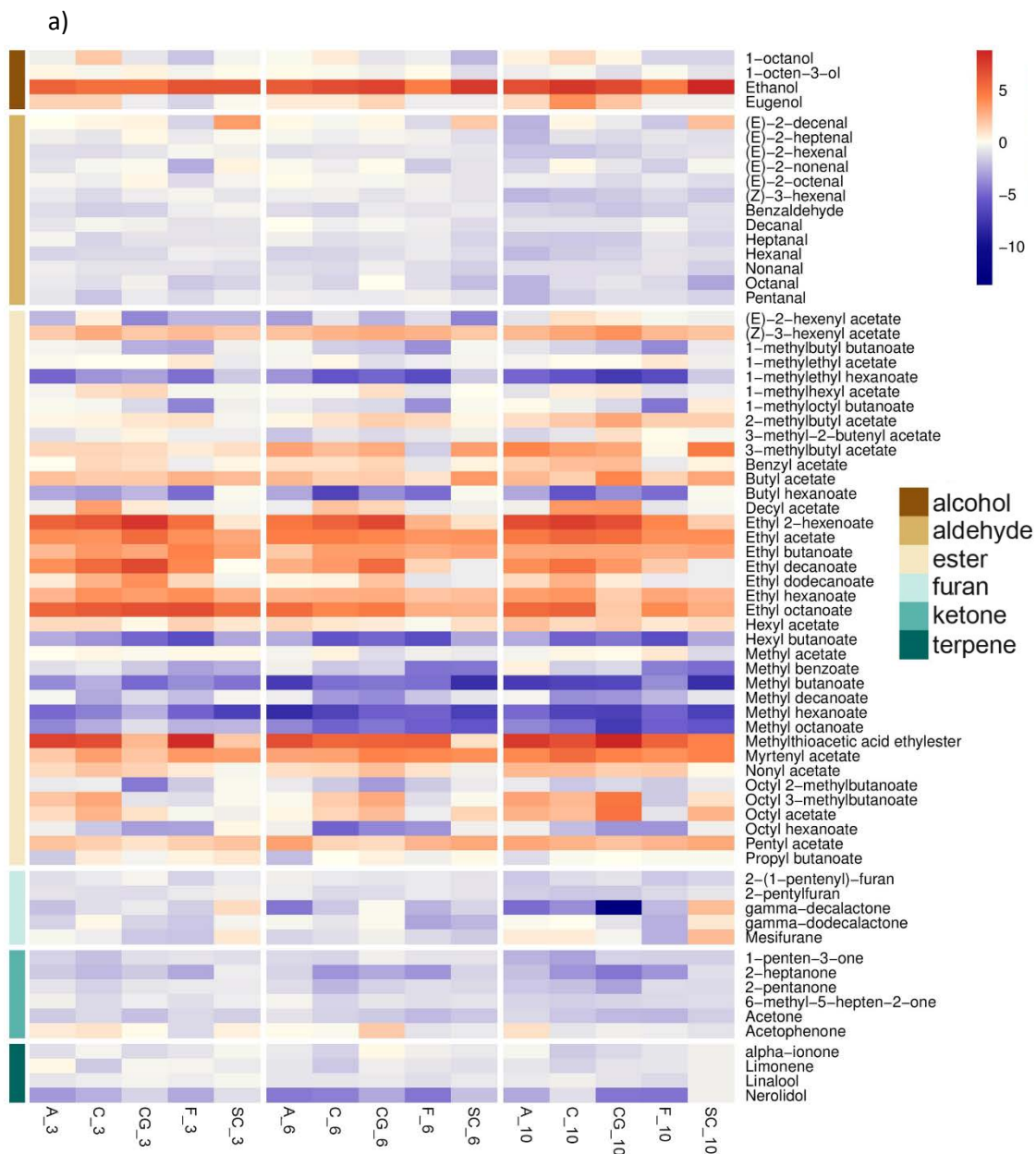
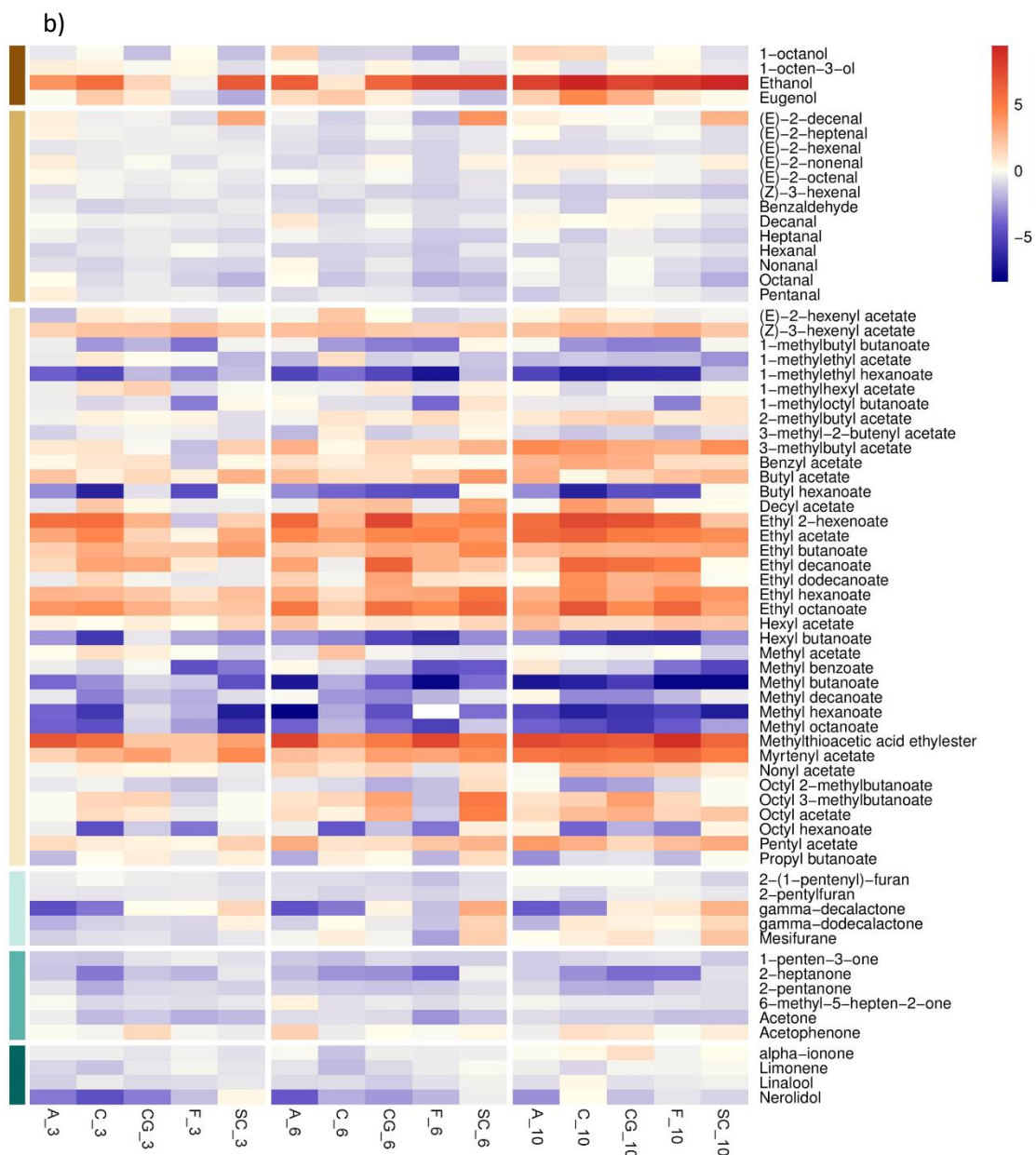


Figure 18: heatmaps representing the log₂ fold change in secondary metabolites when compared to T0 fruits for samples kept in normal atmosphere (a), in CO₂-enriched atmosphere (b) and in O₃-enriched atmosphere (c). A: 'Amiga', C: 'Camarosa', CG: 'Candongga', F: 'Fortuna', SC: 'Santa Clara'.





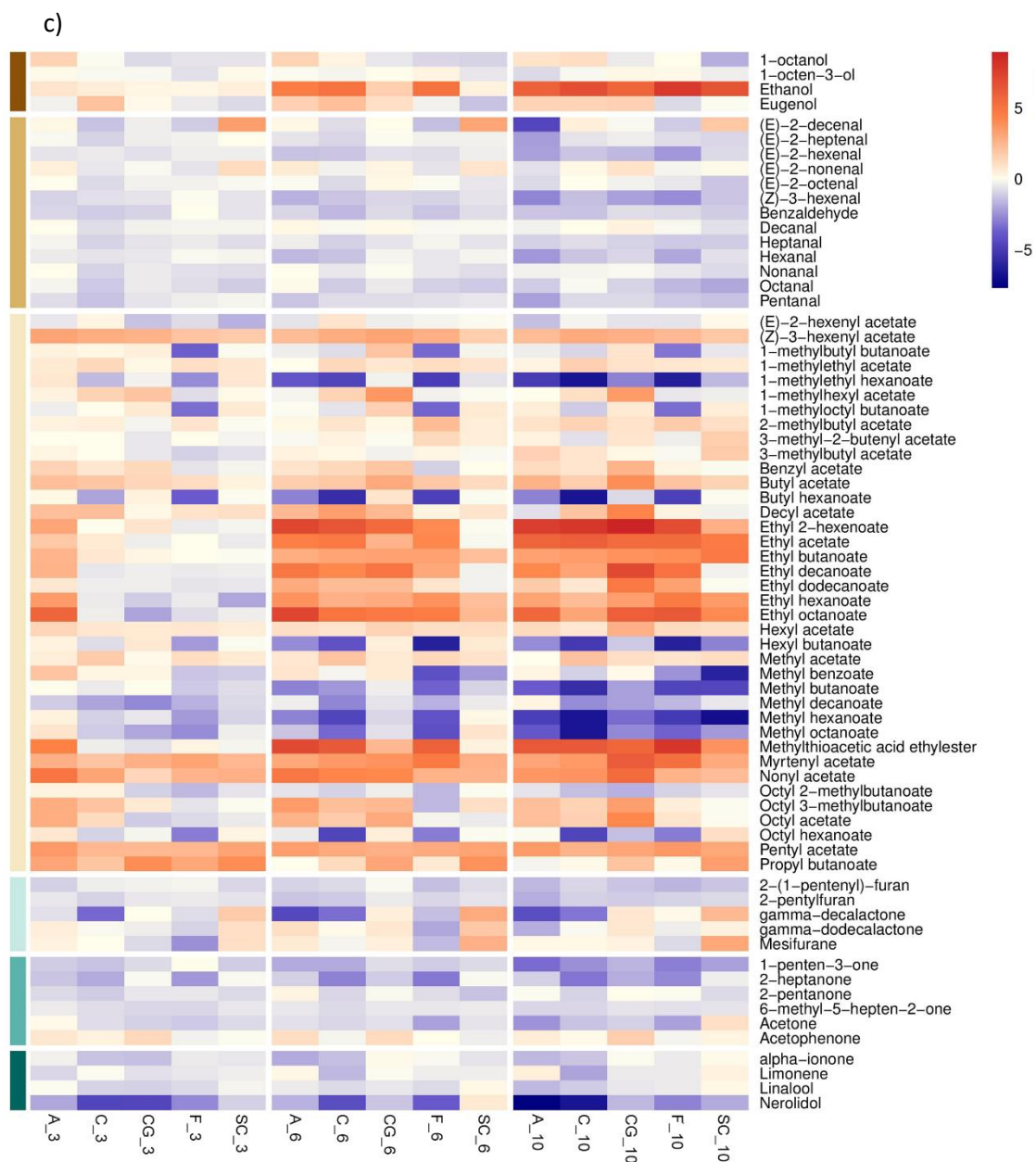


Figure 19: heatmaps representing the log₂ fold change in volatiles when compared to T0 fruits for samples kept in normal atmosphere (a), in CO₂-enriched atmosphere (b) and in O₃-enriched atmosphere (c). A: 'Amiga', C: 'Camarosa', CG: 'Candongga', F: 'Fortuna', SC: 'Santa Clara'.

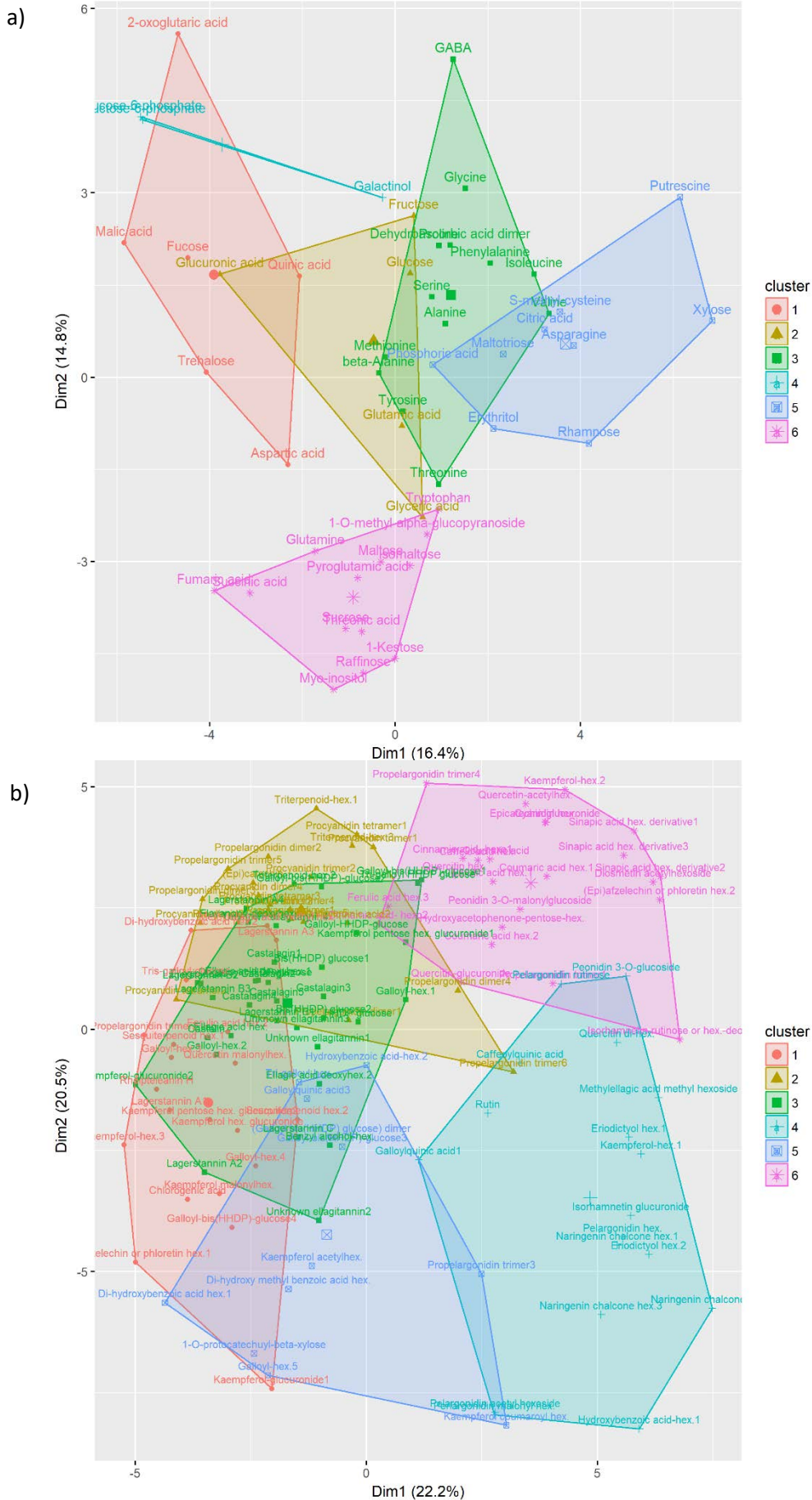
4) K-means clustering

K-means clustering is an unsupervised algorithm that classifies a given data set through a certain number of clusters (K clusters) fixed *a priori*. One K center per cluster is defined, far away as much as possible from each other. Each observation, belonging to a data set, is associated to the nearest K center, allowing to form clusters of the different observations (Kanungo *et al.*, 2002). The first step when using K-means clustering is to indicate the number of K clusters that will be generated in the final solution. Elbow, Silhouette and Gap statistic methods have been used to help finding the appropriate numbers of clusters in primary, secondary metabolites and volatiles. In addition, and to further clarify the appropriate numbers of clusters, visualizations of the obtained clusters were plotted (Figure 20). The number of clusters was set as six for primary, secondary metabolites and volatiles. Primary, secondary metabolites and volatiles with their cluster attribution are listed in Annexes 11, 12 and 13, respectively. Representation of metabolite profiles within each cluster is shown in Figure 21 (primary metabolites), Figure 22 (secondary metabolites) and Figure 23 (volatiles).

Regarding the evolution of primary metabolites trend along postharvest, clusters 2 and 5 had the most striking features. Indeed, in cluster 2 a peak in metabolite content was observed in all the cultivars after 10 days in CO₂-enriched atmosphere, indicating that the levels of these compounds were increasing along postharvest in this condition. On the other hand, 'Amiga', 'Camarosa' and 'Candongga' showed another peak after 3 days in normal atmosphere, followed by a decrease in the 6 and 10-day samples. Cluster 2 grouped 13 metabolites, 12 amino acids, including GABA, glycine and β -alanine, and dehydroascorbic acid dimer. Cluster 5 was composed of metabolites (fructose-6-phosphate, glucose-6-phosphate and galactinol) which presented a clear increase in the O₃-enriched atmosphere samples. Interestingly, in 'Camarosa' cultivar, cluster 3 grouped metabolites with opposite trends between normal atmosphere (decrease along postharvest) and both CO₂ and O₃ modified atmospheres (increase along postharvest). Important quality traits associated metabolites, such as organic acids and sugars, were found in this cluster (Figure 21).

As mentioned above, it is more complicated to see common trends concerning secondary metabolites evolution in the different postharvest samples and the five studied cultivars. For example, cluster 4 (mainly ellagitannins and kaempferol derivatives) grouped metabolites which were decreased along postharvest in the three tested treatments in 'Camarosa'. In the other cultivars, the behavior of the metabolites within cluster 4 was not so obvious, and in 'Amiga' an increase along postharvest was observed in the samples kept in CO₂- and O₃-enriched atmospheres. Cluster 6, which principally comprised flavonoids, including pelargonidin-hexose and other anthocyanins, also showed a fluctuating behavior along postharvest. However, the behavior was not consistent between treatments and cultivars (Figure 22).

Clusters 2 and 3 grouped volatiles based on their increase along postharvest in the different treatments and their decrease respectively. Cluster 2 was basically composed by ethanol and esters, while cluster 3 included aldehydes and furans. In 'Camarosa' and 'Candongá' cultivars, cluster 5 (mainly comprised of esters) grouped metabolites which showed a clear decrease in the samples kept in normal atmosphere (Figure 23).



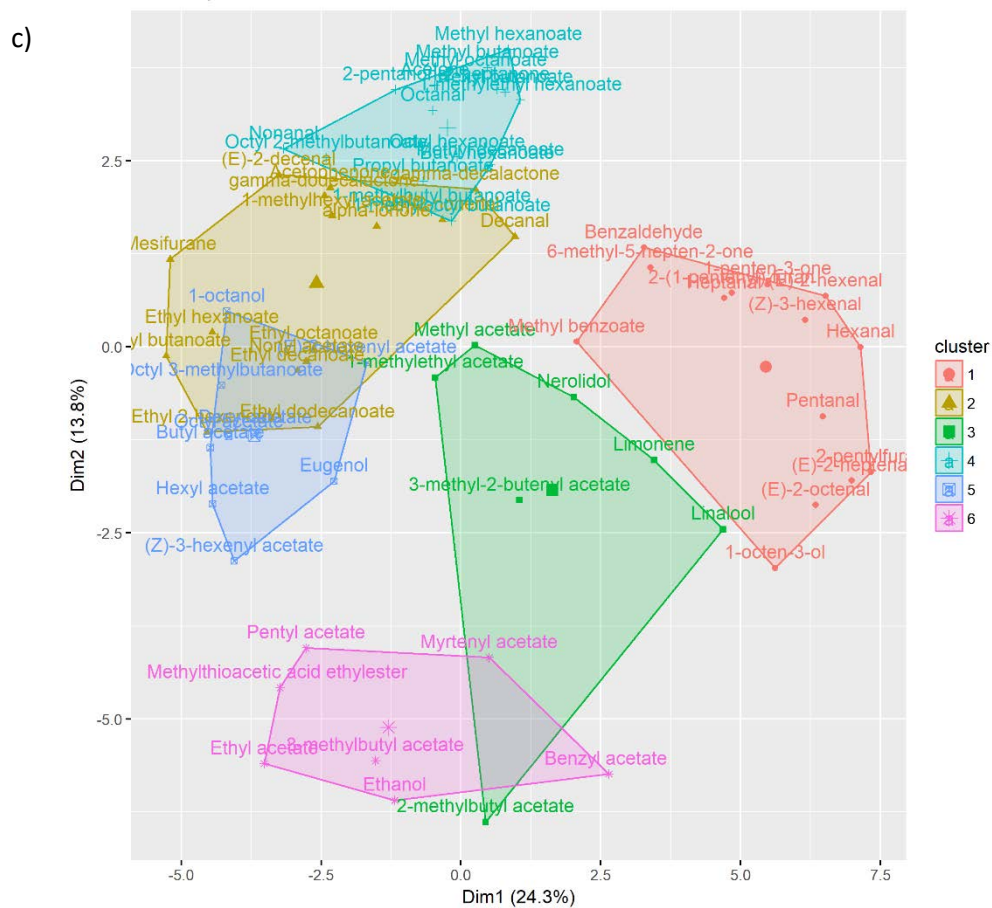
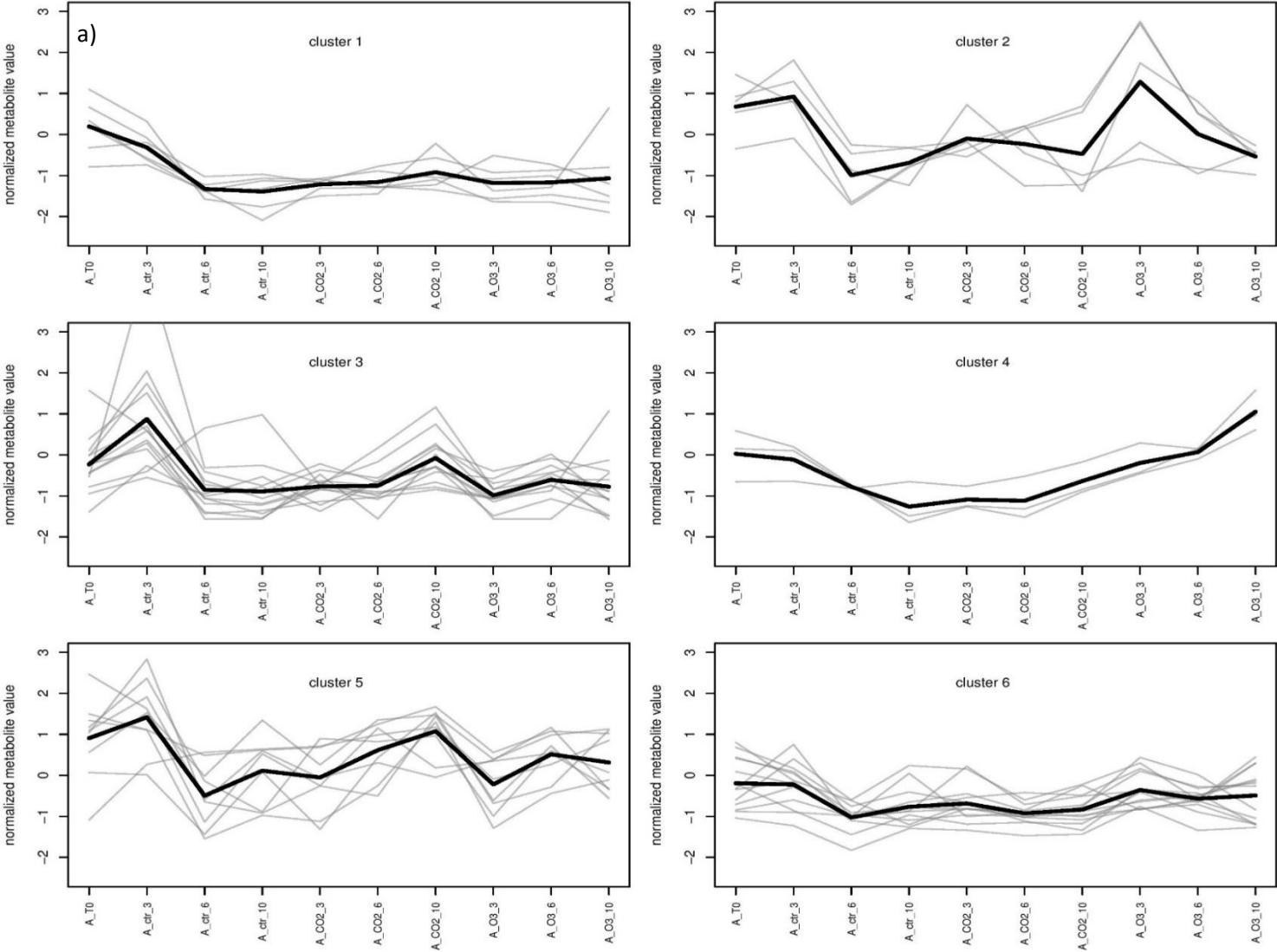
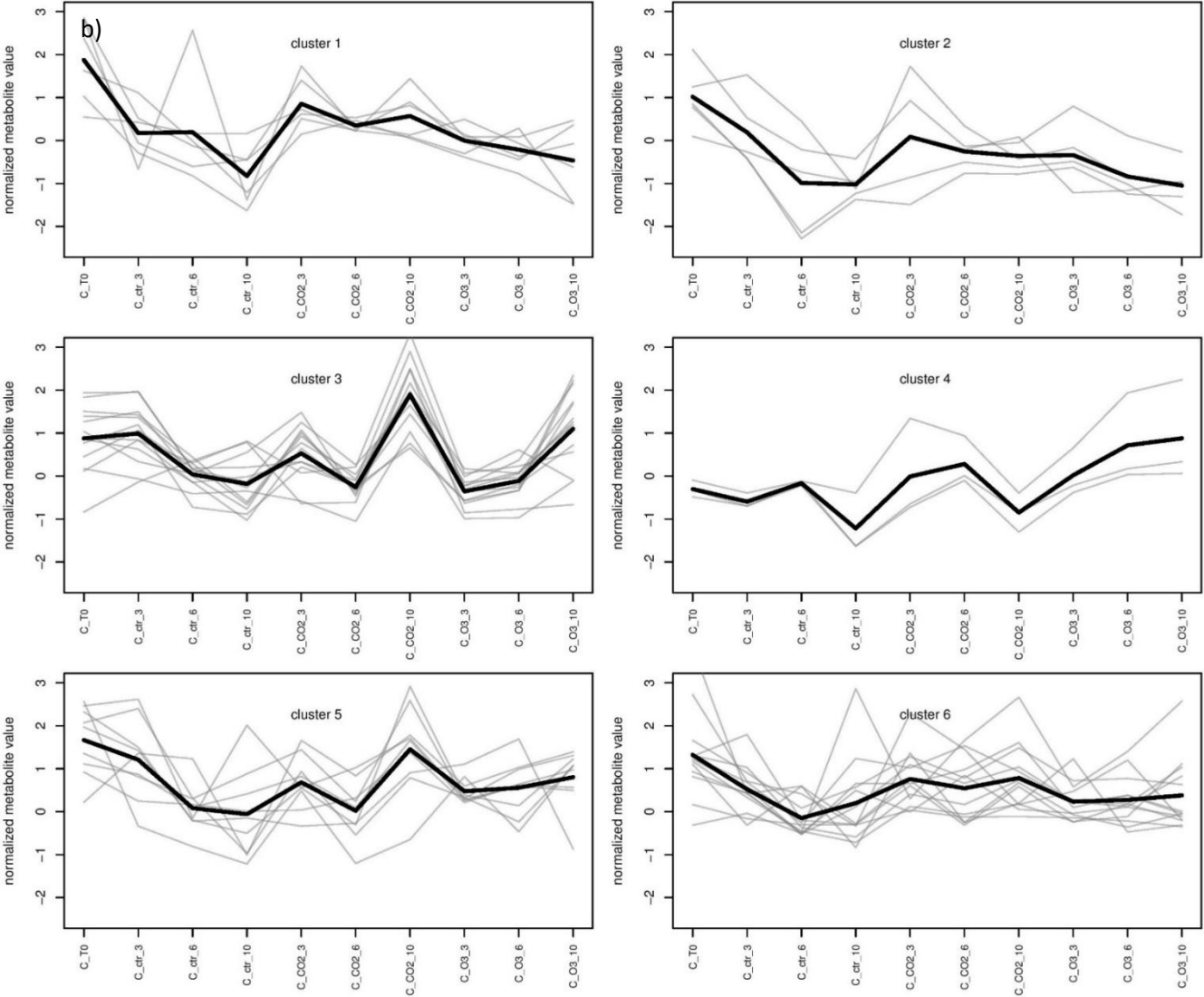
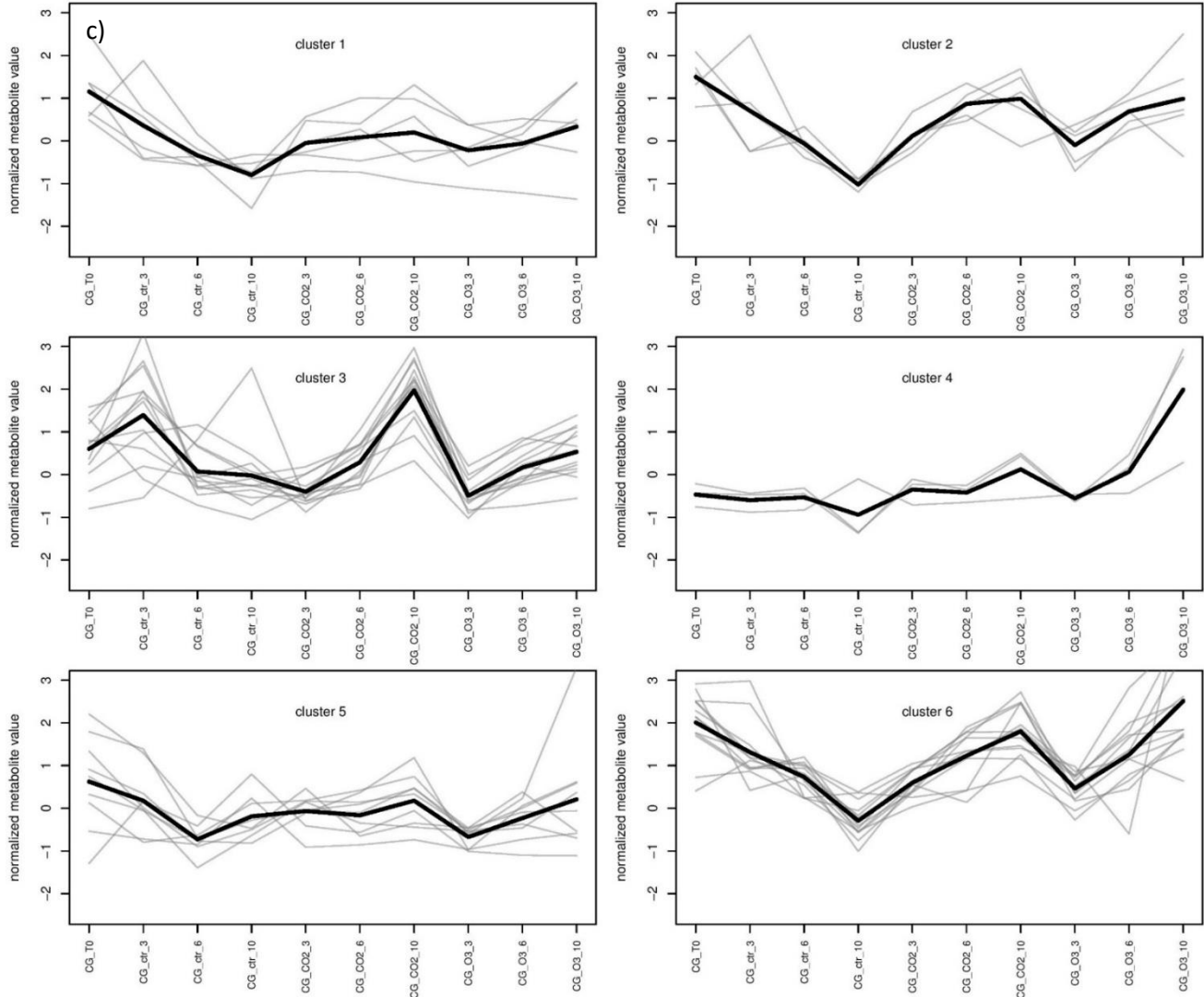
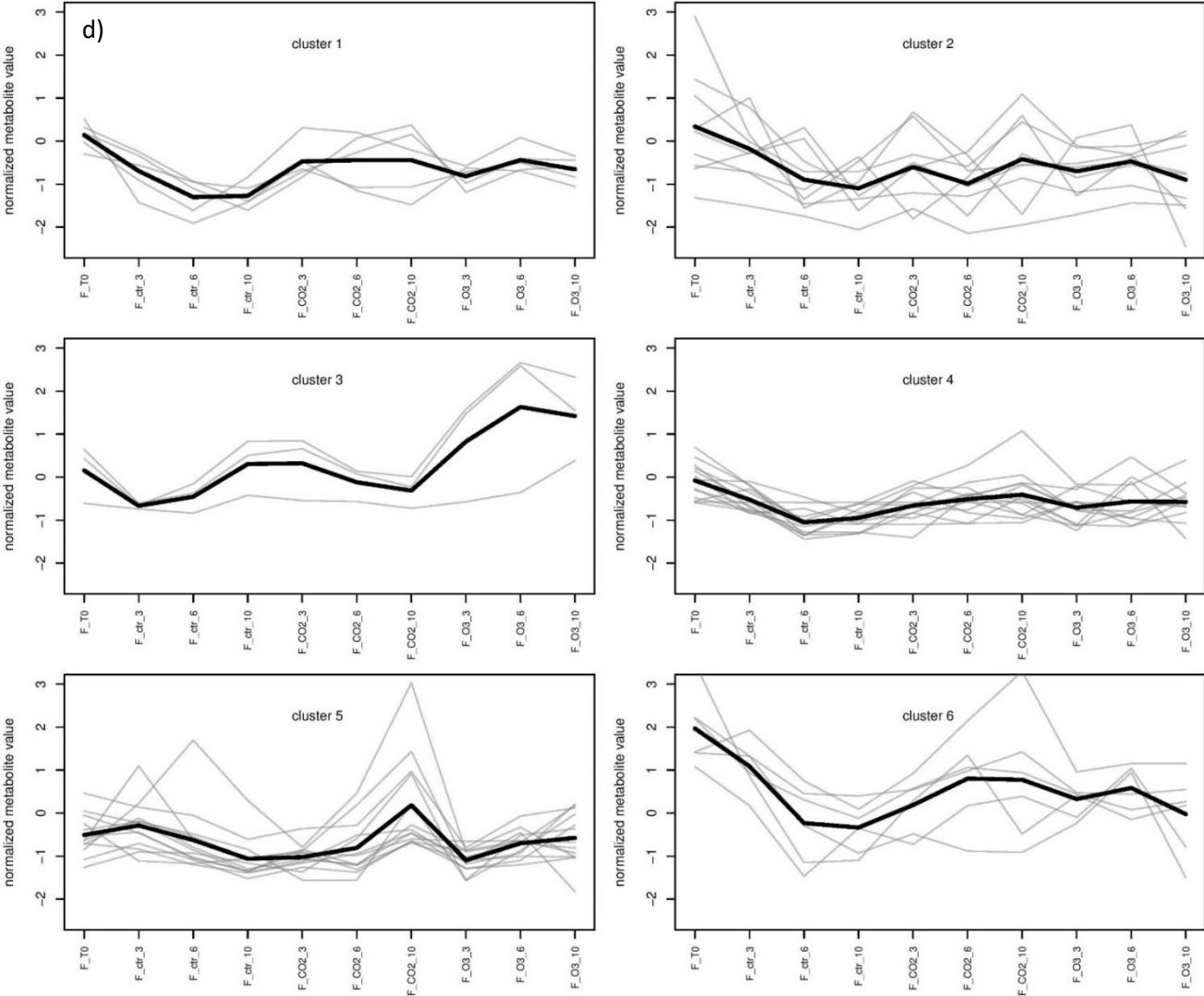


Figure 20: PCA of the six K clusters for primary (a), secondary metabolites (b) and volatiles (c).









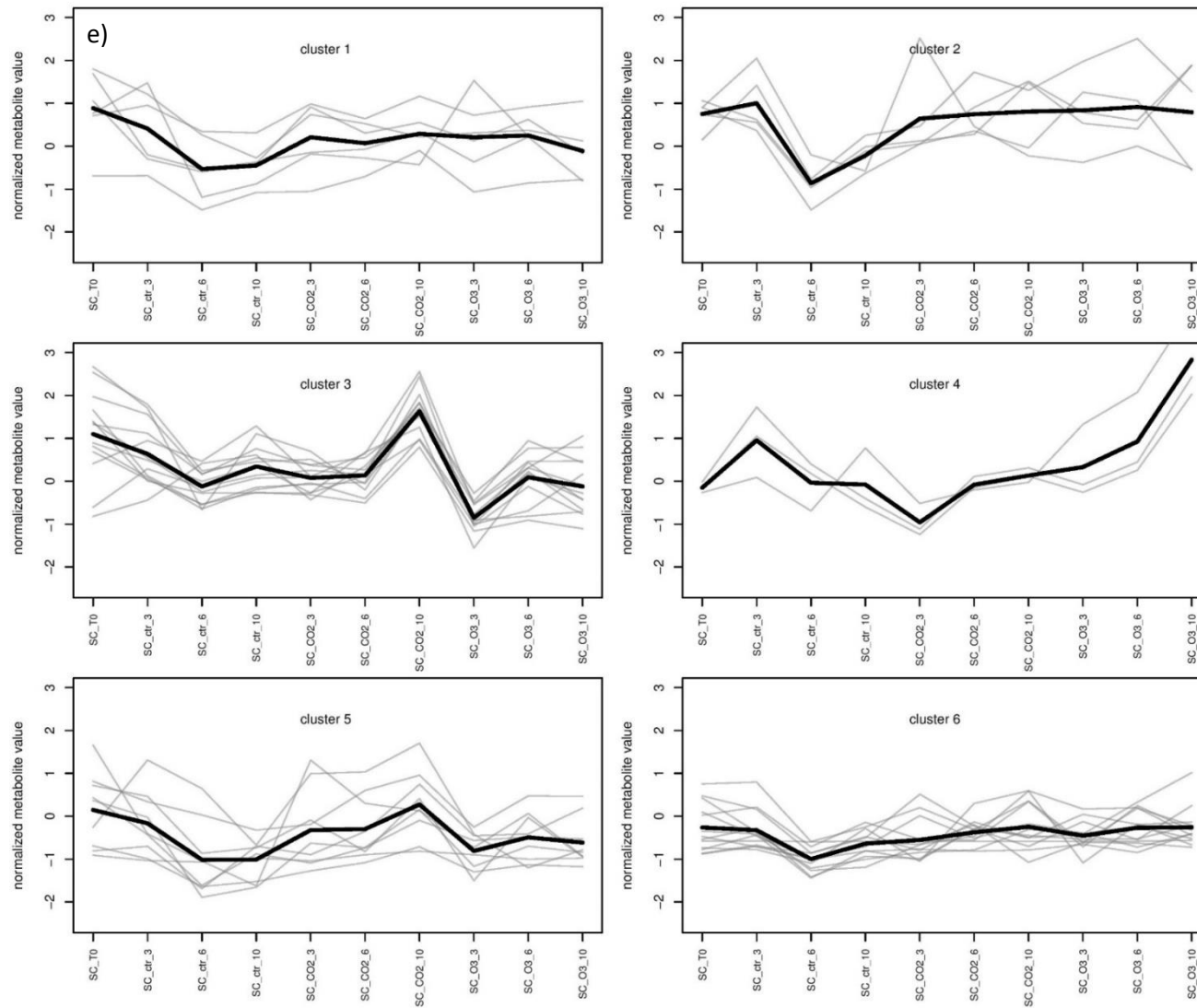
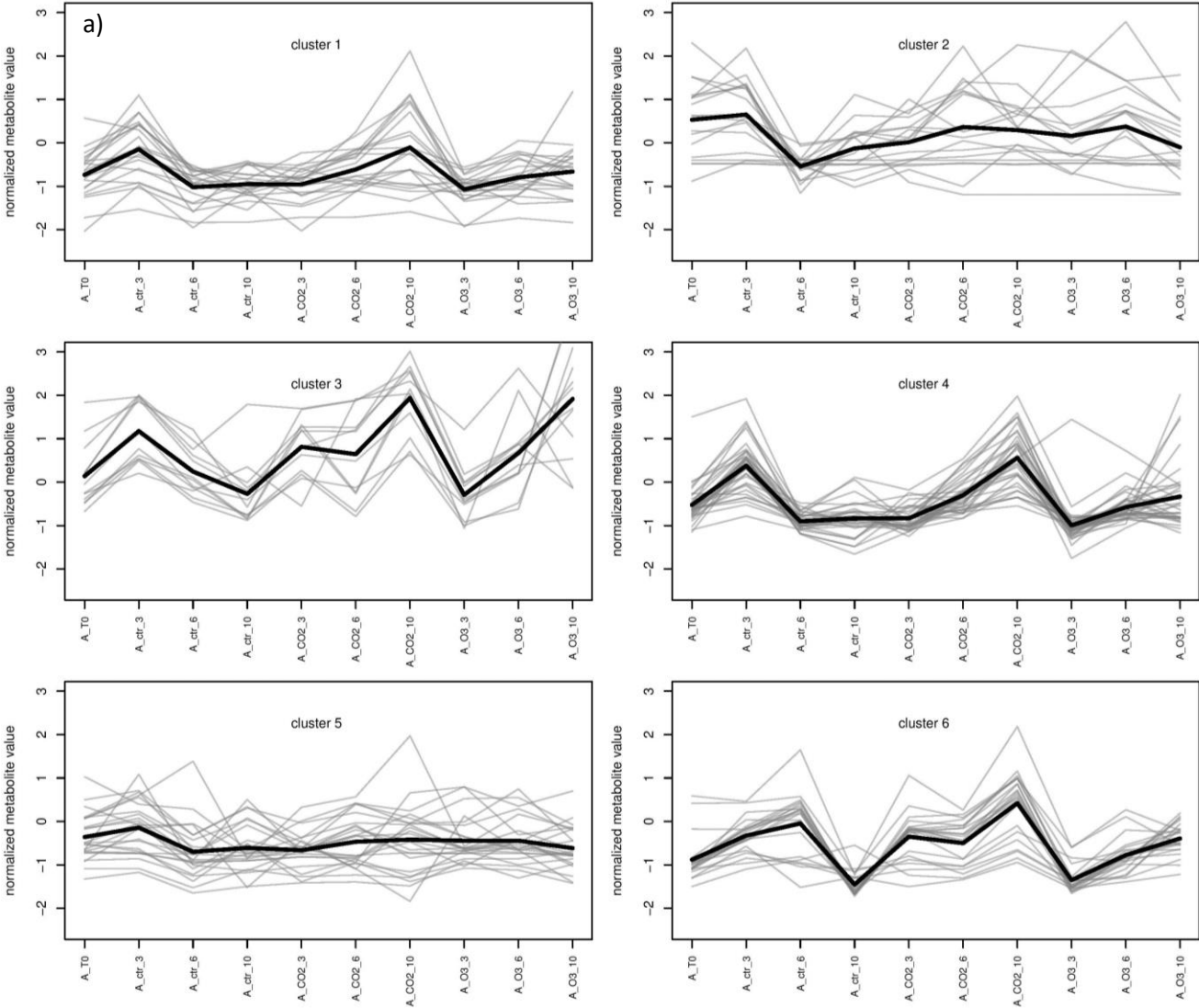
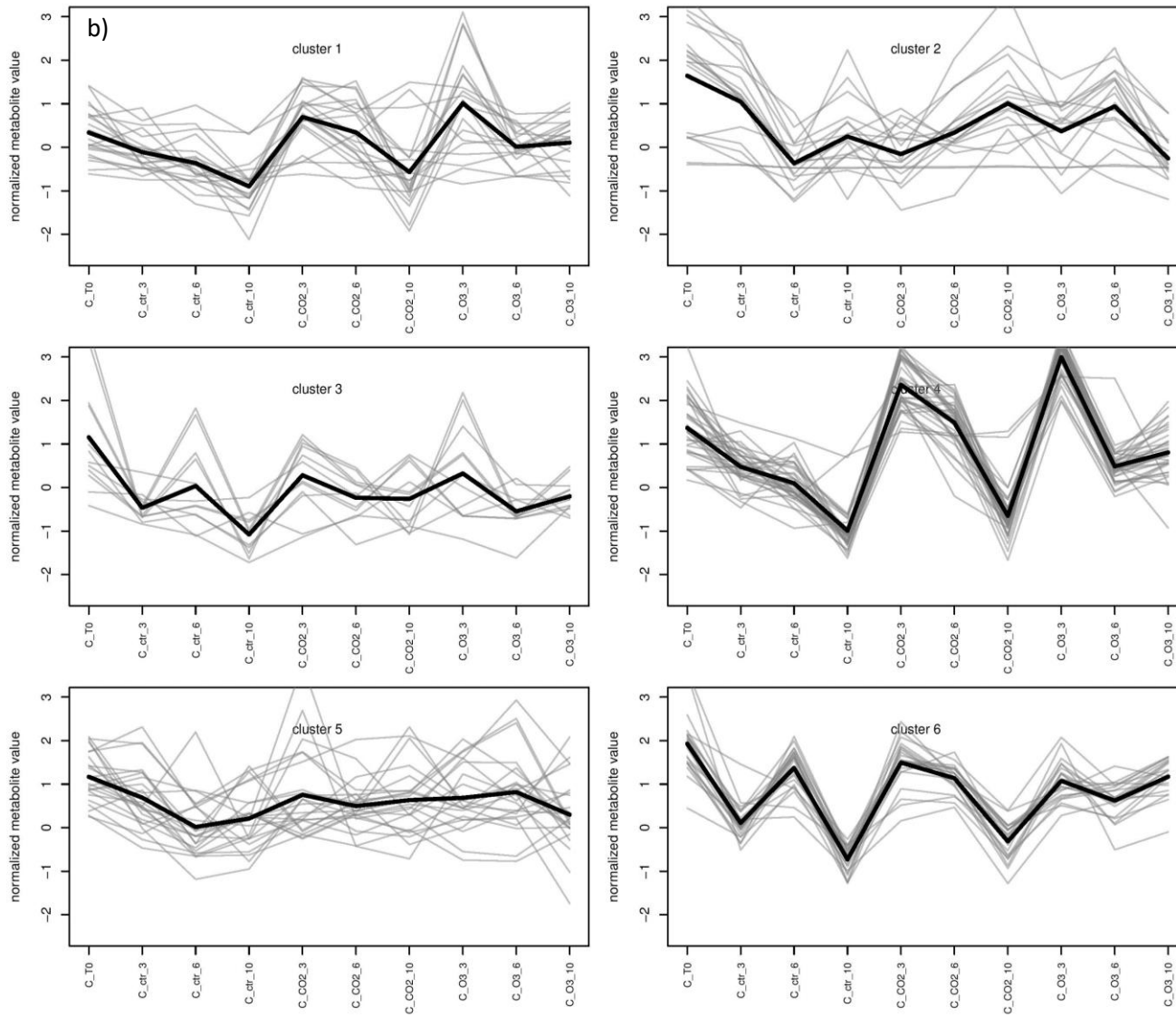
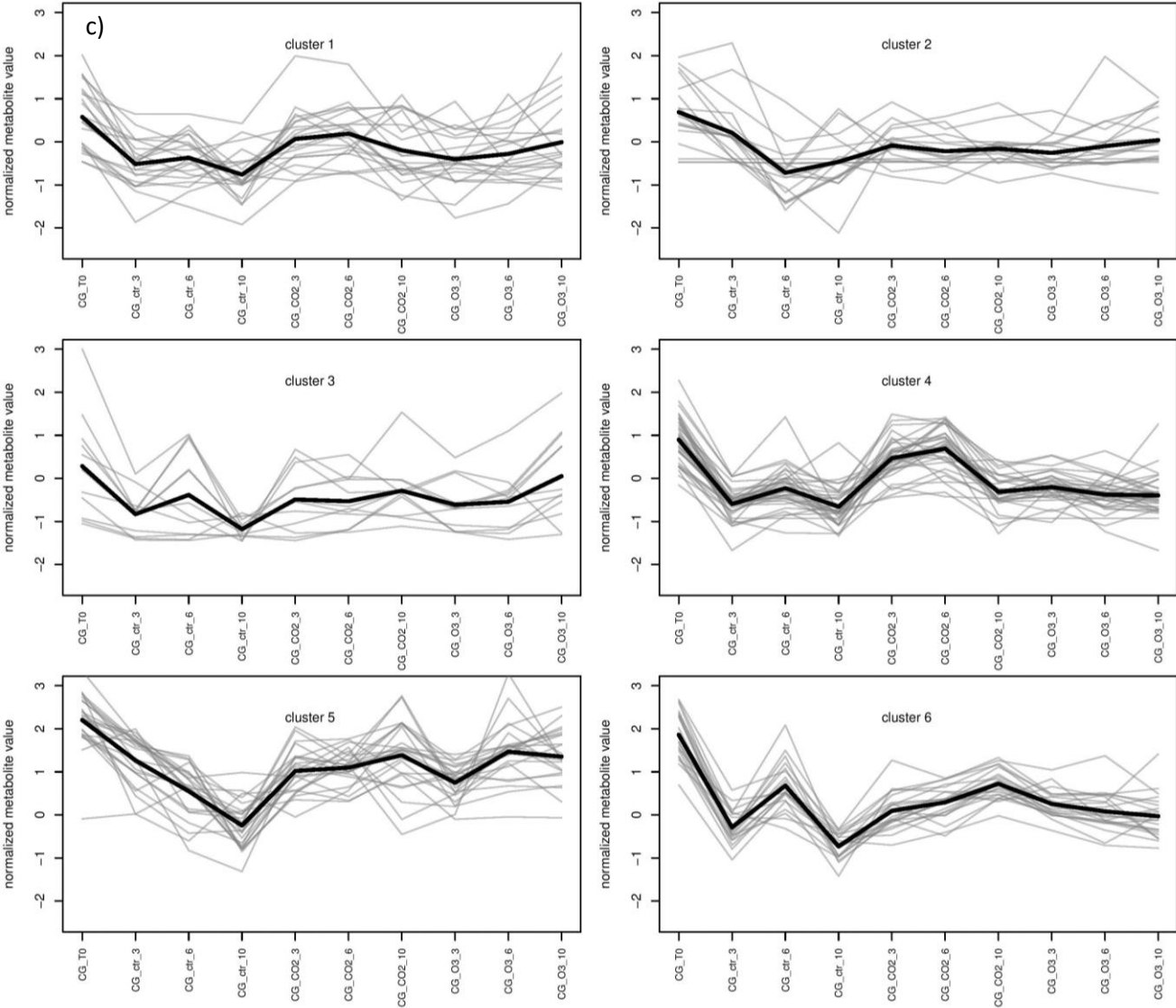
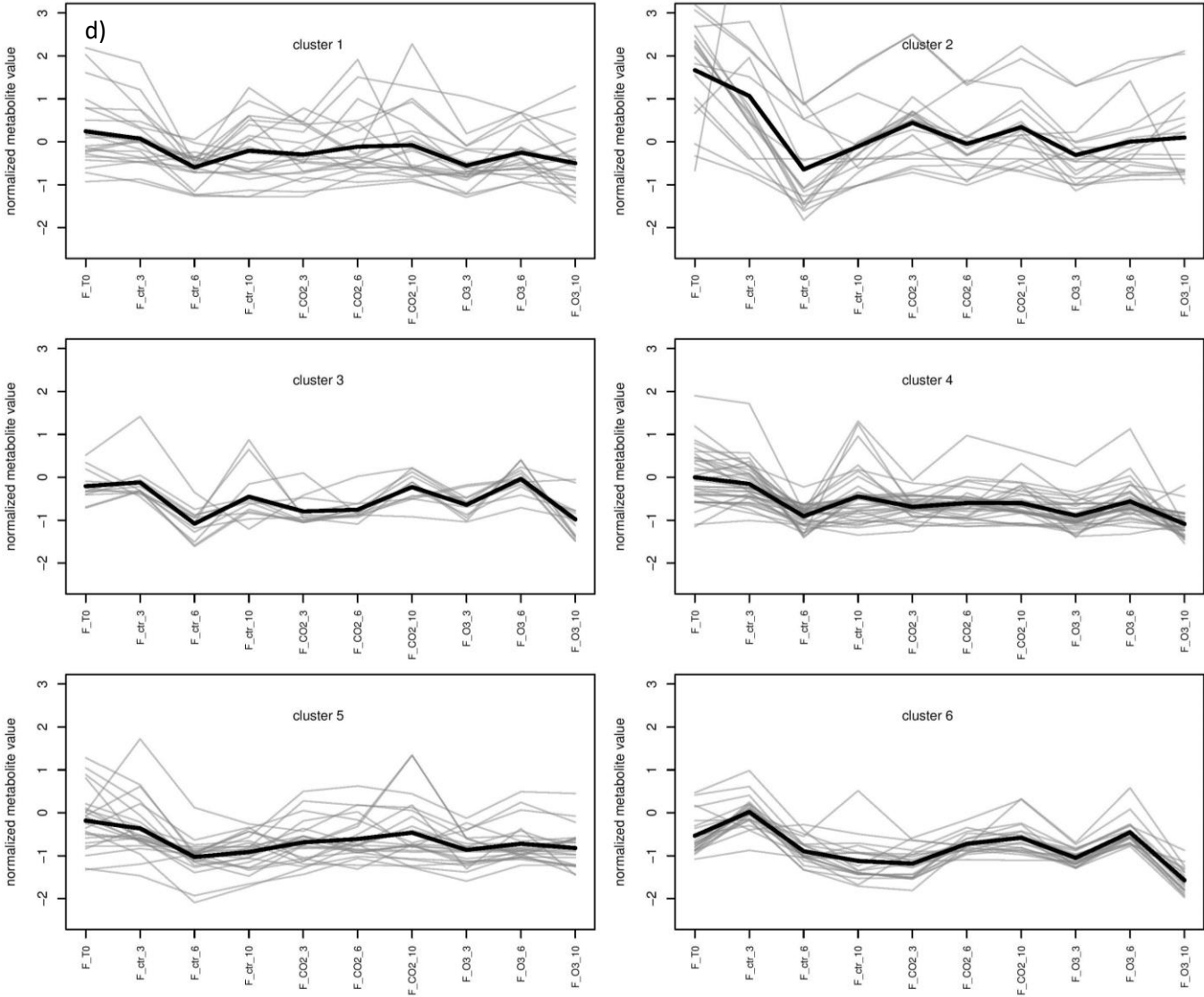


Figure 21: Representation of primary metabolite profiles in the six *K* clusters, ordered by treatments (T0, normal, CO₂-enriched and O₃-enriched atmospheres) and by time (3, 6 and 10 days of treatment). Grey lines indicate the profile of each individual metabolite, while the black line shows the value the *K* center in each sample. a) 'Amiga' cultivar, b) 'Camarosa' cultivar, c) 'Candongá' cultivar, d) 'Fortuna' cultivar and e) 'Santa Clara' cultivar.









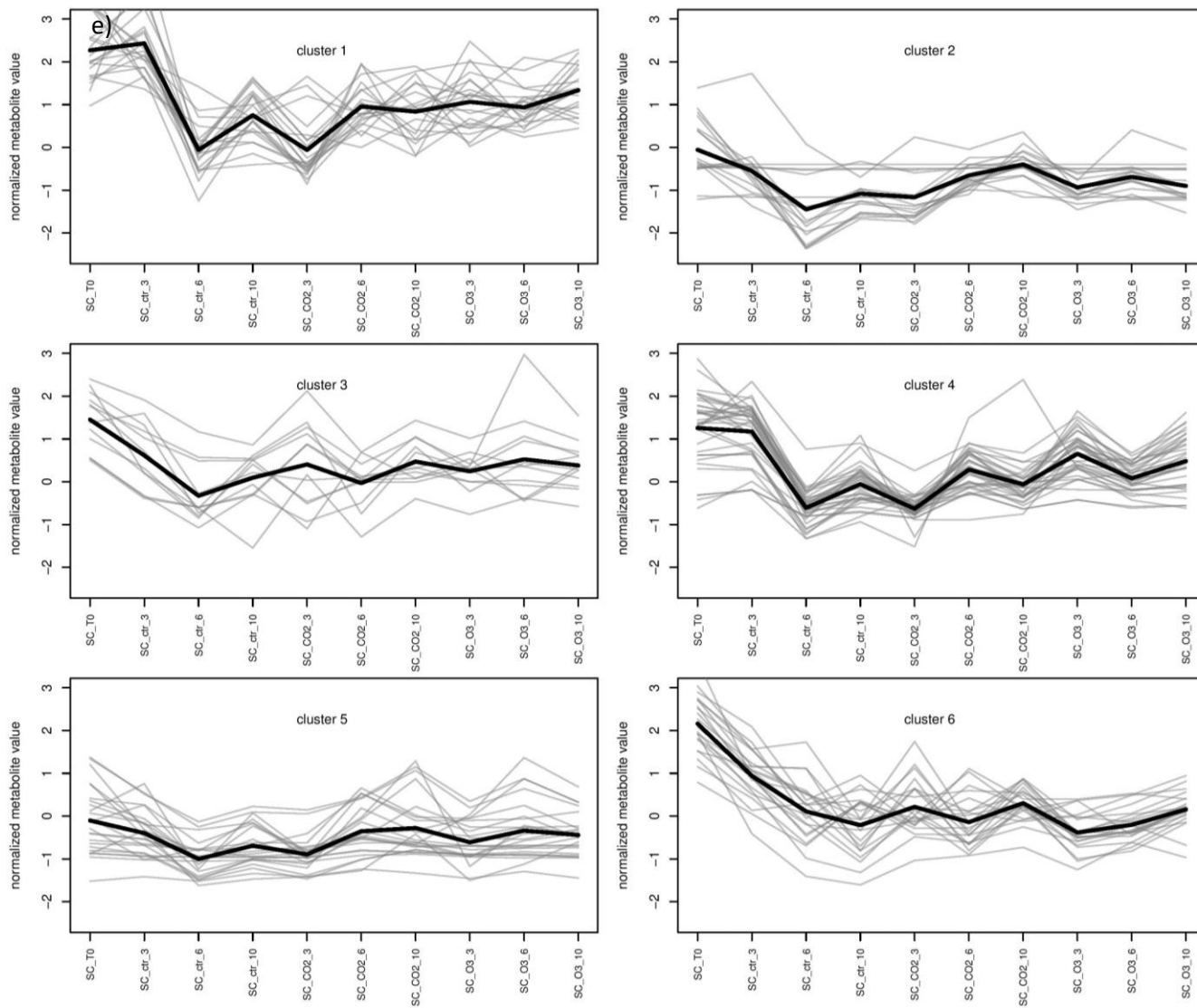
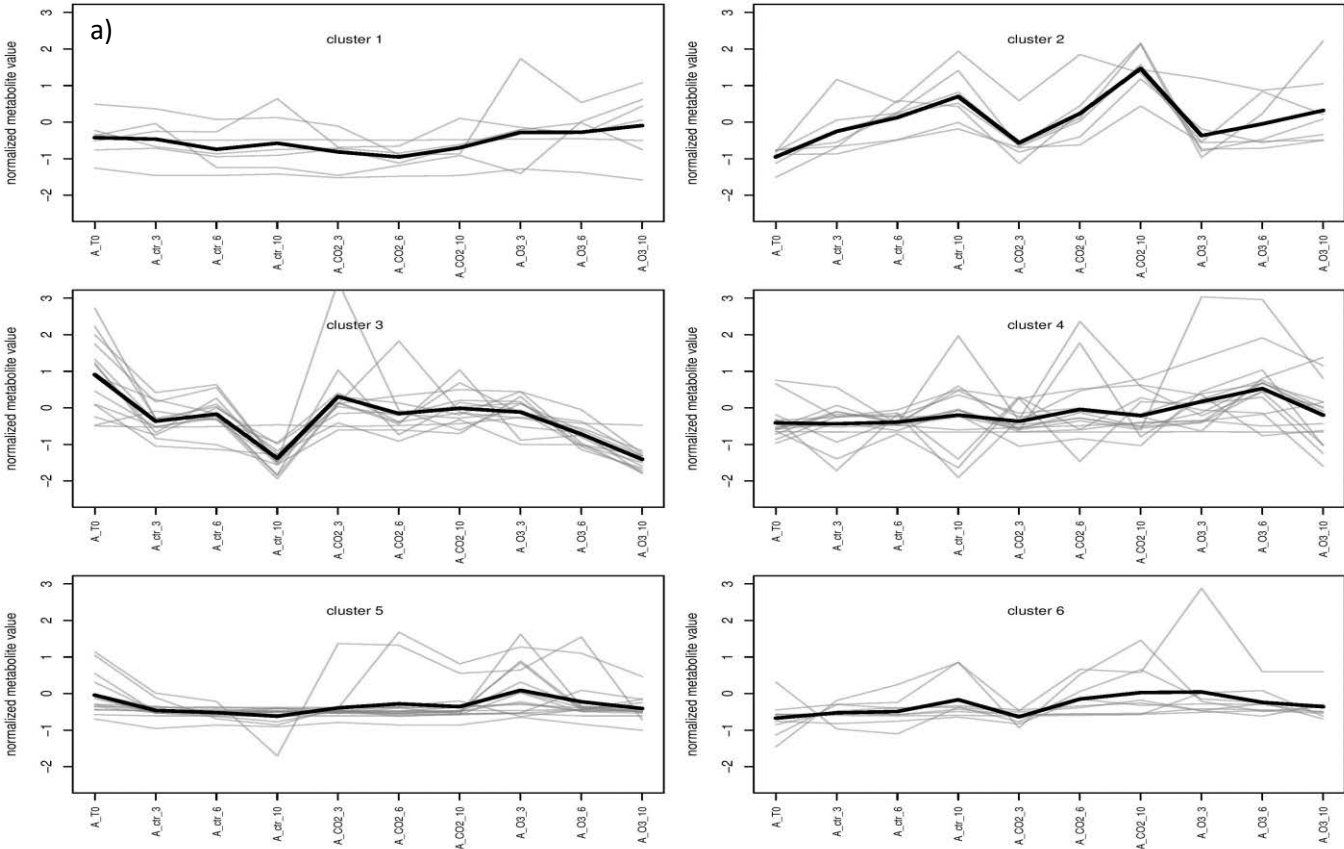
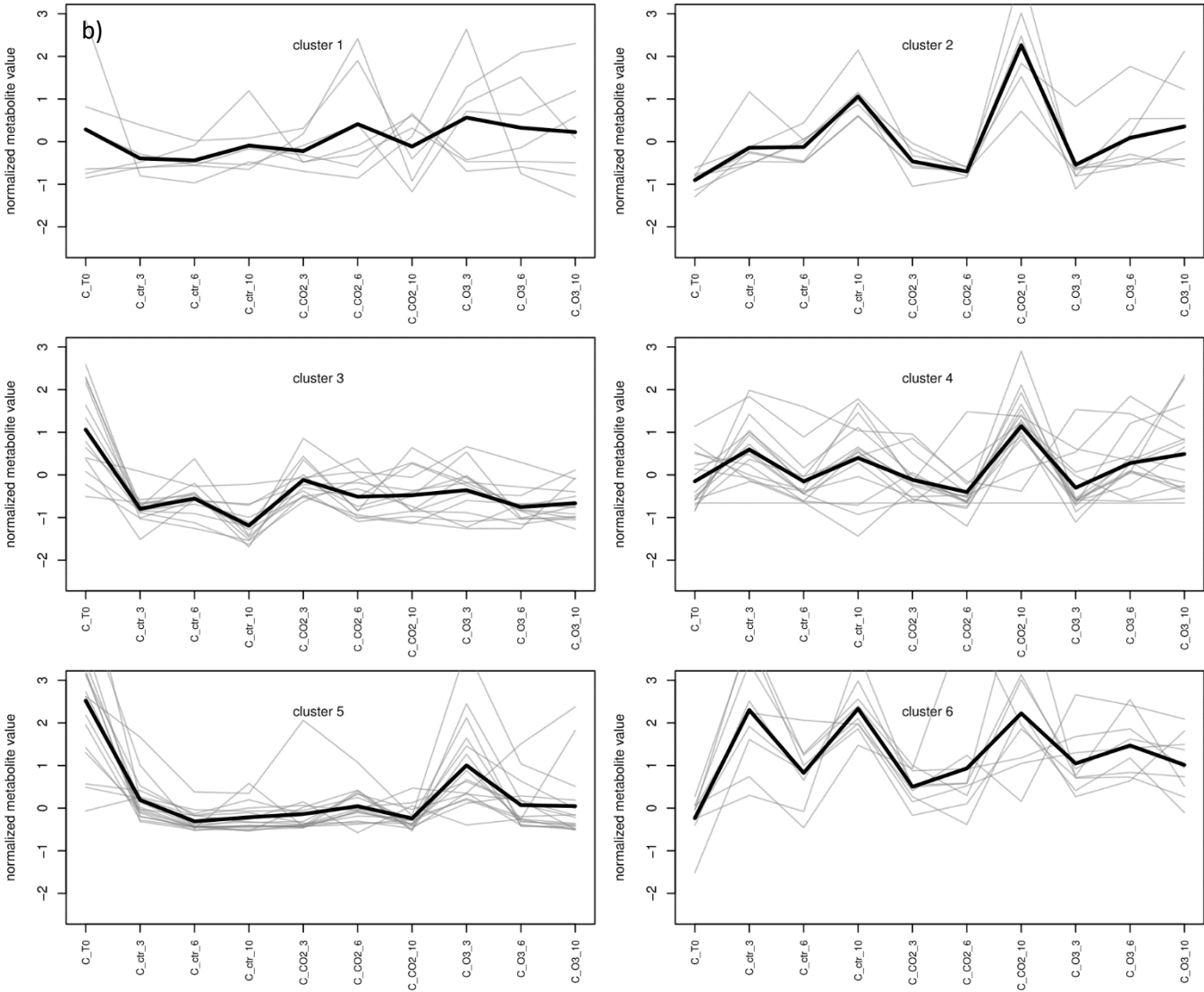
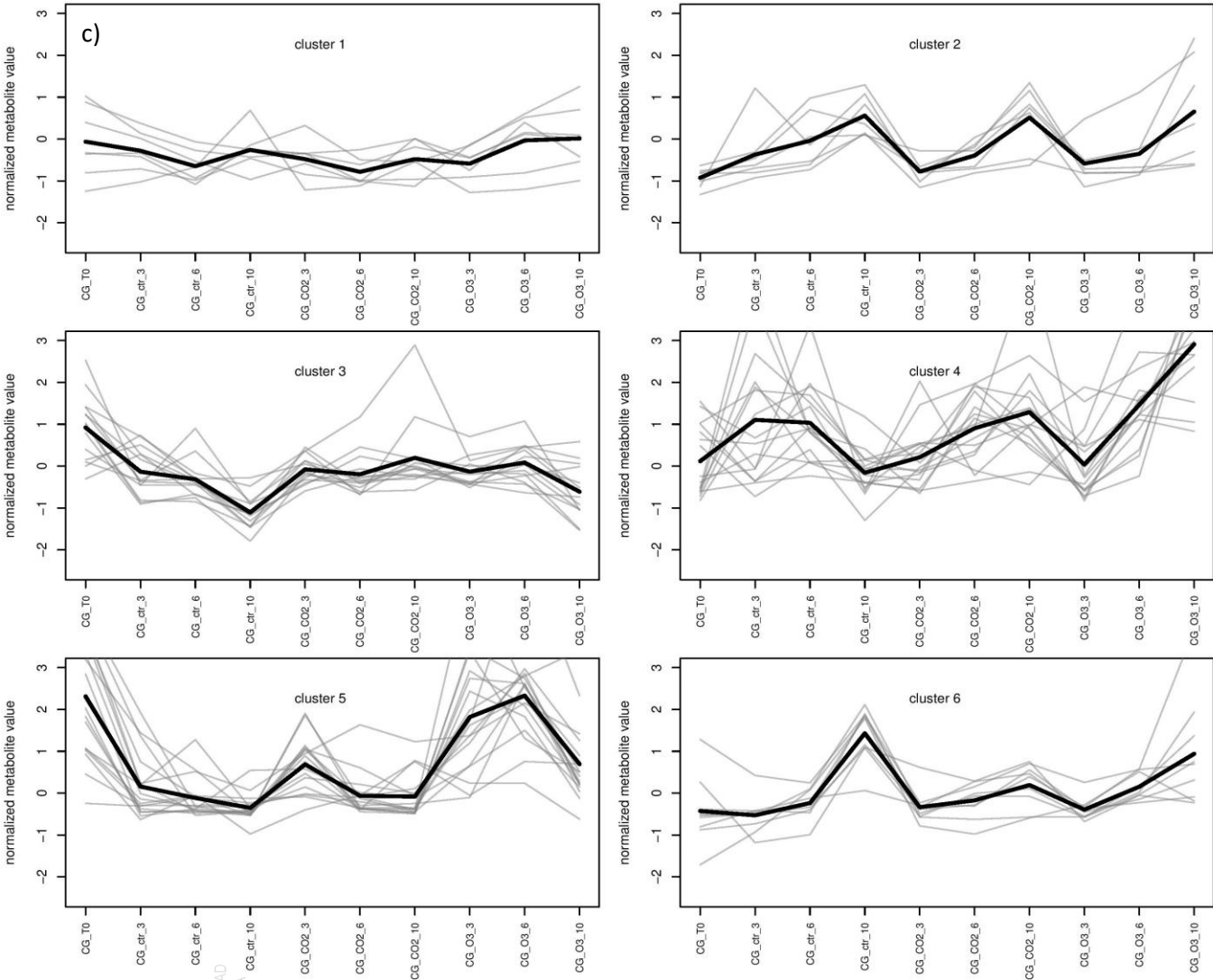
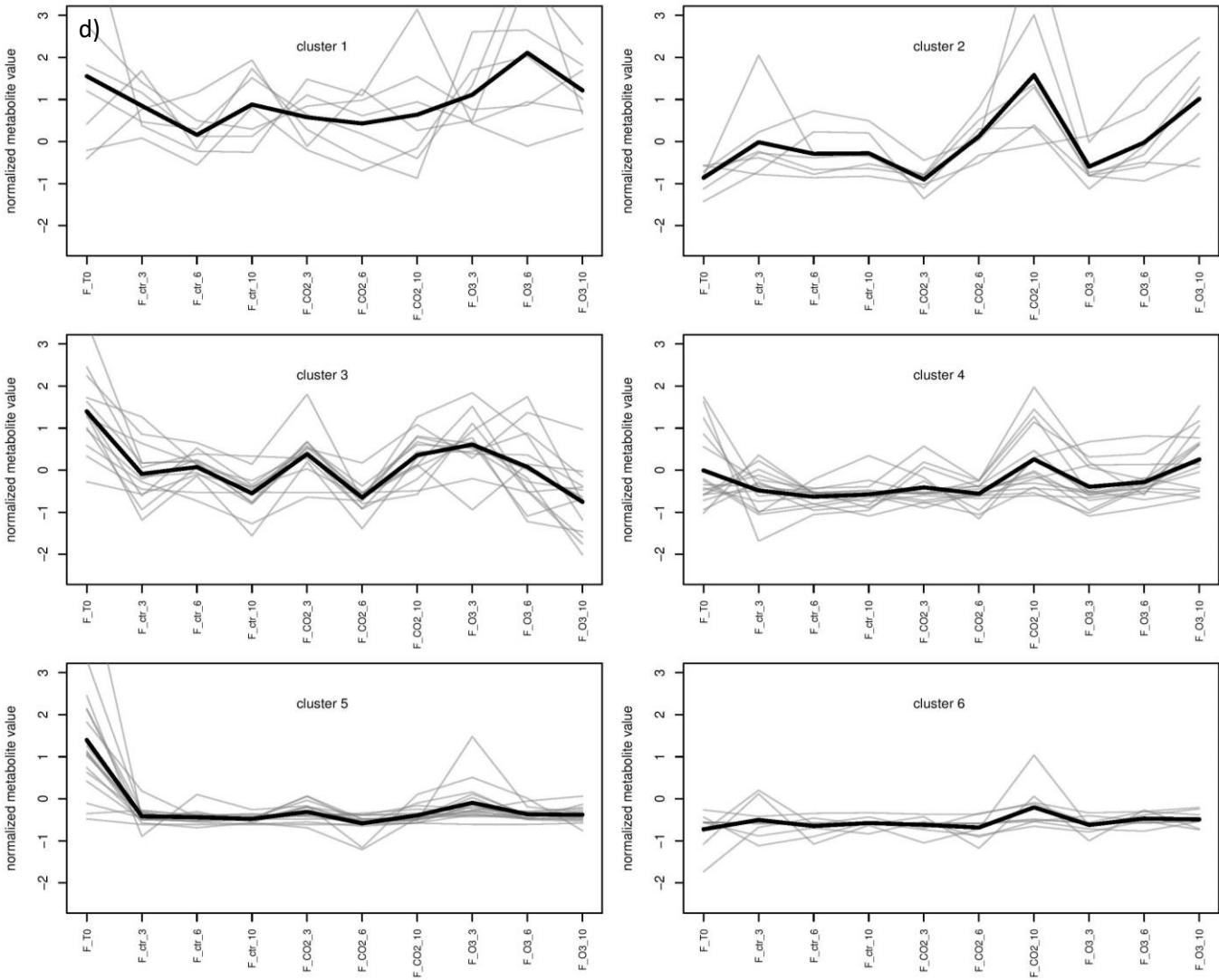


Figure 22: Representation of secondary metabolite profiles in the six K clusters, ordered by treatments (T0, normal, CO₂-enriched and O₃-enriched atmospheres) and by time (3, 6 and 10 days). Grey lines indicate the profile of each individual metabolite, while the black line shows the value the K center in each sample. a) 'Amiga' cultivar, b) 'Camarosa' cultivar, c) 'Candonga' cultivar, d) 'Fortuna' cultivar and e) 'Santa Clara' cultivar.









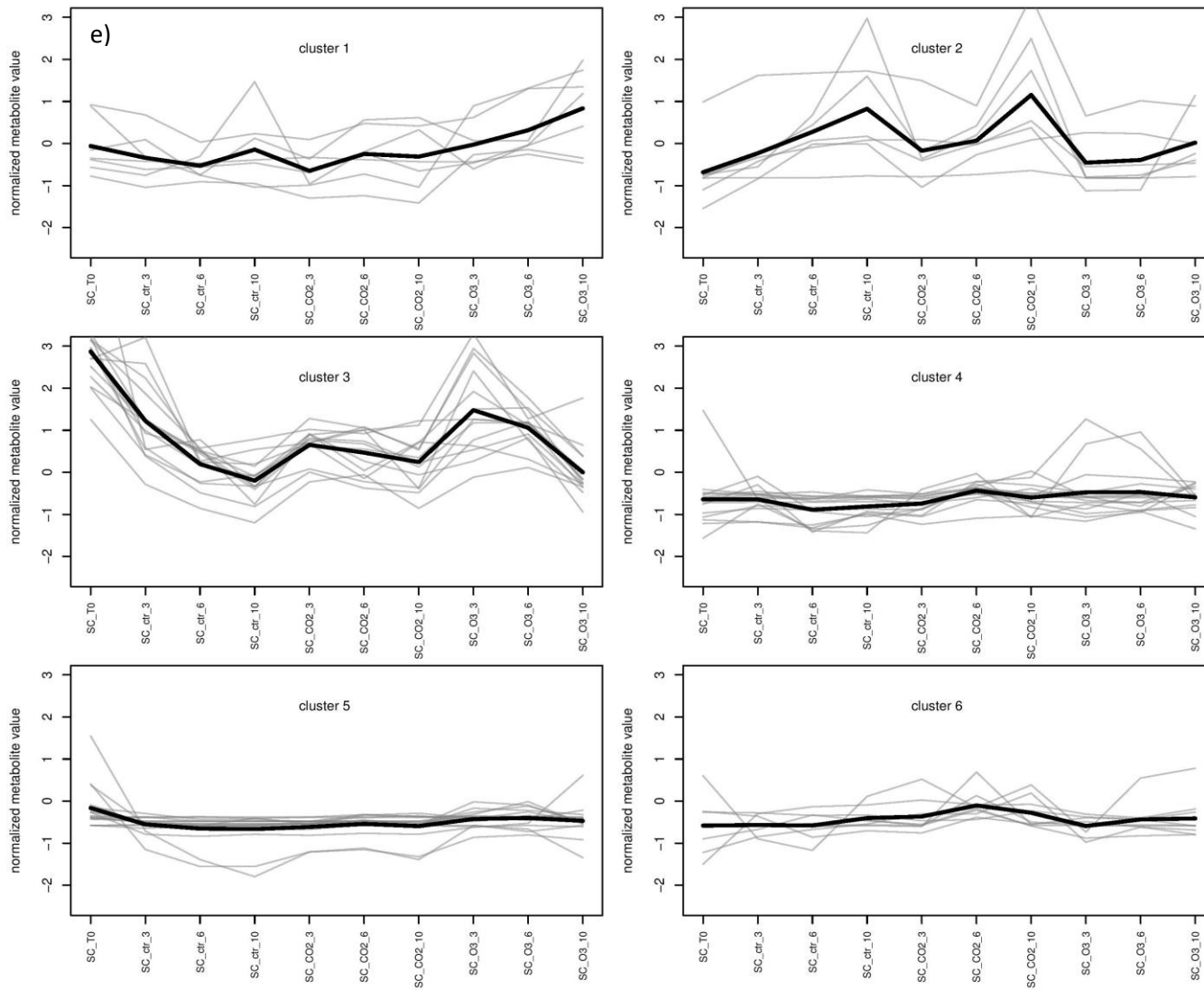


Figure 23: Representation of volatiles profiles in the six *K* clusters, ordered by treatments (T0, normal, CO₂-enriched and O₃-enriched atmospheres) and by time (3, 6 and 10 days). Grey lines indicate the profile of each individual metabolite, while the black line shows the value the *K* center in each sample. a) 'Amiga' cultivar, b) 'Camarosa' cultivar, c) 'Candonga' cultivar, d) 'Fortuna' cultivar and e) 'Santa Clara' cultivar.

Discussion

Strawberry are particularly sensitive to postharvest, resulting in the deterioration of fruits quality attributes, and as a consequence, in important economic losses. In climacteric fruits, several approaches are used in the industry to control fruit ripening and postpone postharvest damages. However, in non-climacteric fruits, such as strawberries, little is known about the regulatory mechanisms controlling senescence and thus, methods to prevent shelf life damages are limited. In this study, a combination of metabolomics techniques allowed us to shed light on metabolic changes occurring in different postharvest treatments used in food industry. Low temperature, alone or in combination with controlled atmosphere conditions, is the most common method in order to decrease respiration and reduce postharvest losses. It is important to take into account that these strategies represent abiotic stresses for the fruits and that different metabolic pathways are activated to deal with them (Pedreschi and Lurie, 2015). In addition, we evaluated effects of postharvest senescence in different genotypes, in order to compare the reproducibility of the responses between them.

As room temperature treatment was not including in this assay, we can only discuss the effect of modified atmospheres when compared to normal atmosphere and how they influence fruit quality attributes. Indeed, the three tested treatments shared the cold storage, which normally is accompanied by water loss from the fruit, particularly during the cool down period. As a consequence, the fruit is more sensitive to softening, browning and peel damage (Pedreschi and Lurie, 2015). For this reason, it is not surprising to see damage symptoms appearing along postharvest (Figure 2). Softening of the fruits was apparent after 6 days in all the cultivars and treatments. However, it is important to notice that both modified atmospheres treatments presented less severe damages than normal atmosphere condition after 6 days of storage. It can be explained by the expected reduction of respiration in hypoxic situation (low O₂ and high CO₂). On the other hand, ozone treatment can decrease the negative effect of pathogens on the stored fruits, and as a consequence, reduce damage symptoms. Regarding cell wall metabolism, it is normal to observe a decrease of fruit firmness during postharvest (Figure 3), which is related to water loss and

softening. Nevertheless, the observed softening symptom differences between treatments was not completely reflected with fruit firmness values. Indeed, it seems that modified atmospheres had a positive effect on firmness only in 'Santa Clara' fruits (CO₂-enriched atmosphere) and 'Camarosa' (O₃-enriched atmosphere) in agreement with observations made by Nadas *et al.* (2003). Indeed, it was observed a delay in softening induced by ozone in 'Camarosa' fruits. As well, Li *et al.* (2015) observed an increase in firmness in strawberry fruits (cv. 'Akihime') kept in CO₂-enriched atmosphere when comparing to normal atmosphere combined with cold and room temperature storage. Similarly, Alamar *et al.* (2017) described an increase of firmness in strawberry fruits (cv. 'Sonata') stored in CO₂-enriched atmosphere.

Soluble solid content (SSC) is another parameter related to fruit quality, and is expected to decrease during storage, as previously reported in strawberry (Gil *et al.*, 1997; Pelayo *et al.*, 2003; Mishra and Kar, 2014). For most of the strawberry cultivars tested in this study, modified atmospheres did not seem to affect SSC, as described by Li *et al.* (2015). However, we observed an increase in SSC for cv. 'Amiga' during postharvest for fruits kept in both modified atmospheres (Figure 4). Onopiuk *et al.* (2016) also observed that ozonized 'Honeoye' strawberries had a higher SSC than control fruits.

Primary metabolites

Primary metabolism provides energy and biosynthetic precursors to support fruit growth and maturation. In addition, it is essential for fruit quality, as it provides the major components of most fruits (Beauvoit *et al.*, 2018). During postharvest, it has been described important metabolic shifts when comparing to the fruit metabolism during growth and ripening *in planta* (Oms-Oliu *et al.*, 2011; Ding *et al.*, 2015; Yun *et al.*, 2016; Yuan *et al.*, 2017). For these reasons, a deeper look was taken onto the evolution of sugars and acids during the different tested treatments.

A small group of primary metabolites was able to separate T0 fruits from postharvest samples by PLS-DA (Figure 12a) and its behavior was also striking when analyzing log₂ fold change and *K*-means clustering (Figures 14, 17 and

21). These metabolites include succinic acid, galactinol, putrescine and the amino acids GABA, β -alanine, glycine and to a lesser extent proline.

GABA was increased in the three postharvest treatments, even if the increase was lower and retarded in the fruits kept in O₃-enriched atmosphere, when compared to the other two conditions (Figure 17). GABA is a non-proteinogenic amino acid which increase in plant cells has been connected to different abiotic stresses (Palma *et al.*, 2014; Michaeli and Fromm, 2015). GABA is mainly synthesized from glutamic acid, and is associated with TCA cycle through GABA shunt. It is considered an important component in the balance between carbon and nitrogen metabolism in the cell, playing a key role in pH regulation, energy and respiration processes (Sun *et al.*, 2013). Previous studies in *Citrus* postharvest also showed an increase of GABA content, which can be consequence of the activation of the GABA shunt pathway and its function in the regulation of organic acid catabolism processes (Sun *et al.*, 2013; Tang *et al.*, 2016). In addition, GABA accumulation has been related with oxygen deficiency and the onset of injury symptoms due to controlled atmosphere storage (Chiu *et al.*, 2015). The accumulation of GABA coincident with CO₂ treatment injury could involve a mechanism designed to counteract cytosolic acidification resulting from CO₂ dissolution (Shelp *et al.*, 2012; Lum *et al.*, 2016).

On the other hand, GABA is also connected with other metabolites which showed a striking behavior in the postharvest samples and which are known to be involved in stress tolerance, i.e. β -alanine, proline and putrescine (Gupta *et al.*, 2013). Indeed, several biological functions related to cold stress has been associated with putrescine (Kaplan *et al.*, 2007; Rohloff *et al.*, 2012), which synthesis is tightly connected to the metabolism of several amino acids and which degradation yields GABA and β -alanine. Furthermore, proline is also connected via GABA metabolism in stressed tissues (Bouchereau *et al.*, 1999; Shelp *et al.*, 2012; Palma *et al.*, 2014). Proline levels were higher in fruits kept in normal and CO₂-enriched atmospheres, coinciding with the highest accumulation of GABA in postharvest samples. On the other hand, succinic acid levels were enhanced in the samples from the two modified atmospheres. During GABA catabolism, GABA is converted to succinic acid by the action of two enzymes (GABA transaminase and succinic semi-aldehyde dehydrogenase). Succinic acid acts

both as an electron donor to mitochondrial electron transport chain and as an intermediate of TCA cycle (Shelp *et al.*, 2012). For these reasons, it can play an important role in energy balance and respiration during fruit senescence, together with GABA.

Apart from its relation with cold tolerance and GABA metabolism, polyamines, such as putrescine, have been suggested to function in maintaining membrane stability under stress conditions and growing evidence associate putrescine with modulation of antioxidant system (Gill and Tuteja, 2010; Moreno *et al.*, 2018).

Galactinol was strongly induced in the samples kept in O₃-enriched atmosphere and in some cultivars kept in CO₂ and normal atmospheres. Interestingly, galactinol is an alcohol sugar which has been described to be involved in cold response in peach (Bustamante *et al.*, 2016) and strawberry (Davik *et al.*, 2013). In addition, galactinol and sucrose take part in raffinose synthesis, and the raffinose pathway has been described as an essential cold-inducible biosynthetic route (Kaplan *et al.*, 2007). Sugars can serve as osmoprotectants of biological membranes, stabilizing macromolecular structures (Bustamante *et al.*, 2016). Salvi *et al.* (2017) observed in chickpea that galactinol and raffinose contents were significantly increased in response to various abiotic stresses, including oxidative stress, due to the up-regulation of the galactinol synthase activity. Both galactinol and raffinose, apart from their osmoprotectant role, can act as antioxidant molecules, having the ability to scavenge hydroxyl radicals and thus decrease ROS (Nishizawa *et al.*, 2008). This could explain why galactinol is strongly induced in postharvest strawberry kept in ozone atmosphere.

Finally, two phosphorylated sugars, glucose- and fructose-6-phosphate were increased in the fruits from the O₃-enriched atmosphere treatment, while in normal atmosphere the increase was less obvious and was not observed in CO₂ treatment (Figures 12a, 14, 17 and 21). This increase could be related to the higher ROS scavenging capacity of the hexose phosphates in comparison with the non-phosphorylated sugars and their induction due to oxidative stress (Spasojević *et al.*, 2009; Rohloff *et al.*, 2012).

Secondary metabolites

As plants have to deal with numerous challenges including a series of abiotic and biotic stresses, they developed a more specific and specialized metabolism, known as secondary metabolism, which allows them to resist adverse conditions (Mouradov and Spangenberg, 2014). Then, it is expected that secondary metabolite content will be affected during postharvest. Indeed, it has been demonstrated that postharvest has an impact on the phenolic content in strawberries, being the temperature of storage a key factor affecting the stability of these compounds (Ayala-Zavala *et al.*, 2004; Cordenunsi *et al.*, 2005; Shin *et al.*, 2008; Jin *et al.*, 2011). Changes have been attributed to the degradation of phytochemicals by the presence of oxygen, light and polyphenol oxidase activity and to the anthocyanin synthesis in harvested fruit (Holcroft and Kader, 1999; Goulas and Manganaris, 2011). Surprisingly and with the exception of a few metabolites, no drastic changes were observed along the postharvest when compared to the T0 fruits, and it was difficult to observe common trends between cultivars (Figures 15 and 18). PLS-DA analysis was partially able to separate T0 samples from postharvest ones, with a few metabolites being outlined (Figure 12b). Flavonoids naringenin chalcone hexose 2, eriodictyol hexose 2, kaempferol hexose 1, propelargonidin trimer 3 and pelargonidin-hexose, and the hydroxybenzoic acid hexose 1 were correlated with T0 fruits (meaning that they were generally decreased along postharvest), and also grouped together in *K* cluster 6 (Figure 22). The main anthocyanin pigment, pelargonidin-hexose, was found in this cluster and was mainly decreased in the postharvest samples. Anthocyanin synthesis and accumulation have been reported in strawberry and other fruits during their postharvest life (Goulas and Manganaris, 2011; Goulas *et al.*, 2015). However, it seems that their accumulation is temperature-dependent and that low temperature storage does not favor it (Ayala-Zavala *et al.*, 2004; Shin *et al.*, 2007). Indeed, it has been seen that the activity of the phenylalanine ammonia-lyase (PAL), which catalyzes the first step of the phenylpropanoid pathway, increased at room temperature (Trakulnaleumsai *et al.*, 2006). In addition, Holcroft and Kader (1999) reported that CO₂ treatment led to a lower accumulation of anthocyanins and a decrease in PAL activity. Nevertheless, our results did not reflect any change between CO₂ and the other

treatments. All metabolites, with the exception of rutin and quercetin acetylhexose, weighed negatively for PLS-DA component 1, which roughly separated samples based on the duration of the postharvest treatments (Figure 13b). The interpretation is that there is a general decrease of secondary metabolites during postharvest senescence, independently of the treatment. Interestingly, only 'Amiga' cultivar showed a slight increase in polyphenol content (mainly flavonoids and ellagitannins), mainly after 3 days in normal atmosphere and 10 days in CO₂-enriched atmosphere (Figure 15a). Curiously, T0 fruits of this cultivar presented lower content of most secondary metabolites when compared to the other varieties used in this study (Figure 6). Anyway, it would be interesting to measure antioxidant capacity of the different postharvest samples, to figure out how it is affected by the changes in polyphenol composition.

Volatiles

Fruit aroma pattern is directly influenced by its maturity stage, so important changes are expected to occur in volatile content during postharvest storage (Lester, 2006). Indeed, some drastic alterations were observed in volatile profiles when compared to the T0 fruits (Figures 16 and 19). Interestingly, most extreme changes were conserved in the different cultivars, and the most striking difference between treatments was observed in samples kept in ozone-enriched atmosphere during 3 days. Indeed, for most volatiles, alterations were attenuated in comparison with the same duration of normal and CO₂-enriched atmospheres.

Most aldehydes, furans, ketones and terpenes were slightly reduced during postharvest treatments. Aldehydes are important for the green and unripe notes in strawberry aroma, and their concentrations are decreasing along ripening (Ménager *et al.*, 2004; Rodríguez *et al.*, 2013; Vandendriessche *et al.*, 2013). For this reason, it is not unexpected that they presented low levels during fruit senescence, and that they correlated with T0 fruit samples in PLS-DA analysis (Figure 12c). *FaQR*, a quinone oxidoreductase, and *FaOMT*, an O-methyltransferase, are involved in the synthesis of furans volatiles (Lunkenbein *et al.*, 2006; Raab *et al.*, 2006). It has been described that *FaQR* activity declined remarkably at low temperature and in CO₂-enriched atmosphere when compared

to room temperature storage (Li *et al.*, 2015) while FaOMT activity increased with the temperature (Fu *et al.*, 2017a), which can explain the relative low levels of these volatiles observed in the postharvest samples. Fu *et al.* (2017a) also observed that terpene level increase during postharvest is strongly influenced by temperature. Once again, the storage temperature used in this experiment could explain why terpene levels were slightly decreased.

On the other hand, ester concentration increases extraordinarily during ripening, conferring floral and fruity scent to mature fruit (Rodríguez *et al.*, 2013). Interestingly, esters could be divided into two groups with contrasting behavior in the postharvest treatments. Indeed, some of them were strongly increased, while other were strongly decreased along postharvest. Methyl esters were predominantly decreased while ethyl esters increased (Figures 16 and 19). Miszczak *et al.* (1995) also observed an increase in the ratio of ethyl to methyl esters in 'Kent' strawberry cultivar. This difference can be due to a low rate of methyl alcohol biosynthesis, which is precursor of methyl esters, while the precursor of ethyl esters, ethanol, is strongly induced during postharvest. Ke *et al.* (1994) also pointed out an increase in ethanol which correlates with an increase in ethyl esters in strawberry fruits (cv. 'Chandler') stored in low O₂ and/or high CO₂. The levels of ethanol were strongly induced in the three tested postharvest treatments, even if an initial delay in the accumulation was observed in the fruits kept in O₃-enriched atmosphere and in some samples kept in CO₂-enriched atmosphere (Figure 19). In other fruits, such as mandarins, increase of ethyl esters was also observed during cold storage (Tietel *et al.*, 2012).

Sulfur volatiles, which influence strawberry aroma due to their low odor thresholds, have been seen to be drastically increased during ripening and over-ripening stages (Du *et al.*, 2011). Methylthioacetic acid ethylester was strongly increased in the postharvest samples, confirming this tendency observed in 'Strawberry Festival' and 'Florida Radiance'.

The use of modified atmospheres could result in the fruit possessing an 'off' flavor. Indeed, high CO₂ atmosphere has been shown to cause changes in the activity of enzymes involved in the fermentative metabolism, resulting in increasing levels of acetaldehyde, ethanol and ethyl lactate, which confer

undesirable aroma to the strawberry fruit (Kader, 2003; Ponce-Valadez *et al.*, 2009). However, this accumulation of ethanol due to CO₂ atmosphere seems cultivar-specific, as Ponce-Valadez *et al.* (2009) only observed it in 'Jewel' cultivar while 'Cavendish' did not accumulate it under the same storage conditions. In the fruits of the five cultivars kept at 4°C in normal atmosphere, ethanol level was already strongly increased after 3 days of treatment (Figure 19), while in fruits kept in O₃-enriched atmosphere the increase was delayed until 6 days. The use of ozone treatment during postharvest has already been reported to affect the development of volatiles, even if it is not clear if it leads to the formation of 'off' flavor. Pérez *et al.* (1999) and Nadas *et al.* (2003) observed a reduction in the volatile emission as a consequence of ozone treatment combined with cold storage. This is concordant with the result obtained in this study, which showed a reduced increase in ethyl esters content after 3 days of storage in O₃ atmosphere, when compared to the other treatments. However, after 6 and 10 days of storage, levels of ethyl esters were similar between the three treatments (Figure 19). It was suggested that the reduced volatile emission in ozonized fruits could be a consequence of a physical alteration of the fruit surface, as no clear difference in the activity of the enzymes involved in aroma synthesis was found (Pérez *et al.*, 1999).

Conclusion

Metabolome analysis of harvested strawberry fruits kept in different commonly used postharvest treatments allowed the identification of metabolic processes related to abiotic stresses (cold and oxidative stresses). In addition, changes in fruit metabolism has a strong impact on the volatile profiles, suggesting important changes in fruit palatability and consumer acceptance. Descriptive and statistical approaches pointed out the effect of O₃-enriched atmosphere in mitigating volatiles changes in the initial phase of postharvest when compared to normal and CO₂-enriched atmospheres. Deeper bioinformatics analysis are ongoing, in order to understand the metabolic pathways and regulatory mechanisms underlying fruit senescence.

Conclusions

According to our initial objectives, the conclusions derived from this thesis are:

1. A high number of mQTL controlling primary and secondary metabolite contents in a F_1 *F. x ananassa* population were identified in all the homoeology groups of *Fragaria* octoploid map, with main cluster hotspots in HG IV and HG V, indicating linkage or pleiotropic effect of *loci*.
2. Stable QTL, detected over the two harvests, were found for 17 primary metabolites and 45 secondary metabolites. These QTLs could be used for designing breeding strategies to improve the organoleptic and nutritional characteristics of strawberry.
3. Based on its map location and predicted function, a candidate gene within a stable mQTL for ellagic acid hexose content has been identified. Stable transgenic strawberry plants, overexpressing and silencing the candidate, have been generated and will allow a functional analysis of this gene.
4. Likewise, deeper analysis of the identified mQTL genomic regions will allow the identification of new candidate genes controlling strawberry fruit metabolite content.
5. Postharvest storage of strawberry fruit cultivars induced changes in primary and secondary metabolites, and the most drastic compositional changes were observed in aroma profile. Several common responses and metabolic shifts were observed between the different tested postharvest treatments. In addition, different storage atmospheres influenced the behavior of specific metabolites.
6. Multivariate statistical approaches were used to highlight the most striking features occurring in senescent strawberry fruit metabolism, and network-

based methods will allow to point out the regulatory factors underlying fruit senescence.

Resumen de la tesis en castellano

La Universidad de Málaga pide un resumen de la tesis en español (mínimo 5000 palabras) cuando ha sido escrito en un idioma diferente.

CAPÍTULO 1: Introducción general

La fresa (*Fragaria x ananassa*) es un fruto de baya muy apreciado por su delicado sabor y su alto valor nutricional. España, con una producción anual de 366.161 toneladas métricas, se consolida como el sexto país productor de este fruto a nivel mundial, concentrando más del 95% de su producción en la provincia de Huelva, Andalucía (Sur de España).

La fresa pertenece a la familia Rosaceae y al género *Fragaria*, que comprende unas 20 especies diferentes y que se caracterizan por un número amplio de ploidías, que van desde diploide a decaploide. La fresa cultivada, *F. x ananassa*, es octoploide y cuenta con 4 subgenomas diferentes, uno de los cuales está relacionado con la especie diploide silvestre *F. vesca* y tres de ellos, con la diploide *F. iinumae* (Tenessen *et al.*, 2014). La secuenciación del genoma de *F. vesca*, su colinealidad y macrosintenia con el de *F. x ananassa* ha permitido que la especie silvestre se convierta en un modelo para los estudios genéticos del género *Fragaria*.

Las características organolépticas y nutritivas definen la calidad del fruto, e incluyen componentes de sabor, aroma, color y firmeza, así como el contenido en compuestos saludables. Los procesos fisiológicos que conducen el desarrollo y maduración del fruto de fresa, y los cambios metabólicos que ocurren durante su vida postcosecha, son responsables de la calidad final del fruto encontrado por el consumidor.

El metabolismo central del fruto, conocido también como *metabolismo primario*, es responsable del contenido en azúcares y ácidos que influyen directamente en el sabor del fruto. Además, los metabolitos que conforman el metabolismo primario sirven de precursores para el metabolismo especializado del fruto (*metabolismo secundario*) y para la síntesis de compuestos volátiles, los cuales son responsables del típico aroma por el cual reconocemos y valoramos la

calidad del fruto (Vandendriessche *et al.*, 2013). Por otro lado, la fresa es especialmente rica en ácido ascórbico y fólico, y su alto contenido en polifenoles (metabolitos secundarios), la convierte en un aporte esencial de la dieta humana. De esta manera es reconocida como una importante fuente de metabolitos con acción antioxidante, antiinflamatoria y antihipertensiva (Mazzoni *et al.*, 2015).

El fruto de fresa se caracteriza por tener una vida postcosecha muy corta, siendo especialmente sensible a daños mecánicos y ataques por parte de patógenos (Feliziani y Romanazzi, 2016). Con el fin de retrasar la rápida senescencia del fruto y, de este modo, evitar pérdidas económicas, varias estrategias están siendo empleadas en la industria, entre las cuales se encuentran el almacenamiento a baja temperatura y/o el uso de atmósfera controlada o modificada (Pedreschi y Lurie, 2015). Sin embargo, existe muy poca información sobre los cambios metabólicos y-regulatorios que controlan la senescencia del fruto de fresa durante su postcosecha.

Herramientas para la mejora de la calidad de frutos

Debido a su complejidad fenotípica y su herencia poligénica, en la agricultura tradicional, se ha tendido a favorecer caracteres discriminantes como el color y el tamaño de fruto, entre otros, pero se ha descuidado la importancia de incluir caracteres relacionados con calidad de fruto, como la presencia de metabolitos importantes de incorporar en una dieta saludable. Sin embargo, con el avance de la tecnología de secuenciación masiva y algoritmos de análisis modernos, el desarrollo de marcadores y mapas genéticos, el mapeo de *loci* de carácter cuantitativo (QTL por sus siglas en inglés) ha permitido la identificación de genes y *loci* relacionados con calidad de fruto en fresa y otros cultivos (Zorrilla-Fontanesi *et al.*, 2011, 2012; Zeballos *et al.*, 2016; Capel *et al.*, 2017). Además, el reciente desarrollo de técnicas metabolómicas de alto rendimiento, ha permitido la identificación simultánea de un amplio rango y número de metabolitos, convirtiéndose en una poderosa herramienta para la identificación de QTL involucrados en calidad de fruto (Alseekh *et al.*, 2015; Ballester *et al.*, 2016; Urrutia *et al.*, 2017). En este sentido, la espectrometría de masa es una tecnología muy sensible que puede ser usada en combinación con técnicas de

separación, como la cromatografía líquida (LC) o gaseosa (GC), facilitando el análisis de extractos biológicos de alta complejidad (Dettmer *et al.*, 2007).

Objetivos

Se plantean los siguientes objetivos para esta tesis:

1. Identificación de QTL para el contenido en metabolitos primarios y secundarios (mQTL) involucrados en las características organolépticas y nutritivas de la fresa cultivada (*F. x ananassa*), usando la población de mapeo F₁ '232' x'1392'.
2. Identificación de factores regulatorios a nivel genómico y metabolómico relacionados con la pérdida de calidad organoléptica y nutritiva del fruto de fresa durante su vida postcosecha.

CAPÍTULO 2: Identificación de *loci* de carácter cuantitativo (QTL) y genes candidatos para el contenido en metabolitos primarios del fruto de fresa

Introducción

Tradicionalmente, los programas de mejora de fresa se han centrado en el desarrollo de variedades que presenten a nivel de fruto, un mayor tamaño, un mayor rendimiento (kg/planta) y mayor resistencia a enfermedades. Sin embargo, recientemente las preferencias de los consumidores han llevado a los productores a elegir variedades con mejor sabor, con mayor contenido de azúcares y una proporción equilibrada entre azúcares y ácidos (Jouquand *et al.*, 2008). El mapeo de QTL, junto a la caracterización metabolómica del fruto, aportan una valiosa información para el análisis en la búsqueda del control genético de los atributos relacionados con el sabor del fruto y, la información adquirida tras este análisis, permitiría el desarrollo de nuevas variedades mediante el uso de selección asistida por marcadores. Por ejemplo, en estudios realizados en variedades de fresa comercial, se han identificado QTLs asociados con el contenido de compuestos volátiles y otros metabolitos como glucosa, fructosa, sacarosa y los ácidos málico, cítrico y ascórbico (Zorrilla-Fontanesi *et al.*, 2011, 2012; Lerceteau-Köhler *et al.*, 2012).

El objetivo de este trabajo es la caracterización de la variación y control genético del metabolismo primario del fruto de fresa. Para ello ha sido usada la población de mapeo F₁, que deriva de un cruzamiento entre dos líneas, '232' y '1392', que presentan un fenotipo contrastante, difiriendo en características de dulzor, acidez y contenido en ácido ascórbico (L-AA), entre otras. A fin de conseguir este objetivo, se ha medido el contenido en metabolitos primarios en la población. Se han identificado varios mQTL que putativamente controlan los niveles de los metabolitos primarios estudiados. Estos, a su vez, se han podido comparar con QTL previamente descritos en la misma población para el contenido en sólidos solubles y acidez titulable. Finalmente, se han propuesto una serie de genes candidatos para algunos de los metabolitos, por su localización dentro de los intervalos de confianza de los QTL detectados y su posible función anotada en el reciente ensamblaje del genoma de *F. vesca* (Shulaev *et al.*, 2011; Tenessen *et al.*, 2014; Edger *et al.*, 2018).

Resultados y discusión

Variación en la composición metabólica de la población de mapeo '232' x '1392'

Durante dos temporadas y utilizando el protocolo descrito en Osorio *et al.* (2012), se ha evaluado y parcialmente cuantificado el contenido de metabolitos primarios en muestras provenientes de la población en estudio y de sus dos líneas parentales, '232' y '1392'. Como resultado de esto, se han identificado 50 metabolitos, que incluyen aminoácidos, ácidos orgánicos, azúcares y una poliamina. Tras su análisis se observó un alto nivel de divergencia en el metabolismo primario entre las dos líneas parentales. Así, por ejemplo, la línea '232' presenta niveles significativamente más bajos que la línea '1392' en 14 de los metabolitos analizados.

La utilización de análisis estadísticos como el agrupamiento jerárquico (HCA, por sus siglas en inglés de *hierarchical cluster analysis*) y el cálculo de correlaciones, mediante el uso del coeficiente de Pearson, permitieron establecer relaciones y correlaciones entre los diferentes metabolitos. Como resultado de esto, fueron encontradas 665 y 697 correlaciones positivas y significativas en las temporadas 2013 y 2014 respectivamente. Por otro lado, sólo 50 y 8 correlaciones, fueron

negativas, respectivamente. Tras el análisis HCA, los metabolitos se clasificaron en dos grupos. El primer grupo agrupa principalmente a azúcares, mientras el segundo a aminoácidos.

Identificación de mQTL para metabolismo primario en frutos de fresa

Para el análisis de QTL se utilizó el mapa integrado y previamente generado de la población '232' x '1392', que comprende 2089 marcadores repartidos en los 33 grupos de ligamiento (Sánchez-Sevilla *et al.*, 2015). Además de los metabolitos primarios identificados, se incluyó en el análisis el contenido de sólidos solubles, de ácido ascórbico (L-AA) y los resultados de los análisis realizados para determinar la acidez titulable. Fueron identificados 133 QTL para 47 características fenotípicas, de los cuales solamente 20 se consideraron estables en las dos temporadas analizadas. El bajo número de QTL estables podría indicar que el contenido en metabolitos primarios está altamente afectado por el ambiente y contrasta con el contenido de compuestos volátiles medidos en la misma población, donde el 50% de los QTL detectados fueron estables entre las distintas temporadas (Zorrilla-Fontanesi *et al.*, 2012). Se detectaron QTLs a lo largo de los siete grupos de homología (HG, por su sigla en inglés) del mapa de la población y se encontraron agrupaciones de QTL en todos los HG, sugiriendo ligamiento o efectos pleiotrópicos de *loci*. La asociación más grande de QTL se situó en el HG V, con una agrupación de QTL relacionadas con la acidez titulable, pH y varios metabolitos de la categoría de ácidos orgánicos. QTL del grupo de ligamiento (LG) V-2 y V-4 fueron asociados con tres azúcares, dos ácidos orgánicos y cinco aminoácidos. En estudios anteriores, fueron identificados QTL para ácidos y azúcares en el HG V, aproximadamente el mismo intervalo cromosómico, lo que podría indicar que *loci* comunes controlan el contenido de esos metabolitos en múltiples fondos genéticos. Otros QTLs comunes con esos estudios fueron detectados en HG VI y II, aportando una mayor posibilidad de identificar marcadores fiables para la selección de caracteres de calidad en fruto (Lerceteau-Köhler *et al.*, 2012; Castro and Lewers, 2016; Verma *et al.*, 2017).

Además, se identificaron varios QTLs para metabolitos primarios en regiones genómicas solapantes de diferentes LG del mismo HG, sugiriendo la presencia de *homoeo*-QTL.

Asociaciones entre QTL y marcadores génicos que controlan la variación de ácidos y azúcares

QTL estables, que explican un porcentaje importante de la variación (22-30%) han sido identificados en el LG V-4 para los metabolitos sacarosa y rafinosa. En el intervalo de confianza de dichos QTL, fueron encontrados siete posibles genes candidatos relacionados con el metabolismo de azúcares, basándonos en su anotación y, además de considerar su expresión genética en frutos rojos de *F. x ananassa* cv. 'Camarosa' (Sánchez-Sevilla *et al.*, 2017). El análisis de expresión, mediante PCR cuantitativa en frutos rojos de líneas F₁ de la población en estudio, con niveles contrastantes de sacarosa y rafinosa y de sus parentales, señaló como candidato en la variación de los niveles de azúcares el gen *FvH4_5g03890*, que codificaría para una glucosa-6-fosfato epimerasa. En paralelo, se ha detectado un QTL estable para el ácido succínico. Este fue detectado en el mismo grupo de ligamiento y con un intervalo de confianza solapando el de los QTL para sacarosa y rafinosa. Además, los alelos que afectan la variación de esos tres metabolitos son heredados de la línea parental '232' y modifican su contenido en la misma dirección. Por lo tanto, existe la posibilidad que un solo gen, con efectos pleiotrópicos, controle el contenido en sacarosa, rafinosa y ácido succínico. Alternativamente, otro gen, ligado al *locus* detectado para los dos azúcares, puede ser responsable de los niveles de ácido succínico. De hecho, un factor de ensamblaje mitocondrial de la succinato deshidrogenasa (*FvH4_5g09730*) fue localizado en el intervalo de confianza del QTL, aunque no se vio diferencia de expresión entre líneas F₁ con niveles contrastantes del metabolito. Así, se plantea la necesidad de realizar nuevos estudios para determinar si los cambios en las secuencias de los genes candidatos identificados pueden ser responsables de las variaciones metabólicas detectadas.

Manosa-6-fosfato isomerasa, gen candidato en la modulación del contenido de L-AA

Tres QTL fueron identificados en la población bajo estudio que podrían modular el contenido en L-AA (Zorrilla-Fontanesi *et al.*, 2011). En el presente estudio, se repitió el mapeo de QTL para ese carácter y usando el mapa integrado de los dos parentales, se obtuvieron resultados similares a los descritos previamente (Zorrilla-Fontanesi *et al.*, 2011). El QTL más importante, que explicaría entre un 27.7% y 35.5% de la variación, ha sido detectado en el LG V-1, localizándose junto a un QTL asociado a la variación de contenido de ácido dehidroascórbico. El posterior análisis reveló un candidato, el gen *FvH4_5g21090*, con alta homología a un gen que codifica una proteína manosa-6-fosfato isomerasa de *Arabidopsis*. Tras la identificación, se ha validado su posible implicación mediante análisis de expresión diferencial usando datos obtenidos por RNASeq y PCR cuantitativa entre grupos de líneas F₁ con bajos y altos niveles de L-AA respectivamente. Este candidato catalizaría la isomerización entre la D-fructosa-6-fosfato y la D-manosa-6-fosfato en una de las rutas de síntesis del L-AA descritas en plantas (Maruta *et al.*, 2008).

En conclusión, se han identificado varios genes mediante mapeo de QTL para el contenido en metabolitos primarios del fruto de fresa. Futuros estudios funcionales permitirán la validación de dichos candidatos y su uso potencial en la selección asistida por marcadores de variedades con unas altas características nutricionales y organolépticas.

CAPÍTULO 3: Identificación de *loci* de carácter cuantitativo (QTL) y genes candidatos que regulen el contenido en metabolitos secundarios del fruto de fresa

Introducción

Debido a su alto contenido en compuestos fenólicos, que provienen del ácido shikímico y de la ruta de los fenilpropanoides, la fresa presenta una alta actividad antioxidante. Estudios en animales han demostrado que poseen propiedades antiinflamatoria y antihipertensiva (Giampieri *et al.*, 2015). Dentro de los polifenoles presentes en el fruto, los flavonoides son los más abundantes. Estos están compuestos principalmente por antocianinas, que son responsables del color rojo del fruto maduro. Además, pero en menor cantidad, el fruto presenta

concentraciones razonables de flavonoles, flavanoles y proantocianidinas. Otros compuestos fenólicos importantes en la composición del fruto de fresa son los taninos hidrolizables (elagitaninos y galotaninos) y los ácidos fenólicos (ácidos hidroxicinámicos y hidroxibenzoicos).

La enzima clave en la síntesis de los compuestos fenólicos es la fenilalanina amonio liasa (*PAL*) que redirige el flujo de carbono del metabolismo primario al metabolismo secundario (Vogt, 2010). La formación de 4-coumaroil CoA es un paso clave en la ruta ya que proporciona un precursor directo para la síntesis de los flavonoides. Los ácidos fenólicos son principalmente derivados de los ácidos cumárico, cafeico y ferúlico sintetizados a partir del ácido cinámico. Existe muy poca información sobre la formación de los taninos hidrolizables, sin embargo, se especula que el ácido gálico, el núcleo de la estructura de estos compuestos, proviene de la deshidrogenación del 5-deshidroschikimato (Bontpart *et al.*, 2016).

Dentro del estudio de las características organolépticas y nutritivas de la población '232' x '1392', se han llevado a cabo análisis metabolómicos del metabolismo secundario de las líneas F₁ y de sus parentales. Para ello se han combinado técnicas de detección y análisis de metabolitos, mediante Cromatografía Líquida de alta eficacia asociada a Espectrometría de Masa (UPLC-qOrbitrap-MS/MS), seguido de análisis genéticos mediante mapeo de QTL para la identificación de regiones genómicas y posibles genes candidatos involucrados en la síntesis y/o regulación de los polifenoles encontrados en el fruto de fresa.

Resultados y discusión

Variación en la composición de metabolitos secundarios en la población '232' x '1392'

Mediante el uso de tecnologías de separación y detección de compuestos, UPLC-qOrbitrap-MS/MS, se identificaron 130 metabolitos secundarios, de los cuales 125 son polifenoles y 5 terpenoides. Dentro del grupo de polifenoles y en relación con su abundancia en el fruto de fresa, se detectaron 55 flavonoides, 49 taninos hidrolizables y 21 derivados de ácidos fenólicos. 33 metabolitos mostraron diferencias significativas entre ambos parentales en las dos cosechas estudiadas y otros 43 en sólo una temporada. Se observó en la progenie un alto

rango de variación en el contenido de metabolitos secundarios. Además, se pudo observar una segregación transgresiva en ambas direcciones para la mayoría de los metabolitos. A pesar de que se había descrito previamente una diferencia significativa entre las líneas parentales en el contenido de antocianinas responsables del color del fruto maduro (Zorrilla-Fontanesi *et al.*, 2011), en este estudio solamente se detectó una disminución significativa del pigmento minoritario cianidina hexosa en el parental '232'. Como esperábamos, nuestros análisis de HCA y estudios de correlaciones entre metabolitos indicaron relaciones positivas fuertes entre compuestos pertenecientes a la misma clase. Sorprendentemente, se obtuvieron muy pocas correlaciones negativas entre metabolitos de diferentes clases.

Identificación de QTL que controlan el contenido de metabolitos secundarios en la población '232' x '1392'

En este estudio, el mapeo de QTL se ha llevado a cabo de la misma manera que fue descrito en el capítulo anterior. 465 asociaciones significativas fueron detectadas entre marcadores y 116 de los 130 metabolitos secundarios identificados. De esos QTL, fueron considerados estables sólo 110, mediante la coincidencia del mismo compuesto en regiones cromosómicas parecidas en los dos años estudiados.

En los siete grupos de homología se detectaron agrupaciones de QTL para metabolitos biosintéticamente relacionados y para diferentes isómeros del mismo compuesto, indicando la presencia de *loci* controlando los niveles de metabolitos secundarios de manera coordinada. Similar al análisis de QTL llevado a cabo para el estudio del metabolismo primario, fueron observadas importantes asociaciones de QTL en HG V (LG V-2 y LG V-4), indicando que los genes involucrados en la biosíntesis de metabolitos se distribuyen de manera desigual a lo largo del genoma. Igualmente, y, como se ha propuesto en estudios realizados en *Arabidopsis*, estos resultados podrían sugerir la presencia de genes reguladores que controlen la acumulación de metabolitos en un mayor orden jerárquico (Lisec *et al.*, 2008).

Estudios previos realizados en *F. x ananassa* y *F. vesca* señalaron la presencia de QTL relacionados con el metabolismo de los polifenoles en el cromosoma 5

o HG V (Lerceteau-Köhler *et al.*, 2012; Urrutia *et al.*, 2015a,b; Castro and Lewers, 2016). En nuestro análisis, QTL para el contenido en pelargonidina, el pigmento mayoritario, y otras antocianinas fueron detectados en LG V-2 y se pueden relacionar con QTL para el contenido total en antocianinas y para el color de fruto previamente descritos en la población '232' x '1392' por Zorrilla-Fontanesi *et al.* (2011). Además, en el LG V-2, se observaron varios QTL para otros flavonoides, sugiriendo la posibilidad que el *locus* responsable de la variación de color y del contenido en antocianinas está actuando corriente arriba en la ruta de síntesis de los flavonoides. Otra agrupación de QTL en LG V-4 para flavonoides evoca la probabilidad de un homoeo-QTL. Otra asociación importante de QTL para flavonoides se detectó en LG I-2. *FaMYB10*, un factor de transcripción clave en el control de la síntesis de los fenilpropanoides, se encuentra en el cromosoma 1 y podría colocalizar con algunos de los QTL detectados (Zhang *et al.*, 2017). El estudio más detallado de esas regiones genómicas permitiría identificar *loci* relacionados con esta importante clase de metabolitos.

Análisis de candidatos en los LG I-2 y LG IV-1 relacionados con el metabolismo de elagitaninos: gen *FvH4_1g16310*

Se detectaron agrupaciones de QTL relacionados con el metabolismo de taninos hidrolizables en LG I-2, LG IV-1, LG II-4 y LG V-1. Un QTL estable asociado con el ácido elágico hexosa isómero 2 destacó en el LG I-2, debido al alto porcentaje de variación fenotípica que explicaba, sugiriendo la presencia de un gen clave en el control de este metabolito. Un análisis más detallado de la región genómica delimitada por el intervalo de confianza de ese QTL llevó a la identificación de ocho candidatos que podrían tener relación con el metabolismo de los elagitaninos. De la misma manera, se centró la búsqueda de genes candidatos en el LG IV-1, y más específicamente en el intervalo de confianza de QTL estables para dos isómeros de elagitaninos explicando un alto porcentaje de variación fenotípica. Análisis de expresión de los candidatos seleccionados en ambos grupos de ligamiento mediante PCR cuantitativa y en líneas con niveles contrastantes de los distintos metabolitos relacionados con los QTL, permitió la identificación de una acetiltransferasa (gen *FvH4_1g16310*), relacionada con los niveles de ácido elágico hexosa 2. Considerando su anotación, este gen podría estar involucrado en el metabolismo de los elagitaninos, debido a que codificaría

una enzima perteneciente a la categoría EC.2.3.1.90 (“ β -glucogallin O-galloyltransferases”). Estas enzimas, que pertenecen a las aciltransferasas, catalizan la formación de los precursores en la síntesis de los elagitaninos (Niemetz and Gross, 2001). Por lo tanto, el gen candidato identificado actuaría corriente arriba en la ruta biosintética de los taninos hidrolizables, por lo que podría afectar los niveles de varios compuestos de esta clase. De esta manera, se ha transformado tejido vegetal y mediante cultivo *in vitro*, se han obtenido plantas transgénicas de fresa que sobreexpresan y silencian el gen *FvH4_1g16310*. Con ellas se pretende realizar un estudio funcional de los frutos para aclarar el papel de este gen en el metabolismo de los elagitaninos.

CAPÍTULO 4: Perfil metabolómico durante la senescencia de postcosecha en frutos de diferentes cultivares de fresa

Introducción

La senescencia de los frutos es un proceso biológico complejo, inevitable y negativo para fines comerciales, ya que conduce a un deterioro rápido de los atributos de calidad del fruto, influyendo en su sabor, textura y apariencia (Tietel *et al.*, 2012). Sin embargo, se conoce poco de los cambios a nivel metabólico durante el proceso de senescencia y, del mismo modo, de los factores regulatorios que controlan estos procesos. Estudios metabolómicos señalaron ciertos metabolitos importantes en este proceso, debido a su relación con la vida postcosecha del fruto (Oms-Oliu *et al.*, 2011; Yuan *et al.*, 2017; Sun *et al.*, 2017), esta área de estudio aún está lejos de ser dilucidada.

En la actualidad, se emplean distintos métodos para retrasar la senescencia de los frutos. Estos suelen tener en común el almacenamiento en frío y en atmósferas modificadas que limitan el crecimiento de microorganismos e interfieren en el intercambio gaseoso. A pesar de ello, hay poca información disponible sobre las respuestas metabólicas y genéticas de los frutos sometidos a tratamientos postcosecha en estas condiciones. Se ha observado que el uso de atmósfera modificada puede prevenir los daños por bajas temperaturas. (Sanhuesa *et al.*, 2015). Asimismo, se ha sugerido que niveles altos de CO₂ pueden mejorar la calidad de la fresa durante la postcosecha, como

consecuencia de una disminución en la tasa de respiración (Sanhuez *et al.*, 2015; Feliziani and Romanazzi, 2016). Además, se ha observado que el uso de atmósfera enriquecida en ozono (O₃) aumenta los niveles de L-AA en frutos de fresa (Pérez *et al.*, 1999). Por otro lado, se ha demostrado que estos tratamientos también pueden influir negativamente sobre aspectos importantes del fruto como son el color y el aroma (Shamaila *et al.*, 1992; Pérez *et al.*, 1999). Las ciencias “ómicas” permiten aportar luz sobre las respuestas globales del fruto sometido a tratamientos de postcosecha. En fresa, un estudio combinando proteómica con análisis del volatiloma confirmó que el contenido en volátiles era menor en frutos almacenados en frío y que este patrón podía correlacionarse con el contenido en proteínas implicadas en la síntesis de volátiles (Li *et al.*, 2015). Sin embargo, hasta donde sabemos, no se ha descrito la respuesta global del metaboloma del fruto de fresa sometido a frío o a frío en combinación con algún tipo de atmósfera modificada. Debido a esto, en este estudio proponemos caracterizar metabólicamente cinco variedades de fresa comerciales (*F. x ananassa* cv. ‘Amiga’, cv. ‘Camarosa’, cv. ‘Candongga’, cv. ‘Fortuna’ y cv. ‘Santa Clara’) sometidas durante un periodo de diez días a distintos tratamientos de postcosecha. Estos tratamientos consisten en el uso de bajas temperaturas (4°C), combinadas con atmósfera enriquecida en CO₂ (10% CO₂ y 11% O₂) y en O₃ (0.35 ppm). Después de 3, 6 y 10 días de tratamientos se tomaron muestras para su análisis mediante GC-MS y LC-MS.

Resultados y discusión

Perfiles metabólicos en frutos de fresa

Mediante GC-TOF/MS se identificaron 49 metabolitos primarios y mediante LC-qOrbitrap-MS/MS 132 metabolitos secundarios. Además, 70 compuestos volátiles fueron detectados y semi-cuantificados por microextracción en fase sólida en espacio de cabeza acoplada a GC-MS (HS-SPME-GC-MS). Tras un análisis de agrupamiento jerárquico de los perfiles metabólicos de las cinco variedades empleadas en este estudio, dio como resultado una mayor similitud entre los cultivares ‘Camarosa’ y ‘Candongga’, ambos con altos niveles relativos de los tres sets de metabolitos (primarios, secundarios y volátiles), comparando con el resto de los cultivares. Al contrario, el cv. ‘Amiga’ presentó niveles más

bajos de metabolitos, mientras 'Fortuna' y 'Santa Clara' tenían niveles intermedios. Considerando que son diferentes cultivares y su selección se basa en el reflejo del fenotipo (visible y metabólico), era de esperar respuestas también diferentes durante la postcosecha de los frutos.

Cambios metabólicos en el fruto de fresa durante postcosecha

A continuación, aproximaciones estadísticas multivariantes, incluyendo agrupamiento jerárquico, análisis discriminante de mínimos cuadrados parciales y algoritmo *k*-means, se llevaron a cabo para destacar los cambios en el metabolismo durante la vida postcosecha de la fresa.

Metabolismo primario

Como es de esperar, ciertos cambios en el metabolismo primario deberían producirse durante la senescencia, debido a que parte de estos metabolitos pueden ser usados para proveer energía y precursores para soportar la maduración del fruto. De manera interesante, un pequeño grupo de metabolitos primarios destacó por diferenciar los frutos controles de las muestras de postcosecha y mostrar perfil parecido en los diferentes tratamientos y variedades. Esos metabolitos incluyen el ácido succínico, el galactinol, la putrescina y los aminoácidos GABA, β -alanina, glicina y prolina.

El GABA une el metabolismo del carbono con el del nitrógeno, jugando un papel clave en la regulación del pH, la energía y respiración celular. Su aumento en tejido vegetal se ha relacionado con diferentes situaciones de estrés abiótico, incluido frío y deficiencia en oxígeno (Michaeli and Fromm, 2015; Chiu *et al.*, 2015) y su incremento durante la postcosecha ya fue descrita en cítricos (Sun *et al.*, 2013; Tang *et al.*, 2016). La poliamina putrescina se ha relacionado con situaciones de estrés por frío y con la modulación de sistema antioxidante, y su degradación forma β -alanina y GABA (Rohloff *et al.*, 2012; Moreno *et al.*, 2018).

Los niveles de galactinol se mostraron especialmente altos en los frutos almacenados en atmósfera enriquecida en ozono. Ese metabolito ha sido descrito por su papel en respuesta de frío en melocotón y, además, se ha visto que podría tener una función antioxidante por su capacidad de actuar sobre las

especies reactivas del oxígeno (ROS) (Nishizawa *et al.*, 2008; Bustamante *et al.*, 2016).

Al ser comparados los tratamientos entre sí, destacaron dos azúcares fosfatos (glucosa- y fructosa-6-fosfato), que permitieron diferenciar fácilmente las muestras provenientes del tratamiento con ozono. Esos dos intermediarios metabólicos podrían ver aumentados sus niveles en presencia de ozono, tal vez por su mayor capacidad de captura de ROS si se comparan con metabolitos azúcares no fosfatos (Rohloff *et al.*, 2012).

Metabolismo secundario

Debido a su carácter sésil, la planta es incapaz de adaptarse al medio sin recurrir a metabolitos especiales. Es entendido que una de las funciones de este metabolismo especializado es ayudar a contender los diferentes estreses, bióticos y abióticos, a los cuales están sometidas. Estudios previos señalan que el contenido en polifenoles se podría ver afectado por el almacenamiento postcosecha y que uno de los parámetros clave en la estabilidad de estos compuestos es la temperatura (Jin *et al.*, 2011). Sorprendentemente, pocos cambios drásticos fueron observados en los perfiles de los polifenoles a lo largo de la postcosecha y ha sido difícil detectar algún patrón común entre las variedades. Se han contrastado los resultados y fue posible distinguir cambios principalmente observados en el descenso de la concentración de una serie de metabolitos respecto a los frutos usados como control, indicando el efecto que la postcosecha tiene sobre éstos. Por ejemplo, la pelargonidina hexosa, la principal antocianina responsable del color del fruto y cuya acumulación durante la postcosecha ha sido previamente descrita (Goulas *et al.*, 2015), muestra la tendencia descrita. Sin embargo, y no descartable, la baja temperatura de almacenamiento usada en este estudio posiblemente no favoreció la síntesis de antocianinas ni de los compuestos fenilpropanoides en general, esto debido a que la actividad de la enzima clave en esta ruta (PAL), se ha reportado altamente afectada por la temperatura (Holcroft and Kader, 1999). Sin embargo, altamente destacable el comportamiento del cv. 'Amiga', ya que es la única variedad cuyo contenido en flavonoides y elagitaninos fue incrementado ligeramente a lo largo

de la postcosecha. Curiosamente, es también la variedad que presentó niveles más bajos de metabolitos secundarios en los frutos controles.

Volátiles

La cantidad de compuestos volátiles generados y emanados al ambiente por el fruto está directamente influenciado por su estadio de madurez, por lo que fue de esperar cambios importantes durante su vida postcosecha influenciados por los tratamientos desarrollados en este estudio. De este modo, fue posible observar diferencias drásticas entre frutos control y los provenientes de los tratamientos de postcosecha. Una serie de compuestos fuertemente incrementados y otros disminuidos fue la tónica que ha marcado el análisis individual de este grupo en particular. Así, la atmósfera enriquecida en ozono provocó una atenuación en los cambios observados durante la postcosecha, por lo menos durante los tres primeros días de tratamiento. Este resultado es concordante con la observación de Pérez *et al.* (1999) y Nadas *et al.* (2003) que señalaron el uso de ozono como responsable del descenso de la emisión de volátiles.

La mayoría de los aldehídos, furanos, cetonas y terpenos presentaron una ligera disminución durante la postcosecha. Los aldehídos confieren notas inmaduras al aroma de fresa y disminuyen a lo largo de la maduración. Además, se ha visto que la actividad de enzimas clave en el metabolismo de los furanos disminuye fuertemente con el descenso de la temperatura y con el uso de atmósfera enriquecida en CO₂ (Li *et al.*, 2015; Fu *et al.*, 2017). Al contrario, los niveles de los esterres aumentan durante la maduración de la fresa, representando hasta el 90% de los volátiles presentes en frutos maduros, confiriéndoles un aroma frutal y floral. En los tres tratamientos de postcosecha, el contenido en esterres etílicos aumentó fuertemente en los frutos, mientras que el de los esterres metílicos disminuyó de manera importante. Esas diferencias podrían deberse a una baja síntesis de alcohol metílico, precursor de los esterres metílicos, mientras que el precursor de los esterres etílicos, el etanol, está muy inducido durante la postcosecha. Efectivamente, se observó un incremento importante de etanol, aunque el uso de atmósferas modificadas provocó un retraso inicial en su acumulación. Esta observación parece en contradicción con resultados previos

que destacaron que el uso de CO₂ favorece la producción de un aroma no deseado, por la formación de etanol y otros volátiles como consecuencia del metabolismo fermentativo del fruto (Ponce-Valadez *et al.*, 2009). Sin embargo, la directa comparación entre los tratamientos llevados a cabo entre los diferentes estudios no es posible.

En general, el análisis del metaboloma del fruto sometido a tratamientos de postcosecha ha permitido la identificación de una serie de procesos relacionados con estrés abiótico, como cambios debido a frío y estrés oxidativo, con evidencia en cambios del perfil aromático del fruto, que vienen determinados a su vez por cambios bioquímicos en el metabolismo central del fruto senescente. Los compuestos fenólicos se vieron menos afectados, posiblemente por el uso de bajas temperaturas. El tratamiento de ozono ha destacado por la fácil discriminación que sus datos producen al ser contrastados con el resto de los tratamientos en estudio.

Conclusiones generales

1. Ha sido identificado un gran número de QTL que putativamente controlan el contenido de metabolitos primarios y secundarios en la población de mapeo F1 '232' x '1392'.
2. Los QTL mayoritarios y estables detectados han sido propuestos como parte de las herramientas para el desarrollo moderno de nuevas variedades con características organolépticas y nutritivas superiores.
3. Se ha propuesto un gen candidato que controlaría la producción de ácido elágico hexosa y se han generado plantas transgénicas estables, que permitirán su comprobación mediante análisis funcional.

4. Se han propuesto regiones genómicas delimitadas por los QTL, las que posibilitarán la identificación de nuevos genes candidatos que controlen el contenido de diferentes metabolitos en el fruto de fresa.
5. Los tratamientos de postcosecha realizados en este estudio han producido cambios en el contenido de metabolitos primarios, secundarios y volátiles. Las diferencias más drásticas fueron observadas en compuestos relacionados con el aroma.
6. Análisis estadísticos multivariantes han permitido resaltar las características discriminatorias en el metabolismo senescente del fruto de fresa a través de los distintos tratamientos llevados a cabo.

References

- Adrian M, Jeandet P, Veneau J, Weston LA, Bessis R.** 1997. Biological activity of resveratrol, a stilbenic compound from grapevines, against *Botrytis cinerea*, the causal agent for gray mold. *Journal of Chemical Ecology* **23**, 1689–1702.
- Agar IT, Streif J, Bangerth F.** 1997. Effect of high CO₂ and controlled atmosphere (CA) on the ascorbic and dehydroascorbic acid content of some berry fruits. *Postharvest Biology and Technology* **11**, 47–55.
- Aharoni A, O'Connell AP.** 2002. Gene expression analysis of strawberry achene and receptacle maturation using DNA microarrays. *Journal of Experimental Botany* **53**, 2073–2087.
- Aked J.** 2002. Maintaining the postharvest quality of fruits and vegetables A2. In: Jongen W, ed. *Fruit and Vegetable Processing*. 119–149.
- Alamar MC, Collings E, Cools K, Terry LA.** 2017. Impact of controlled atmosphere scheduling on strawberry and imported avocado fruit. *Postharvest Biology and Technology* **134**, 76–86.
- Almeida JRM, D'Amico E, Preuss A, et al.** 2007. Characterization of major enzymes and genes involved in flavonoid and proanthocyanidin biosynthesis during fruit development in strawberry (*Fragaria × ananassa*). *Archives of Biochemistry and Biophysics* **465**, 61–71.
- Almenar E, Hernández-Muñoz P, Lagarón JM, Catalá R, Gavara R.** 2006. Controlled atmosphere storage of wild strawberry fruit (*Fragaria vesca* L.). *Journal of Agricultural and Food Chemistry* **54**, 86–91.
- Alseekh S, Tohge T, Wendenberg R, et al.** 2015. Identification and Mode of Inheritance of Quantitative Trait Loci for Secondary Metabolite Abundance in Tomato. *The Plant Cell* **27**, 485–512.
- Alvarez-Suarez JM, Giampieri F, Tulipani S, et al.** 2014. One-month strawberry-rich anthocyanin supplementation ameliorates cardiovascular risk, oxidative stress markers and platelet activation in humans. *Journal of Nutritional Biochemistry* **25**, 289–294.
- Argyris JM, Díaz A, Ruggieri V, Fernández M, Jahrmann T, Gibon Y, Picó B, Martín-Hernández AM, Monforte AJ, Garcia-Mas J.** 2017. QTL Analyses in Multiple Populations Employed for the Fine Mapping and Identification of Candidate Genes at a Locus Affecting Sugar Accumulation in Melon (*Cucumis melo* L.). *Frontiers in Plant Science* **8**.
- Ayala-Zavala JF, Wang SY, Wang CY, González-Aguilar GA.** 2004. Effect of storage temperatures on antioxidant capacity and aroma compounds in strawberry fruit. *LWT - Food Science and Technology* **37**, 687–695.
- Azzi-Achkouty S, Estephan N, Ouaini N, Rutledge DN.** 2017. Headspace solid-phase microextraction for wine volatile analysis. *Critical Reviews in Food Science and Nutrition* **57**,

2009–2020.

Bakker J, Bridle P, Bellworthy SJ. 1994. Strawberry juice colour: A study of the quantitative and qualitative pigment composition of juices from 39 genotypes. *Journal of the Science of Food and Agriculture* **64**, 31–37.

Ballester A-R, Tikunov Y, Molthoff J, Grandillo S, Viquez-Zamora M, de Vos R, de Maagd RA, van Heusden S, Bovy AG. 2016. Identification of Loci Affecting Accumulation of Secondary Metabolites in Tomato Fruit of a *Solanum lycopersicum* × *Solanum chmielewskii* Introgression Line Population. *Frontiers in Plant Science* **7**, 1–14.

Barceló M, El-Mansouri I, Mercado JA, Quesada MA, Alfaro FP. 1998. Regeneration and transformation via *Agrobacterium tumefaciens* of the strawberry cultivar Chandler. *Plant Cell, Tissue and Organ Culture* **54**, 29–36.

Bassil N V, Davis TM, Zhang H, et al. 2015. Development and preliminary evaluation of a 90 K Axiom® SNP array for the allo-octoploid cultivated strawberry *Fragaria* × *ananassa*. *BMC Genomics* **16**, 155.

Batley N, Le Mière P, Tehranifar A, Cekic C, Taylor S, Shrikes K, Hadley P, Greenland A, Darby J, Wilkinson M. 1998. Genetic and environmental control of flowering in strawberry. In: Gray D., In: Cockshull K., In: Seymore G., In: Thomas B, eds. Genetic and environmental manipulation of horticultural crops. Wallingford, UK, 111–131.

Beauvoit B, Belouah I, Bertin N, et al. 2018. Putting primary metabolism into perspective to obtain better fruits. *Annals of Botany* **122**, 1–21.

Begou O, Gika HG, Wilson ID, Theodoridis G. 2017. Hyphenated MS-based targeted approaches in metabolomics. *The Analyst* **142**, 3079–3100.

Bogs J. 2005. Proanthocyanidin Synthesis and Expression of Genes Encoding Leucoanthocyanidin Reductase and Anthocyanidin Reductase in Developing Grape Berries and Grapevine Leaves. *Plant Physiology* **139**, 652–663.

Bontpart T, Cheynier V, Ageorges A, Terrier N. 2015. BAHD or SCPL acyltransferase? What a dilemma for acylation in the world of plant phenolic compounds. *New Phytologist* **208**, 695–707.

Bontpart T, Marlin T, Vialet S, Guiraud JL, Pinasseau L, Meudec E, Sommerer N, Cheynier V, Terrier N. 2016. Two shikimate dehydrogenases, VvSDH3 and VvSDH4, are involved in gallic acid biosynthesis in grapevine. *Journal of Experimental Botany* **67**, 3537–3550.

Bouchereau A, Aziz A, Larher F, Martin-Tanguy J. 1999. Polyamines and environmental challenges: recent development. *Plant Science* **140**, 103–125.

Bustamante CA, Monti LL, Gabilondo J, Scossa F, Valentini G, Budde CO, Lara M V., Fernie AR, Drincovich MF. 2016. Differential Metabolic Rearrangements after Cold Storage Are Correlated with Chilling Injury Resistance of Peach Fruits. *Frontiers in Plant Science* **7**, 1–15.

Le Cao KA, Rohart F, Gonzalez I, Dejean S, Gautier B, Bartolo F, Monget P, Coquery J, Yao F, Liquet B. 2017. mixOmics: Omics Data Integration Project. R package version 6.3.1.

Capel C, Yuste-Lisbona FJ, López-Casado G, Angosto T, Heredia A, Cuartero J, Fernández-Muñoz R, Lozano R, Capel J. 2017. QTL mapping of fruit mineral contents provides new chances for molecular breeding of tomato nutritional traits. *Theoretical and Applied Genetics* **130**, 903–913.

Carbone F, Preuss A, De Vos RCH, D'Amico E, Perrotta G, Bovy AG, Martens S, Rosati C. 2009. Developmental, genetic and environmental factors affect the expression of flavonoid genes, enzymes and metabolites in strawberry fruits. *Plant, Cell and Environment* **32**, 1117–1131.

Casañal A, Zander U, Muñoz C, Dupeux F, Luque I, Botella MA, Schwab W, Valpuesta V, Marquez JA. 2013. The strawberry pathogenesis-related 10 (PR-10) Fra a proteins control flavonoid biosynthesis by binding to metabolic intermediates. *Journal of Biological Chemistry* **288**, 35322–35332.

Castro P, Lewers KS. 2016. Identification of quantitative trait loci (QTL) for fruit-quality traits and number of weeks of flowering in the cultivated strawberry. *Molecular Breeding* **36**, 1–19.

Centeno DC, Osorio S, Nunes-Nesi A, et al. 2011. Malate Plays a Crucial Role in Starch Metabolism, Ripening, and Soluble Solid Content of Tomato Fruit and Affects Postharvest Softening. *The Plant Cell* **23**, 162–184.

Chambers A, Carle S, Njuguna W, Chamala S, Bassil N, Whitaker VM, Barbazuk WB, Folta KM. 2013. A genome-enabled, high-throughput, and multiplexed fingerprinting platform for strawberry (*Fragaria L.*). *Molecular Breeding* **31**, 615–629.

Chambers AH, Pillet J, Plotto A, Bai J, Whitaker VM, Folta KM. 2014. Identification of a strawberry flavor gene candidate using an integrated genetic-genomic-analytical chemistry approach. *BMC genomics* **15**, 217.

Chen J, Mao L, Lu W, Ying T, Luo Z. 2016. Transcriptome profiling of postharvest strawberry fruit in response to exogenous auxin and abscisic acid. *Planta* **243**, 183–197.

Chiu GZ, Shelp BJ, Bowley SR, DeEll JR, Bozzo GG. 2015. Controlled atmosphere-related injury in 'Honeycrisp' apples is associated with γ -aminobutyrate accumulation. *Canadian Journal of Plant Science* **95**, 879–886.

Churchill GA, Doerge RW. 1994. Empirical threshold values for quantitative trait mapping. *Genetics* **138**, 963–971.

Coberly LC, Rausher MD. 2003. Analysis of a chalcone synthase mutant in *Ipomoea purpurea* reveals a novel function for flavonoids: Amelioration of heat stress. *Molecular Ecology* **12**, 1113–1124.

Collard BCY, Jahufer MZZ, Brouwer JB, Pang ECK. 2005. An introduction to markers,

quantitative trait loci (QTL) mapping and marker-assisted selection for crop improvement: The basic concepts. *Euphytica* **142**, 169–196.

Cordenunsi BR, Genovese MI, Oliveira Do Nascimento JR, Aymoto Hassimotto NM, José Dos Santos R, Lajolo FM. 2005. Effects of temperature on the chemical composition and antioxidant activity of three strawberry cultivars. *Food Chemistry* **91**, 113–121.

Crespo P, Giné J, Terry LA, Carlen C. 2010. Characterisation of major taste and health-related compounds of four strawberry genotypes grown at different Swiss production sites. *Food Chemistry* **122**, 16–24.

Cruz-Mendivil A, López-Valenzuela JA, Calderón-Vázquez CL, Vega-García MO, Reyes-Moreno C, Valdez-Ortiz A. 2015. Transcriptional changes associated with chilling tolerance and susceptibility in 'Micro-Tom' tomato fruit using RNA-Seq. *Postharvest Biology and Technology* **99**, 141–151.

Cruz-Rus E, Sesmero R, Ángel-Pérez JA, Sánchez-Sevilla JF, Ulrich D, Amaya I. 2017. Validation of a PCR test to predict the presence of flavor volatiles mesifurane and γ -decalactone in fruits of cultivated strawberry (*Fragaria* \times *ananassa*). *Molecular Breeding* **37**, 131.

Curtolo M, Cristofani-Yaly M, Gazaffi R, Takita MA, Figueira A, Machado MA. 2017. QTL mapping for fruit quality in Citrus using DArTseq markers. *BMC Genomics* **18**, 1–16.

Davik J, Koehler G, From B, Torp T, Rohloff J, Eidem P, Wilson RC, Sønsteby A, Randall SK, Alsheikh M. 2013. Dehydrin, alcohol dehydrogenase, and central metabolite levels are associated with cold tolerance in diploid strawberry (*Fragaria* spp.). *Planta* **237**, 265–277.

DeBolt S, Cook DR, Ford CM. 2006. L-tartaric acid synthesis from vitamin C in higher plants. *Proceedings of the National Academy of Sciences of the United States of America* **103**, 5608–13.

Deluc LG, Quilici DR, Decendit A, Grimplet J, Wheatley MD, Schlauch KA, Mérillon JM, Cushman JC, Cramer GR. 2009. Water deficit alters differentially metabolic pathways affecting important flavor and quality traits in grape berries of Cabernet Sauvignon and Chardonnay. *BMC Genomics* **10**, 1–33.

Denzel K, Schilling G, Gross GG. 1988. Biosynthesis of gallotannins. Enzymatic conversion of 1,6-digalloylglucose to 1,2,6-trigalloylglucose. *Planta* **176**, 135–137.

Dercks W, Creasy LL. 1989. The significance of stilbene phytoalexins in the *Plasmopara viticola*-grapevine interaction. *Physiological and Molecular Plant Pathology* **34**, 189–202.

Dettmer K, Aronov PA, Hammock BD. 2007. Mass spectrometry-based metabolomics. *Mass Spectrometry Reviews* **26**, 51–78.

Diamanti J, Capocasa F, Balducci F, Battino M, Hancock J, Mezzetti B. 2012. Increasing Strawberry Fruit Sensorial and Nutritional Quality Using Wild and Cultivated Germplasm. *PLoS ONE* **7**.

- Dijk T Van, Pagliarani G, Pikunova A, Noordijk Y, Yilmaz-temel H, Meulenbroek B, Visser RGF, Weg E Van De.** 2014. Genomic rearrangements and signatures of breeding in the allo-octoploid strawberry as revealed through an allele dose based SSR linkage map. *BMC plant biology*, 1–16.
- Ding Y, Chang J, Ma Q, et al.** 2015. Network Analysis of Postharvest Senescence Process in Citrus Fruits Revealed by Transcriptomic and Metabolomic Profiling. *Plant Physiology* **168**, 357–376.
- Dirlewanger E, Cosson P, Tavaud M, Aranzana M, Poizat C, Zanetto A, Arús P, Laigret F.** 2002. Development of microsatellite markers in peach [*Prunus persica* (L.) Batsch] and their use in genetic diversity analysis in peach and sweet cherry (*Prunus avium* L.). *Theoretical and Applied Genetics* **105**, 127–138.
- Dobson P, Graham J, Stewart D, Brennan R, Hackett CA, McDougall GJ.** 2012. Over-seasons analysis of quantitative trait loci affecting phenolic content and antioxidant capacity in raspberry. *Journal of Agricultural and Food Chemistry* **60**, 5360–5366.
- Doerge RW.** 2002. Mapping and analysis of quantitative trait loci in experimental populations. *Nature Reviews Genetics* **3**, 43.
- Du X, Song M, Rouseff R.** 2011. Identification of new strawberry sulfur volatiles and changes during maturation. *Journal of Agricultural and Food Chemistry* **59**, 1293–1300.
- Dunemann F, Ulrich D, Malysheva-Otto L, Weber WE, Longhi S, Velasco R, Costa F.** 2012. Functional allelic diversity of the apple alcohol acyl-transferase gene *MdAAT1* associated with fruit ester volatile contents in apple cultivars. *Molecular Breeding* **29**, 609–625.
- Edger PP, VanBuren R, Colle M, et al.** 2018. Single-molecule sequencing and optical mapping yields an improved genome of woodland strawberry (*Fragaria vesca*) with chromosome-scale contiguity. *GigaScience* **7**, 1–7.
- Eduardo I, Chietera G, Pirona R, Pacheco I, Troggio M, Banchi E, Bassi D, Rossini L, Vecchietti A, Pozzi C.** 2013. Genetic dissection of aroma volatile compounds from the essential oil of peach fruit: QTL analysis and identification of candidate genes using dense SNP maps. *Tree Genetics & Genomes* **9**, 189–204.
- Ernst M, Silva DB, Silva RR, Vêncio RZN, Lopes NP.** 2014. Mass spectrometry in plant metabolomics strategies: from analytical platforms to data acquisition and processing. *Natural product reports* **31**, 784–806.
- Eshed Y, Zamir D.** 1995. An introgression line population of *Lycopersicon pennellii* in the cultivated tomato enables the identification and fine mapping of yield-associated QTL. *Genetics* **141**, 1147–62.
- Fait A, Hanhineva K, Beleggia R, Dai N, Rogachev I, Nikiforova VJ, Fernie AR, Aharoni A.**

2008a. Reconfiguration of the achene and receptacle metabolic networks during strawberry fruit development. *Plant physiology* **148**, 730–750.

Fait A, Hanhineva K, Beleggia R, Dai N, Rogachev I, Nikiforova VJ, Fernie AR, Aharoni A. 2008b. Reconfiguration of the achene and receptacle metabolic networks during strawberry fruit development. *Plant physiology* **148**, 730–750.

Farneti B, Di Guardo M, Khomenko I, Cappellin L, Biasioli F, Velasco R, Costa F. 2017. Genome-wide association study unravels the genetic control of the apple volatilome and its interplay with fruit texture. *Journal of Experimental Botany* **68**, 1467–1478.

Feliziani E, Romanazzi G. 2016. Postharvest decay of strawberry fruit: Etiology, epidemiology, and disease management. *Journal of Berry Research* **6**, 47–63.

Fiehn O, Wohlgemuth G, Scholz M, Kind T, Lee DY, Lu Y, Moon S, Nikolau B. 2008. Quality control for plant metabolomics: Reporting MSI-compliant studies. *Plant Journal* **53**, 691–704.

Forbes-Hernandez TY, Gasparrini M, Afrin S, Bompadre S, Mezzetti B, Quiles JL, Giampieri F, Battino M. 2016. The Healthy Effects of Strawberry Polyphenols: Which Strategy behind Antioxidant Capacity? *Critical Reviews in Food Science and Nutrition* **56**, S46–S59.

Forney CF, Kalt W, Jordan M a. 2000. The composition of strawberry aroma is influenced by cultivar, maturity, and storage. *HortScience* **35**, 1022–1026.

Fournier-Level A, Le Cunff L, Gomez C, Doligez A, Ageorges A, Roux C, Bertrand Y, Souquet JM, Cheynier V, This P. 2009. Quantitative genetic bases of anthocyanin variation in grape (*Vitis vinifera* L. ssp. *sativa*) berry: A quantitative trait locus to quantitative trait nucleotide integrated study. *Genetics* **183**, 1127–1139.

Fu X, Cheng S, Zhang Y, Du B, Feng C, Zhou Y, Mei X, Jiang Y, Duan X, Yang Z. 2017a. Differential responses of four biosynthetic pathways of aroma compounds in postharvest strawberry (*Fragaria × ananassa* Duch.) under interaction of light and temperature. *Food Chemistry* **221**, 356–364.

Fu Y-B, Yang M-H, Zeng F, Biligetü B. 2017b. Searching for an Accurate Marker-Based Prediction of an Individual Quantitative Trait in Molecular Plant Breeding. *Frontiers in Plant Science* **8**, 1–12.

Galli V, da Silva Messias R, Perin EC, Borowski JM, Bamberg AL, Rombaldi CV. 2016. Mild salt stress improves strawberry fruit quality. *LWT - Food Science and Technology* **73**, 693–699.

Giampieri F, Forbes-Hernandez TY, Gasparrini M, Alvarez-Suarez JM, Afrin S, Bompadre S, Quiles JL, Mezzetti B, Battino M. 2015. Strawberry as a health promoter: an evidence based review. *Food Funct.* **6**, 1386–1398.

Giampieri F, Tulipani S, Alvarez-Suarez JM, Quiles JL, Mezzetti B, Battino M. 2012. The strawberry: Composition, nutritional quality, and impact on human health. *Nutrition* **28**, 9–19.

- Giavalisco P, Li Y, Matthes A, Eckhardt A, Hubberten HM, Hesse H, Segu S, Hummel J, Köhl K, Willmitzer L.** 2011. Elemental formula annotation of polar and lipophilic metabolites using ^{13}C , ^{15}N and ^{34}S isotope labelling, in combination with high-resolution mass spectrometry. *Plant Journal* **68**, 364–376.
- Gil MI, Holcroft DM, Kader AA.** 1997. Changes in Strawberry Anthocyanins and Other Polyphenols in Response to Carbon Dioxide Treatments. *Journal of Agricultural and Food Chemistry* **45**, 1662–1667.
- Gill SS, Tuteja N.** 2010. Polyamines and abiotic stress tolerance in plants. *Plant Signaling & Behavior* **5**, 26–33.
- Gillaspy G, Ben-David H, Gruissem W.** 1993. Fruits : A Developmental Perspective. *Plant Cell* **5**, 1439–1451.
- Giovannoni J.** 2004. Genetic regulation of fruit development and ripening. *The Plant Cell Online* **16**, 170–181.
- Gorny JR, Kader AA.** 1996. Regulation of ethylene biosynthesis in climacteric apple fruit by elevated CO_2 and reduced O_2 atmospheres. *Postharvest Biology and Technology* **9**, 311–323.
- Goulas V, Manganaris GA.** 2011. The effect of postharvest ripening on strawberry bioactive composition and antioxidant potential. *Journal of the Science of Food and Agriculture* **91**, 1907–1914.
- Goulas V, Minas IS, Kourdoulas PM, Lazaridou A, Molassiotis AN, Gerothanassis IP, Manganaris GA.** 2015. ^1H NMR Metabolic Fingerprinting to Probe Temporal Postharvest Changes on Qualitative Attributes and Phytochemical Profile of Sweet Cherry Fruit. *Frontiers in Plant Science* **6**, 1–11.
- Griesser M, Hoffmann T, Bellido ML, Rosati C, Fink B, Kurtzer R, Aharoni A, Muñoz-Blanco J, Schwab W.** 2008. Redirection of flavonoid biosynthesis through the down-regulation of an anthocyanidin glucosyltransferase in ripening strawberry fruit. *Plant physiology* **146**, 1528–1539.
- Gromski PS, Muhamadali H, Ellis DI, Xu Y, Correa E, Turner ML, Goodacre R.** 2015. A tutorial review: Metabolomics and partial least squares-discriminant analysis - a marriage of convenience or a shotgun wedding. *Analytica Chimica Acta* **879**, 10–23.
- Grover A, Sharma PC.** 2016. Development and use of molecular markers: Past and present. *Critical Reviews in Biotechnology* **36**, 290–302.
- Gupta K, Dey A, Gupta B.** 2013. Plant polyamines in abiotic stress responses. *Acta Physiologiae Plantarum* **35**, 2015–2036.
- Hackett CA.** 2002. Statistical methods for QTL mapping in cereals. *Plant Molecular Biology* **48**, 585–599.

- Halbwirth H, Puhl I, Haas U, Jezik K, Treutter D, Stich K.** 2006. Two-phase flavonoid formation in developing strawberry (*Fragaria x ananassa*) fruit. *Journal of Agricultural and Food Chemistry* **54**, 1479–1485.
- Han Y, Dang R, Li J, Jiang J, Zhang N, Jia M, Wei L, Li Z, Li B, Jia W.** 2015. SUCROSE NONFERMENTING1-RELATED PROTEIN KINASE2.6, an ortholog of OPEN STOMATA1, is a negative regulator of strawberry fruit development and ripening. *Plant physiology* **167**, 915–30.
- Hancock JF.** 1999. *Strawberries*. New York, NY: CABI.
- Hanhineva K.** 2011. Recent Advances in Strawberry Metabolomics. *Genes, Genomes and Genomics* **5**, 65–75.
- Hannum SM.** 2004. Potential Impact of Strawberries on Human Health : A Review of the Science Potential Impact of Strawberries on Human Health : A Review. *Critical Reviews in Food Science and Nutrition* **44**, 1–17.
- Heigh DF.** 1956. Volatile compounds produced by apples. I. Aldehydes and ketones. *Journal of the Science of Food and Agriculture* **7**, 396–411.
- Hoffmann L.** 2004. Silencing of Hydroxycinnamoyl-Coenzyme A Shikimate / Quinate Hydroxycinnamoyltransferase Affects Phenylpropanoid Biosynthesis. **16**, 1446–1465.
- Hoffmann T, Kalinowski G, Schwab W.** 2006. RNAi-induced silencing of gene expression in strawberry fruit (*Fragaria x ananassa*) by agroinfiltration: A rapid assay for gene function analysis. *Plant Journal* **48**, 818–826.
- Hoffmann T, Kurtzer R, Skowranek K, Kießling P, Fridman E, Pichersky E, Schwab W.** 2011. Metabolic engineering in strawberry fruit uncovers a dormant biosynthetic pathway. *Metabolic Engineering* **13**, 527–531.
- Holcroft DM, Kader AA.** 1999. Carbon dioxide-induced changes in color and anthocyanin synthesis of stored strawberry fruit. *HortScience* **34**, 1244–1248.
- Hu LY, Hu SL, Wu J, Li YH, Zheng JL, Wei ZJ, Liu J, Wang HL, Liu YS, Zhang H.** 2012. Hydrogen sulfide prolongs postharvest shelf life of strawberry and plays an antioxidative role in fruits. *Journal of Agricultural and Food Chemistry* **60**, 8684–8693.
- Isobe SN, Hirakawa H, Sato S, et al.** 2013. Construction of an Integrated High Density Simple Sequence Repeat Linkage Map in Cultivated Strawberry (*Fragaria x ananassa*) and its Applicability. *DNA Research* **20**, 79–92.
- Jansen RC.** 1993. Interval mapping of multiple quantitative trait loci. *Genetics* **135**, 205 LP-211.
- Jansen RC, Stam P.** 1994. High resolution of quantitative traits into multiple loci via interval mapping. *Genetics* **136**, 1447 LP-1455.
- Jetti RR, Yang E, Kurnianta A, Finn C, Qian MC.** 2007. Quantification of selected aroma-active

compounds in strawberries by headspace solid-phase microextraction gas chromatography and correlation with sensory descriptive analysis. *Journal of Food Science* **72**.

Jia H-F, Chai Y-M, Li C-L, Lu D, Luo J-J, Qin L, Shen Y-Y. 2011. Abscisic Acid Plays an Important Role in the Regulation of Strawberry Fruit Ripening. *Plant Physiology* **157**, 188–199.

Jia H, Wang Y, Sun M, et al. 2013. Sucrose functions as a signal involved in the regulation of strawberry fruit development and ripening. *New Phytologist* **198**, 453–465.

Jin P, Wang SY, Wang CY, Zheng Y. 2011. Effect of cultural system and storage temperature on antioxidant capacity and phenolic compounds in strawberries. *Food Chemistry* **124**, 262–270.

Johnson AL, Govindarajulu R, Ashman T. 2014. Bioclimatic evaluation of geographical range in *Fragaria* (Rosaceae): consequences of variation in breeding system, ploidy and species age. *Botanical Journal of the Linnean Society* **176**, 99–114.

Jonsson P, Gullberg J, Nordström A, Kusano M, Kowalczyk M, Sjöström M, Moritz T. 2004. A Strategy for Identifying Differences in Large Series of Metabolomic Samples Analyzed by GC/MS. *Analytical Chemistry* **76**, 1738–1745.

Josuttis M, Verrall S, Stewart D, Kru E, Mcdougall GJ. 2013. Genetic and Environmental Effects on Tannin Composition in Strawberry (*Fragaria × ananassa*) Cultivars Grown in Different European Locations. *Journal of Agricultural and Food Chemistry* **61**, 790–800.

Jung S, Staton M, Lee T, Blenda A, Svancara R, Abbott A, Main D. 2008. GDR (Genome Database for Rosaceae): Integrated web-database for Rosaceae genomics and genetics data. *Nucleic Acids Research* **36**, 1034–1040.

Kader AA. 2003. Atmosphere modification. In: Bartz JA, In: Brecht JK, eds. *Postharvest physiology and pathology of vegetables*. New York, NY, 229–246.

Kallio H, Hakala M, Pelkkikangas AM, Lapveteläinen A. 2000. Sugars and acids of strawberry varieties. *European Food Research and Technology* **212**, 81–85.

Kanungo T, Mount DM, Netanyahu NS, Piatko CD, Silverman R, Wu AY. 2002. An efficient k-means clustering algorithm: analysis and implementation. *IEEE Transactions on Pattern Analysis and Machine Intelligence* **24**, 881–892.

Kaplan F, Kopka J, Sung DY, Zhao W, Popp M, Porat R, Guy CL. 2007. Transcript and metabolite profiling during cold acclimation of *Arabidopsis* reveals an intricate relationship of cold-regulated gene expression with modifications in metabolite content. *Plant Journal* **50**, 967–981.

Karimi M, Inze D, Depicker A. 2002. GATEWAY vectors for *Agrobacterium*-mediated plant transformation. *Trends in Plant Science* **7**, 193–195.

Ke D, Zhou L, Kader AA. 1994. Mode of Oxygen and Carbon Dioxide Action on Strawberry Ester Biosynthesis. *J. Amer. Soc. Hort. Sci.* **119**, 971–975.

- Keurentjes JJB, Fu J, de Vos CHR, Lommen A, Hall RD, Bino RJ, van der Plas LHW, Jansen RC, Vreugdenhil D, Koornneef M.** 2006. The genetics of plant metabolism. *Nature Genetics* **38**, 842–849.
- Khan SA, Chibon PY, De Vos RCH, et al.** 2012. Genetic analysis of metabolites in apple fruits indicates an mQTL hotspot for phenolic compounds on linkage group 16. *Journal of Experimental Botany* **63**, 2895–2908.
- Klee HJ.** 2010. Improving the flavor of fresh fruits: Genomics, biochemistry, and biotechnology. *New Phytologist* **187**, 44–56.
- Klee HJ, Giovannoni JJ.** 2011. Genetics and control of tomato fruit ripening and quality attributes. *Annual Review of Genetics* **45**, 41–59.
- Kobayashi H, Naciri-Graven Y, Broughton WJ, Perret X.** 2004. Flavonoids induce temporal shifts in gene-expression of nod-box controlled loci in *Rhizobium* sp. NGR234. *Molecular Microbiology* **51**, 335–347.
- Kolde R.** 2015. pheatmap: Pretty Heatmaps. R package version 1.0.8.
- Kopka J, Schauer N, Krueger S, et al.** 2005. GMD@CSB.DB: The Golm metabolome database. *Bioinformatics* **21**, 1635–1638.
- Koyuncu M, Dilmaçunal T.** 2010. Determination of vitamin C and organic acid changes in strawberry by HPLC during cold storage. *Notulae Botanicae Horti Agrobotanici Cluj-Napoca* **38**, 95–98.
- Lander ES, Botstein S.** 1989. Mapping mendelian factors underlying quantitative traits using RFLP linkage maps. *Genetics* **121**, 185.
- Lauxmann MA, Brun B, Borsani J, Bustamante CA, Budde CO, Lara M V., Drincovich MF.** 2012. Transcriptomic Profiling during the Post-Harvest of Heat-Treated Dixiland *Prunus persica* Fruits: Common and Distinct Response to Heat and Cold. *PLoS ONE* **7**, 1–16.
- Van Leeuwen C, Destrac-Irvine A, Ollat N.** 2017. Modified grape composition under climate change conditions requires adaptations in the vineyard. *Journal International des Sciences de la Vigne et du Vin* **51**, 147–154.
- Lehman EL.** 1975. *Nonparametrics*. New York, NY.
- Lepiniec L, Debeaujon I, Routaboul J-M, Baudry A, Pourcel L, Nesi N, Caboche M.** 2006. Genetics and Biochemistry of Seed Flavonoids. *Annual Review of Plant Biology* **57**, 405–430.
- Lerceteau-Köhler E, Guérin G, Laigret F, Denoyes-Rothan B.** 2003. Characterization of mixed disomic and polysomic inheritance in the octoploid strawberry (*Fragaria x ananassa*) using AFLP mapping. *Theoretical and Applied Genetics* **107**, 619–628.
- Lerceteau-Köhler E, Moing A, Guérin G, Renaud C, Petit A, Rothan C, Denoyes B.** 2012.

Genetic dissection of fruit quality traits in the octoploid cultivated strawberry highlights the role of homoeo-QTL in their control. *TAG. Theoretical and applied genetics* **124**, 1059–77.

Lester GE. 2006. Environmental Regulation of Human Health Nutrients (Ascorbic Acid , 13-Carotene , and Folic Acid) in Fruits and Vegetables. *HortScience* **41**, 59–64.

Li L, Li D, Luo Z, Huang X, Li X. 2016. Proteomic Response and Quality Maintenance in Postharvest Fruit of Strawberry (*Fragaria × ananassa*) to Exogenous Cytokinin. *Scientific Reports* **6**, 1–11.

Li L, Luo Z, Huang X, Zhang L, Zhao P, Ma H, Li X, Ban Z, Liu X. 2015. Label-free quantitative proteomics to investigate strawberry fruit proteome changes under controlled atmosphere and low temperature storage. *Journal of Proteomics* **120**, 44–57.

Lisec J, Meyer RC, Steinfath M, et al. 2008. Identification of metabolic and biomass QTL in *Arabidopsis thaliana* in a parallel analysis of RIL and IL populations. *Plant Journal* **53**, 960–972.

Liston A, Cronn R, Ashman TL. 2014. *Fragaria*: A genus with deep historical roots and ripe for evolutionary and ecological insights. *American Journal of Botany* **101**, 1686–1699.

Liu B-H. 1998. *Genomics: Linkage Mapping and QTL Analysis*. Boca Raton, Florida.

Liu DJ, Chen JY, Lu WJ. 2011. Expression and regulation of the early auxin-responsive Aux/IAA genes during strawberry fruit development. *Molecular Biology Reports* **38**, 1187–1193.

Liu Y, Gao L, Liu L, Yang Q, Lu Z, Nie Z, Wang Y, Xia T. 2012. Purification and characterization of a novel galloyltransferase involved in catechin galloylation in the tea plant (*Camellia sinensis*). *Journal of Biological Chemistry* **287**, 44406–44417.

López MG, Zanon MI, Pratta GR, et al. 2015. Metabolic analyses of interspecific tomato recombinant inbred lines for fruit quality improvement. *Metabolomics* **11**, 1416–1431.

Luedemann A, Strassburg K, Erban A, Kopka J. 2008. TagFinder for the quantitative analysis of gas chromatography - Mass spectrometry (GC-MS)-based metabolite profiling experiments. *Bioinformatics* **24**, 732–737.

Luengwilai K, Beckles DM, Pluemjit O, Siriphanich J. 2014. Postharvest quality and storage life of 'Makapuno' coconut (*Cocos nucifera* L.). *Scientia Horticulturae* **175**, 105–110.

Lum GB, Brikis CJ, Deyman KL, Subedi S, DeEil JR, Shelp BJ, Bozzo GG. 2016. Pre-storage conditioning ameliorates the negative impact of 1-methylcyclopropene on physiological injury and modifies the response of antioxidants and γ -aminobutyrate in 'Honeycrisp' apples exposed to controlled-atmosphere conditions. *Postharvest Biology and Technology* **116**, 115–128.

Lunkenbein S, Salentijn EMJ, Coiner H a., Boone MJ, Krens F a., Schwab W. 2006. Up- and down-regulation of *Fragaria × ananassa* O-methyltransferase: Impacts on furanone and phenylpropanoid metabolism. *Journal of Experimental Botany* **57**, 2445–2453.

- Ma B, Zhao S, Wu B, et al.** 2016. Construction of a high density linkage map and its application in the identification of QTLs for soluble sugar and organic acid components in apple. *Tree Genetics and Genomes* **12**, 1–10.
- Macheix JJ, Fleuriet A.** 1993. Phenolics in fruits and fruit products: progress and prospects. In: Scalbert A, ed. *Polyphenolic Phenomena*. Paris, France, 157–163.
- Mandal SM, Chakraborty D, Dey S.** 2010. Phenolic acids act as signaling molecules in plant-microbe symbioses. *Plant Signaling and Behavior* **5**, 359–368.
- Mangaraj S, Goswami TK.** 2009. Modified atmosphere packaging—an ideal food preservation technique. *J Food Sci Tech.* **46**, 399–410.
- Mattila P, Kumpulainen J.** 2002. Determination of free and total phenolic acids in plant-derived foods by HPLC with diode-array detection. *Journal of Agricultural and Food Chemistry* **50**, 3660–3667.
- Mazzoni L, Perez-Lopez P, Giampieri F, Alvarez-Suarez JM, Gasparrini M, Forbes-Hernandez TY, Quiles JL, Mezzetti B, Battino M.** 2016. The genetic aspects of berries: From field to health. *Journal of the Science of Food and Agriculture* **96**, 365–371.
- McAtee P, Karim S, Schaffer R, David K.** 2013. A dynamic interplay between phytohormones is required for fruit development, maturation, and ripening. *Frontiers in Plant Science* **4**, 1–7.
- Medina-Minguez JJ.** 2017. *Distribución Varietal en el Cultivo de Fresa en Huelva. Campaña 2016-2017*. Sevilla.
- Medina-Puche L, Cumplido-Laso G, Amil-Ruiz F, Hoffmann T, Ring L, Rodríguez-Franco A, Caballero JL, Schwab W, Muñoz-Blanco J, Blanco-Portales R.** 2014. MYB10 plays a major role in the regulation of flavonoid/phenylpropanoid metabolism during ripening of *Fragaria × ananassa* fruits. *Journal of Experimental Botany* **65**, 401–417.
- Meir S, Naiman D, Akerman M, Hyman JY, Zauberman G, Fuchs Y.** 1997. Prolonged storage of 'Hass' avocado fruit using modified atmosphere packaging. *Postharvest Biology and Technology* **12**, 51–60.
- Mellidou I, Buts K, Hatoum D, et al.** 2014. Transcriptomic events associated with internal browning of apple during postharvest storage. *BMC Plant Biology* **14**, 1–17.
- Ménager I, Jost M, Aubert C.** 2004. Changes in Physicochemical Characteristics and Volatile Constituents of Strawberry (Cv. Cigaline) during Maturation. *Journal of Agricultural and Food Chemistry* **52**, 1248–1254.
- Michaeli S, Fromm H.** 2015. Closing the loop on the GABA shunt in plants: are GABA metabolism and signaling entwined? *Frontiers in Plant Science* **6**, 1–7.
- Mishra R, Kar A.** 2014. Effect of storage on the physicochemical and flavour attributes of two

cultivars of strawberry cultivated in Northern India. *The Scientific World Journal* **2014**.

Miszczak A, Forney CF, Prange RK. 1995. Development of aroma volatiles and color during postharvest ripening of 'kent' strawberries. *Journal of American Society for Horticultural Science* **120**, 650–655.

Mitcham EJ. 2004. Strawberry. In: Gross KC,, In: Wang CY,, In: Saltveit ME, eds. *The Commercial Storage of Fruits, Vegetables, and Florist and Nursery Crops*.

Mittasch J, Böttcher C, Frolova N, Bönn M, Milkowski C. 2014. Identification of UGT84A13 as a candidate enzyme for the first committed step of gallotannin biosynthesis in pedunculate oak (*Quercus robur*). *Phytochemistry* **99**, 44–51.

Molina-Hidalgo FJ, Franco AR, Villatoro C, Medina-Puche L, Mercado J a., Hidalgo M a., Monfort A, Caballero JL, Muñoz-Blanco J, Blanco-Portales R. 2013. The strawberry (*Fragaria×ananassa*) fruit-specific rhamnogalacturonate lyase 1 (FaRGLyase1) gene encodes an enzyme involved in the degradation of cell-wall middle lamellae. *Journal of Experimental Botany* **64**, 1471–1483.

Monforte AJ, Friedman E, Zamir D, Tanksley SD. 2001. Comparison of a set of allelic QTL-NILs for chromosome 4 of tomato: Deductions about natural variation and implications for germplasm utilization. *Theoretical and Applied Genetics* **102**, 572–590.

Moose SP, Mumm RH. 2008. Molecular Plant Breeding as the Foundation for 21st Century Crop Improvement. *Plant Physiology* **147**, 969–977.

Moreira N, Lopes P, Cabral M, Guedes de Pinho P. 2016. HS-SPME/GC-MS methodologies for the analysis of volatile compounds in cork material. *European Food Research and Technology* **242**, 457–466.

Moreno AS, Perotti VE, Margarit E, Bello F, Vázquez DE, Podestá FE, Tripodi KEJ. 2018. Metabolic profiling and quality assessment during the postharvest of two tangor varieties subjected to heat treatments. *Postharvest Biology and Technology* **142**, 10–18.

Motilva MJ, Serra A, Macià A. 2013. Analysis of food polyphenols by ultra high-performance liquid chromatography coupled to mass spectrometry: An overview. *Journal of Chromatography A* **1292**, 66–82.

Mouradov A, Spangenberg G. 2014. Flavonoids: a metabolic network mediating plants adaptation to their real estate. *Frontiers in Plant Science* **5**, 1–16.

Mullen W, Yokota T, Lean MEJ, Crozier A. 2003. Analysis of ellagitannins and conjugates of ellagic acid and quercetin in raspberry fruits by LC-MSn. *Phytochemistry* **64**, 617–624.

Nadas A, Olmo M, García JM. 2003. Growth of *Botrytis cinerea* and strawberry quality in ozone-enriched atmospheres. *Journal of Food Science* **68**, 1798–1802.

- Niehaus JU, Gross GG.** 1997. A Gallotannin Degrading Esterase From Leaves of Pedunculate Oak. *Phytochemistry* **45**, 1555–1560.
- Niemetz R, Gross GG.** 2005. Enzymology of gallotannin and ellagitannin biosynthesis. *Phytochemistry* **66**, 2001–2011.
- Nishizawa A, Yabuta Y, Shigeoka S.** 2008. Galactinol and Raffinose Constitute a Novel Function to Protect Plants from Oxidative Damage. *Plant Physiology* **147**, 1251–1263.
- Njuguna W, Liston A, Cronn R, Ashman TL, Bassil N.** 2013. Insights into phylogeny, sex function and age of *Fragaria* based on whole chloroplast genome sequencing. *Molecular Phylogenetics and Evolution* **66**, 17–29.
- Nogata Y, Yoza K, Kusumoto K, Ohta H.** 1996. Changes in molecular weight and carbohydrate composition of cell wall polyuronide and hemicellulose during ripening in strawberry fruit. In: Visser J., In: Voragen AGJ, eds. *Pectins and Pectinases*. 591–596.
- Olbricht K, Ulrich D, Weiss K, Grafe C.** 2011. Variation in the amounts of selected volatiles in a model population of *Fragaria* × *ananassa* Duch. as influenced by harvest year. *Journal of Agricultural and Food Chemistry* **59**, 944–952.
- Oms-Oliu G, Hertog MLATM, Van de Poel B, Ampofo-Asiama J, Geeraerd AH, Nicolai BM.** 2011. Metabolic characterization of tomato fruit during preharvest development, ripening, and postharvest shelf-life. *Postharvest Biology and Technology* **62**, 7–16.
- Onopiuk A, Póltorak A, Wyrwicz J, et al.** 2016. Impact of ozonisation on pro-health properties and antioxidant capacity of 'Honeoye' strawberry fruit. *CyTA - Journal of Food* **15**, 1–7.
- Oosumi T, Gruszewski HA, Blischak LA, Baxter AJ, Wadl PA, Shuman JL, Veilleux RE, Shulaev V.** 2006. High-efficiency transformation of the diploid strawberry (*Fragaria vesca*) for functional genomics. *Planta* **223**, 1219–1230.
- Ornelas-Paz JDJ, Yahia EM, Ramírez-Bustamante N, Pérez-Martínez JD, Escalante-Minakata MDP, Ibarra-Junquera V, Acosta-Muñiz C, Guerrero-Prieto V, Ochoa-Reyes E.** 2013. Physical attributes and chemical composition of organic strawberry fruit (*Fragaria* × *ananassa* Duch, Cv. Albion) at six stages of ripening. *Food Chemistry* **138**, 372–381.
- Osborn TC, Chris Pires J, Birchler JA, et al.** 2003. Understanding mechanisms of novel gene expression in polyploids. *Trends in Genetics* **19**, 141–147.
- Osorio S, Castillejo C, Quesada MA, Medina-Escobar N, Brownsey GJ, Suau R, Heredia A, Botella MA, Valpuesta V.** 2008. Partial demethylation of oligogalacturonides by pectin methyl esterase 1 is required for eliciting defence responses in wild strawberry (*Fragaria vesca*). *Plant Journal* **54**, 43–55.
- Osorio S, Do PT, Fernie AR.** 2012. Profiling primary metabolites of tomato fruit with gas chromatography/mass spectrometry. *Methods in Molecular Biology* **860**, 101–109.

Palma F, Carvajal F, Jamilena M, Garrido D. 2014. Contribution of polyamines and other related metabolites to the maintenance of zucchini fruit quality during cold storage. *Plant Physiology and Biochemistry* **82**, 161–171.

Paniagua C, Blanco-Portales R, Barceló-Muñoz M, García-Gago J a., Waldron KW, Quesada MA, Muñoz-Blanco J, Mercado JA. 2016. Antisense down-regulation of the strawberry β -galactosidase gene Fa β Gal4 increases cell wall galactose levels and reduces fruit softening. *Journal of Experimental Botany* **67**, 619–631.

Pareiman MA, Storms DH, Kirschke CP, Huang L, Zunino SJ. 2012. Dietary strawberry powder reduces blood glucose concentrations in obese and lean C57BL/6 mice, and selectively lowers plasma C-reactive protein in lean mice. *British Journal of Nutrition* **108**, 1789–1799.

Paterson AH, Lander ES, Hewitt JD, Peterson S, Lincoln SE, Tanksley SD. 1988. Resolution of quantitative traits into Mendelian factors by using a complete linkage map of restriction fragment length polymorphisms. *Nature* **335**, 721.

Pedreschi R, Lurie S. 2015. Advances and current challenges in understanding postharvest abiotic stresses in perishables. *Postharvest Biology and Technology* **107**, 77–89.

Pelayo C, Ebeler SE, Kader a. a. 2003. Postharvest life and flavor quality of three strawberry cultivars kept at 5°C in air or air+20 kPa CO₂. *Postharvest Biology and Technology* **27**, 171–183.

Pérez AG, Olías R, Sanz C, Olías JM. 1996. Furanones in Strawberries: Evolution during Ripening and Postharvest Shelf Life. *Journal of Agricultural and Food Chemistry* **44**, 3620–3624.

Pérez AG, Sanz C, Ríos JJ, Olías R, Olías JM. 1999. Effects of ozone treatment on postharvest strawberry quality. *Journal of Agricultural and Food Chemistry* **47**, 1652–1656.

Perkins-Veazie P. 1995. Growth and ripening of strawberry fruit. *Horticultural Reviews* **17**, 267–297.

Perry RH, Cooks RG, Noll RJ. 2008. Orbitrap mass spectrometry: Instrumentation, ion motion and applications. *Mass Spectrometry Reviews* **27**, 661–699.

Pesis E, Aharoni D, Aharon Z, Ben-Arie R, Aharoni N, Fuchs Y. 2000. Modified atmosphere and modified humidity packaging alleviates chilling injury symptoms in mango fruit. *Postharvest Biology and Technology* **19**, 93–101.

Petrussa E, Braidot E, Zancani M, Peresson C, Bertolini A, Patui S, Vianello A. 2013. Plant flavonoids-biosynthesis, transport and involvement in stress responses. *International Journal of Molecular Sciences* **14**, 14950–14973.

Phan NT, Sim S. 2017. Genomic Tools and Their Implications for Vegetable Breeding. *Horticultural Science and Technology* **35**, 149–164.

- Piljac-Žegarac J, Šamec D.** 2011. Antioxidant stability of small fruits in postharvest storage at room and refrigerator temperatures. *Food Research International* **44**, 345–350.
- Ponce-Valadez M, Fellman SM, Giovannoni J, Gan SS, Watkins CB.** 2009. Differential fruit gene expression in two strawberry cultivars in response to elevated CO₂ during storage revealed by a heterologous fruit microarray approach. *Postharvest Biology and Technology* **51**, 131–140.
- Popovsky-Sarid S, Borovsky Y, Faigenboim A, Parsons EP, Lohrey GT, Alkalai-Tuvia S, Fallik E, Jenks MA, Paran I.** 2017. Genetic and biochemical analysis reveals linked QTLs determining natural variation for fruit post-harvest water loss in pepper (*Capsicum*). *Theoretical and Applied Genetics* **130**, 445–459.
- Pott DM, Vallarino JG, Osorio S, Amaya I.** 2018. Fruit Ripening and QTL for Fruit Quality in the Octoploid Strawberry. *The Genomes of Rosaceous Berries and Their Wild Relatives*. Springer International Publishing, 95–113.
- Qin G, Meng X, Wang Q, Tian S.** 2009. Oxidative damage of mitochondrial proteins contributes to fruit senescence: A redox proteomics analysis. *Journal of Proteome Research* **8**, 2449–2462.
- Raab T, López-Ráez JA, Klein D, Caballero JL, Moyano E, Schwab W, Muñoz-Blanco J.** 2006. FaQR, Required for the Biosynthesis of the Strawberry Flavor Compound 4-Hydroxy-2,5-Dimethyl-3(2H)-Furanone, Encodes an Enone Oxidoreductase. *the Plant Cell Online* **18**, 1023–1037.
- Rambla JL, López-Gresa MP, Bellés JM, Graneli A.** 2015. Metabolomic Profiling of Plant Tissues. In: Alonso JM, In: Stepanova AN, eds. *Plant Functional Genomics and Protocols*, *Methods in Molecular Biology*. New York, NY: Springer Science+Businesss, 221–235.
- Remberg SF, Soørnsteby A, Aaby K, Heide OM.** 2010. Influence of postflowering temperature on fruit size and chemical composition of glen ample raspberry (*Rubus Idaeus L.*). *Journal of Agricultural and Food Chemistry* **58**, 9120–9128.
- Ring L, Yeh S-Y, Hücherig S, et al.** 2013. Metabolic interaction between anthocyanin and lignin biosynthesis is associated with peroxidase FaPRX27 in strawberry fruit. *Plant physiology* **163**, 43–60.
- Rodríguez A, Alquézar B, Peña L.** 2013. Fruit aromas in mature fleshy fruits as signals of readiness for predation and seed dispersal. *New Phytologist* **197**, 36–48.
- Roessner U, Luedemann a, Brust D, Fiehn O, Linke T, Willmitzer L, Fernie a.** 2001. Metabolic profiling allows comprehensive phenotyping of genetically or environmentally modified plant systems. *The Plant cell* **13**, 11–29.
- Rohloff J, Kopka J, Erban A, Winge P, Wilson RC, Bones AM, Davik J, Randall SK, Alsheikh MK.** 2012. Metabolite profiling reveals novel multi-level cold responses in the diploid model *Fragaria vesca* (woodland strawberry). *Phytochemistry* **77**, 99–109.

Rosli HG, Civello PM, Martínez GA. 2004. Changes in cell wall composition of three *Fragaria x ananassa* cultivars with different softening rate during ripening. *Plant Physiology and Biochemistry* **42**, 823–831.

Rousseau-Gueutin M, Lerceteau-Köhler E, Barrot L, Sargent DJ, Monfort A, Simpson D, Arús P, Guérin G, Denoyes-Rothan B. 2008. Comparative genetic mapping between octoploid and diploid *Fragaria* species reveals a high level of colinearity between their genomes and the essentially disomic behavior of the cultivated octoploid strawberry. *Genetics* **179**, 2045–60.

Rowe HC, Hansen BG, Halkier BA, Kliebenstein DJ. 2008. Biochemical Networks and Epistasis Shape the *Arabidopsis thaliana* Metabolome. *the Plant Cell Online* **20**, 1199–1216.

RStudio Team. 2016. RStudio: Integrated Development Environment for R.

Rudell DR, Mattheis JP, Curry EA. 2008. Prestorage ultraviolet-white light irradiation alters apple peel metabolome. *Journal of Agricultural and Food Chemistry* **56**, 1138–1147.

Sainsbury F, Thuenemann EC, Lomonossoff GP. 2009. PEAQ: Versatile expression vectors for easy and quick transient expression of heterologous proteins in plants. *Plant Biotechnology Journal* **7**, 682–693.

Salvi P, Kamble NU, Majee M. 2017. Stress-Inducible Galactinol Synthase of Chickpea (*CaGolS*) is Implicated in Heat and Oxidative Stress Tolerance Through Reducing Stress-Induced Excessive Reactive Oxygen Species Accumulation. *Plant and Cell Physiology* **59**, 155–166.

Sánchez-Sevilla JF, Cruz-Rus E, Valpuesta V, Botella M a, Amaya I. 2014. Deciphering gamma-decalactone biosynthesis in strawberry fruit using a combination of genetic mapping, RNA-Seq and eQTL analyses. *BMC Genomics* **15**, 218.

Sánchez-Sevilla JF, Horvath A, Botella MA, Gaston A, Folta K, Kilian A, Denoyes B, Amaya I. 2015. Diversity arrays technology (DArT) marker platforms for diversity analysis and linkage mapping in a complex crop, the octoploid cultivated strawberry (*Fragaria x ananassa*). *PLoS ONE* **10**.

Sánchez-Sevilla JF, Vallarino JG, Osorio S, Bombarely A, Posé D, Merchante C, Botella MA, Amaya I, Valpuesta V. 2017. Gene expression atlas of fruit ripening and transcriptome assembly from RNA-seq data in octoploid strawberry (*Fragaria x ananassa*). *Scientific Reports* **7**, 1–13.

Sánchez G, Martínez J, Romeu J, García J, Monforte AJ, Badenes ML, Granell A. 2014. The peach volatilome modularity is reflected at the genetic and environmental response levels in a QTL mapping population. *BMC Plant Biology* **14**.

Sanhueza D, Vizoso P, Balic I, Campos-Vargas R, Meneses C. 2015. Transcriptomic analysis of fruit stored under cold conditions using controlled atmosphere in *Prunus persica* cv. “Red Pearl”. *Frontiers in Plant Science* **6**, 1–12.

Sargent DJ, Fernández-Fernández F, Ruiz-Roja JJ, Sutherland G, Passey A, Whitehouse AB, Simpson DW. 2009. A genetic linkage map of the cultivated strawberry (*Fragaria x ananassa*) and its comparison to the diploid *Fragaria* reference map. *Molecular bioSystems* **24**, 293–303.

Sargent DJ, Passey T, Šurbanovski N, Lopez Girona E, Kuchta P, Davik J, Harrison R, Passey A, Whitehouse AB, Simpson DW. 2012. A microsatellite linkage map for the cultivated strawberry (*Fragaria x ananassa*) suggests extensive regions of homozygosity in the genome that may have resulted from breeding and selection. *Theoretical and Applied Genetics* **124**, 1229–1240.

Sargent DJ, Yang Y, Surbanovski N, Bianco L, Buti M, Velasco R, Giongo L, Davis TM. 2016. HaploSNP affinities and linkage map positions illuminate subgenome composition in the octoploid , cultivated strawberry (*Fragaria x ananassa*). *Plant Science* **242**, 140–150.

Savoi S, Wong DCJ, Arapitsas P, Miculan M, Bucchetti B, Peterlunger E, Fait A, Mattivi F, Castellarin SD. 2016. Transcriptome and metabolite profiling reveals that prolonged drought modulates the phenylpropanoid and terpenoid pathway in white grapes (*Vitis vinifera* L.). *BMC Plant Biology* **16**, 1–17.

Schauer N, Semel Y, Roessner U, et al. 2006. Comprehensive metabolic profiling and phenotyping of interspecific introgression lines for tomato improvement. *Nature biotechnology* **24**, 447–454.

Schieberle P, Hofmann T. 1997. Evaluation of the Character Impact Odorants in Fresh Strawberry Juice by Quantitative Measurements and Sensory Studies on Model Mixtures. *Journal of Agricultural and Food Chemistry* **45**, 227–232.

Schulenburg K, Feller A, Hoffmann T, Schecker JH, Martens S, Schwab W. 2016. Formation of β -glucogallin, the precursor of ellagic acid in strawberry and raspberry. *Journal of Experimental Botany* **67**, 2299–2308.

Schwieterman ML, Colquhoun TA, Jaworski EA, et al. 2014. Strawberry flavor: Diverse chemical compositions, a seasonal influence, and effects on sensory perception. *PLoS ONE* **9**.

Serek M, Tamari G, Sisler EC, Borochoy A. 1995. Inhibition of ethylene-induced cellular senescence symptoms by 1-methylcyclopropene, a new inhibitor of ethylene action. *Physiologia Plantarum* **94**, 229–232.

Shamaila M, Powrie WD, Skura BJ. 1992. Analysis of Volatile Compounds from Strawberry Fruit Stored under Modified Atmosphere Packaging (MAP). *Journal of Food Science* **57**, 1173–1176.

Shapiro ASS, Wilk MB. 1965. An Analysis of Variance Test for Normality (Complete Samples) Published by: Oxford University Press on behalf of Biometrika Trust Stable URL : <http://www.jstor.org/stable/2333709> Accessed : 25-04-2016 16 : 06 UTC An analysis of varianc. *Biometrika* **52**, 591–611.

- Shelp BJ, Mullen RT, Waller JC.** 2012. Compartmentation of GABA metabolism raises intriguing questions. *Trends in Plant Science* **17**, 57–59.
- Shin Y, Liu RH, Nock JF, Holliday D, Watkins CB.** 2007. Temperature and relative humidity effects on quality, total ascorbic acid, phenolics and flavonoid concentrations, and antioxidant activity of strawberry. *Postharvest Biology and Technology* **45**, 349–357.
- Shin Y, Ryu JA, Liu RH, Nock JF, Polar-Cabrera K, Watkins CB.** 2008. Fruit quality, antioxidant contents and activity, and antiproliferative activity of strawberry fruit stored in elevated CO₂ atmospheres. *Journal of Food Science* **73**.
- Shulaev V, Korban SS, Sosinski B, et al.** 2008. Multiple Models for Rosaceae Genomics. *Plant Physiology* **147**, 985–1003.
- Shulaev V, Sargent DJ, Crowhurst RN, et al.** 2011. The genome of woodland strawberry (*Fragaria vesca*). *Nature Genetics* **43**, 109–116.
- da Silva FL, Escribano-Bailón MT, Pérez Alonso JJ, Rivas-Gonzalo JC, Santos-Buelga C.** 2007. Anthocyanin pigments in strawberry. *LWT - Food Science and Technology* **40**, 374–382.
- Silva O, Duarte A, Pimentel M, Viegas S, Barroso H, Machado J, Pires I, Cabrita J, Gomes E.** 1997. Antimicrobial activity of *Terminalia macroptera* root. *Journal of Ethnopharmacology* **57**, 203–207.
- Slovin J, Michael T.** 2011. Strawberry. Part 3 structural and functional genomics. In: Folta K,, In: Kole C, eds. *Genetics, genomics and breeding of berries*. Enfield, 162–193.
- Soegiarto L, Wills RBH.** 2004. Short term fumigation with nitric oxide gas in air to extend the postharvest life of broccoli, green bean, and bok choy. *HortTechnology* **14**, 538–540.
- Song C, Hong X, Zhao S, Liu J, Schulenburg K, Huang F-C, Franz-Oberdorf K, Schwab W.** 2016. Glucosylation of 4-Hydroxy-2,5-Dimethyl-3(2H)-Furanone, the Key Strawberry Flavor Compound in Strawberry Fruit. *Plant Physiology* **171**, 139–151.
- Spasojević I, Mojović M, Blagojević D, Spasić SD, Jones DR, Nikolić-Kokić A, Spasić MB.** 2009. Relevance of the capacity of phosphorylated fructose to scavenge the hydroxyl radical. *Carbohydrate Research* **344**, 80–84.
- Spigler RB, Lewers KS, Johnson AL, Ashman TL.** 2010. Comparative mapping reveals autosomal origin of sex chromosome in octoploid *Fragaria virginiana*. *Journal of Heredity* **101**, 107–117.
- Stewart D, Dhungana S, Clark R, Pathmasiri W, McRitchie S, Sumner S.** 2015. Chapter 4 - Omics Technologies Used in Systems Biology. In: Fry RCBT-SB in T and EH, ed. Boston: Academic Press, 57–83.
- Sun J, Janisiewicz WJ, Nichols B, Jurick WM, Chen P.** 2017. Composition of phenolic

compounds in wild apple with multiple resistance mechanisms against postharvest blue mold decay. *Postharvest Biology and Technology* **127**, 68–75.

Sun L, Zhang M, Ren J, Qi J, Zhang G, Leng P. 2010. Reciprocity between abscisic acid and ethylene at the onset of berry ripening and after harvest. *BMC Plant Biology* **10**.

Sun X, Zhu A, Liu S, et al. 2013. Integration of Metabolomics and Subcellular Organelle Expression Microarray to Increase Understanding the Organic Acid Changes in Post-harvest Citrus Fruit. *Journal of Integrative Plant Biology* **55**, 1038–1053.

Tang N, Deng W, Hu N, Chen N, Li Z. 2016. Metabolite and transcriptomic analysis reveals metabolic and regulatory features associated with Powell orange pulp deterioration during room temperature and cold storage. *Postharvest Biology and Technology* **112**, 75–86.

Tanksley SD. 1993. Mapping Polygenes. *Annual Review of Genetics* **27**, 205–233.

Team RC. 2017. R: A Language and Environment for Statistical Computing.

Tenessen JA, Govindarajulu R, Ashman TL, Liston A. 2014. Evolutionary origins and dynamics of octoploid strawberry subgenomes revealed by dense targeted capture linkage maps. *Genome Biology and Evolution* **6**, 3295–3313.

Thill J, Miosic S, Gotame TP, et al. 2013. Differential expression of flavonoid 3'-hydroxylase during fruit development establishes the different B-ring hydroxylation patterns of flavonoids in *Fragaria x ananassa* and *Fragaria vesca*. *Plant Physiology and Biochemistry* **72**, 72–78.

Thompson EP, Davies JM, Glover BJ. 2010. Identifying the transporters of different flavonoids in plants. *Plant Signaling and Behavior* **5**, 860–863.

Tieman D, Zhu G, Resende MFR, et al. 2017. A chemical genetic roadmap to improved tomato flavor. *Science (New York, N.Y.)* **355**, 391–394.

Tietel Z, Lewinsohn E, Fallik E, Porat R. 2012. Importance of storage temperatures in maintaining flavor and quality of mandarins. *Postharvest Biology and Technology* **64**, 175–182.

Tietel Z, Plotto A, Fallik E, Lewinsohn E, Porat R. 2011. Taste and aroma of fresh and stored mandarins. *Journal of the Science of Food and Agriculture* **91**, 14–23.

Trakulnaleumsai C, Ketsa S, Van Doorn WG. 2006. Temperature effects on peel spotting in 'Sucrier' banana fruit. *Postharvest Biology and Technology* **39**, 285–290.

Tulipani S, Marzban G, Herndl A, Laimer M, Mezzetti B, Battino M. 2011. Influence of environmental and genetic factors on health-related compounds in strawberry. *Food Chemistry* **124**, 906–913.

Tulipani S, Mezzetti B, Battino M. 2009. Impact of strawberries on human health: Insight into marginally discussed bioactive compounds for the Mediterranean diet. *Public Health Nutrition* **12**, 1656–1662.

- Tulipani S, Mezzetti B, Capocasa F, Bompadre S, Beekwilder J, Vos CHR De, Capanoglu E, Bovy A, Battino M.** 2008. Antioxidants , Phenolic Compounds , and Nutritional Quality of Different Strawberry Genotypes Quality of Different Strawberry Genotypes. *Journal of Agricultural and Food Chemistry* **56**, 696–704.
- Ulrich D, Hoberg E, Rapp A, Kecke S.** 1997. Analysis of strawberry flavour - discrimination of aroma types by quantification of volatile compounds. *Zeitschrift für Lebensmitteluntersuchung und -Forschung A* **205**, 218–223.
- Ulrich D, Komes D, Olbricht K, Hoberg E.** 2007. Diversity of aroma patterns in wild and cultivated *Fragaria* accessions. *Genetic Resources and Crop Evolution* **54**, 1185–1196.
- Ulrich D, Olbricht K.** 2013. Diversity of volatile patterns in sixteen *Fragaria vesca* L . accessions in comparison to cultivars of *Fragaria × ananassa*. *Journal of Applied Botany and Food Quality* **46**, 37–46.
- Urrutia M, Bonet J, Arús P, Monfort A.** 2015a. A near-isogenic line (NIL) collection in diploid strawberry and its use in the genetic analysis of morphologic, phenotypic and nutritional characters. *Theoretical and Applied Genetics* **128**, 1261–1275.
- Urrutia M, Rambla JL, Alexiou KG, Granell A, Monfort A.** 2017. Genetic analysis of the wild strawberry (*Fragaria vesca*) volatile composition. *Plant Physiology and Biochemistry* **121**, 99–117.
- Urrutia M, Schwab W, Hoffmann T, Monfort A.** 2015b. Genetic dissection of the (poly)phenol profile of diploid strawberry (*Fragaria vesca*) fruits using a NIL collection. *Plant Science*.
- Vallarino JG, Osorio S, Bombarely A, et al.** 2015. Central role of FaGAMYB in the transition of the strawberry receptacle from development to ripening. *New Phytologist*, 482–496.
- Vandendriessche T, Vermeir S, Mayayo Martinez C, Hendrickx Y, Lammertyn J, Nicolai BM, Hertog ML a TM.** 2013. Effect of ripening and inter-cultivar differences on strawberry quality. *LWT - Food Science and Technology* **52**, 62–70.
- Verma S, Zurn JD, Salinas N, Mathey MM, Denoyes B, Hancock JF, Finn CE, Bassil N V., Whitaker VM.** 2017. Clarifying sub-genomic positions of QTLs for flowering habit and fruit quality in U.S. strawberry (*Fragariaananassa*) breeding populations using pedigree-based QTL analysis. *Horticulture Research* **4**, 1–9.
- Versari A, Paola Parpinello G, Battista Torielli G, Ferrarini R, Giulivo C.** 2001. Stilbene compounds and stilbene synthase expression during ripening, wilting, and UV treatment in grape cv. Corvina. *Journal of Agricultural and Food Chemistry* **49**, 5531–5536.
- Vogt T.** 2010. Phenylpropanoid biosynthesis. *Molecular Plant* **3**, 2–20.
- Wahyuni Y, Stahl-Hermes V, Ballester A-R, et al.** 2014. Genetic mapping of semi-polar metabolites in pepper fruits (*Capsicum* sp.): towards unravelling the molecular regulation of

flavonoid quantitative trait loci. *Molecular breeding : new strategies in plant improvement* **33**, 503–518.

Wang H, Cao G, Prior RL. 1996. Total antioxidant capacity of fruits. *Journal of Agricultural and Food Chemistry* **44**, 701–705.

Wang SY, Lin HS. 2000. Antioxidant activity in fruits and leaves of blackberry, raspberry, and strawberry varies with cultivar and developmental stage. *Journal of Agricultural and Food Chemistry* **48**, 140–146.

Wang SY, Zheng W. 2001. Effect of plant growth temperature on antioxidant capacity in strawberry. *J Agric Food Chem* **49**, 4977–4982.

Weebadde CK, Wang D, Finn CE, Lewers KS, Luby JJ, Bushakra J, Sjulín TM, Hancock JF. 2008. Using a linkage mapping approach to identify QTL for day-neutrality in the octoploid strawberry. *Plant Breeding* **127**, 94–101.

Wentzell AM, Rowe HC, Hansen BG, Ticconi C, Halkier BA, Kliebenstein DJ. 2007. Linking metabolic QTLs with network and cis-eQTLs controlling biosynthetic pathways. *PLoS Genetics* **3**, 1687–1701.

Werner RA, Rossmann A, Schwarz C, Bacher A, Schmidt HL, Eisenreich W. 2004. Biosynthesis of gallic acid in *Rhus typhina*: Discrimination between alternative pathways from natural oxygen isotope abundance. *Phytochemistry* **65**, 2809–2813.

Wickham H. 2009. *ggplot2: Elegant Graphics for Data Analysis*. New York, NY, .

Widhalm JR, Dudareva N. 2015. A familiar ring to it: Biosynthesis of plant benzoic acids. *Molecular Plant* **8**, 83–97.

Winkel-Shirley B. 2001. Flavonoid Biosynthesis. A Colorful Model for Genetics, Biochemistry, Cell Biology, and Biotechnology. *Plant Physiology* **126**, 485–493.

Würschum T. 2012. Mapping QTL for agronomic traits in breeding populations. *Theoretical and Applied Genetics* **125**, 201–210.

Yang Z, Cao S, Su X, Jiang Y. 2014. Respiratory activity and mitochondrial membrane associated with fruit senescence in postharvest peaches in response to UV-C treatment. *Food Chemistry* **161**, 16–21.

Yauk YK, Chagné D, Tomes S, Matich AJ, Wang MY, Chen X, Maddumage R, Hunt MB, Rowan DD, Atkinson RG. 2015. The O-methyltransferase gene MdoOMT1 is required for biosynthesis of methylated phenylpropenes in ripe apple fruit. *Plant Journal* **82**, 937–950.

Yuan Y, Zhao Y, Yang J, Jiang Y, Lu F, Jia Y, Yang B. 2017. Metabolomic analyses of banana during postharvest senescence by 1H-high resolution-NMR. *Food Chemistry* **218**, 406–412.

Yun Z, Jin S, Ding Y, Wang Z, Gao H, Pan Z, Xu J, Cheng Y, Deng X. 2012. Comparative

transcriptomics and proteomics analysis of citrus fruit, to improve understanding of the effect of low temperature on maintaining fruit quality during lengthy post-harvest storage. *Journal of Experimental Botany* **63**, 2873–2893.

Yun Z, Qu H, Wang H, Zhu F, Zhang Z, Duan X, Yang B, Cheng Y, Jiang Y. 2016. Comparative transcriptome and metabolome provides new insights into the regulatory mechanisms of accelerated senescence in litchi fruit after cold storage. *Scientific Reports* **6**, 1–16.

Zamboni A, Di Carli M, Guzzo F, et al. 2010. Identification of Putative Stage-Specific Grapevine Berry Biomarkers and Omics Data Integration into Networks. *Plant Physiology* **154**, 1439–1459.

Zanor MI, Rambla JL, Chaïb J, Steppa A, Medina A, Granell A, Fernie AR, Causse M. 2009. Metabolic characterization of loci affecting sensory attributes in tomato allows an assessment of the influence of the levels of primary metabolites and volatile organic contents. *Journal of Experimental Botany* **60**, 2139–2154.

Zeballos JL, Abidi W, Giménez R, Monforte AJ, Moreno MA, Gogorcena Y. 2016. Mapping QTLs associated with fruit quality traits in peach [*Prunus persica* (L.) Batsch] using SNP maps. *Tree Genetics and Genomes* **12**.

Zeng ZB. 1993. Theoretical basis for separation of multiple linked gene effects in mapping quantitative trait loci. *Proceedings of the National Academy of Sciences* **90**, 10972–10976.

Zeng ZB. 1994. Precision mapping of quantitative trait loci. *Genetics* **136**, 1457 LP-1468.

Zenoni S, Fasoli M, Guzzo F, et al. 2016. Disclosing the Molecular Basis of the Postharvest Life of Berry in Different Grapevine Genotypes. *Plant Physiology* **172**, 1821–1843.

Zhang J, Wang X, Yu O, Tang J, Gu X, Wan X, Fang C. 2011. Metabolic profiling of strawberry (*Fragaria x ananassa* Duch.) during fruit development and maturation. *Journal of Experimental Botany* **62**, 1103–1118.

Zhang J, Zhang Y, Dou Y, Li W, Wang S, Shi W, Sun Y, Zhang Z. 2017. Single nucleotide mutation in FvMYB10 may lead to the yellow fruit in *Fragaria vesca*. *Molecular Breeding* **37**, 1–10.

Zorrilla-Fontanesi Y, Cabeza A, Domínguez P, Medina JJ, Valpuesta V, Denoyes-Rothan B, Sánchez-Sevilla JF, Amaya I. 2011. Quantitative trait loci and underlying candidate genes controlling agronomical and fruit quality traits in octoploid strawberry (*Fragaria x ananassa*). *Theoretical and Applied Genetics* **123**, 755–778.

Zorrilla-Fontanesi Y, Rambla J-L, Cabeza A, Medina JJ, Sánchez-Sevilla JF, Valpuesta V, Botella MA, Granell A, Amaya I. 2012. Genetic analysis of strawberry fruit aroma and identification of O-methyltransferase FaOMT as the locus controlling natural variation in mesifurane content. *Plant physiology* **159**, 851–70.

Zou J, Chen J, Tang N, et al. 2018. Transcriptome analysis of aroma volatile metabolism change

References

in tomato (*Solanum lycopersicum*) fruit under different storage temperatures and 1-MCP treatment. *Postharvest Biology and Technology* **135**, 57–67.

Annexes

Annexes are available in electronic format.

Supplementary material Chapter 2

Annex 1: list of primers used in Chapter 3

Annex 2: relative content (mean value between 2013 and 2014 harvests) of the putatively identified secondary metabolites in the '232'x'1392' population. Values are relativized to the mean value of '1392' parental line.

Annex 3: Tukey's posthoc tests to see if the different treatments (\$Treatment) and their duration (\$Time) significantly changed fruit firmness and SSC during postharvest. ctr, CO₂ and O₃ indicate normal atmosphere, CO₂-enriched and ozone-enriched atmospheres, respectively. 0d, 3d, 6d and 10d indicate T0 samples and three, six and ten days of postharvest treatments, respectively

Annex 4: relative content of the identified primary metabolites in the T0 and postharvest samples.

Annex 5: relative content of the tentatively identified secondary metabolites in the T0 and postharvest samples

Annex 6: relative content of the identified volatiles in the T0 and postharvest samples.

Annex 7: loading plots for PLS-DA analysis shown in Chapter 4.

Annex 8: primary metabolites fold change in the postharvest samples compared to T0 samples.

Annex 9: secondary metabolites fold change in the postharvest samples compared to T0 samples.

Annex 10: volatiles fold change in the postharvest samples compared to T0 samples

Annex 11: cluster attribution for primary metabolites

Annex 12: cluster attribution for secondary metabolites

Annex 13: cluster attribution for volatiles